Universidad de Oviedo

PhD Programme in Natural Resources Engineering

METHODOLOGICAL CONTRIBUTIONS TO THE ATTRIBUTIVE ANALYSIS TOOL FOR SOIL WASHING OPERATIONS

PhD candidate

Xabier Rafael Corres Fuentes

Oviedo, 2024

Universidad de Oviedo

PhD Programme in Natural Resources Engineering

METHODOLOGICAL CONTRIBUTIONS TO THE ATTRIBUTIVE ANALYSIS TOOL FOR SOIL WASHING OPERATIONS

PhD candidate

Xabier Rafael Corres Fuentes

Supervisors

Dr. Diego Baragaño Coto

Dr. Carlos Sierra Fernández

Oviedo, 2024

Universidad de Oviedo

RESUMEN DEL CONTENIDO DE TESIS DOCTORAL

1.- Título de la Tesis	
Español/Otro Idioma: Aportaciones metodológicas a la herramienta del análisis atributivo para operaciones de lavado de suelos	Inglés: Methodological contributions to the attributive analysis tool for soil washing operations

2.- Autor	
Nombre: Xabier Rafael Corres Fuentes	
Programa de Doctorado: Ingeniería de los recursos naturales	
Órgano responsable: Universidad de Oviedo	

RESUMEN (en español)

Esta tesis doctoral presenta un compendio de tres estudios sobre el desarrollo y evolución del método de análisis atributivo como sistema para evaluar técnicas de descontaminación de suelos. El método de análisis atributivo ha experimentado una evolución significativa, pasando de una forma básica a un enfoque más robusto y multidimensional, lo que ha permitido mejorar su precisión y efectividad.

Inicialmente, el método de análisis atributivo básico (BAA) se centró en maximizar la recuperación y minimizar el rendimiento, estableciendo una base fundamental para evaluar las condiciones de separación. Este enfoque, junto con el factor de corrección por distancia al objetivo, identificó configuraciones experimentales prometedoras en la aplicación de la separación electrostática para la descontaminación de suelos.

A partir del análisis del BAA, se observó que el algoritmo priorizaba la minimización del rendimiento sobre la maximización de la recuperación. Mientras que la relación entre el índice de calidad y la recuperación era lineal, la relación con el rendimiento era inversamente cuadrática. Además, el método mostró una notable sensibilidad a la dispersión de los datos de recuperación y rendimiento. En respuesta, se introdujo una corrección basada en el inverso de la desviación estándar y una normalización de los parámetros para penalizar configuraciones experimentales con mayores variaciones. Estas modificaciones dieron lugar al método de análisis atributivo penalizado (PPAA-U).

Posteriormente, se incorporaron dos modificaciones adicionales. La primera consistió en un criterio para identificar experimentos "fallidos", definidos como aquellos con valores de rendimiento superiores a los de recuperación, ya que estos escenarios presentan una baja eficiencia en los procesos de descontaminación de suelos. Además, se estableció que la fracción concentrada en EPTs (elementos potencialmente tóxicos) sería aquella que tuviera un valor de recuperación superior al rendimiento en el 50% o más de los EPTs objetivo. Esta regla heurística permitió discernir el concentrado de las colas. La segunda modificación añadió un tercer parámetro al análisis atributivo: la ley del EPT en el concentrado (λ), con el objetivo de mejorar la precisión del método en la identificación de las condiciones óptimas de concentración. Esto dio lugar al análisis atributivo penalizado de tres parámetros (3PPAA-U).

Sin la corrección objetivo-distancia, el 3PPAA-U es al menos tan eficaz en la selección de las BUC (mejores condiciones de uso) como los métodos basados en otros criterios. Con la corrección adicional, el 3PPAA-U supera a las técnicas convencionales, mejorando así la evaluación de los procedimientos de lavado de suelos.

La técnica del análisis atributivo ha avanzado significativamente a lo largo de la investigación, permitiendo mejoras continuas en la precisión de la evaluación de la eficiencia de los procedimientos de separación. Sin embargo, el enfoque 3PPAA-U sigue siendo un método heurístico y no definitivo para determinar las BUC. Aunque proporciona un enfoque metódico e imparcial para evaluar y contrastar varias opciones, se basa en suposiciones y simplificaciones que pueden pasar por alto algunas complejidades asociadas a los procedimientos de lavado de suelos. Por lo tanto, esta metodología debe emplearse con cautela y como un indicador de configuraciones experimentales prometedoras, complementada con consideraciones subjetivas y cualitativas como el riesgo, el coste y la viabilidad. El 3PPAA-U debe ser utilizado con un enfoque crítico y en combinación con otras técnicas, y su metodología podrá ampliarse en

futuros estudios para evaluar una mayor variedad de factores esenciales para la eficacia de las operaciones de lavado de suelos.

RESUMEN (en Inglés)

This PhD thesis presents a compendium of three studies on the development and evolution of the Attributive Analysis (AA) method as a system for evaluating soil decontamination techniques. The AA has significantly evolved from its initial form to a more robust and multidimensional approach, enhancing its accuracy and effectiveness.

Initially, the basic Attributive Analysis (BAA) method focused on maximizing recovery and minimizing yield, providing a fundamental basis for evaluating separation conditions. This approach, combined with the distance-to-target correction factor, identified promising experimental setups for the application of electrostatic separation in soil remediation.

Upon analyzing the BAA, it was observed that the algorithm prioritized minimizing yield over maximizing recovery. While the relationship between the quality index and recovery was linear, throughput exhibited an inverse square relationship. Additionally, the method showed considerable sensitivity to variability in recovery and yield data. To address this, a correction for the inverse of the standard deviation and normalization of parameters were introduced to penalize experimental setups with high data variability. These modifications led to the development of the Penalized Attributive Analysis (PPAA-U) method.

Subsequently, two further modifications were implemented. The first involved introducing a criterion to identify "failed" experiments—those with yield values exceeding recovery values. Such scenarios are of limited interest for soil remediation due to their reduced efficiency compared to setups with higher recovery values. Additionally, it was established that the fraction concentrated in potentially toxic elements (PTEs) should have a recovery value higher than the yield in 50% or more of the target PTEs. This rule was used as a heuristic to distinguish between concentrates and tailings. The second modification incorporated a third parameter into the attributive analysis: the grade of PTEs in the concentrate. This aimed to enhance the precision of the method in identifying optimal concentration conditions, leading to the development of the Penalized Three-Parameter Attributive Analysis (3PPAA-U).

Without the target-distance correction, 3PPAA-U is at least as effective in selecting the best upgrading conditions (BUC) as methods based on other criteria. With the additional correction, it outperforms conventional techniques, potentially improving the performance evaluation of soil washing procedures.

The Attributive Analysis technique has undergone significant development, resulting in continuous improvements in assessing separation procedure efficiency. However, the 3PPAA-U approach remains a heuristic method for determining BUCs, rather than a definitive tool. While it provides a systematic and unbiased framework for evaluating and comparing options, it is based on assumptions and simplifications that may overlook some complexities of soil washing procedures. Thus, it should be used as an indicator of promising experimental configurations rather than a final decision-making tool. Subjective factors such as risk, cost, and feasibility should also be considered in the decision-making process. Consequently, the 3PPAA-U should be employed cautiously and critically, alongside other techniques. Future studies may expand this methodology to incorporate a broader range of factors critical to the effectiveness of soil washing operations.

Universidad de Oviedo

SR. PRESIDENTE DE LA COMISIÓN ACADÉMICA DEL PROGRAMA DE DOCTORADO EN INGENIERÍA DE LOS RECURSOS NATURALES

Acknowledgements.

I would like to express my deepest gratitude to all those who have supported me throughout my academic journey. To my friends, colleagues, and professors, you have my most sincere gratitude. However, there are a few individuals who deserve a more special and heartfelt recognition:

First and foremost, I would like to express my sincere gratitude to my supervisor and friend, Associate Professor Carlos Sierra Fernández, of the Department of Mining Technology, Topography, and Structures at the University of León. For his trust, guidance, encouragement, understanding, and motivation throughout the course of this thesis and, hopefully, in the years to come. I owe you a great debt.

Likewise, I extend my gratitude to Dr. Diego Baragaño Coto, Researcher at the Carbon Science and Technology Institute (INCAR-CSIC), for his invaluable collaboration and guidance throughout this thesis.

I would also like to thank all the co-authors of the research papers for their contributions and for the significant role they have played in this project.

Finally, I cannot express enough gratitude to my family, for their help throughout these years in everything I have done, and for their sincere joy in all my accomplishments as if they were their own.

Thanks to all of you, for everything you have done for me and for every moment along the way.

Contribution of the author to the published work.

The candidate declares the authorship of all the chapters of this thesis, presented as a compendium of research articles. Chapter I (Introduction) has been completely compiled by him. Chapters II, III and IV comprise the research articles. The field, laboratory and computing tasks, as well as the redaction of the articles have also been conducted by the student under the supervision of the rest of the authors of each paper. Chemical analyses were subcontracted to the commercial laboratory Actlabs (Canada) or to the Scientific and Technical Services of the University of Oviedo. Chapters V and VI (Results, discussion and conclusions) were also contributed by the candidate.

Abstract.

This PhD thesis presents a compendium of three studies on the development and evolution of the Attributive Analysis (AA) method as a system for evaluating soil decontamination techniques. The AA has significantly evolved from its initial form to a more robust and multidimensional approach, enhancing its accuracy and effectiveness.

Initially, the basic Attributive Analysis (BAA) method focused on maximizing recovery and minimizing yield, providing a fundamental basis for evaluating separation conditions. This approach, combined with the distance-to-target correction factor, identified promising experimental setups for the application of electrostatic separation in soil remediation.

Upon analyzing the BAA, it was observed that the algorithm prioritized minimizing yield over maximizing recovery. While the relationship between the quality index and recovery was linear, throughput exhibited an inverse square relationship. Additionally, the method showed considerable sensitivity to variability in recovery and yield data. To address this, a correction for the inverse of the standard deviation and normalization of parameters were introduced to penalize experimental setups with high data variability. These modifications led to the development of the Penalized Attributive Analysis (PPAA-U) method.

Subsequently, two further modifications were implemented. The first involved introducing a criterion to identify "failed" experiments—those with yield values exceeding recovery values. Such scenarios are of limited interest for soil remediation due to their reduced efficiency compared to setups with higher recovery values. Additionally, it was established that the fraction concentrated in potentially toxic elements (PTEs) should have a recovery value higher than the yield in 50% or more of the target PTEs. This rule was used as a heuristic to distinguish between concentrates and tailings. The second modification incorporated a third parameter into the attributive analysis: the grade of PTEs in the concentrate. This aimed to enhance the precision of the method in identifying optimal concentration conditions, leading to the development of the Penalized Three-Parameter Attributive Analysis (3PPAA-U).

Without the target-distance correction, 3PPAA-U is at least as effective in selecting the best upgrading conditions (BUC) as methods based on other criteria. With the additional correction, it outperforms conventional techniques, potentially improving the performance evaluation of soil washing procedures.

The Attributive Analysis technique has undergone significant development, resulting in continuous improvements in assessing separation procedure efficiency. However, the 3PPAA-U approach remains a heuristic method for determining BUCs, rather than a definitive tool. While it provides a systematic and unbiased framework for evaluating and comparing options, it is based on assumptions and simplifications that may overlook some complexities of soil washing procedures. Thus, it should be used as an indicator of promising experimental configurations rather than a final decision-making tool. Subjective factors such as risk, cost, and feasibility should also be considered in the decision-making process. Consequently, the 3PPAA-U should be employed cautiously and critically, alongside other techniques. Future studies may expand this methodology to incorporate a broader range of factors critical to the effectiveness of soil washing operations.

Resumen.

Esta tesis doctoral presenta un compendio de tres estudios sobre el desarrollo y evolución del método de análisis atributivo como sistema para evaluar técnicas de descontaminación de suelos. El método de análisis atributivo ha experimentado una evolución significativa, pasando de una forma básica a un enfoque más robusto y multidimensional, lo que ha permitido mejorar su precisión y efectividad.

Inicialmente, el método de análisis atributivo básico (BAA) se centró en maximizar la recuperación y minimizar el rendimiento, estableciendo una base fundamental para evaluar las condiciones de separación. Este enfoque, junto con el factor de corrección por distancia al objetivo, identificó configuraciones experimentales prometedoras en la aplicación de la separación electrostática para la descontaminación de suelos.

A partir del análisis del BAA, se observó que el algoritmo priorizaba la minimización del rendimiento sobre la maximización de la recuperación. Mientras que la relación entre el índice de calidad y la recuperación era lineal, la relación con el rendimiento era inversamente cuadrática. Además, el método mostró una notable sensibilidad a la dispersión de los datos de recuperación y rendimiento. En respuesta, se introdujo una corrección basada en el inverso de la desviación estándar y una normalización de los parámetros para penalizar configuraciones experimentales con mayores variaciones. Estas modificaciones dieron lugar al método de análisis atributivo penalizado (PPAA-U).

Posteriormente, se incorporaron dos modificaciones adicionales. La primera consistió en un criterio para identificar experimentos "fallidos", definidos como aquellos con valores de rendimiento superiores a los de recuperación, ya que estos escenarios presentan una baja eficiencia en los procesos de descontaminación de suelos. Además, se estableció que la fracción concentrada en EPTs (elementos potencialmente tóxicos) sería aquella que tuviera un valor de recuperación superior al rendimiento en el 50% o más de los EPTs objetivo. Esta regla heurística permitió discernir el concentrado de las colas. La segunda modificación añadió un tercer parámetro al análisis atributivo: la ley del EPT en el concentrado (λ), con el objetivo de mejorar la precisión del método en la identificación de las condiciones óptimas de concentración. Esto dio lugar al análisis atributivo penalizado de tres parámetros (3PPAA-U).

Sin la corrección objetivo-distancia, el 3PPAA-U es al menos tan eficaz en la selección de las BUC (mejores condiciones de uso) como los métodos basados en otros criterios. Con la corrección adicional, el 3PPAA-U supera a las técnicas convencionales, mejorando así la evaluación de los procedimientos de lavado de suelos.

La técnica del análisis atributivo ha avanzado significativamente a lo largo de la investigación, permitiendo mejoras continuas en la precisión de la evaluación de la eficiencia de los procedimientos de separación. Sin embargo, el enfoque 3PPAA-U sigue siendo un método heurístico y no definitivo para determinar las BUC. Aunque proporciona un enfoque metódico e imparcial para evaluar y contrastar varias opciones, se basa en suposiciones y simplificaciones que pueden pasar por alto algunas complejidades asociadas a los procedimientos de lavado de suelos. Por lo tanto, esta metodología debe emplearse con cautela y como un indicador de configuraciones experimentales prometedoras, complementada con consideraciones subjetivas y cualitativas como el riesgo, el coste y la viabilidad. El 3PPAA-U debe ser utilizado con un enfoque crítico y en combinación con otras técnicas, y su metodología podrá ampliarse en futuros estudios para evaluar una mayor variedad de factores esenciales para la eficacia de las operaciones de lavado de suelos.

Table of Contents

Table of Figures and Tables

Universidad de Oviedo

CHAPTER I: Introduction

1. Background

Many industries in today's economic society have been impacted by the crises we have faced over the past few decades, including the steel, mining, chemical, textile, and port sectors (Vieira et al., 2024). Each of them has accompanying facilities that vary in size and complexity, but they all have one thing in common: when they close for any reason, they typically leave behind polluted land, which is frequently found in metropolitan or peri-urban settings (Chowdhury et al., 2023).

However, obsolescence is another factor that contributes to the creation of such polluted soils in addition to the many economic crises. Three categories apply to this (Riedel, 2010):

- Physical: The facility's state has deteriorated due to neglect, affecting its elements and structure.
- Functional: The facility no longer serves the original purpose for which it was built because of technological advancements.
- Internal: when a facility closes because the cost of the resource being used is reduced, for instance.

The sectors that produce the most polluted land are, in the first place, the industrial sector, followed by the service sector and the oil and gas industry.

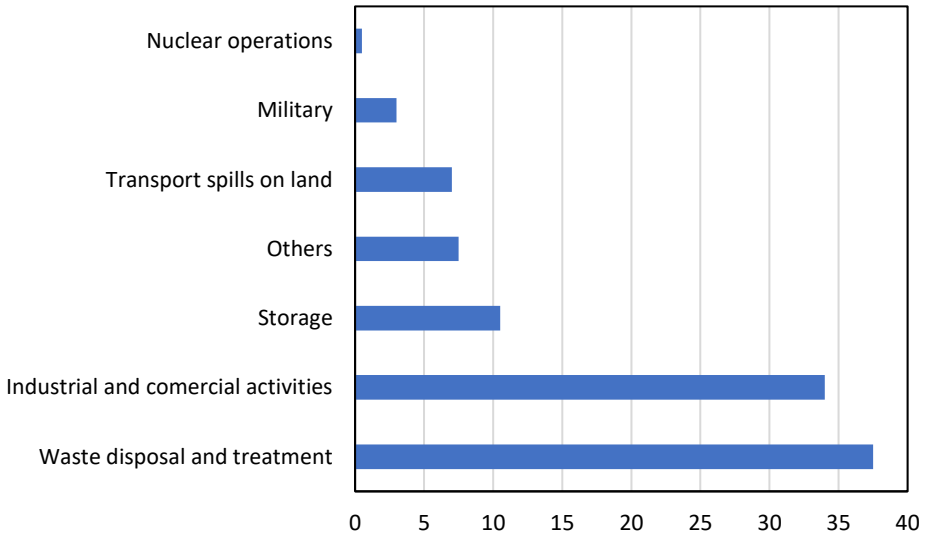

Figure 1.- Key sources of contamination in Europe (EEA, 2014).

Heavy metals, mineral oils, and polycyclic aromatic hydrocarbons are the three most common forms of contamination in the globe (EEA, 2014).

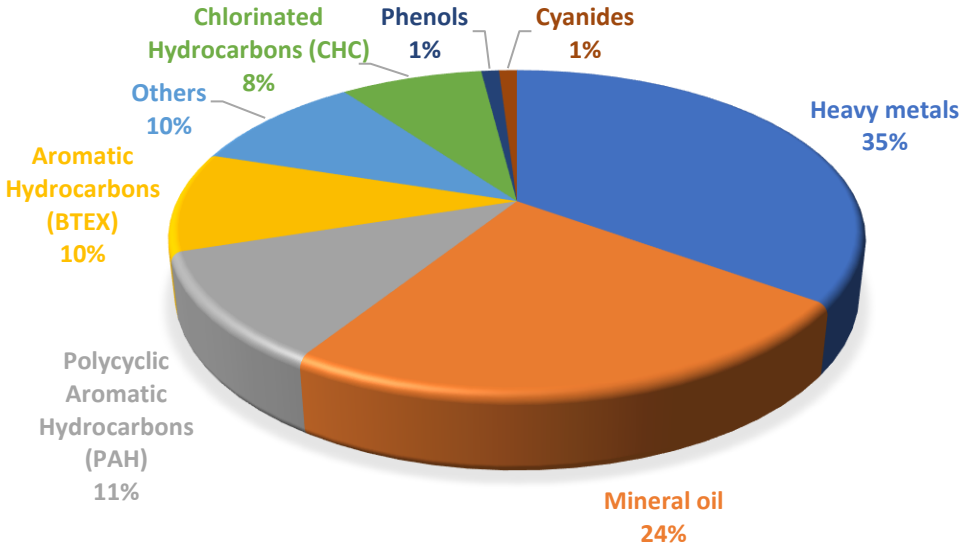

Figure 2.- Overview of pollutants in soil reported in Europe (EEA, 2014).

Europe's and the world's urban planning have experienced a variety of situations. The process of rebuilding cities following World War II came after the industrial revolution, which first produced the explosion of the structures that gave rise to these contaminated regions. Then, in the 1960s, the outskirts and suburbs of the major cities started to come alive, and in the 1970s, as environmental awareness grew, the renovations started and continued for the next twenty years. All of this ultimately resulted in the modern notions of circular economy and sustainable development (Wang et al., 2024).

2. Heavy metals

Industrialization has advanced rapidly during the past century. As a result, there is now a greater demand for the reckless exploitation of the Earth's natural resources, which is aggravating the global problem of environmental pollution (Drenning, 2021). Among these contaminants, there is one group with an enormous prevalence, heavy metals. These pollutants are a class of potentially toxic elements (PTEs) that pose a serious threat to both human health and the environment. They are harmful both physiologically and industrially. Although this kind of soil pollution has existed since antiquity, it only became a significant issue with the industrial revolution and the huge worldwide mining output it produced (Shahid et al., 2015). The global mean yearly discharges of Pb, Ni, Mn, Cu, and Hg are 15,000 tons, 3.4, 5, 15, and 1 million tons, respectively, indicating that the contamination is obviously becoming worse all over the world (Popova et al., 2012).

The most common metals in polluted soils are Pb, Cr, As, Zn, Cd, Cu and Hg, sorted from most prevalent to least prevalent (Vieira et al., 2024). Heavy metals that can be found in polluted soils include nickel (Ni), chromium (Cr), copper (Cu), cobalt (Co), zinc (Zn), manganese (Mn), aluminum (Al), arsenic (As), lead (Pb), cadmium (Cd) and mercury (Hg). These last four substances are among the 20 most dangerous substances reviewed by the Toxicology and Disease Registry (ATSDR, 2012).

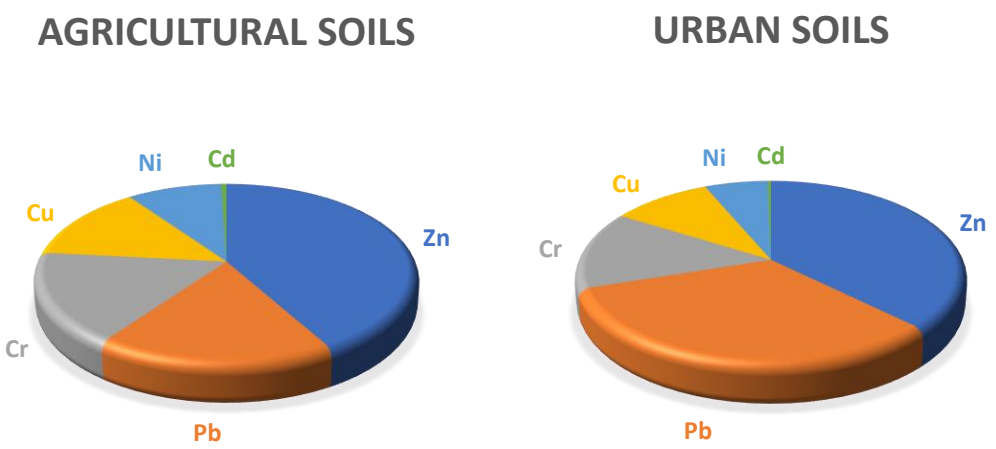

Figure 3.- Most prevalent heavy metals in soils (C. Li et al., 2019).

One of the main issues with heavy metal-polluted soils for human health is that they cannot be used for agriculture because the food grown there would absorb more heavy metals, which can pose a serious health risk (Pierart et al., 2015; Xiong et al., 2016). According to Romero et al. (2024), there are several diseases and hazards associated with them, including cancer, cardiovascular disease, cognitive decline, chronic anemia, and harm to the kidneys, neurological system, brain, skin, and bones.

However, the issues caused by heavy metals are not limited to agriculture; their overabundance can also lead to the degradation of the soil ecosystem and the environmental issues that follow (Panagos et al., 2024a).

Many nations are tackling these issues, but their approaches, technologies, and levels of knowledge vary widely (Baldantoni et al., 2016; Ko et al., 2015). It is estimated that there are over 10 million polluted sites in the world, with heavy metals accounting for half of them (He et al., 2015). Because industrial operations are more common in developed nations, most of these sites are located there (Foucault et al., 2013; Goix et al., 2014). The U.S. Environmental Protection Agency (EPA) has designated over 50,000 locations

contaminated with heavy metals as priorities for immediate decontamination. There are 600,000 hectares of heavy metal contamination in the U.S. alone (Vieira et al., 2024). Nevertheless, it is evident that increased focus is being directed toward this issue, as evidenced by the recent initiation of various European programs addressing it (Panagos et al., 2024b).

The state of California permits concentrations of heavy metals no higher than those found in 75% of the orchards in the San Francisco area in the United States (Gorospe, 2012). Several agricultural areas in Europe are also known to be contaminated, most likely as a result of their proximity to mining areas (Foucault et al., 2013; Goix et al., 2014).

According to data provided by the Chinese Ministry of Land Resources and Ministry of Environmental Protection (Bulletin on National Soil Pollution Survey), the situation is more dire in China, where 4 million hectares of arable land (2.9% of the total) are classified as moderately or seriously polluted. According to reports, heavy metal contamination affects 25% of China's agriculture area, which results in a 10 million tons annual loss in agricultural productivity (Shi et al., 2023). Arsenic contamination in particular is a serious issue, with soils containing up to 41 times the permitted quantity of this element in China (Yu et al., 2024; Wei et al., 2009).

Europe may contain more than 3 million polluted sites, according to the European Environment Agency (EEA). Of the 250,000 contaminated sites in EEA member nations, 80,000 have been cleaned up, while the remaining 500,000 are extremely contaminated and require urgent cleanup. Furthermore, according to European Commission data, the number of polluted sites recorded in 2016 exceeded 650,000 (Vieira et al., 2024).

However, this issue also arises in underdeveloped or less developed nations. Heavy metal pollution of soils in Pakistan, India, Bangladesh, and other countries has resulted from the use of untreated wastewater (both industrial and urban) for crop irrigation (Khan et al., 2008).

2.1. Definition and properties

The definition of the term "heavy metals" has been the subject of continuous debate. Due to either their high atomic weight or their high density (above 5 g/cm^3), they are classified as heavy metals. Other, more inclusive definitions of "heavy metals" demand an atomic mass greater than 23 or an atomic number greater than 20; these definitions are extremely

erroneous and perplexing. Considering both different definitions, the using of atomic mass criterion, the maximum number of elements designated as "heavy metals" rockets high to 99 out of the total 118 (Duffus, 2002).

The term "heavy metal" is now used to refer to metallic chemical elements and metalloids that are harmful to both humans and the environment. Toxic substances include several metalloids and lighter metals including selenium, arsenic, and aluminium. While some heavy metals, like the element gold, are normally not hazardous, they have been referred to be heavy metals (Gautam et al., 2016; Tchounwou et al., 2012).

On the other hand, several of them, including lead, chromium, thallium, arsenic, cadmium, and others, are known to represent the "dark side of chemistry" since they are hazardous even at low concentrations (Duruibe et al., 2007).

Metalloids frequently form covalent bonds, which gives them toxicological characteristics. The ability to covalently bond with organic groups is one of this property's two most significant effects. Since they bind to non-metallic components of biological macromolecules, they produce lipophilic ions and compounds that can have harmful effects (Ballabio et al., 2021; Drenning et al., 2021). The distribution of metalloids in the biosphere and their hazardous response are different from those of the same element's simple ionic forms because of being lipophilic. Tributyltin oxide and hazardous methylated versions of arsenic are examples of lyophilic chemicals. The sulfhydryl groups of the protein can bind lead and mercury as examples of non-metallic elements. There are four ways that heavy metals can get into a person: by contaminated food, contaminated air, contaminated water, and through skin contact from industrial, residential, pharmaceutical, and agricultural regions (Walker et al., 2012).

Metals are not biodegradable and cannot be broken down. By enclosing the active component in a protein or storing them in intracellular granules in an insoluble form to be expelled in the organism's feces or for long-term storage, organisms can detoxify metal ions. The heavy metals bioaccumulate in our systems after being ingested or absorbed into them. As a result, they are considered dangerous. Biological and physiological issues are brought on by this bioaccumulation produced by an extensively used in agriculture, industry, medicine, and other fields, with the result that they have gotten into our soils, rivers, and atmosphere (Panagos et al., 2021; Tchounwou et al., 2012).

2.2. Features of soil contamination by heavy metals

The main differential characteristics of heavy metal soil contamination are the following (Li et al., 2019):

- Broad dissemination: The global prevalence of heavy metal contamination has increased along with the growth of the economy and society. It poses practically a major threat to all nations. Two of the top 10 environmental incidents in history have involved heavy metal contamination.
- Strong latency: Because heavy metal contamination has no colour and no smell, it is hard to detect. It doesn't immediately cause any overt environmental harm. Nevertheless, heavy metals in the soil have the potential to become activated and seriously harm the ecosystem when they surpass the environmental tolerance or when the environment changes. Thus, chemical time bombs (CTBs) are typically the cause of heavy metal pollution.
- Irreversibility and difficulty of remediation: If there is pollution in the air or water, it can be resolved by dilution and self-purification when the pollution sources are turned off. To remove heavy metal contamination and enhance soil quality, self-purification or dilution methods present challenges. It may require a century or more to rehabilitate certain heavy metal-polluted soils. As a result, the process of remediating heavy metal pollution is relatively lengthy and requires a significant financial investment.
- Complex heavy metal contamination: One heavy metal used to be the primary cause of soil pollution. Nonetheless, several heavy metals have been linked to an increase in instances in recent years. The combined effects of multiple heavy metals will always intensify the effects of each heavy metal alone.

2.3. Environmental impact

However, problems caused by heavy metals not only affect agriculture, but their excessive presence can also lead to degradation of soil ecosystems and related environmental problems.

2.3.1. Effects through soils

Heavy metals in soils are a severe problem because they can enter food chains and disrupt the entire ecosystem. Even while organic pollutants have a potential for biodegradation,

the presence of heavy metals in the environment slows down their biodegradation rate, which doubles the amount of environmental pollution caused by both organic pollutants and heavy metals. Risks from heavy metals to people, animals, plants, and ecosystems as a whole come in many different forms. These include direct consumption, plant uptake, food chains, intake of tainted water, and changes to the pH, porosity, colour, and natural chemistry of the soil, all of which have an effect on the soil's quality (Musilova et al., 2016).

Worldwide, the introduction of a pollutant, particularly heavy metals, into a soil ecosystem can lead to a variety of customary and specific changes in the diversity and composition of the microbial community as well as in the population density and typical activity of the soil microbiome (Ashraf & Ali, 2007; Dulya et al., 2024). For instance, Cd is a heavy metal that can be rather harmful to living things (Šabanović et al., 2018). In spite of this, exposure to metals might enhance the populations of microorganisms that are resistant to them (Xie et al., 2014).

2.3.2. Effects through water

Although only small amounts of heavy metals can be detected in water sources, they are nevertheless extremely poisonous and represent major health risks to both people and other organisms. This is due to the fact that a metal's level of toxicity varies on a variety of variables, including the species to which it is exposed, its nature, its biological function, and the length of time the organisms are exposed to the metal. Food chains serve as symbols for the interactions between organisms. As a result, all species are impacted by heavy metal poisoning of water. Because heavy metal concentrations rise in the food chain, humans, an example of an organism that feeds at the top, are more vulnerable to major health issues (Lee et al., 2002).

2.3.3. Effects on plants

According to Chibuike & Obiora (2014), plants growing in heavy metal-polluted soils show decreased growth, efficiency, and productivity. The main problem for plants in heavy metal-containing media is that harmful ions build up and important cations like iron, potassium, and manganese are less concentrated (Howe et al., 2004).

For instance, harmful heavy metals that are not good for plants, such as Cr, Hg, U, Zn, Ag, Se, As, Ni, and Au, can slow down the growth of plants by reducing photosynthesis,

the uptake of minerals by the plants, and the activity of essential enzymes (Nematian & Kazemeini, 2013). Furthermore, by interfering with physiological and biochemical processes that support plant growth and development, heavy metals like Pb poison plants (Pourrut et al., 2011; Sharma & Dubey, 2005).

The following are the principal problems on plants caused by heavy metal contamination (Naveed et al., 2023):

- Photosynthesis disruption.
- Delays in biochemical processes.
- A decrease in crop yield.
- Slowed growth.
- pH soils changes.
- Mass reduction of dry seeds.
- Interferes with cell division.
- Reduces the height, flower weight, and fruit and tiller panicle weight.

The effects of each heavy metal changes and has its own toxicity, effects and limits:

- Lead: The majority of the Pb that plants absorb from the soil is deposited in their roots. Evidence suggests that Pb is also absorbed by leaves, with a likelihood that it may spread to other regions of the plant (Emamverdian et al., 2015). Pb poisons plants in a variety of ways, which includes preventing the germination of some type of seeds by lowering the germination rate (Li et al., 2018), impairing the early seedling growth of different plants and hindering stem and root elongation (Ahmad et al., 2011; Begum et al., 2011; Fahad et al., 2019; Sędzik et al., 2019; Zhang et al., 2018).
- Cadmium: High levels of Cd in the soil cause damage to plants, as shown in the form of stunted development, chlorosis, scorching of the root tips, and eventual death (Gao et al., 2022).
- Chromium: The morphological, biochemical, metabolic, and physiological processes of plants can be disturbed by high concentrations of Cr^{3+} (Kapoor et al., 2020). Cr reduces seed dry mass and prevents the premature growth of leaves and stem to some plants (Ahmad et al., 2012; Akinci & Akinci, 2010; Anjum et al., 2010) and inhibits cell division, which lowers plant height (Ma et al., 2016; Zhu et al., 2025).

- Mercury: Surplus levels of Hg in *Oryza sativa* (rice) inhibit growth, slow the development of tillers and panicles, and lower yield (Du et al., 2005).
- Manganese: The way that different plants react to Mn toxicity varies. Some plants shorten their roots and shoots, like Vicia faba, while others reduce their chlorophyll content, like *Mentha spicata* (Arya & Roy, 2011), *Pisum sativum*, and *Lycopersicon esculentum* (Doncheva et al., 2005).

2.3.4. Effect on animals

Studies on the bioaccumulation of heavy metals in wildlife have generally found a relationship between the target organ and the studied species. For instance, Bilandžić et al. (2012) examined HM bioaccumulation in wild carnivores and found that the Eurasian badger had the greatest Cd levels in its kidney and liver. Cu content in the liver reduced in the studied species, which followed the following pattern: Brown bear > Pine marten > Eurasian lynx > Gray wolf > Eurasian badger. The highest quantities were found in the muscles (As, Cu, Pb), liver (As, Cd, Cu, Pb), and kidneys (Cd, Pb) of the Eurasian badger and the kidneys (As, Cu, Hg) of the Pine marten. However, there are conflicting findings about how exposure to HM affects people's health in the scientific literature. Levengood & Heske (2008) demonstrated that, when compared to those who had not been exposed to Cd and Zn pollution, white-footed mice that dwell in such an environment had the highest liver Cd, Cu, and Zn concentrations. Despite the detected bioaccumulation levels, the health of the individuals (as measured by reproductive and fitness indicators) remained unchanged.

2.3.5. Effect on ecosystems

Ecosystems are dynamic, open systems that emit matter and energy while maintaining a stable equilibrium between their biotic and abiotic components (Williams, 2002). The presence of heavy metals may disrupt the stability of an ecosystem (Gall et al., 2015). The major factors that determine how well heavy metals are incorporated into an ecosystem are their bioavailability and, later, how well they fit into the trophic chain, reaching their highest concentrations in the highest levels of the chain, a process called "biomagnification" (Hossain et al., 2012; Kim et al., 2015). Heavy metals may or may not have an impact on ecosystems in this scenario, depending on its intensity and duration, or if one of the processes that preserve the integrity of the ecosystem (such as nutrient

cycles or energy outflow) is hampered by the loss of biodiversity (Vijver & Peijnenburg, 2011).

Few ecotoxicological investigations have examined the biomagnification of heavy metals along the trophic chain and its consequences on ecosystem integrity, focusing instead on the measurement of pollutant concentrations in soils, their bioavailability, and bioaccumulation (Gall et al., 2015). Metal cations adhere to negatively charged soil particles like clay and organic matter, and when they separate from these particles, they enter the soluble soil fraction, where they are bioavailable and have the potential to bioaccumulate in various organisms. This is the first step in the incorporation of heavy metals into ecosystems (Kim et al., 2015).

To thrive and survive, microorganisms, plants, and invertebrate species have systems for incorporating trace metals (such Cu, Ni, Fe, Co, Mn, and Mg), yet they can be hazardous in greater doses. Additionally, these same mechanisms make it easier for non-trace metals (As, Cd, Hg, and Pb), which are extremely hazardous at low concentrations, to enter organisms (Gadd, 2010).

Microorganisms are essential components of soils because they help plants, which make up the first trophic level in terrestrial ecosystems, recycle nutrients and inorganic elements such minerals and trace metals (Harris, 2009). However, heavy metal pollution may alter the structure and biodiversity of microorganism communities, which has an impact on the soil processes in which they take part (Boshoff et al., 2014; Giller et al., 2009). For instance, changes in microbe metabolic activities and development have been shown (Boshoff et al., 2014; Microbiology & Abdousalam, 2010). These modifications have an impact on the breakdown of organic matter, which decreases nutrient accumulation and availability for plants and jeopardizes matter and energy fluxes at the base of the trophic chains (Boshoff et al., 2014).

On the other hand, soil invertebrates, such as crustaceans, snails, and earthworms that live in leaf litter and consume organic materials with high heavy metal concentrations, can bioaccumulate them due to their preferred eating habits (Rogival et al., 2007).

2.3.6. Human Health problems

Soils polluted by heavy metals pose several problems for human health, including the fact that they cannot be used for agriculture because food produced on these soils will absorb

large amounts of this components, which can pose a major health risk (Pierart et al., 2015; Xiong et al., 2016). The risks and diseases they can give rise to include conditions such as cardiovascular disease, cancer, cognitive decline, chronic anemia and damage to the kidneys, nervous system, brain, skin and bones (Järup, 2003).

Heavy metals have been shown to have an impact on cellular organelles and parts of the cell, including the mitochondria, nucleus, lysosomes, cell membrane, and enzymes. It has been discovered that metal ions interact with DNA and nuclear proteins, resulting to DNA damage and ultimately modulating cell cycle, inducing apoptosis, or promoting the development of cancer (Tchounwou et al., 2012).

Over the past few decades, the hazards to human health have increased due to the excessive entry of heavy metals into plants and soil; heavy metals have turned into an increasingly harmful kind of environmental pollution (Gratão et al., 2005). The potential threat to public health thus arises from accumulation along the food chain (Jiwan & Kalamdhad, 2011).

Heavy metals are the primary cause of several life-threatening retrogressive disorders that impact humans, including cancers, Parkinson's disease, atherosclerosis, and Alzheimer's disease (Muszyńska & Hanus-Fajerska, 2015). Additionally, eating foods contaminated with heavy metals may cause humans to consume significantly fewer essential nutrients, which can lower immune system effectiveness (Harmanescu et al., 2011; Jan et al., 2015), decelerate the growth of foetuses in the womb (Khan et al., 2008), cause dietary-related illnesses, and increase the risk of upper gastrointestinal tumors (Türkdoğan et al., 2003).

Several cellular organelles and parts of biological systems, including cell membranes, mitochondria, lysosomes, endoplasmic reticulum, nuclei, and several enzymes involved in metabolism, detoxification, and damage repair, have been documented to be affected by heavy metals (Wang et al., 2001). It has been discovered that metal ions interact with nuclear proteins and DNA in cells, resulting in DNA damage and conformational changes that may influence cell-cycle progression, carcinogenesis, or apoptosis (Beyersmann et al., 2008).

They are all known to cause numerous organ harm even at low exposure levels because they are all systemic toxins. These metals are also categorized as "known" or "probable" human carcinogens by the US Environmental Protection Agency (US EPA) and the International Agency for Research on Cancer (IARC), respectively, based on

epidemiological and experimental studies demonstrating an association between exposure and the incidence of cancer in humans and animals. Many molecular components of heavy metal-induced toxicity and carcinogenicity are involved, some of which are not well characterized or understood. However, it is recognized that each metal has distinct characteristics and physicochemical traits that give rise to its own toxicological modes of action (Tchounwou et al., 2012).

The same element can serve as both a poison and a medicine, depending on how concentrated it is in the body; the dose determines the physiological consequences. Because of this, certain innocuous substances at higher concentrations can have very toxic effects, whereas highly toxic substances at lower concentrations can have nongenetic effects, that is, they can have a therapeutic effect on the body (Skalny & Skalny, 2014).

Every element has a range of appropriate concentrations needed to carry out crucial biological tasks inside the body; therefore, when an enzyme's actions are compromised, either an excessive build-up or a deficiency result in major disruptions within the body. Most of the elements that make up the human body are only found in their coordination compounds. The methods in which these metals and their ligands act as activators or inhibitors toward distinct enzymes performing different jobs in the body determine their significant significance in the treatment of various diseases and the development of the body (Kumar et al., 2021).

The effects of heavy metals in the human health depends on the specific pollutant, the role it plays in the body:

- Iron: The body's excessive iron build-up causes a rise in intracellular ferritin levels. Overconsumption of iron also leads to hepatic and pancreatic dysfunction, which results in type II diabetes mellitus, as well as impaired cardiovascular system functioning, or cardiomyopathy. Specifically, iron deposition in the endocardium or epicardium and cardiomyocytes is the cause of hyperferremic cardiomyopathy. Diastolic and systolic dysfunction are associated with this hyperferremic cardiomyopathy, and if they persist long enough, they may cause a heart attack (Hider & Kong, 2013).
- Zinc: The human body is highly poisonous when zinc levels are excessive. Although there have been many studies on zinc shortage, the harmful consequences of zinc have not been well investigated. Workers in the zinc-

smelting sector have been shown to exhibit myeloneuropathy. Sensation abnormalities, tactile hallucinations, tactile allodynia, and paraesthesia are brought on by an overabundance of zinc in the human body. Additionally, it has been noted that symptoms of zinc excess may also indicate a copper shortage (Lanska & Remler, 2014).

- Copper: The build-up of free copper in the body is the cause of a great deal of illnesses, including prion disease, Huntington chorea, Alzheimer's disease, and lateral amyotrophic sclerosis. Even though these diseases have intricate pathogenetic pathways, an excess of copper is extremely common in all stages. Increased amyloid-β protein plaque build-up in intracellular space is thought to be the etiology of Alzheimer's disease because it causes synaptic dysfunction. Degenerative alterations in dopaminergic neurons and the substantia nigra are noted in Parkinson disease. Localized copper build-up in brain tissue results in decreased blood ceruloplasmin and copper concentrations. Furthermore, it has been noted that the age of Parkinson disease onset is negatively correlated with blood ceruloplasmin levels. High copper levels are typically seen in patients with chronic cholelithiasis (Bharucha et al., 2008; Jomova et al., 2010; Squitti, 2012; Squitti et al., 2008).
- Manganese: When the body contains too much manganese, it can have harmful consequences, particularly on the central nervous system and lead to neurological disorders. A high manganese diet disrupts the hypothalamus-hypophysial system, which results in elevated prolactin synthesis and decreased dopamine secretion in dopaminergic brain areas. Additionally, manganese overload promotes the synthesis of melanin by mediating the oxidation of DOPA from DOPA. Skin depigmentation may be a sign of Mn dyshomeostasis, which controls the metabolism of melanin (Shin et al., 2015).
- Selenium: Along with its beneficial effects, an overabundance of selenium in the body can have some negative impacts on health. Numerous investigations have demonstrated a connection between selenium overdose and type II diabetes and obesity. Metabolic syndrome and liver steatosis are linked to elevated level of FGF-21 and SEPP1 fetuin-A. The synthesis of these molecules results in increased levels of low-density lipoprotein, decreased levels of high-density lipoprotein, glucose utilization (GLUT-1), and impaired insulin resistance (Yoo & Choi, 2015).

- Iodine: Overuse of iodine by the thyroid results in increased production of proinflammatory cytokines, oxidative stress, damage to the thyrocytes, generation of free radicals, production of anti-Tg antibodies, and immune cell infiltration of the thyroid tissue (Burek & Rose, 2008; Dijkstra et al., 2007).
- Cobalt: Overloading the body with cobalt prevents DNA from being repaired, which damages it and triggers apoptosis. In addition, it raises the risk of lung cancer and causes allergic rhinitis and lung illness. Additionally, polycythemia, cardiomyopathy, and hypothyroidism can all develop reversibly when there is an excess of cobalt (Catalani et al., 2012; Simonsen et al., 2012).

2.3.7. Prevalence

Many countries face heavy metal prevalence problems, but they have significant differences in perceptions, strategies, and technologies to address them (Baldantoni et al., 2016; Ko et al., 2015). It is estimated that more than 10 million sites are contaminated worldwide, half of which are contaminated with heavy metals (He et al., 2015). Of these sites, the majority are in developed countries due to the higher prevalence of industrial processes (Foucault et al., 2013; Goix et al., 2014). In the United States alone, 600,000 hectares are contaminated with heavy metals, and the United States Environmental Protection Agency (EPA) has designated more than 50,000 heavy metal contaminated areas a priority for urgent decontamination (Glass, 2001).

In the United States, it is estimated that 75% of orchards in the San Francisco area have heavy metal concentrations above California's (Gorospe, 2012) and some agricultural areas in Europe are known to be heavily contaminated, possibly due to their proximity to mining areas (Foucault et al., 2013; Goix et al., 2014).

In China, the situation is more serious, with about 4 million hectares of arable land (2.9% of the total) being moderately or severely polluted, according to information released by the Ministry of Land Resources and the Ministry of Environmental Protection of China (National Soil Contamination Survey Bulletin). It has also been reported that 25% of total arable land in China is contaminated with heavy metals, resulting in a loss of 10 million tons of agricultural output annually (Hongbo et al., 2011). The issue of arsenic is of particular concern, with soils contaminated up to 41 times the allowable concentration in China for this element (Liao et al., 2005; Liu et al., 2005; WEI et al., 2009).

As it was already stated, according to the European Environment Agency (EEA), there are more than 3 million potentially contaminated sites in Europe, and the EEA estimates that contaminated sites could increase by 50% by 2025 (EEA, 2009).

But in underdeveloped or developing countries, this problem also exists. The use of untreated wastewater (both industrial and municipal) for crop irrigation has caused heavy metal contamination of soil in Pakistan, India, Bangladesh, etc. (Khan et al., 2015).

2.4. Sources of heavy metal pollution

Although heavy metals are naturally present in the crust of the earth, human activity has enriched certain elements to poisonous and hazardous levels in some locations. But these riches may also be the result of natural processes. Heavy metals are mostly mobilized by human action during their physical (extraction, smelting) or chemical (reductive) release from ores and the following processing for various purposes, in addition to the leaching and mitigation of heavy metals by erosion and weathering. The use of heavy metals in (agro)industrial, home, automotive, medical, electrical, and other technological applications is another mechanism that releases them into the environment. As a result, they are widely distributed in both aquatic and terrestrial settings (Tchounwou et al., 2012).

2.4.1. Natural sources

Numerous investigations have identified certain heavy metal natural sources. Natural emissions of heavy metals take place under various and specific environmental circumstances. Volcanic eruptions, sea-salt sprays, forest fires, rock weathering, biogenic sources, and wind-borne soil particles are a few examples of these emissions. Metals may be released from their endemic spheres and end up in other environmental compartments because of natural weathering processes. Hydroxides, oxides, sulphides, sulphates, phosphates, silicates, and organic compounds are all forms of heavy metals (Herawati et al., 2000).

Due to the underlying parent rock's weathering, certain metals may naturally arise in soils. Because of this, there are numerous regions in the world where heavy metal contamination of soil happens naturally and has only one source: the local geology. High quantities of heavy metals will be found in soils that were produced on rocks that contained such minerals (Pourrut et al., 2011).

2.4.2. Artificial sources

Heavy metal use has dramatically increased, which has led to an impending rise in metallic substances in both the terrestrial environment and the aquatic environment (Gautam et al., 2016). Among the existing sources of heavy metal pollution from human activities, we can highlight:

2.4.2.1. Fertilizers

Plants require both important micronutrients and macronutrients (N, P, K, S, Ca, and Mg) in order to grow and complete their life cycle. Some soils lack the heavy metals (Co, Cu, Fe, Mn, Mo, Ni, and Zn) necessary for good plant growth (Lasat, 1999). These can be added to the soil or sprayed on the leaves of plants to help them grow healthily. In intensive farming systems, significant amounts of fertilizers are routinely put to the soil in order to supply enough N, P, and K for crop growth. Heavy metal impurities, such as Cd and Pb, are present in trace amounts in the compounds used to supply these elements. These impurities have the potential to considerably increase the quantity of heavy metals in the soil following continuous fertilizer application (Mossel et al., 1995).

2.4.2.2. Pesticides

For many years, lead arsenate was utilized in fruit orchards as a parasite bug pest controller. In New Zealand and Australia, arsenic-containing compounds were also widely used to suppress cattle ticks and pests in banana plantations. Timbers were preserved using formulations of Cu, Cr, and As (CCA). Such contamination may give rise to issues, especially in the event that the sites are used for uses other than agriculture. These materials have been used more locally, confined to certain locations or crops, than fertilizers (McLaughlin et al., 2000).

2.4.2.3. Biosolids and Manures

Heavy metals can end up in the soil as a result of applying a lot of biosolids (such composts, livestock manures, and municipal sewage sludge) to land (Basta et al., 2005). Manures from chickens, cattle, and pigs are examples of animal wastes that are frequently added to crops and grasslands in the form of solids or slurries (Sumner, 2000). While most manures are considered excellent fertilizers, the pig and poultry industries also face the risk of metal contamination of the soil due to the addition of Cu and Zn to diets as growth promoters and the As found in chicken health products (Sumner, 2000).

2.4.2.4. Wastewater

Waste water is reportedly used to irrigate 20 million hectares of agricultural land globally. Studies conducted in a number of Asian and African cities indicate that half of the vegetables supplied to urban areas come from agriculture based on wastewater irrigation (Bjuhr, 2007). The main concern of farmers is increasing their yields and income; they are typically unconcerned about environmental advantages or hazards. Even while wastewater effluents typically have relatively modest metal concentrations, long-term irrigation of such land can eventually lead to soil deposition of heavy metals.

2.4.2.5. Metal Mining and Milling Processes

Numerous nations have been left with the legacy of widespread metal contamination in their soils due to the mining and milling of metal ores in conjunction with industry. Tailings are directly dumped into natural depressions during mining, including wetlands on the site, which causes higher concentrations (DeVolder et al., 2003). Soil contamination resulting from extensive mining and smelting of lead and zinc ore has put human and ecological health at risk. Numerous restoration techniques employed for these sites are time-consuming, costly, and might not be able to increase soil productivity. Human exposure to soil heavy metals is correlated with their bioavailability.

2.4.2.6. Industrial Wastes

Other materials, which vary greatly in composition, are produced by a wide range of sectors, including textile, tanning, petrochemicals from unintentional oil spills or the use of petroleum-based products, insecticides, and pharmaceutical facilities. Few of them are advantageous to forestry or agriculture, even though some are disposed of on land. Furthermore, a lot of them are rarely, if ever, applied to land and may be dangerous due to the presence of harmful organic compounds or heavy metals (Zn, Pb, and Cr). Others have no soil conditioning qualities or very little plant nutrition (Sumner, 2000).

3. Soil washing in heavy metal contamination

Due to its capacity to permanently remove these substances from soil, a variety of procedures commonly utilized in heavy metal decontamination are collectively referred to as "soil washing" (Dermont et al., 2008a). Physical separation, chemical extraction, or a mix of the two forms their basic foundation. The first involves separating soil particles that contain metals, which concentrates pollutants into a smaller fraction of soil. By utilizing the physical variations between the two assemblies (size, density, hydrophobic characteristics, magnetism, etc.), this is accomplished. quite comparable to the mining industry's mineral processing.

Chemical extraction, on the other hand, is based on the desorption and dissolution of metals present in the soil by chemical reagents such as acids or complexing agents, which is very close to the hydrometallurgical process. Figure 4 shows the flowcharts for each type of washing very schematically.

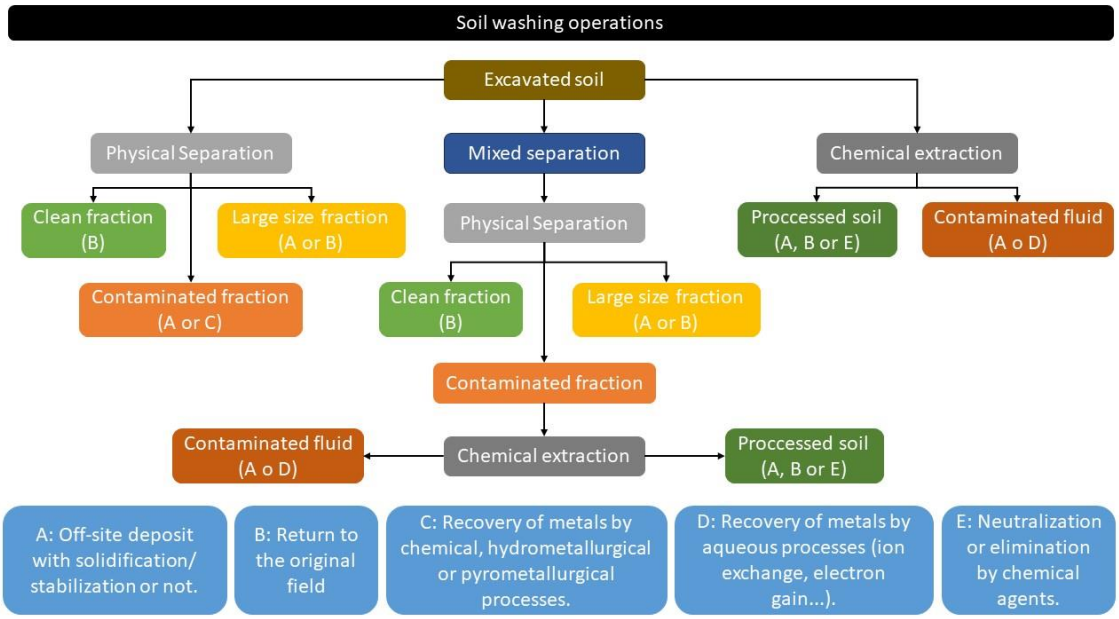

Figure 4.- Diagram of typical options used in soil washing processes. Adapted from (Dermont et al., 2008a).

3.1. Physical separation

As mentioned above, the physical separation methods used to remove contaminants from the soil are very similar to those used in mineral processing in the mining industry. There are a large number of parameters that affect the efficiency of physical separation, among which we can highlight the particle size distribution, shape, clay content, moisture

content, heterogeneity, etc. of the soil matrix, density difference between soil matrix and metal contamination, magnetic field properties, etc. (Dermont et al., 2008a).

The most important factors to consider before starting a soil physical separation project are the degree of removal, the percentage of fine particles, and the volume of soil to be treated (Sierra et al., 2013). The degree of release refers to, over a particular period, the percentage of free particles relative to the total number of fixed and free particles (Wills & Napier-Munn, 2006). The shape, morphology, and mineralogical relationship of the metal contamination particles determine the degree of liberation (Dermont et al., 2008b).

The percentage of fine particles is an important factor because many physical separation processes are governed by particle size classification, which can greatly affect their performance or even their feasibility. Therefore, if the soil is rich in silt or clay and therefore contaminants are more likely to be found in the form of fine particles, chemical extraction should be used (Dermont et al., 2008a; Sierra et al., 2013).

Physical separation methods offer several advantages (Dermont et al., 2008a):

- These techniques can handle metallic and organic pollutants in the same system.
- In comparison to other approaches, the volume of solids containing contaminants is greatly decreased, whether the method is landfill or metal recovery.
- It will be less expensive to reclaim the treated land. - Metal can be recycled after extraction.
- Large-scale processing facilities exist that enable on-site processing.
- All matter separation technologies have a solid track record in the mining sector and, as a result, typically have low operating costs.

However, they also have some disadvantages (Dermont et al., 2008a):

- To set up these operations, substantial equipment and space are needed.
- For on-site pollution treatment, the amount of soil that needs to be treated must be significant—more than 5000 tons—in order to be economically feasible.
- Washing the water used in the operations and the evacuation of leftovers in places outside of polluted soil may be necessary, which would dramatically raise operational expenses.

3.1.1. Soil characterization for selecting the optimal physical soil washing technic

A detailed characterization process of the site, soil, and contaminant is necessary for the successful execution of a physical separation cleanup. The following factors are crucial in this process of characterization (Williford & Mark Bricka, 2000):

- Physical parameters: the two most important factors are the particles size distribution, to asses if there is need for a pre-treatment to reduce the particles sizes or if the soil is too thin for a soil washing process (< 0.063 mm), and the moisture content, to make and adequate pre-treatment and to ensure a proper transfer if needed.
- Chemical parameters: as the organics, concentration, volatility and partition coefficient. To identify the pollutants, evaluate the effectiveness of their separation and washing, the interaction of hydrophobic molecules, the compatibility of the washing fluid, and the changes in the washing fluid with the contaminants; for a steady supply, pre-blending can be necessary; determine contaminant partitioning by using the jar methodology. Other chemical parameters as pH and buffering capacity are also important because may have an impact on the need for pre-treatment, equipment compatibility, building materials, and wash fluid compatibility.
- Metals: Concentration and species of components (particular jar test) will affect metal mobility, posttreatment, and compatibility with washing fluid.
- Humics acid: The amount of organic matter in the soil will influence the way pollutants adsorb on vital areas such as wetlands and marine environments.

The following situations make treatment challenging or impossible (Dermont et al., 2008b):

- The metal contaminants are firmly bound to soil particles.
- There is little to no difference in the density or surface characteristics of metal-bearing particles and the soil matrix
- There is a high degree of variability in the chemical forms of the metals.
- The metals are present in all fractions of the polluted soil's particle size
- The soil contains an excessive amount of silt or clay (more than 30%–50%)
- The soil has a high humics content.
- The soil contains highly viscous organic compounds.

3.1.1.1. Hydrodynamic classification

Hydrodynamic classification, also referred to as "hydroclassification," is the process of separating particles into water flow by centrifugal force (hydrocyclone) or according to the velocity at which they descend through water flow (sedimentation, elutriation, and fluidization). Particle size-based separation is the primary objective using variations in the particle settling velocity (Drzymała & Swatek, 2007). The main principle of this technic is the addition of water to the feed pulp, which is introduced in an opposite direction to the settling particles. Typically, they are made up of several sorting units where particles are sorted out and a vertical water circulation rises through each one (Wills & Finch, 2015). Units arranged in series improve overall recoveries, whereas units arranged in parallel enable smaller, more effective units to manage large flows (Williford & Bricka, 2000). They can be conducted in media that is fixed, in media that is moving sideways, vertically, horizontally, or in the form of a pulsing or spiral stream (Drzymała & Swatek, 2007).

The term "underflow" refers to the hydraulic separation product that contains particles that settle quickly, and "overflow" refers to the second product that contains particles that settle more slowly. In addition to removing extremely fine particles from the feed and separating heavier and larger particles from lighter and smaller ones, hydraulic separators can also be used to divide the feed into narrow size fractions, limit the lower and upper range of particle sizes due to applied technology requirements, and control size reduction during grinding (Drzymała & Swatek, 2007).

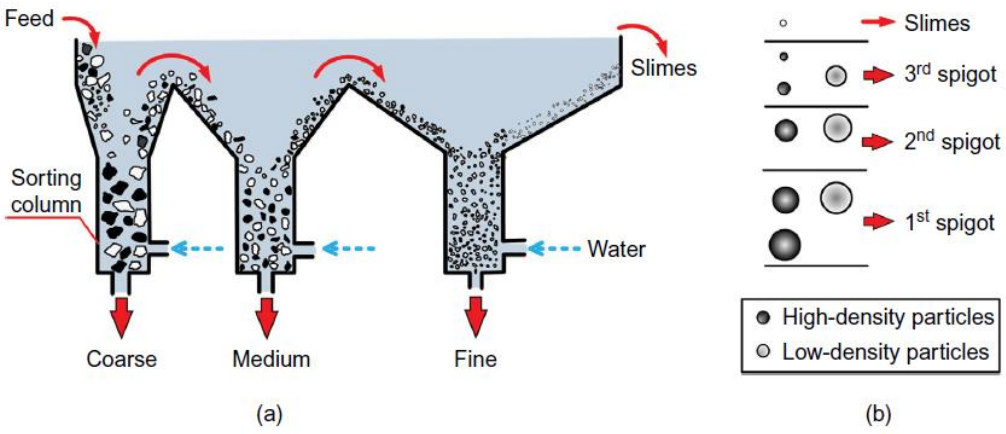

Figure 5.- (a) Principle of hydraulic classifier, and (b) spigot products (Wills & Finch, 2015).

In order to produce a product sequence through the different units, with the bigger and denser particles in the first column and the finer in the later ones, the rising currents are graded from higher to lower velocity. Every subsequent vessel is larger than the one before it to handle all the water from previous phases and to gradually lower the surface velocity of the fluid passing from one vessel to the next. The classifier can provide a concentrating effect because of the high ratio of sizes of evenly falling particles, and the first unit product is often the one with the highest grade, even being sufficiently rich to be categorized as a concentrate (Wills & Finch, 2015).

The hydrodynamic classifiers can be differentiated as follows (Drzymała & Swatek, 2007):

- Sedimentation: the particles descend vertically or almost vertically in water after being fed from the upper section of the container. The separation occurs due to the disparity in their settling velocities. Water overflow and fine, light particles (slow settling) are taken out of the classifier while fast-settling particles are extracted using suitable mechanical mechanisms (mechanical classifiers) or as an underflow at the bottom of the tank (non-mechanical or coil classifier). The feed particles in a tiny model coil classifier go in four directions, (1-4) producing four concentration regions (A–D). Particle concentration is low in region A due to its quickly exit through the overflow. Mixed particles travel in region B, arriving to the overflow or underflow. The big particles travel through region C in an almost vertically movement to the region D, large particles are sent to the underflow through a spiral device.

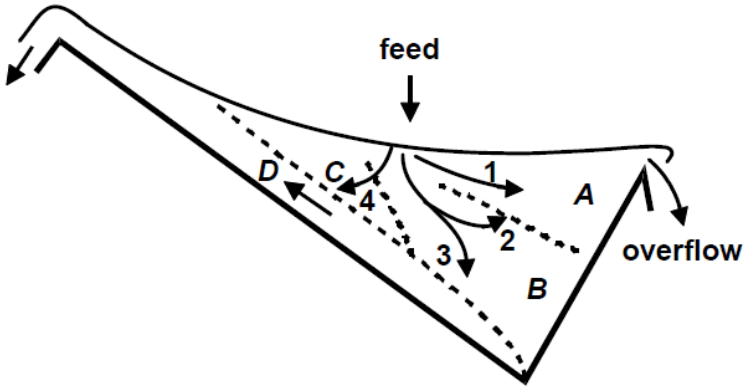

Figure 6.- Regions and direction of particles moevement in a coil classifier(Drzymała & Swatek, 2007).

- Fluidizing classification: this equipment are characterized by a stream of water beneath the tank, affecting the forces balance and sedimentation velocity. The water flow carries the particles whose sedimentation velocity can't beat the upward-moving flow to the overflow, while the underflow is directed toward the particles with a higher sedimentation velocity.
- Classification in horizontal stream of medium: Particles experience diagonal settling when an additional horizontal force acts on them in addition to the other forces (gravity, buoyancy, and resistance). One side of the separator supplies the feed, while the other side removes the overflow.
- Hydrocyclones: these machines take the advantage of a spiral pattern as they pass through the classifier. This type of movement is caused by the separator's cylindrical shape as well as forcing the feed stream tangent to the classifier wall. Centrifugal force, the primary separating force, acts on the particles because of their spiral movement. Hydrocyclones are the most frequently used in the soil washing process. Because the centrifugal force is stronger than the gravitational one, it takes less time to accomplish separation.

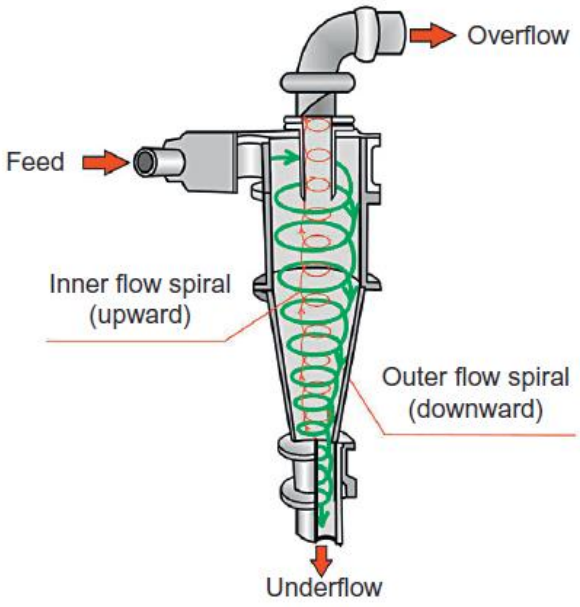

Figure 7.- Principal flows of a hydrocyclon (Wills & Finch, 2015).

In general, hydrocyclones are small in comparison to other separation equipment and have low capital and operating costs (Williford & Mark Bricka, 2000). This technique can be utilized in large-scale facilities (ex-situ treatments) or mobile plants (on-site treatments), making it very adaptable, affordable, and very easy to operate (Pearl et al., 2006).

3.1.1.2. Gravity concentrations

Gravity concentration is the process of separating the metal-bearing particles from the soil matrix with different, specific densities from one another in a fluid by gravity and one or more additional forces, typically provided by a viscous fluid, such air or water, which resists motion (Dermont et al., 2008b; Fuerstenau & Han, 2003; Wills & Finch, 2015). Particle size, shape, and weight all contribute to settling, but variations in the densities of the individual particles is the most important determinant (Dermont et al., 2008b; King, 2012).

When the gravity separation is performed slowly in a liquid, without any other forces apart from gravity and buoyancy, the classification occurs due to the difference between the density of the fluid and the particles (float and sink mechanism). When the process includes dynamic forces, other factors such as friction affect the separation (Drzymała & Swatek, 2007). Therefore, larger particles will be affected more than smaller ones, so particle size has an effect on the efficiency of gravity processes. To make the relative motion of the particles specific to gravity and to lessen the size effect, close size control of feeds to gravity processes is necessary in practice (Dermont et al., 2008b; Wills & Finch, 2015). Another factor regarding the size effect on gravity separation are slimes, or ultra-fine particles, which increase the viscosity of the slurry and obfuscate visual cut-points, decreasing the sharpness of separation (Wills & Finch, 2015).

Usually, the gravity separation is carried out in water. But most solid substances have a higher density so it usually requires liquids with a density greater water (heavy liquids). Sometimes the classification may be done using two or more liquids, with more phases and suspensions layers (Drzymała & Swatek, 2007). The two main categories of gravity separation operations are autogenous medium devices (Reichert cone, sluice, jig…) and produced medium devices. Within the first category, the process of separation occurs within a synthetic liquid medium whose density lies in the middle of the two components to be separated. The particulate material in autogenous media devices creates an environment with an effective density that causes stratification, or the separation of particles with different densities. A third class of gravity separators (spiral concentrator and the shaking table) depend on intricate physical mechanisms to achieve a separation between particles with varying densities (King, 2012).

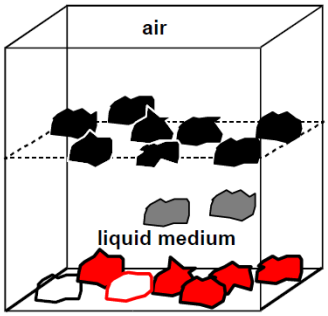

Figure 8.- Principle of gravity separation (Drzymała & Swatek, 2007).

When particles have a limited density distribution or a wide size distribution, gravity separation is ineffective (Williford & Bricka, 2000). Taggart's "concentration criterion" can be used to measure the efficacy of density separation (Bouchard, 2001), establishing a value of more than 2.5 for relatively simple circumstances (Wills & Finch, 2015). The range of 130-mm to 74-µm is optimal for gravity concentration, being problematic under 74 µm, and not applicable below 15 µm unless unusual circumstances arise (Fuerstenau & Han, 2003).

Maintaining the proper water balance in the plant is one of the most crucial parts of gravity circuit operations. The ideal feed pulp density for almost all gravity concentrators is attained with very little deviation, and this departure leads to a sharp drop in efficiency (Wills & Finch, 2015). Gravity concentration is frequently a cheap and efficient approach for mineral concentration if the minerals are freed at a coarse size (Fuerstenau & Han, 2003), if the soil and contaminant particles have a notable difference in density (Dermont et al., 2008b; Wills & Finch, 2015).

Jigs, shaking tables, and spirals are the most popular gravity concentrators that are used on a wide scale for treating soil (Dermont et al., 2008c; Wills & Finch, 2015). Shaking tables and spirals are better suited to handle fine to medium/coarse sand fractions (63–2000 µm), whereas mineral jigs are typically used to treat coarse sand fractions (800–2000 µm) or gravel fractions (2000–6000 µm). With MGS-Mozley, fractions of silt/clay (<63µm) and very fine sand (63–125µm) can be treated (Dermont et al., 2008b). The most common Gravity separators are described as follows (Wills & Finch, 2015):

- Jigs: Jigs are continuously operating devices used for classification by pulsating water streams. Sedimentation and stratification of the silt are caused by water moving lower in the stream, whereas water moving upward through a screen loosens the sediment. The main soil exploited parameter is different densities

between particles and the separation is made by a dam and gate that are positioned properly.

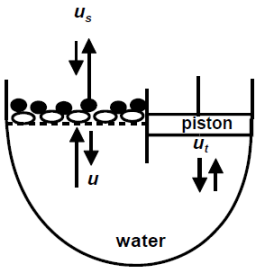

Figure 9.- Pulsating (jig) system (Drzymała & Swatek, 2007).

- Spirals: It is made up of a modified semicircular cross-section helical conduit. At the top of the spiral, feed pulp with a solid content of 15–45% by weight and a size range of 3 mm to 75 μm is introduced. As the pulp flows downward in a spiral pattern, the combined effects of centrifugal force, the particle's different settling rates, and the interstitial trickling through the flowing particle bed cause the particles to stratify. The intricate workings of these processes are greatly impacted by the density and size of the slurry. The lowest points of the cross-section have ports for the removal of particles with a higher specific gravity. When wash-water is introduced at the stream's inner edge, it crosses the concentrate band outward. Splitters that are adjustable regulate the width of the concentrate band that is withdrawn at the ports. Tailings are released from the bottom of the spiral conduit as the concentrate grade gradually drops from the descending ports.

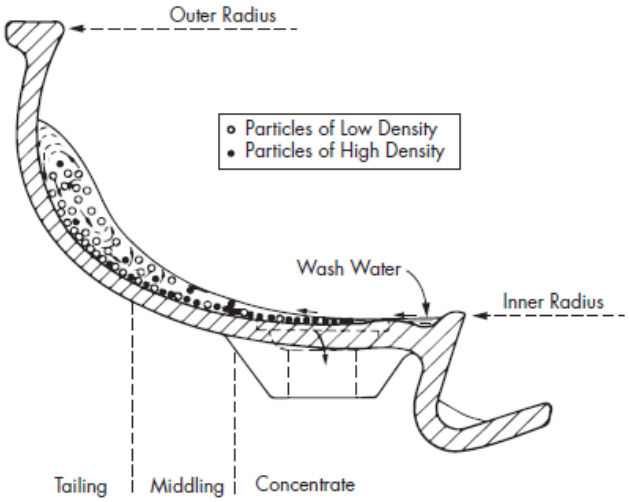

Figure 10.- The density-based particle separation is provided by the fluid flow pattern along the spiral trough's cross section (Kawatra & Young, 2019).

- Shaking tables: The water nearest to the surface is slowed down by the friction of the water absorbed on the surface as a film of flowing water passes over a level, incline surface; the velocity increases in the direction of the water's surface. Small particles will not travel as quickly as large particles if mineral particles are added to the film because they will be buried in the slower-moving section. The material will shift laterally because particles with a high specific gravity will travel more slowly than particles with a lower specific gravity. The shakingtable concentrator, which is arguably the most metallurgically efficient type of gravity concentrator, uses the flowing film to effectively separate small dense particles from coarse light particles. It is used to treat smaller, more challenging flow-streams and to create finished concentrates from the byproducts of other gravity system types.

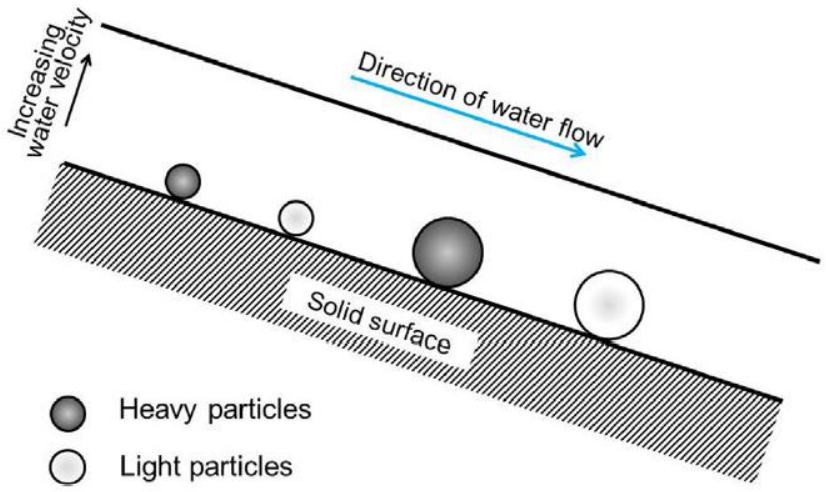

Figure 11.- Action in a flowing film (Wills & Finch, 2015).

3.1.1.3. Froth flotation

Flotation is the most significant, adaptable, and popular method of mineral processing, and its applications and uses are always being expanded to handle larger volumes and new regions (King, 2012; Wills & Finch, 2015).

Flotation is a selective method that can be applied to complicated ores making use of the different degrees of hydrophobicity between the desired and undesired gangue minerals (Wills & Finch, 2015) or to extract metal-containing particles from the soil matrix, depending on the context (Dermont et al., 2008b). In a direct flotation concentration, the gangue remains in the pulp or tailing while the mineral is typically moved to the foam, or

float fraction. The opposite of this is reverse flotation, which separates the gangue from the float fraction (Wills & Finch, 2015).

This method is based on three phases (solids, water, and froth) and numerous subprocesses and interactions. The three main mechanisms are involved in the material recovery process via flotation from the pulp (Wills & Finch, 2015): the selective attachment to air bubbles (tru flotation), The water that travels through the foam (entrainment) and particles in the foam that are physically trapped in air bubbles (aggregation).

The capacity of the different materials in the separation process to be wetted with a liquid in the presence of a gas phase is characterized by its hydrophobicity. In the mineral processing industry, materials that readily wet with water are referred to as hydrophilic, whereas those that have a low affinity for wetting are referred to as hydrophobic. Particles stick to a gas bubble because they are hydrophobic, creating a particle-air aggregate that is lighter than water and rises to the surface. Particles that are hydrophilic sink. Contact angle is a metric used to quantify the degree of hydrophobicity shown by different substances. Hydrophilic materials have a contact angle of zero, whereas hydrophobic ones have a contact angle greater than zero (Drzymała & Swatek, 2007).

The bulk of particles recovered to the concentrate are attached to air bubbles. While physical entrapment and entrainment degree have a role in the separation efficiency, real flotation remains the predominant mechanism. To accomplish a sufficient separation, it is crucial to regulate the stability of the froth phase, where these minerals drain. For the desirable finished product, multiple flotation stages (circuits) are needed. The purpose of the froth phase is to improve the flotation process's overall selectivity by minimizing the amount of entrained material recovered to the concentrate stream and holding onto the attached material. This raises the concentrate grade while attempting to keep the decline in useful recovery to a minimum (Wills & Finch, 2015).

Three processes make up this separation method (Dermont et al., 2008b; King, 2012):

- Attaching the required metal-bearing particles to the air bubbles: particles with suitable surface qualities can adhere to rising bubbles and be transported upward, eventually reaching the slurry's surface.
- Collecting the bubbles into a foam portion: Rising bubbles can and do collide with suspended solid particles. A bubble can take many particles to the top of the

slurry and will come into contact with particles numerous times as it rises through the slurry.

- Removing the foam fraction, which floats up the slurry: the surface of the slurry is kept covered with a layer of foam where retained particles are collected at the edge, near the lip of the froth weir. The foam flows over due to its inherent mobility, which helps with the recovery process. Occasionally, mechanical paddles are used to aid in the recovery process

Only if the mineral particles are somewhat hydrophobic, or resistant to water, will they be able to adhere to the air bubbles. Once at the surface, the air bubbles will only be able to hold the mineral particles in place if they are able to create a stable froth; if not, they will rupture and release the mineral particles. It is required to employ the various chemical substances known as flotation reagents in order to create the adequate conditions. Because most minerals are not naturally water-repellent, flotation reagents need to be added to the pulp. The collectors are the most crucial reagents because they adsorb on mineral surfaces, making them hydrophobic. A rather stable froth is maintained with the aid of the frothers. Regulators are used to regulate the flotation process; they also regulate the pH of the system by either activating or depressing mineral adhesion to air bubbles (Wills & Finch, 2015). Certain minerals, like sulphur, can float because they are hydrophobic by nature, but the majority of minerals are hydrophilic and must be treated to become hydrophobic by adding specific surface-active substances known as collectors. To accomplish separation, flotation and related auxiliary processes employ a variety of organic and inorganic chemicals, such as flocculants, extenders, collectors, frothers, activators, depressants, and deactivators. Surfactants called collectors, frothers, and extenders are added to minerals to provide them hydrophobicity, enable selective adsorption of the collector, or remove flotation interference caused by different dissolved or colloidal species (Fuerstenau & Han, 2003)

The heterogeneity of the metal compounds, the metal distribution over the various particle size fractions, the presence of high organic matter contents, and the proportion of very fine particles <10µm are the main factors influencing the floatability of metal-bearing particles in the context of soil remediation (Vanthuyne et al., 2003). In the finer part of the particle size range, flotation columns typically have a substantially better efficiency than flotation cells (Dermont et al., 2008c).

In the mineral business, froth flotation is frequently employed, specially with metal sulphides, which are simpler to separate than carbonates and oxides (Bouchard, 2001). The removal of metals from sediments and soils, mainly Cd, Cu, Pb, and Zn, has been accomplished with success using foam flotation (Vanthuyne et al., 2003; Vanthuyne & Maes, 2002, 2007). Nonetheless, froth flotation is still not as widely employed as other technologies for soil washing in the restoration process (Dermont et al., 2008b).

Most mechanical flotation cells have trouble selectively floating metal-bearing tiny particles (<10 μm) due to entrainment and trapping of the fine hydrophilic gangue particles (Vanthuyne & Maes, 2007). Bubbles cannot carry heavy and coarse particles, hence typical flotation devices are less effective when it comes to floating large particles (>200–300 μm) (Bouchard, 2001). The separation in froth (SIF) method is more suited for separation in the coarser particle size range as compared to conventional flotation technologies (Bouchard, 2001). Only relatively fine particles can be used in this method; any larger particles will cause the bubble to lose its load since their adhesion to the particle will be less than its weight (Wills & Finch, 2015).

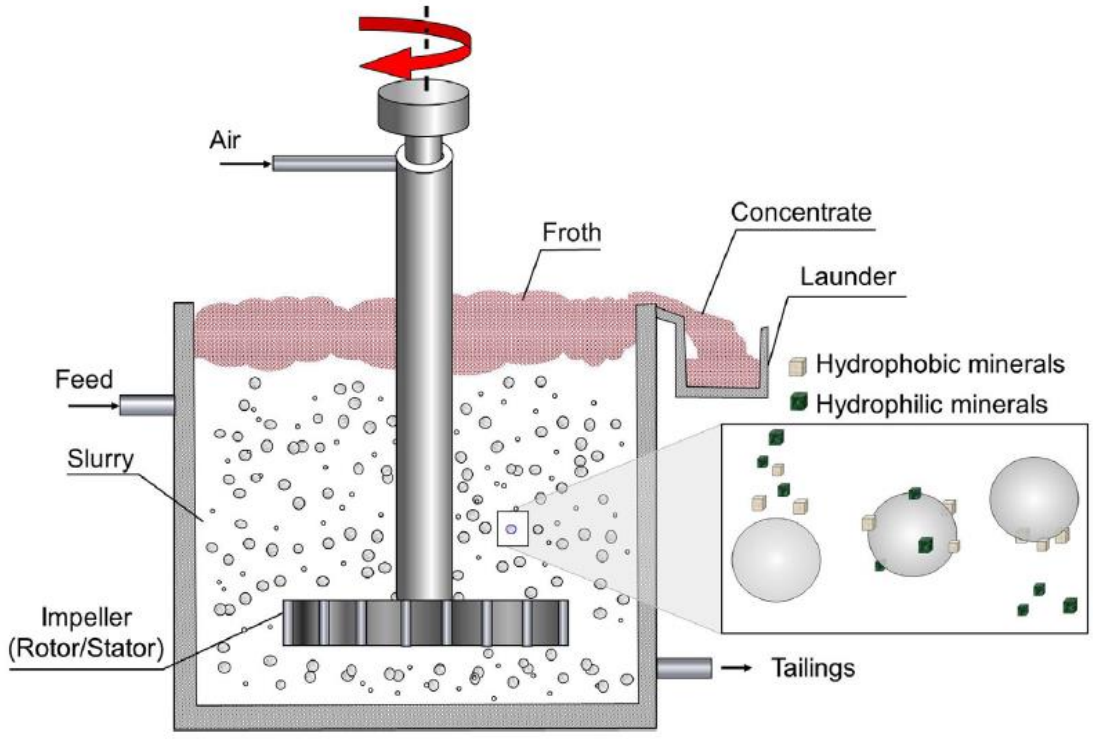

Figure 12.- Principle of froth flotation (Wills & Finch, 2015).

In order to release trapped particles, flotation machines guarantee that pulp flows into good, active contact with bubbles which levitate to the top of the cell. Production flotation

machines can be broadly classified into two categories based on the methods used to deliver air into the cell. There are numerous variants of these sorts that enable varying agitation intensities and flow patterns in apparatuses of various dimensions and forms. Pneumatic and mechanical machines are the two basic categories (Fuerstenau & Han, 2003):

- Pneumatic: Baffles or perforated bases in pneumatic machines distribute air entering the turbulent pulp into bubbles, maximizing the air's potential to come into touch with the mineral particles. The pulp is dispersed through agitation. These cells have fewer moving components, which makes them technically simpler, but their performance is also less effective.
- Mechanical: A mechanically driven impeller agitates the pulp to achieve dispersion. Mechanical machines use one of two types of aeration and pulp flow systems: open flow with no wiers and air intake through suction from the impeller's rotation or an external blower, or cell-to-cell flow with adjustable wiers between cells.

The column flotation technique improves separation through the application of the counter current principle by lowering particle entrapment The absence of an impeller or any other agitation mechanism (lowering energy and maintenance costs) is the primary operational distinction from mechanical flotation cells. Another significant distinction is that, in the majority of ore-processing applications, wash water must be sprayed into the froth at the top of the column. This cannot be done in a mechanical cell since the froth may be killed. A significant determinant of flotation recovery and selectivity as well as column operating stability is the amount of wash water injected. Column flotation involves feeding the ore into the column through a distributor situated at approximately two-thirds of the column's height, removing tails from the bottom, allowing concentrate to overflow at the top, and creating air bubbles at the bottom of the column using a porous sparger (Fuerstenau & Han, 2003).

3.1.1.4. Magnetic separation

Magnetic separation is a mechanical process that divides substances from a mixture according to their magnetic susceptibility by applying a magnetic force (Svoboda, 2004). In order to concentrate Fe ores and fe-containing minerals, this technology has been widely utilized in mineral processing (Wills & Finch, 2015). Additionally, it has been

applied in soil washing to eliminate pollutants from polluted soils by taking advantage of variations in their magnetic susceptibility.

Magnetic susceptibility is the magnitude that indicates a substance's level of magnetization when a magnetic field is applied (Blundell, 2001). From an engineering perspective, all substances possess some degree of magnetic properties, and minerals are typically categorized based on these characteristics. Therefore, materials having a high positive magnetic susceptibility are typically referred to as "magnetic," and materials having a low positive susceptibility are called "weakly magnetic." While the latter typically relate to the para- and antiferro-magnetic materials, which seldom enhance the magnetic flux density in their surroundings, the former include ferri and ferro-magnetic materials, which are distinguished by their ability to multiply the magnetic flux density inside them. On the other hand, materials that are typically classified as "nonmagnetic" are referred to as diamagnetic because they exhibit a negative magnetic susceptibility, which weakens the magnetic field when it exists (Cullity & Graham, 2008). Although diamagnetism is present in all materials to some extent, it is typically a minor effect that may be disregarded or a minor adjustment to a major effect.

Practically speaking, this means that substances that have a positive magnetic susceptibility are drawn to a magnetic field, while substances that have a negative value are marginally repelled from the magnet. Low-intensity magnetic separators can thus be used to easily separate ferro- and ferri-magnetic materials from other materials, while high-intensity magnetic separation is used to extract fine para- and antiferro-magnetic particles from a mixture that contains diamagnetic particles (Drzymała & Swatek, 2007).

Similar to this, the magnetic susceptibilities of pollutants and minerals found in soil can range from being mostly positive (ferro and ferri minerals) to being negative (organic matter) and intermediate (paramagnetic minerals and organometallics) (Dermont et al., 2008b; Sierra et al., 2013). Additionally, the formation of organometallics and the presence of Fe and Mn oxyhydroxides, which are chemically active and preferentially adsorb other metals on their surface (regardless of their magnetic properties) aid in the separation process because, similar to the previous instance, they have positive magnetic susceptibilities and can be separated by HIMS (High-Intensity Magnetic Separation).

Magnetism-based separation worked best with grain sizes larger than 250 mm and less well with smaller particle sizes (Boente et al., 2017).

The two types of magnetic separators are low- and high-intensity machines, which are further divided into wet-feed and dry-feed separators (Wills & Finch, 2015):

- Low-intensity magnetic separation (LIMS): The concentration of strongly magnetic coarse grains is the primary application for dry LIMS, frequently performed in drum separators. Wet techniques are applied below the 0.5 cm size range because they result in significantly reduced dust loss and a cleaner product. Mos frequent application of wet LIMS is to concentrate ferromagnetic sands. In essence, they are made up of a revolving non-magnetic drum with three to six stationary magnets of alternating polarity, whose magnetization changes gradually in different directions. The gangue is left in the tailings compartment while magnetic particles are raised by the magnets, pinned to the drum, and transported out of the field. Water is added to the apparatus to create a current that maintains the pulp's suspension.
- High-intensity magnetic separation (HIMS): It is only possible to successfully extract very weakly paramagnetic minerals from an ore feed if high-intensity fields of 2 Tesla or more can be generated (Drzymała & Swatek, 2007; Svoboda, 2004). IRMs or induced roll magnetic separators, are the most frequently used (mainly applied to handle phosphate rock, glass sands, wolframite, beach sands, and tin ores). Phosphoric steel laminates are squeezed together on a non-magnetic stainless-steel shaft to form the roll. Magnetic particles are grasped, carried out of the field's effect, and deposited into the magnetics compartment, while nonmagnetic particles are ejected off the roll to the tailings fraction (the location of the splitter plates that cut into the material's discharge direction is crucial). Because the precise grinding required to assure full liberation of the magnetic fraction makes it impossible to concentrate ores by dry high-intensity techniques, WHIMS, or continuous wet high-intensity magnetic, lower the minimum particle size for efficient separation and enable magnetic concentration of those ores. In some flowsheets, a wet concentration system can replace costly drying processes.

3.1.1.5. Electrostatic separation

Utilizing the differences in electrical conductivity between the various species present in the mineral or substance to be treated, electrostatic separation is a technique. It might seem like a universal method of separation because all minerals have some variation in conductivity, but processing circumstances limit its use (Wills & Finch, 2015). Typically,

it is employed with granular feeds that range in size from 40 microns to 1 millimeter (Kawatra & Young, 2019).

The degree to which the particles to be removed from the feed differ electrically conductivity determines how efficient this procedure will be. It is also possible to use certain chemical agents that change the conductivity of the minerals being separated (Mohanta & Dwari, 2020). This method's primary drawbacks are its low capacity for fine sizes and requirement for a dry, monolayer feed (Kawatra & Young, 2019).

The three main processes in which the electrostatic separation is based, are described as follows (Kawatra & Young, 2019; Wills & Finch, 2015):

- Lifting effect: The process of pure electrostatic separation uses an electric field to polarize materials according to their varying inclinations. Separation is possible even with relatively equal conductivities thanks to this phenomenon. Pure electrostatic separation is not particularly effective and is highly sensitive to variations in humidity and temperature.
- Fixing effect: Through the image effect, the non-conductive particles act as an electrode of the opposite sign by receiving charge from an electrode, holding onto it, and adhering to the surface of a transport roller that is connected to ground. Separation is made possible by the variations in the electric charge released by conductive and non-conductive particles.
- Triboelectrification: This phenomenon stems from some materials' propensity to interchange electrons through friction, which causes the materials to charge in opposite directions. The charging process is dependent on several variables, including temperature, ambient conditions, and contact speed. Particle size is another crucial component; research has shown that minerals operate better in environments with finer particle sizes.

The high intensity roll separator, electrostatic plate separator (and its screen variant), and triboelectric separator (free-fall and belt) are the three types of electrostatic separators utilized in the business; the first two are the most commonly employed (Fuerstenau & Han, 2003; Kawatra & Young, 2019):

- High intensity roll separator: It is supplied onto a cylinder facing an electrode, which ionizes the air, after both the fixing and lifting effects. By creating an image effect, the charging of the particles attracts the cylinder, which functions as an

electrode of the opposite sign. The conductive particles will discharge on the cylinder after exiting the electrode's region of effect, losing their attraction and returning to a normal trajectory that will be dependent on the cylinder's rotation speed. Conversely, the non-conductive particles, which are later removed by a brush, will not be discharged and will stay attached to the cylinder even after passing through the electrostatic field.

- Electrostatic plate separator: Using the elevation effect, the particles are fed onto a curved or inclined plate that is connected to the ground so that they pass beneath an elliptical plate or tube that is positioned parallel to the plate, acting as a non-ionizing electrode. The conductive particles are affected by this electrode's high static field, which attracts them to it by charging them in the opposite direction of the electrode. A trajectory that crosses a divider that is appropriately positioned for the separation will be produced by the force of attraction between the electrode and the inertia of the particles sliding along the plate. In the meantime, the non-conductive particles will land on the opposite side of the divider by following the path indicated by the plate.
- Triboelectrostatic belt separators (STCs): in which feed is supplied into a small space between two parallel flat electrodes. Triboelectrostatic charging of the particles is produced by the action of an open mesh belt traveling at a high speed between the electrodes, which has an open area of roughly 60% that permits particles to flow through with ease. The electric field forces will draw the negatively charged particles toward the lower positive electrode and the positively charged particles toward the upper negatively charged electrode. Two particle fluxes are thus produced, one toward each end of the tape in accordance with their respective charges.

3.2. Chemical extraction

Chemical extraction uses a liquid containing a specific chemical agent such as a metal extractor present in the soil. Extractive metallurgical processes and more specifically hydrometallurgical processes are widely used in the recovery of metals from ores, concentrates, wastes, recycled materials, and soil decontamination (Gupta & Mukherjee, 1990).

Most notably, solutions in which metals dissolve during chemical leaching or the conversion of metals into more soluble compounds, such as employing valence modifications to generate soluble metal salts, which are utilized to improve solubility. Acids, salts, and solutions with a high chlorine content, chelators, surfactants, and reducing or oxidizing agents are among the most often employed solutions in these procedures.

The decontamination efficiency of these methods depends mainly on the geochemistry of the soil, the nature of the contaminant metal, the dose and chemical composition of the extract, and the process conditions. However, if two specific factors are highlighted, the two most relevant relate to the properties of the contaminating metal. Distribution of different metals and their association with specific soil substrates. The fractions most likely to be decontaminated by these processes are the carbonates and those involving iron and manganese oxides (Dermont et al., 2008a).

This method can be effective and interesting, but it certainly brings more disadvantages than advantages when applying this technology on a large scale. It is true that it can be very interesting for very fine soils, as it can dissolve several types of contaminants independent of this factor, and the extracted metals can be recovered and recycled in a variety of ways. method (Dermont et al., 2008a). But it should also be noted that it is not particularly interesting from an economic point of view, since the use of chemical agents makes it very expensive to use this technology, as well as the greatest difficulty in handling. and purify the water used in the processes (Griffiths, 1995). But the real problem lies in the environmental factor, as treated soil often cannot be used for regeneration or deposited on the same land it was extracted from because chemical processes have altered the properties of the soil. physicochemical and microbiological properties. Likewise, the disposal and/or treatment of sludge from metal extraction can be very difficult. It is therefore a method of little economic benefit in most cases and when chemical agents themselves can cause other environmental problems (Dermont et al., 2008a).

3.3. Combination of physical separation and chemical extraction

The typical combination used is physical separation initially based on size classification, density or flotation, followed by chemical extraction (Dermont et al., 2008a). This is due to the assumption that contaminants are more concentrated in the fine parts of the soil,

resulting in a smaller amount of soil that needs to be treated with chemical agents. In this way, the cost of chemical processes and their environmental problems can be reduced by applying them to a smaller volume of material (Griffiths, 1995).

4. Attributive analysis

Multiple objectives are common in decision-making difficulties, and these purposes sometimes conflict with one another in that progress toward one aim can only be made at the expense of some of the others. Therefore, the trade-off between the levels of fulfillment of each target must be considered by the decision-maker. Furthermore, there may be a large level of uncertainty in genuine decision-making situations, making it impossible to anticipate with certainty what would happen if each choice is chosen. As a result, making decisions in certain situations can be beyond our ability for thought, necessitating a rigorous examination (Jiménez Martín et al., 2003)

A procedure based on the isolation and study of specified traits that are subsequently synthesized is known as attribute analysis. In contrast to subjective assessments that rely too heavily on the experience and bias of a single expert, it first offers a series of concrete actions and techniques that are easily repeated (Wandibba, 1982).

Typically, methods for cleaning soil rely on technologies for processing minerals (Gupta & Yan, 2016; Wills & Finch, 2015). The ideal goal of a soil washing technique is to optimize a specific contaminant's recovery and lower the ratio of concentration of that fraction by concentrating it in a smaller volume of soil than the initial one (Sierra et al., 2010). But in cases where multiple pollutants had to be treated at once, is needed the use of a technique to modify the choice of recoveries and concentration ratios in order to get satisfactory results for a number of contaminants rather than just one (Pero-Sanz, 2000). However, it is challenging to evaluate the procedure' performance due to the numerous factors in each trial. As a result, comparing experiments necessitates the use of a tool that can rate their quality (Boente et al., 2017).

Achieving a methodology which evaluates the capacity of a given soil washing process for more than one contaminant and being able to compare the results for different configurations of the same procedure or even between several technics, is a difficult task. Attributive analysis makes just that.

Imagine a procedure where “A” and “B” are the most important parameters for its effectiveness. The investigation runs “x” experiments varying the configuration and having each one different result. Between all the experiments, the desire outcome would have the combination of maximum “A” and “B” values, so a quality index (I) based on those guidelines is calculated as follows:

$$QI^i = \frac{A^i}{Max\{A\}} + \frac{B^i}{Max\{B\}}$$

$$QI_{optimal} = Max\{QI^i\}$$

Where:

- QI^i: quality index of the “i” configuration.
- A^i and B^i: specific “A” and “B” values of the experiment “i”, respectively.
- $Max\{A\}$ and $Max\{B\}$: maximum value of “A” and “B” of the “x” experiments.
- $QI_{optimal}$: resulto f the best configuration.

The experiment with the highest QI value, would the best configuration of this process.

But in the case of soil washing targeting more than one contaminant, those measured parameters would be for each one of the contaminants. So, there would be “A” and “B” values for each contaminant “j” (from a total of “y”) in every “i” configuration of the experiments making the calculations as follows:

$$QI_j^i = \frac{A_j^i}{Max\{A_j\}} + \frac{B_j^i}{Max\{B_j\}};\ QI^i = \sum_{j=1}^{y} Q_j^i$$

$$QI_{optimal} = Max\{QI^i\}$$

Where:

- QI_j^i: quality index of the “i” configuration for the “j” contaminant.
- QI^i: quality index of the “i” configuration.
- A_j^i and B_j^i: specific “A” and “B” values of the experiment “i” for the “j” contaminant, respectively.
- $Max\{A_j\}\ Max\{B_j\}$: maximum value of “A” and “B” of the “x” experiments for the “j” element.
- $QI_{optimal}$: result of the best configuration.

More parameters and correction factors can be applied to this methodology, being able to achieve infinite combinations and results, adapting to each scenario.

5. References

Agency for toxic substance and disease registry, U. S. (2012). *Toxicological profile for cadmium*. Department of Health and Humans Services, Public Health Service, Centers for Disease Control, Atlanta, Georgia, USA. https://scholar.google.com/scholar_lookup?title=Agency%20for%20Toxic%20Substance%20and%20Disease%20Registry%2C%20U.S.%20toxicological%20profile%20for%20cadmium&publication_year=2012&author=ATSDR

Ahmad, I., Zahir, Z. A., Bot, P. J., Akhtar, M. J., & Jamil, A. (2012). *Effect of cadmium on seed germination and seedling growth of four wheat (Triticum aestivum L.) cultivars*. *44*(5), 1569–1574. https://www.researchgate.net/publication/236016436

Ahmad, M. S. A., Ashraf, M., Tabassam, Q., Hussain, M., & Firdous, H. (2011). Lead (Pb)-induced regulation of growth, photosynthesis, and mineral nutrition in maize (zea mays L.) plants at early growth stages. *Biological Trace Element Research*, *144*(1–3), 1229–1239. https://doi.org/10.1007/S12011-011-9099-5/FIGURES/4

Akinci, I. E., & Akinci, S. (2010). Effect of chromium toxicity on germination and early seedling growth in melon (Cucumis melo L.). *African Journal of Biotechnology*, *9*(29), 4589–4594. https://doi.org/10.4314/AJB.V9I29

Anjum, M. F., Zia, M. A., Ashraf, M., & Khalid, Z. M. (2010). Effect of Chromium on Growth Attributes in Sunflower (Helianthus annuus L.). *Survival and Sustainability*, 985–994. https://doi.org/10.1007/978-3-540-95991-5_93

Arya, S. K., & Roy, B. K. (2011). Manganese induced changes in growth, chlorophyll content and antioxidants activity in seedlings of broad bean (Vicia faba L.). *Journal of Environmental Biology*, *32*(6), 707–711.

Ashraf, R., & Ali, A. (2007). EFFECT OF HEAVY METALS ON SOIL MICROBIAL COMMUNITY AND MUNG BEANS SEED GERMINATION. *Pak. J. Bot*, *39*(2), 629–636.

Ballabio, C., Jiskra, M., Osterwalder, S., Borrelli, P., Montanarella, L., Panagos, P. (2021). A spatial assessment of mercury content in the European Union topsoil. *Science of The Total Environment* 769, 144755. https://doi.org/10.1016/j.scitotenv.2020.144755

Baldantoni, D., Morra, L., Zaccardelli, M., & Alfani, A. (2016). Cadmium accumulation in leaves of leafy vegetables. *Ecotoxicology and Environmental Safety*, *123*, 89–94. https://doi.org/10.1016/J.ECOENV.2015.05.019

Basta, N. T., Ryan, J. A., & Chaney, R. L. (2005). Trace element chemistry in residual-treated soil: key concepts and metal bioavailability. *Journal of Environmental Quality*, *34*(1), 49–63. https://doi.org/10.2134/JEQ2005.0049DUP

Begum, P., Ikhtiari, R., & Fugetsu, B. (2011). *Graphene phytotoxicity in the seedling stage of cabbage, tomato, red spinach, and lettuce*. https://doi.org/10.1016/j.carbon.2011.05.029

Beyersmann, D., toxicology, A. H.-A. of, & 2008, undefined. (2008). Carcinogenic metal compounds: recent insight into molecular and cellular mechanisms. *SpringerD Beyersmann, A HartwigArchives of Toxicology, 2008•Springer*, *82*(8), 493–512. https://doi.org/10.1007/s00204-008-0313-y

Bharucha, K. J., Friedman, J. K., Vincent, A. S., & Ross, E. D. (2008). Lower serum ceruloplasmin levels correlate with younger age of onset in Parkinson's disease. *Journal of Neurology*, *255*(12), 1957–1962. https://doi.org/10.1007/S00415-009-0063-7

Bilandžić, N., Dežcrossed D Signek, D., Sedak, M., Crossed D Signokić, M., Šimić, B., Rudan, N., Brstilo, M., & Lisicin, T. (2012). Trace elements in tissues of wild carnivores and omnivores in Croatia. *Bulletin of Environmental Contamination and Toxicology*, *88*(1), 94–99. https://doi.org/10.1007/S00128-011-0449-Y

Bjuhr, J. (2007). *Trace metals in soils irrigated with waste water in a periurban area downstream Hanoi City, Vietnam*.

Blundell, Stephen. (2001). *Magnetism in condensed matter*. 238. https://books.google.com/books/about/Magnetism_in_Condensed_Matter.html?hl=es&id=zP9QEAAAQBAJ

Boente, C., Sierra, C., Rodríguez-Valdés, E., Menéndez-Aguado, J. M., & Gallego, J. R. (2017). Soil washing optimization by means of attributive analysis: Case study for the removal of potentially toxic elements from soil contaminated with pyrite ash. *Journal of Cleaner Production*, *142*, 2693–2699. https://doi.org/10.1016/J.JCLEPRO.2016.11.007

Boshoff, M., De Jonge, M., Dardenne, F., Blust, R., & Bervoets, L. (2014). The impact of metal pollution on soil faunal and microbial activity in two grassland ecosystems. *Environmental Research*, *134*, 169–180. https://doi.org/10.1016/J.ENVRES.2014.06.024

Bouchard, S. (2001). *Traitement du minerai : flottation, méthodes physiques*. 373.

Burek, C. L., & Rose, N. R. (2008). Autoimmune thyroiditis and ROS. *Autoimmunity Reviews*, *7*(7), 530–537. https://doi.org/10.1016/J.AUTREV.2008.04.006

Catalani, S., Rizzetti, M. C., Padovani, A., & Apostoli, P. (2012). Neurotoxicity of cobalt. *Human & Experimental Toxicology*, *31*(5), 421–437. https://doi.org/10.1177/0960327111414280

Chowdhury, S., Kain, J.-H., Adelfio, M., Volchko, Y., Norrman, J. (2023). Transforming brownfields into urban greenspaces: A working process for stakeholder analysis. *PLoS ONE* 18(1), e0278747. https://doi.org/10.1371/journal.pone.0278747

Chibuike, G. U., & Obiora, S. C. (2014). Heavy metal polluted soils: Effect on plants and bioremediation methods. *Applied and Environmental Soil Science*, *2014*. https://doi.org/10.1155/2014/752708

Cullity, B. D., & Graham, C. D. (2008). Introduction to Magnetic Materials. *Introduction to Magnetic Materials*. https://doi.org/10.1002/9780470386323

Dermont, G., Bergeron, M., Mercier, G., & Richer-Laflèche, M. (2008a). Metal-Contaminated Soils: Remediation Practices and Treatment Technologies. *Practice Periodical of Hazardous, Toxic, and Radioactive Waste Management*, *12*(3), 188–209. https://doi.org/10.1061/(ASCE)1090-025X(2008)12:3(188)

Dermont, G., Bergeron, M., Mercier, G., & Richer-Laflèche, M. (2008b). Soil washing for metal removal: A review of physical/chemical technologies and field applications. *Journal of Hazardous Materials*, *152*(1), 1–31. https://doi.org/10.1016/J.JHAZMAT.2007.10.043

Dermont, G., Bergeron, M., Mercier, G., & Richer-Laflèche, M. (2008c). Soil washing for metal removal: A review of physical/chemical technologies and field applications. In *Journal of Hazardous Materials* (Vol. 152, Issue 1, pp. 1–31). https://doi.org/10.1016/j.jhazmat.2007.10.043

DeVolder, P. S., Brown, S. L., Hesterberg, D., & Pandya, K. (2003). Metal Bioavailability and Speciation in a Wetland Tailings Repository Amended with Biosolids Compost, Wood Ash, and Sulfate. *Journal of Environment Quality*, *32*(3), 851. https://doi.org/10.2134/JEQ2003.0851

Dijkstra, B., Prichard, R. S., Lee, A., Kelly, L. M., Smyth, P. P. A., Crotty, T., McDermott, E. W., Hill, A. D. K., & O'Higgins, N. (2007). Changing patterns of thyroid carcinoma. *Irish Journal of Medical Science*, *176*(2), 87–90. https://doi.org/10.1007/S11845-007-0041-Y

Doncheva, S., Georgieva, K., Vassileva, V., Stoyanova, Z., Popov, N., & Ignatov, G. (2005). Effects of succinate on manganese toxicity in pea plants. *Journal of Plant Nutrition*, *28*(1), 47–62. https://doi.org/10.1081/PLN-200042161

Drenning, P. (2021). Soil Functions and Ecosystem Services: A Literature Review (Part 2/2). https://doi.org/10.13140/RG.2.2.23922.63685

Drzymała, Jan., & Swatek, A. (2007). *Mineral processing : foundations of theory and practice of minerallurgy*. University of Technology.

Du, X., Zhu, Y.-G., Liu, W.-J., & Zhao, X.-S. (2005). Uptake of mercury (Hg) by seedlings of rice (Oryza sativa L.) grown in solution culture and interactions with arsenate uptake. *Environmental and Experimental Botany*, *54*, 1–7. https://doi.org/10.1016/j.envexpbot.2004.05.001

Duffus, J. H. (2002). "heavy metals" - A meaningless term? (IUPAC technical report). *Pure and Applied Chemistry*, *74*(5), 793–807. https://doi.org/10.1351/PAC200274050793/MACHINEREADABLECITATION/RIS

Dulya, O., Mikryukov, V., Shchepkin, D., Pent, M., Tamm, H., Guazzini, M., Panagos, P., Jones, A., Orgiazzi, A., Marroni, F., Bahram, M., Tedersoo, L. (2024). A trait-based ecological perspective on the soil microbial antibiotic-related genetic machinery. *Environment International* 190, 108917. https://doi.org/10.1016/j.envint.2024.108917

Duruibe, J. O., Ogwuegbu, M. O. C., & Egwurugwu. (2007). Heavy metal pollution and human biotoxic effects. *International Journal of Physical Sciences*, *2*(5), 112–118. http://www.academicjournals.org/IJPS

EEA. (2009). *Overview of economic activities causing soil contamination in some WCE and SEE countries*. Eruopean Evironment Agency (EEA). https://www.eea.europa.eu/data-and-maps/figures/overview-of-economic-activities-causing-soil-contamination-in-some-wce-and-see-countries-pct-of-investigated-sites

EEA (European Environment Agency). (2014). *Progress in management of contaminated sites*. *Lsi 003*, CSI 015/LSI 003. https://doi.org/10.2788/4658

Emamverdian, A., Ding, Y., Mokhberdoran, F., & Xie, Y. (2015). Heavy metal stress and some mechanisms of plant defense response. *Scientific World Journal*, *2015*. https://doi.org/10.1155/2015/756120

Fahad, S., Rehman, A., Shahzad, B., Tanveer, M., Saud, S., Kamran, M., Ihtisham, M., Khan, S. U., Turan, V., & ur Rahman, M. H. (2019). Rice Responses and Tolerance to Metal/Metalloid Toxicity. *Advances in Rice Research for Abiotic Stress Tolerance*, 299–312. https://doi.org/10.1016/B978-0-12-814332-2.00014-9

Foucault, Y., Lévêque, T., Xiong, T., Schreck, E., Austruy, A., Shahid, M., & Dumat, C. (2013). Green manure plants for remediation of soils polluted by metals and metalloids: Ecotoxicity and human bioavailability assessment. *Chemosphere*, *93*(7), 1430–1435. https://doi.org/10.1016/J.CHEMOSPHERE.2013.07.040

Fuerstenau, M. C., & Han, K. N. (2003). *Principles of mineral processing*. Society for Mining, Metallurgy, and Exploration.

G. Vijver, M., & Peijnenburg, W. J. G. M. (2011). Metals and Metalloids in Terrestrial Systems: Bioaccumulation,Biomagnification and Subsequent Adverse Effects. *Ecological Impacts of Toxic Chemicals (Open Access)*, 43–62. https://doi.org/10.2174/978160805121210043

Gadd, G. M. (2010). Metals, minerals and microbes: geomicrobiology and bioremediation. *Microbiology (Reading, England)*, *156*(Pt 3), 609–643. https://doi.org/10.1099/MIC.0.037143-0

Gall, J. E., Boyd, R. S., & Rajakaruna, N. (2015). Transfer of heavy metals through terrestrial food webs: a review. *Environmental Monitoring and Assessment*, *187*(4). https://doi.org/10.1007/S10661-015-4436-3

Gao, P. P., Zhang, X. M., Xue, P. Y., Dong, J. W., Dong, Y., Zhao, Q. L., Geng, L. P., Lu, Y., Zhao, J. J., & Liu, W. J. (2022). Mechanism of Pb accumulation in Chinese cabbage leaves: Stomata and trichomes regulate foliar uptake of Pb in atmospheric PM2.5. *Environmental Pollution*, *293*, 118585. https://doi.org/10.1016/J.ENVPOL.2021.118585

Gautam, P. K., Gautam, R. K., Chattopadhyaya, M. C., Banerjee, S., Chattopadhyaya, M. C., & Pandey, J. D. (2016). *Heavy metals in the environment: Fate, transport,*

toxicity and remediation technologies. https://www.researchgate.net/publication/314465070

Giller, K. E., Witter, E., & McGrath, S. P. (2009). Heavy metals and soil microbes. *Soil Biology and Biochemistry*, *41*(10), 2031–2037. https://doi.org/10.1016/J.SOILBIO.2009.04.026

Glass, D. J. (2001). Phytoremediation of Toxic Metals. Using Plants to Clean Up the Environment-Book Review. *Plant Science*, 15–31.

Goix, S., Lévêque, T., Xiong, T. T., Schreck, E., Baeza-Squiban, A., Geret, F., Uzu, G., Austruy, A., & Dumat, C. (2014). Environmental and health impacts of fine and ultrafine metallic particles: Assessment of threat scores. *Environmental Research*, *133*, 185–194. https://doi.org/10.1016/J.ENVRES.2014.05.015

Gorospe, J. (2012). *GROWING GREENS AND SOILED SOIL: TRENDS IN HEAVY METAL CONTAMINATION IN VEGETABLE GARDENS OF SAN FRANCISCO*.

Gratão, P. L., Polle, A., Lea, P. J., & Azevedo, R. A. (2005). Making the life of heavy metal-stressed plants a little easier. *Functional Plant Biology : FPB*, *32*(6), 481–494. https://doi.org/10.1071/FP05016

Griffiths, R. A. (1995). Soil-washing technology and practice. In *JOURNALOF Journal of Hazardous Materials* (Vol. 40).

Gupta, A., & Yan, D. (2016). Mineral Processing Design and Operations: An Introduction: Second Edition. *Mineral Processing Design and Operations: An Introduction: Second Edition*, 1–850.

Gupta, C. K., & Mukherjee, T. K. (1990). *Hydrometallurgy in extraction processes*.

Harmanescu, M., Alda, L. M., Bordean, D. M., Gogoasa, I., & Gergen, I. (2011). Heavy metals health risk assessment for population via consumption of vegetables grown in old mining area; a case study: Banat County, Romania. *Chemistry Central Journal*, *5*(1). https://doi.org/10.1186/1752-153X-5-64

Harris, J. (2009). Soil microbial communities and restoration ecology: Facilitators or followers? *Science*, *325*(5940), 573–574. https://doi.org/10.1126/SCIENCE.1172975

He, Z., Shen, J., Ni, Z., Tang, J., Song, S., Chen, J., & Zhao, L. (2015). Electrochemically created roughened lead plate for electrochemical reduction of aqueous CO2. *Catalysis Communications*, *72*, 38–42. https://doi.org/10.1016/J.CATCOM.2015.08.024

Herawati, N., Suzuki, S., Hayashi, K., Rivai, I. F., & Koyama, H. (2000). Cadmium, copper, and zinc levels in rice and soil of Japan, Indonesia, and China by soil type. *Bulletin of Environmental Contamination and Toxicology*, *64*(1), 33–39. https://doi.org/10.1007/S001289910006

Hider, R. C., & Kong, X. (2013). Iron: Effect of overload and deficiency. *Metal Ions in Life Sciences*, *13*, 229–294. https://doi.org/10.1007/978-94-007-7500-8_8

Hillel, D. (2004). *ENCYCLOPEDIA OF SOILS IN THE ENVIRONMENT FOUR-VOLUME SET*. www.info.sciencedirect.com.

Hongbo, S., Liye, C., Gang, X., Kun, Y., Lihua, Z., & Junna, S. (2011). *Progress in Phytoremediating Heavy-Metal Contaminated Soils*. 73–90. https://doi.org/10.1007/978-3-642-21408-0_4

Hossain, M. A., Piyatida, P., da Silva, J. A. T., & Fujita, M. (2012). Molecular Mechanism of Heavy Metal Toxicity and Tolerance in Plants: Central Role of Glutathione in Detoxification of Reactive Oxygen Species and Methylglyoxal and in Heavy Metal Chelation. *Journal of Botany*, *2012*, 1–37. https://doi.org/10.1155/2012/872875

Howe, P., Malcolm, H., & Dobson, S. (2004). Enviromental transport, distribution, transformation, and accumulation. *Manganese and Its Compound: Environmental Aspects*.

J. T. Riedel. (2010). Brownfields como oportunidad, Recuperación de sitios ambientalmente degradados en la periferia urbana. In *Facultad de Arquitectura, Diseño y Estudios Urbanos, Pontificia Universidad Católica de Chile*.

Jan, A. T., Azam, M., Siddiqui, K., Ali, A., Choi, I., & Haq, Q. M. R. (2015). Heavy Metals and Human Health: Mechanistic Insight into Toxicity and Counter Defense System of Antioxidants. *International Journal of Molecular Sciences*, *16*(12), 29592. https://doi.org/10.3390/IJMS161226183

Järup, L. (2003). Hazards of heavy metal contamination. *British Medical Bulletin*, *68*, 167–182. https://doi.org/10.1093/BMB/LDG032

Jiménez Martín, A., Ríos Insua, S., & Mateos Caballero, A. (2003). Generic Multi-Attribute Analysis : un Sistema de Ayuda a la Decisión. *Boletín de La Sociedad de Estadística e Investigación Operativa, ISSN 1699-8871, 2003-03, Vol. 19, No. 1*. http://www.seio.es/BEIO/files/BoletinVol19Num1.pdf

Jiwan, S., & Kalamdhad, A. (2011). Effects of Heavy Metals on Soil, Plants, Human Health and Aquatic Life. *International Journal of Research in Chemistry and Environment (IJRCE)*, *1*(2), 15–21. https://www.ijrce.org/index.php/ijrce/article/view/78

Jomova, K., Vondrakova, D., Lawson, M., & Valko, M. (2010). Metals, oxidative stress and neurodegenerative disorders. *Molecular and Cellular Biochemistry*, *345*(1–2), 91–104. https://doi.org/10.1007/S11010-010-0563-X

Jones, D. T., & Hopkin, S. P. (1998). Reduced survival and body size in the terrestrial isopod Porcellio scaber from a metal-polluted environment. *Environmental Pollution*, *99*(2), 215–223. https://doi.org/10.1016/S0269-7491(97)00188-7

Kapoor, D., Bhardwaj, S., Landi, M., Sharma, A., Ramakrishnan, M., & Sharma, A. (2020). The Impact of Drought in Plant Metabolism: How to Exploit Tolerance Mechanisms to Increase Crop Production. *Applied Sciences 2020, Vol. 10, Page 5692*, *10*(16), 5692. https://doi.org/10.3390/APP10165692

Kawatra, S. K., & Young, C. (2019). *SME mineral processing & extractive metallurgy handbook*. 2203.

Khan, M. A., Chattha, M. R., Farooq, K., Jawed, M. A., Farooq, M., Imran, M., Iftkhar, M., & Kasana, M. I. (2015). Effect of farmyard manure levels and NPK applications on the pea plant growth, pod yield and quality . In *Life Sci. Int. J.* (Vol. 9, pp. 3178–3181). https://www.scopus.com/record/display.uri?eid=2-s2.0-85032337691&origin=inward&txGid=a424b993577eeb4cbd1d61752cd236cc

Khan, S., Cao, Q., Zheng, Y. M., Huang, Y. Z., & Zhu, Y. G. (2008). Health risks of heavy metals in contaminated soils and food crops irrigated with wastewater in Beijing, China. *Environmental Pollution*, *152*(3), 686–692. https://doi.org/10.1016/J.ENVPOL.2007.06.056

Kim, R. Y., Yoon, J. K., Kim, T. S., Yang, J. E., Owens, G., & Kim, K. R. (2015). Bioavailability of heavy metals in soils: definitions and practical implementation--a critical review. *Environmental Geochemistry and Health*, *37*(6), 1041–1061. https://doi.org/10.1007/S10653-015-9695-Y

King, R. P. (2012). Modeling and Simulation of Mineral Processing Systems. *Modeling and Simulation of Mineral Processing Systems*, 1–403. https://doi.org/10.1016/C2009-0-26303-3

Ko, M. S., Kim, J. Y., Park, H. S., & Kim, K. W. (2015). Field assessment of arsenic immobilization in soil amended with iron rich acid mine drainage sludge. *Journal of Cleaner Production*, *108*, 1073–1080. https://doi.org/10.1016/J.JCLEPRO.2015.06.076

Kumar., V., Sharma., A., & Cerdà., A. (2021). *Heavy Metals in Environment, Contamination and Remediation*. 1–246.

Lanska, D. J., & Remler, B. (2014). Myelopathy among zinc-smelter workers in Upper Silesia during the late 19th century. *Neurology*, *82*(13), 1175–1179. https://doi.org/10.1212/WNL.0000000000000270

Lasat, M. M. (1999). Phytoextraction of Metals from Contaminated Soil: A Review of Plant/Soil/Metal Interaction and Assessment of Pertinent Agronomic Issues. *Journal of Hazardous Substance Research*, *2*(1), 5. https://doi.org/10.4148/1090-7025.1015

Lee, G., Bigham, J. M., & Faure, G. (2002). Removal of trace metals by coprecipitation with Fe, Al and Mn from natural waters contaminated with acid mine drainage in the Ducktown Mining District, Tennessee. *Applied Geochemistry*, *17*(5), 569–581. https://doi.org/10.1016/S0883-2927(01)00125-1

Levengood, J. M., & Heske, E. J. (2008). Heavy metal exposure, reproductive activity, and demographic patterns in white-footed mice (Peromyscus leucopus) inhabiting a contaminated floodplain wetland. *The Science of the Total Environment*, *389*(2–3), 320–328. https://doi.org/10.1016/J.SCITOTENV.2007.08.050

Li, C., Zhou, K., Qin, W., Tian, C., Qi, M., Yan, X., & Han, W. (2019). A Review on Heavy Metals Contamination in Soil: Effects, Sources, and Remediation

Techniques. *Soil and Sediment Contamination: An International Journal*, *28*(4), 380–394. https://doi.org/10.1080/15320383.2019.1592108

Li, J. T., Gurajala, H. K., Wu, L. H., Van Der Ent, A., Qiu, R. L., Baker, A. J. M., Tang, Y. T., Yang, X. E., & Shu, W. S. (2018). Hyperaccumulator Plants from China: A Synthesis of the Current State of Knowledge. *Environmental Science and Technology*, *52*(21), 11980–11994. https://doi.org/10.1021/ACS.EST.8B01060/SUPPL_FILE/ES8B01060_SI_001.PDF

Liao, X. Y., Chen, T. Bin, Xie, H., & Liu, Y. R. (2005). Soil As contamination and its risk assessment in areas near the industrial districts of Chenzhou City, Southern China. *Environment International*, *31*(6), 791–798. https://doi.org/10.1016/J.ENVINT.2005.05.030

Liu, H., Probst, A., & Liao, B. (2005). Metal contamination of soils and crops affected by the Chenzhou lead/zinc mine spill (Hunan, China). *Science of The Total Environment*, *339*(1–3), 153–166. https://doi.org/10.1016/J.SCITOTENV.2004.07.030

Ma, J., Lv, C., Xu, M., Chen, G., Lv, C., & Gao, Z. (2016). Photosynthesis performance, antioxidant enzymes, and ultrastructural analyses of rice seedlings under chromium stress. *Environmental Science and Pollution Research*, *23*(2), 1768–1778. https://doi.org/10.1007/S11356-015-5439-X/FIGURES/6

McLaughlin, M. J., Hamon, R. E., McLaren, R. G., Speir, T. W., & Rogers, S. L. (2000). Review: A bioavailability-based rationale for controlling metal and metalloid contamination of agricultural land in Australia and New Zealand. *Soil Research*, *38*(6), 1037–1086. https://doi.org/10.1071/SR99128

Microbiology, G., & Abdousalam, A. G. (2010). Effect of heavy metals on soil microbial processes and population. *Egyptian Academic Journal of Biological Sciences, G. Microbiology*, *2*(2), 9–14. https://doi.org/10.21608/EAJBSG.2010.16703

Mohanta, S. K., & Dwari, R. K. (2020). Separation of the coal-quartz mixture using tribo-electrostatic separator: Effect of surface pretreatment. *Advanced Powder Technology*, *31*(8), 3361–3371. https://doi.org/10.1016/j.apt.2020.06.027

Mossel, D. A. A., Corry, J. E. L., Struijk, C. B., & Baird, R. M. (1995). The fate of heavy metals. *The Chemistry of Soil Processes*, *Ed. 1*, 593–620.

Musilova, J., Arvay, J., Vollmannova, A., Toth, T., & Tomas, J. (2016). Environmental Contamination by Heavy Metals in Region with Previous Mining Activity. *Bulletin of Environmental Contamination and Toxicology*, *97*(4), 569–575. https://doi.org/10.1007/S00128-016-1907-3

Muszyńska, E., & Hanus-Fajerska, E. (2015). Why are heavy metal hyperaccumulating plants so amazing? *Biotechnologia*, *96*(4), 265–271. https://doi.org/10.5114/BTA.2015.57730

Naveed, S., Oladoye, P. O., & Alli, Y. A. (2023). Toxic heavy metals: A bibliographic review of risk assessment, toxicity, and phytoremediation technology. *Sustainable*

Chemistry for the Environment, *2*, 100018. https://doi.org/10.1016/J.SCENV.2023.100018

Nematian, M. A., & Kazemeini, F. (2013). *Accumulation of Pb , Zn , Cu and Fe in plants and hyperaccumulator choice in Galali iron mine area , Iran*.

Panagos, P., Broothaerts, N., Ballabio, C., Orgiazzi, A., De Rosa, D., Borrelli, P., Liakos, L., Vieira, D., Van Eynde, E., Navarro, C., Breure, T., Fendrich, A., Köninger, J., Labouyrie, M., Matthews, F., Muntwyler, A., Juan, Jimenez, M., Wojda, P., Jones, A. (2024[a]). How the EU Soil Observatory is providing solid science for healthy soils. *European Journal of Soil Science* 75, e13507. https://doi.org/10.1111/ejss.13507

Panagos, P., Jiskra, M., Borrelli, P., Liakos, L., Ballabio, C. (2021). Mercury in European topsoils: Anthropogenic sources, stocks and fluxes. *Environmental Research* 201, 111556. https://doi.org/10.1016/j.envres.2021.111556

Panagos, P., Robinson, D., Borrelli, P. (2024b). A 1 billion euro mission: A Soil Deal for Europe. *European Journal of Soil Science* 75, e13466. https://doi.org/10.1111/ejss.13466

Pearl, M., Pruijn, M., & Bovendeur, J. (2006). The application of soil washing to the remediation of contaminated soils. *Land Contamination and Reclamation*, *14*(3), 713–726. https://doi.org/10.2462/09670513.680

Pero-Sanz Elorz, J. Antonio. (2000). ciencia e ingenieria de materiales. *Ciencia e Ingenieria de Materiales*. https://www.academia.edu/43840697/ciencia_e_ingenieria_de_materiales

Pierart, A., Shahid, M., Séjalon-Delmas, N., & Dumat, C. (2015). Antimony bioavailability: Knowledge and research perspectives for sustainable agricultures. *Journal of Hazardous Materials*, *289*, 219–234. https://doi.org/10.1016/J.JHAZMAT.2015.02.011

Popova, L. P., Maslenkova, L. T., Ivanova, A., & Stoinova, Z. (2012). Role of salicylic acid in alleviating heavy metal stress. *Environmental Adaptations and Stress Tolerance of Plants in the Era of Climate Change*, 447–466. https://doi.org/10.1007/978-1-4614-0815-4_21

Pourrut, B., Jean, S., Silvestre, J., & Pinelli, E. (2011). Lead-induced DNA damage in Vicia faba root cells: Potential involvement of oxidative stress. *Mutation Research/Genetic Toxicology and Environmental Mutagenesis*, *726*(2), 123–128. https://doi.org/10.1016/J.MRGENTOX.2011.09.001

Pourrut, B., Shahid, M., Dumat, C., Winterton, P., & Pinelli, E. (2011). Lead uptake, toxicity, and detoxification in plants. *Reviews of Environmental Contamination and Toxicology*, *213*, 113–136. https://doi.org/10.1007/978-1-4419-9860-6_4

Rogival, D., Scheirs, J., & Blust, R. (2007). Transfer and accumulation of metals in a soil-diet-wood mouse food chain along a metal pollution gradient. *Environmental Pollution (Barking, Essex : 1987)*, *145*(2), 516–528. https://doi.org/10.1016/J.ENVPOL.2006.04.019

Romero, F., Labouyrie, M., Orgiazzi, A., Ballabio, C., Panagos, P., Jones, A., Tedersoo, L., Bahram, M., Guerra, C., Eisenhauer, N., Tao, D., Delgado-Baquerizo, M., García-Palacios, P., Van der Heijden, M. (2024). Soil health is associated with higher primary productivity across Europe. *Nature Ecology & Evolution* 1–9. https://doi.org/10.1038/s41559-024-02511-8

Schädler, S., Morio, M., Bartke, S., Rohr-Zänker, R., & Finkel, M. (2011). Designing sustainable and economically attractive brownfield revitalization options using an integrated assessment model. *Journal of Environmental Management*, *92*(3), 827–837. https://doi.org/10.1016/J.JENVMAN.2010.10.026

Sędzik, M., Smolik, B., & Krupa-Małkiewicz, M. (2019). Effect of nicotinamide in alleviating stress caused by lead in spring barley seedling. *Journal of Elementology*, *24*(1), 281–291. https://doi.org/10.5601/JELEM.2018.23.2.1582

Shahid, M., Khalid, S., Abbas, G., Shahid, N., Nadeem, M., Sabir, M., Aslam, M., & Dumat, C. (2015). Heavy Metal Stress and Crop Productivity. *Crop Production and Global Environmental Issues*, 1–25. https://doi.org/10.1007/978-3-319-23162-4_1

Shahid, M., Pinelli, E., & Dumat, C. (2012). Review of Pb availability and toxicity to plants in relation with metal speciation; role of synthetic and natural organic ligands. *Journal of Hazardous Materials*, *219*(220), 1–12. https://doi.org/10.1016/j.jhazmat.2012.01.060

Sharma, P., & Dubey, R. S. (2005). Lead toxicity in plants. *Brazilian Journal of Plant Physiology*, *17*(1), 35–52. https://doi.org/10.1590/S1677-04202005000100004

Shi, J., Zhao, D., Ren, F., Huang, L. (2023). Spatiotemporal variation of soil heavy metals in China: The pollution status and risk assessment. *Science of The Total Environment* 871, 161768. https://doi.org/10.1016/j.scitotenv.2023.161768

Shin, D. W., Kim, E. J., Lim, S. W., Shin, Y. C., Oh, K. S., & Kim, E. J. (2015). Association of hair manganese level with symptoms in attention-deficit/hyperactivity disorder. *Psychiatry Investigation*, *12*(1), 66–72. https://doi.org/10.4306/PI.2015.12.1.66

Sierra, C., Gallego, J. R., Afif, E., Menéndez-Aguado, J. M., & González-Coto, F. (2010). Analysis of soil washing effectiveness to remediate a brownfield polluted with pyrite ashes. *Journal of Hazardous Materials*, *180*(1–3), 602–608. https://doi.org/10.1016/J.JHAZMAT.2010.04.075

Sierra, C., Martínez, J., Menéndez-Aguado, J. M., Afif, E., & Gallego, J. R. (2013). High intensity magnetic separation for the clean-up of a site polluted by lead metallurgy. *Journal of Hazardous Materials*, *248–249*(1), 194–201. https://doi.org/10.1016/j.jhazmat.2013.01.011

Simonsen, L. O., Harbak, H., & Bennekou, P. (2012). Cobalt metabolism and toxicology--a brief update. *The Science of the Total Environment*, *432*, 210–215. https://doi.org/10.1016/J.SCITOTENV.2012.06.009

Skalny, A. V., & Skalny, A. V. (2014). Bioelements and Bioelementology in Pharmacology and Nutrition: Fundamental and Practical Aspects. *Pharmacology*

and Nutritional Intervention in the Treatment of Disease. https://doi.org/10.5772/57368

Squitti, R. (2012). Copper dysfunction in Alzheimer's disease: from meta-analysis of biochemical studies to new insight into genetics. *Journal of Trace Elements in Medicine and Biology : Organ of the Society for Minerals and Trace Elements (GMS)*, *26*(2–3), 93–96. https://doi.org/10.1016/J.JTEMB.2012.04.012

Squitti, R., Quattrocchi, C. C., Salustri, C., & Rossini, P. M. (2008). Ceruloplasmin fragmentation is implicated in 'free' copper deregulation of Alzheimer's disease. *Prion*, *2*(1), 23. https://doi.org/10.4161/PRI.2.1.6297

Sumner, M. E. (2000). Beneficial use of effluents, wastes, and biosolids. *Communications in Soil Science and Plant Analysis*, *31*(11–14), 1701–1715. https://doi.org/10.1080/00103620009370532

Svoboda, J. (2004). Magnetic techniques for the treatment of materials. *Magnetic Techniques for the Treatment of Materials*. https://doi.org/10.1007/1-4020-2107-0

Tchounwou, P. B., Yedjou, C. G., Patlolla, A. K., & Sutton, D. J. (2012). Heavy metal toxicity and the environment. *EXS*, *101*, 133–164. https://doi.org/10.1007/978-3-7643-8340-4_6/COVER

Türkdoğan, M. K., Kilicel, F., Kara, K., Tuncer, I., & Uygan, I. (2003). Heavy metals in soil, vegetables and fruits in the endemic upper gastrointestinal cancer region of Turkey. *Environmental Toxicology and Pharmacology*, *13*(3), 175–179. https://doi.org/10.1016/S1382-6689(02)00156-4

Vanthuyne, M., & Maes, A. (2002). The removal of heavy metals from contaminated soil by a combination of sulfidisation and flotation. *The Science of the Total Environment*, *290*(1–3), 69–80. https://doi.org/10.1016/S0048-9697(01)01064-6

Vanthuyne, M., & Maes, A. (2007). The removal of heavy metals from dredged sediments by mechanical Denver flotation: The contribution of true flotation and entrainment. *Land Contamination and Reclamation*, *15*(1), 15–30. https://doi.org/10.2462/09670513.844

Vanthuyne, M., Maes, A., & Cauwenberg, P. (2003). The use of flotation techniques in the remediation of heavy metal contaminated sediments and soils: an overview of controlling factors. *Minerals Engineering*, *16*(11), 1131–1141. https://doi.org/10.1016/J.MINENG.2003.06.012

Walker, C., Sibly, R., Hopkin, S., & Peakall, D. (2012). *Principles of ecotoxicology*. https://books.google.com/books?hl=es&lr=&id=szTGbnooH7QC&oi=fnd&pg=PP1&ots=E8HXsrbxm9&sig=nyui13S0m4IPpoj42dyPnm0kL1c

Wandibba, S. (1982). ATTRIBUTE ANALYSIS AND THE STUDY OF PREHISTORIC POTTERY IN KENYA: AN ESSAY ON METHODOLOGY. *Transafrican Journal of History*, *11*, 167–183.

Wang, F., Xiang, L., Sze-Yin Leung, K., Elsner, M., Zhang, Y., Guo, Y., Pan, B., Sun, H., An, T., Ying, G., Brooks, B.W., Hou, D., Helbling, D.E., Sun, J., Qiu, H., Vogel,

T.M., Zhang, Wei, Gao, Yanzheng, Simpson, M.J., Luo, Yi, Chang, S.X., Su, G., Wong, B.M., Fu, T.-M., Zhu, D., Jobst, K.J., Ge, C., Coulon, F., Harindintwali, J.D., Zeng, X., Wang, H., Fu, Y., Wei, Z., Lohmann, R., Chen, C., Song, Y., Sanchez-Cid, C., Wang, Y., El-Naggar, A., Yao, Y., Huang, Y., Cheuk-Fung Law, J., Gu, Chenggang, Shen, H., Gao, Yanpeng, Qin, C., Li, Hao, Zhang, Tong, Corcoll, N., Liu, M., Alessi, D.S., Li, Hui, Brandt, K.K., Pico, Y., Gu, Cheng, Guo, J., Su, J., Corvini, P., Ye, M., Rocha-Santos, T., He, H., Yang, Y., Tong, M., Zhang, Weina, Suanon, F., Brahushi, F., Wang, Z., Hashsham, S.A., Virta, M., Yuan, Q., Jiang, G., Tremblay, L.A., Bu, Q., Wu, J., Peijnenburg, W., Topp, E., Cao, X., Jiang, X., Zheng, M., Zhang, Taolin, Luo, Yongming, Zhu, L., Li, X., Barceló, D., Chen, J., Xing, B., Amelung, W., Cai, Z., Naidu, R., Shen, Q., Pawliszyn, J., Zhu, Y., Schaeffer, A., Rillig, M.C., Wu, F., Yu, G., Tiedje, J.M. (2024). Emerging Contaminants: A One Health Perspective. *The Innovation.* 5(4), 100612. https://doi.org/10.1016/j.xinn.2024.100612

Wang, S., X. S.-M. (2001). Molecular mechanisms of metal toxicity and carcinogenesis. *SpringerS Wang, X ShiMolecular and Cellular Biochemistry, 2001•Springer*, *222*(1–2), 3–9. https://doi.org/10.1023/A:1017918013293

WEI, C., WANG, C., & YANG, L. (2009). Characterizing spatial distribution and sources of heavy metals in the soils from mining-smelting activities in Shuikoushan, Hunan Province, China. *Journal of Environmental Sciences*, *21*(9), 1230–1236. https://doi.org/10.1016/S1001-0742(08)62409-2

Williams, G. (2002). Ecological Integrity: Integrating Environment, Conservation and Health. *Agriculture, Ecosystems & Environment*, *90*(1), 108. https://doi.org/10.1016/S0167-8809(02)00023-3

Williford, C., & Mark Bricka, R. (2000). Physical Separation of Metal-Contaminated Soils. *Environmental Restoration of Metals-Contaminated Soils*, 121–165. https://doi.org/10.1201/9781420026269.CH7

Wills, B. A., & Finch, J. A. (2015). Wills' mineral processing technology: An introduction to the practical aspects of ore treatment and mineral recovery. *Wills' Mineral Processing Technology: An Introduction to the Practical Aspects of Ore Treatment and Mineral Recovery*, 1–498.

Wills, B. A., & Napier-Munn, T. J. (2006). Mineral Processing Technology: An Introduction to thePractical Aspects of Ore Treatment and Mineral Recovery. In Butterworth-Heinemann (Ed.), *Wills' Mineral Processing Technology* (7th ed). Butterworth-Heinemann. https://doi.org/10.1016/C2010-0-65478-2

Xie, Y., Luo, H., Du, Z., Hu, L., & Fu, J. (2014). Identification of cadmium-resistant fungi related to Cd transportation in bermudagrass [Cynodon dactylon (L.) Pers]. *Chemosphere*, *117*(1), 786–792. https://doi.org/10.1016/J.CHEMOSPHERE.2014.10.037

Xiong, T. T., Austruy, A., Pierart, A., Shahid, M., Schreck, E., Mombo, S., & Dumat, C. (2016). Kinetic study of phytotoxicity induced by foliar lead uptake for vegetables

exposed to fine particles and implications for sustainable urban agriculture. *Journal of Environmental Sciences*, *46*, 16–27. https://doi.org/10.1016/J.JES.2015.08.029

Yoo, H. J., & Choi, K. M. (2015). Hepatokines as a Link between Obesity and Cardiovascular Diseases. *Diabetes & Metabolism Journal*, *39*(1), 10. https://doi.org/10.4093/DMJ.2015.39.1.10

Yu, J., Liu, X., Yang, B., Li, X., Wang, P., Yuan, B., Wang, M., Liang, T., Shi, P., Li, R., Cheng, H., Li, F. (2024). Major influencing factors identification and probabilistic health risk assessment of soil potentially toxic elements pollution in coal and metal mines across China: A systematic review. *Ecotoxicology and Environmental Safety* 274, 116231. https://doi.org/10.1016/j.ecoenv.2024.116231

Yunta, F., Schillaci, C., Panagos, P., Van Eynde, E., Wojda, P., Jones, A. (2024). Quantitative analysis of the compliance of EU Sewage Sludge Directive by using the heavy metal concentrations from LUCAS topsoil database. *Environmental Science and Pollution Research* 1, 16. https://doi.org/10.1007/s11356-024-31835-y

Vieira, D., Yunta, F., Baragaño, D., Evrard, O., Reiff, T., Silva, V., de la Torre, A., Zhang, C., Panagos, P., Jones, A., Wodja, P. (2024). Soil pollution in the European Union – An outlook. *Environmental Science & Policy* 161, 103876. https://doi.org/10.1016/j.envsci.2024.103876

Zhang, T., Xu, W., Lin, X., Yan, H., Ma, M., & He, Z. (2018). *Assessment of heavy metals pollution of soybean grains in North Anhui of China*. ttps://doi.org/10.1016/j.scitotenv.2018.07.335

Zhu, S., Mao, H., Sun, S., Yang, X., Zhao, W., Sheng, L., Chen, Z. (2025). Arbuscular mycorrhizal fungi promote functional gene regulation of phosphorus cycling in rhizosphere microorganisms of Iris tectorum under Cr stress. Journal of Environmental Sciences 151, 187-199. https://doi.org/10.1016/j.jes.2024.02.029

Universidad de Oviedo

CHAPTER II: An evaluation of the feasibility of electrostatic separation for physical soil washing

X. Corres, D. Baragaño, J.M. Menéndez-Aguado, J.R. Gallego, C. Sierra

Environmental Technology & Innovation 32 (2023) 103237

Abstract

We present the first application of electrostatic separation for soil washing. Soil samples were collected from the PTE-containing area of La Cruz in Linares, southern Spain. Using a single-phase high-tension roll separator with voltages ranging from 20 kV to 41.5 kV, we achieved yield values between 0.69% and 9%, with high recovery rates for certain elements such as Zn, Cu, and Mo. SEM-EDX analysis revealed three particle types, including a non-conductive fraction composed of feldspar, a middling fraction composed of mica, and a conductive fraction consisting of PTE-bearing slag grains. Attributive analysis showed that 41.5 kV was the optimal voltage for maximizing PTE concentration. Overall, electrostatic separation is a promising approach for treating soils contaminated with PTEs, particularly in dry climate areas impacted by mining activities.

Keywords

Potentially toxic elements (PTEs), sandy soil, mineral processing, lead, circular economy

1. Introduction

Potentially Toxic Elements (PTEs) are known to be widespread and present complex challenges due to their failure to decompose, difficulties with remediation, toxicity to plants and in the food chain, and damage to soil ecosystems (Beiyuan et al., 2018; Gu et al., 2018; Y. Li et al., 2019). These pollutants are well-known by-products of human activity, including mining, waste disposal, agriculture, electroplating, and coal combustion (Piccolo et al., 2019; Rui et al., 2019; Wu et al., 2015), thus, soil contamination with PTEs is currently one of the most pressing environmental issues we are faced with. Several million hectares of PTE-contaminated soils are found in Europe alone, accounting for nearly 40% of all contaminated soil worldwide (EEA, 2014). Beyond Europe, this issue affects many other nations, principally the USA (Uchimiya et al., 2011), Japan (Makino et al., 2006), and Brazil (França et al., 2017).

PTE-polluted soils can be remediated using physical (soil replacement, physical soil washing, thermal desorption), chemical (chemical soil washing, solidification/stabilisation electrokinetic, vitrification), and biological (phytoremediation, microorganism remediation, animal remediation) (Anderson et al., 1999; Beiyuan et al., 2018; Dermont et al., 2008) treatment methods. Soil washing techniques have their origin in the mining industry and involve either the separation of soils by particle size and density generally using water as the carrier agent (physical washing) or the use of a chemical to extract the contaminant (chemical washing) (Anderson et al., 1999). Such techniques result in a clean fraction that can be backfilled on site and a contaminated fraction that can be disposed of appropriately. In comparison to other methods, physical soil washing is one of the most remarkable decontamination techniques due to its capacity to permanently remove PTEs, fast processing, waste volume reduction, and significant cost/effectiveness ratio (Baragaño et al., 2020; Feng et al., 2020; Khalid et al., 2017; Wang et al., 2018; Xu et al., 2014; L. Zhao et al., 2017).

Electrostatic separation makes use of differences in electrical conductivity between minerals (Inculet, 1984) and on the face of it, this method would seem to be a universal method of separation because all materials exhibit some variation in conductivity. In reality, however, it has several limitations, specifically, its low capacity for fine grain sizes, the processing requirement of a dry monolayer feed, limitations with soil sample variability, sensitivity to moisture and moderate to high energy consumption (mainly due

to drying)(Kawatra & Young, 2019). Typically, this method is used with granular feeds with particle sizes ranging from 40 μm to 1 mm (Kawatra & Young, 2019).

As discussed in Yang et al. (2018), electrostatic separation is widely used for the recovery of ilmenite ore, rutile, and zircon from sands. It also plays a part in many recycling processes, for example in the separation of metal from plastic in lots of scrap electrical cabling (Bedeković & Trbović, 2020; Park et al., 2015), and in the food industry to isolate or concentrate proteins found in various foodstuffs (Kdidi et al., 2019; Tabtabaei et al., 2017, 2019). In addition, the technique is used in the petrochemical industry for desalting crude oil (Aitani, 2004) and for the purification of certain products (Li et al., 2019, 2021; Villot et al., 2012).

Despite its proven effectiveness in many areas, however, electrostatic separation does not appear to have been investigated as a method for soil decontamination. As stated above, one reason for this may be the fact that this method requires a dry feed. The costs involved in drying soils before processing represent a major obstacle to the use of electrostatic separation in a soil washing operation. The site we are considering in this research, La Cruz in the Linares-La Carolina mining district (Southern Andalusia, Spain), side-steps this problem as its Mediterranean climate means there is little rainfall, and its soils are thus completely dry for most of the year (Lorite et al., 2023). Thus, with its arid climate it is an ideal site to test electrostatic separation of soils.

Following from the discussion above, the primary goals of the current study are:

- To evaluate the feasibility of electrostatic separation as part of physical soil washing treatments for soils containing PTEs.
- To explain the underlying aspects of the separation by means of a detailed mineralogical study.
- To test a novel formulation (attributive analysis) for the assessment of separation efficiency and thus determine optimal separation conditions.

2. Materials and methods

2.1. Site description

Galena (PbS) has been mined at La Cruz for over two centuries making it one of the most important led ore mining regions in the world (Lillo Ramos, 1992; Martínez et al., 2007b, 2007a, 2012). The led ore is found in veins with sphalerite (ZnS), chalcopyrite ($CuFeS_2$), and barite ($BaSO_4$) thus processing and extracting the useful ore creates a significant quantity of waste which is often dumped on the land next to mining operations. Moreover, much of the mineral processing at the site considered here involved gravity separation and froth flotation resulting in both medium and fine grain rejects that were then sent to nearby landfills or dumps. In addition, the solid, liquid, and gaseous contaminants produced by the district's foundries remain on these sites in the form of slag and dust, an environmental problem discussed by Adamo et al. (1996) and Li and Thornton (2001) at similar sites in Canada and the UK, respectively. When these industrial residues, containing fractions with a high concentration of heavy metals, are dispersed and dumped on the ground without any prior remediation treatment the action of weathering increases their chemical availability (Loredo et al., 1999; Martínez et al., 2007a) making them even more environmentally hazardous. In this way, mining waste in all its forms constitutes a significant problem for the extensive agricultural areas of the zone (Sierra et al., 2013). Location map is presented in SM1. According to Heliosat (SARAH), the study site receives an average of 3.3 hours of sunlight per day, with 5.82 peak sun hours (PSHs) and an average annual solar radiation of over 5 kwh/m^2 on a horizontal surface (H) (e.g., Pfeifroth et al., 2017). Based on this information, it is evident that solar energy can serve as a viable alternative energy source to power the electrostatic separation process.

2.2. Sample preparation

Samples were taken from 10 randomly selected sites across the location of interest. All samples were taken from the top 35 cm layer of soil; the depth was measured using a stainless-steel calliper and a shovel was used to collect the sample. In total a bulk sample of 25 kg was collected. The sample was then homogenised and kept at room temperature in inert plastic containers until further preparation and analysis. All soil analysis was completed within 15 days of the initial sampling.

The bulk sample was wet sieved in batches for five minutes with a water flow of 0.3 l/min to obtain granulometric fractions of 63, 63-125, 125-250, 250-500, 500-1000, and 1000-2000 µm (ASTM D-422-63, Standard Test Method for Particle-Size Analysis of Soils). Note that, sodium hexametaphosphate and sodium carbonate were used to aid the separation of the silt-clay fraction (<63 µm) from the larger particles. The process was repeated until 3 kg of the 1000-2000 µm fraction was obtained. This fraction was divided into twelve subsamples, which were reserved for further processing in the electrostatic separator. Additional subsamples were taken from each fraction, and these were air dried at 40 °C before being sent for chemical analysis.

2.3. Electrostatic separation

As described above, twelve samples were made from the 1-2 mm fraction of soil collected from the site of interest. Each sample was tested at a different separation voltage with experimental runs at each voltage repeated three times. An average of these results was taken and is presented in this article. The apparatus used was an eForce high voltage electrostatic separator (model EHTP by Outotec) (Fig. 1 and SM2) which is one the few semi-industrial electrostatic separators operating in Europe.

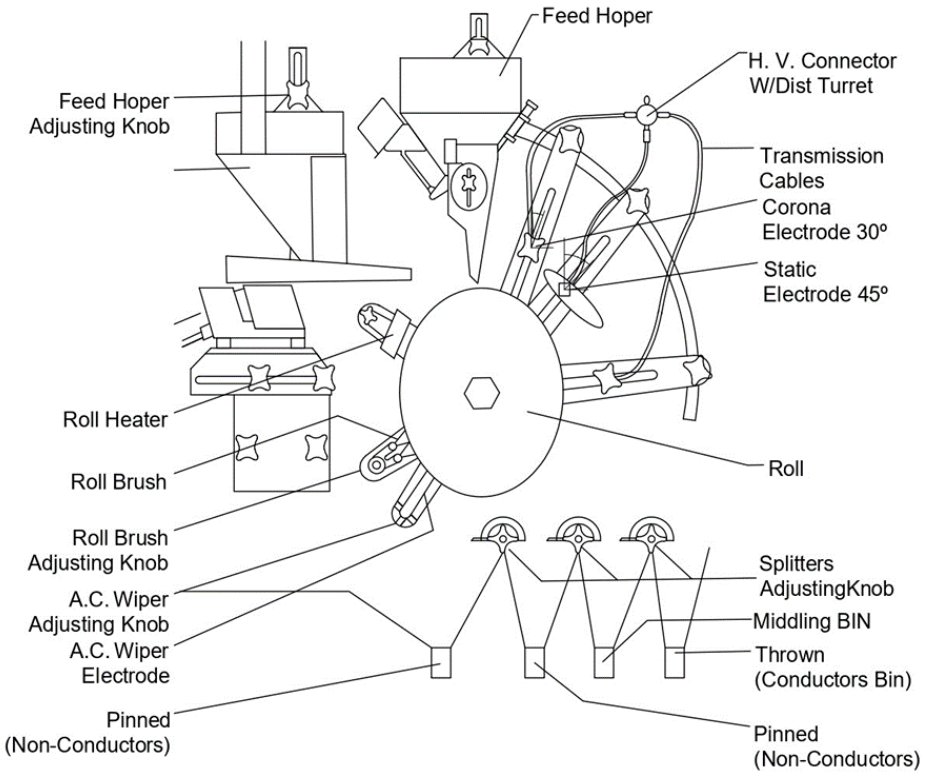

Figure 13.- Scheme of the high voltage electrostatic separation process

The apparatus employed has the following design characteristics:

- Feed particle size range: 0.074-10 mm.
- Treatment capacity: up to 150 kg/h.
- Vibratory tray and hopper with variable speed control for coarser particles and a positive speed feed chute and vibrator hopper for finer particles.
- Hopper with 2 adjustable dividers for the collection of non-conductive, intermediate (middling), and conductive products.
- 2 interchangeable stainless-steel rollers:
    - Of sizes 25.4 and 35.56 cm (10 and 14") in diameter by 15.24 cm (6") wide (industry standards) and
    - Of variable roll speed with a ¼ HP direct drive motor.
- 2 DC electrodes, one corona and the other static, which can be set at a range of voltages to a maximum of 41.5 kV; and 1 AC wiper electrode at 18 kV.
- High voltage transformer, adjustable up to 12,000 VAC.
- Grounded roller brush for particle removal: adjustable and with infrared roller heating capability.

The module was operated under the following conditions:

- Corona electrode angle: 30° with respect to the vertical.
- Electrostatic electrode angle: 45° with respect to vertical.
- Roll speed: 50 rpm.

Samples were fed into the feed hopper and onto the roller. The corona electrode ionizes the surrounding air and charges the particles on the roller as they approach the electrode. Conductive particles lose their charge quickly to the earthed roller and are thrown into the conductors bin due to the centrifugal force of the roller. The more insulating particles retain their charge and will stay on the roller until they are brushed off and fall into either the middlings or insulators bin (depending on particle size and roller speed).

The degree of separation that can be achieved for a given sample will depend on the composition of the sample, roller speed, electrode positions, and separation voltage (the voltage of the corona electrode). In this work, the only variable was the separation voltage which was set at a range of values from 20 kV to 41.5 kV in order to determine the optimum voltage for the soils sampled here.

2.4. Chemical and mineralogical analysis

Before chemical analysis, subsamples (6 from the grain size fractioning and 108 from the separation experiments) needed to be standardized thus, all fractions >125 μm were milled using a vibrating disk mill (RS 100 Retsch) at 400 rpm for 40 sec. Then, representative samples of 1 g were taken from each subsample, and these were subjected to "Aqua regia" ($HCl + HNO_3$) digestion before being sent for ICP-OES analysis at the ISO 9002 accredited laboratories, Actlabs International (Ancaster, Ontario, Canada). Tests returned the total concentrations of the following 36 major and trace elements: Ag, Al, As, Au, B, Ba, Bi, Ca, Cd, Co, Cr, Cu, Fe, Ga, Hg, K, La, Mg, Mn, Mo, Na, Ni, P, Pb, S, Sb, Sc, Se, Sr, Te, Th, Ti, Tl, V, W, Zn. Samples that exceeded the limit of quantification for the previous method (13 in total) were treated in triplicate with Fusion-Inductively Coupled Plasma-Sodium Peroxide Oxidation (FUS-Na_2O_2) in the same laboratories. This process involves sintering the sample at 650°C after oxidizing it with sodium peroxide. The resulting oxidized material was then dissolved in aqueous HNO_3, and various elements in the resulting solution are quantified using ICP-OES (report number: A19-03313).

The subsamples were also examined using a stereoscopic binocular microscope (Nikon SMZ1000) and micrographs were obtained with a high-resolution Nikon DS-Ri1 camera. The morphology and composition of minerals was examined using an SEM-EDX system, comprising a Jeol JSM-6100 scanning electron microscope and an energy dispersive X-ray analyser (INCA Energy 200).

3. Results and discussion

3.1. PTEs concentration in soils

Nine PTEs tested for in this study (As, Cd, Cu, Cr, Hg, Ni, Pb, Sb, and Zn), were found in quantities above the target limits set by current international standards (Buchman, 2008) and three (Cu, Zn, Pb) were significantly above both the intervention limit (Table 1), and the contamination ratio (CR: the quotient of sample concentration and the target value for the element of interest). The concentration of Mo in the soil samples was determined to be below the reference levels. Nevertheless, it was included in the study due to its geochemical importance and economic significance, as well as its notable performance in the separation process. Furthermore, the analysis also incorporated Al and Fe due to their high conductivity. Cu was the most significant soil PTE at the site of interest (176.13 mg/kg to 802.32 mg/kg, mean: 362.7 mg/kg; CR: 106.68) followed by Zn (376.06 mg/kg to 2375.37 mg/kg, mean: 1051.03 mg/kg; CR: 65.69), and, as expected, Pb (1620.25 mg/kg to 3455.43 mg/kg, mean: 2412.81 mg/kg; CR:43.87). Another PTE, As was found to have a CR of similar order to the main 3 PTEs (53.84). In this way, there is a major case for a soil decontamination programme at the site of interest focusing principally on Cu, Zn, and Pb but which might be extended first to As, and later to Ni, Cr, Cd, Sb, and Hg. The soil exhibited a sandy loam texture, like many soils found in Mediterranean regions.

Table 1.- PTEs concentrations in the bulk sample, the international standard (target and intervention limits), and contamination ratio for each PTE tested for in addition to Al, Mo and Fe. Elements marked with an asterisk are those with concentrations surpassing both the intervention and target values.

Element	Concentration (mg/kg)	Dutch Standards (mg/kg) (Buchman, 2008)		Contamination Ratio
		Intervention	Target	
Al	4681.2	-	-	-
As	48.46	55	0.9	53.84
Cd	7.48	12	0.8	9.35
Cr	10.41	220	0.35	29.75
Cu*	362.70	96	3.4	106.68
Fe	19 590.53	-	-	-
Hg	0.76	10	0.3	2.54
Mo	1.71	115	190	3
Ni	9.17	100	0.26	35.28
Pb*	2412.81	530	55	43.87
Sb	11.96	15	3	3.99
Zn*	1051.03	350	16	65.69

3.2. Electrostatic Separation

The results of electrostatic separation were initially assessed according to three standard ore processing parameters: yield (γ), recovery (ε), and enrichment ratio (μ) (Wills & Napier-Munn, 2006). The yield or weight recovery is the quotient of the feed mass and that of the conductive fraction collected for a given experimental run. The recovery is the quotient of the mass of an element of interest found in the conductive fraction and that of the feed for a given experimental run. Finally, the enrichment ratio is the quotient of the concentration of an element of interest found in the conductive fraction and that of the feed for a given experimental run.

Experimental runs were completed for 12 values of corona electrode voltage starting with the highest voltage available (41.5 kV). The voltage was gradually reduced on each subsequent run to determine the optimal operating conditions. At all voltages, we observed lowest yields (γ = 0.69% – 9 %) for the conductive fraction compared to the middlings (γ = 50.68% – 90.59%) and insulating fraction (γ = 8.72% – 48.89%) (Fig. 2).

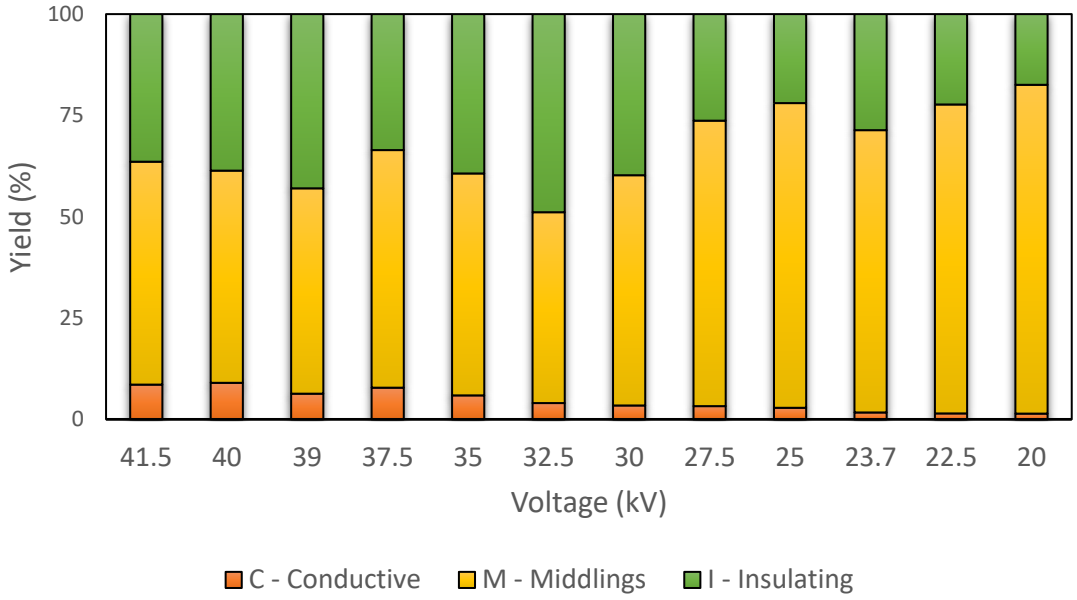

Figure 14.- Yield (γ) distribution between fractions for experimental runs

Looking in detail at the relationship between the yield for the conductive faction and applied voltage, here we found a positive correlation: the higher the voltage, the higher the yield with an almost directly proportional relationship (SM3). This suggests that higher voltages increased the number of conductive particles collected from the feed.

However, higher voltages may also increase the capture of insulating particles, which could reduce recovery, and this highlights the need for more exhaustive study into the selection of an optimal operating voltage.

For most PTEs, the enrichment ratio, μ, is lower for the middlings and insulating fractions (<1% in all cases) compared to the conductive fraction (Table 2). This is a reflection of the fact that most pollutants tested here were metallic or semi-metallic and thus would be expected to report to the conductive fraction.

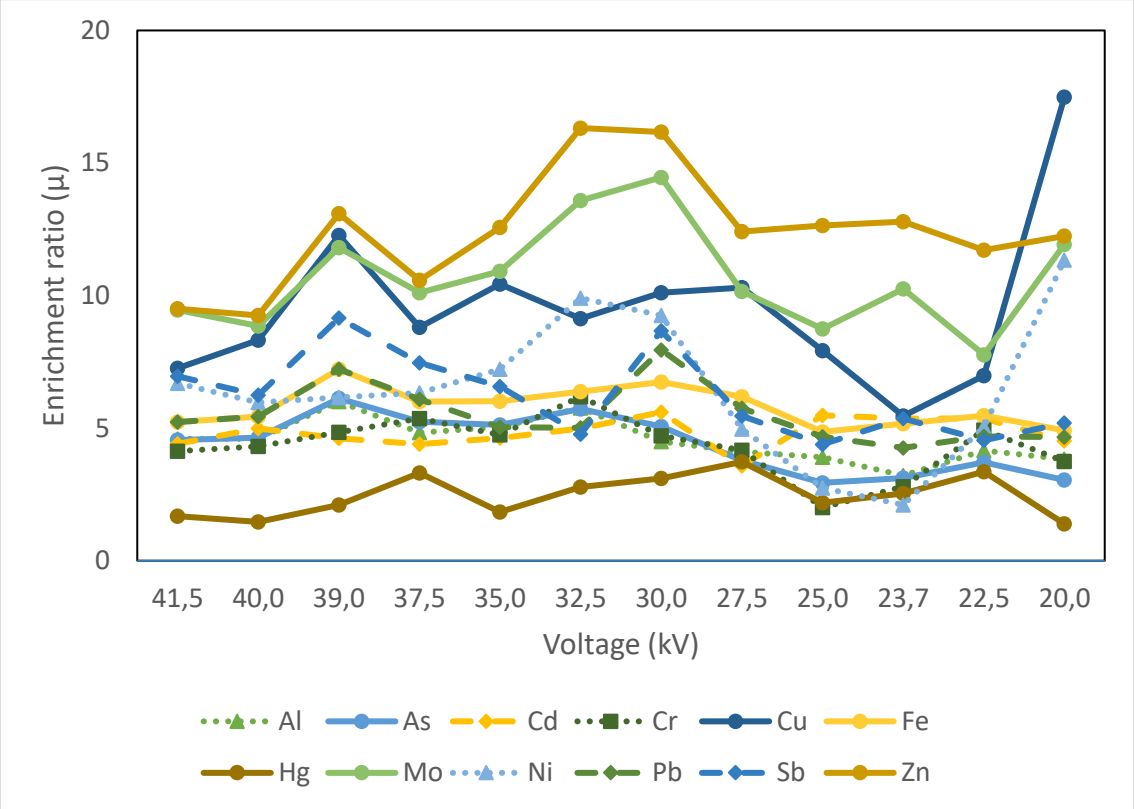

Figure 15.- Enrichment ratio in the conductive fraction for each PTE (plus Al and Fe). Average of three experimental runs at each voltage with a standard error <5%.

No clear tendencies were seen with respect to the enrichment ratios for any of the separated fractions (insulating, middlings, or conductive) and voltage. Considering the specific elements of interest (Fig. 3), here it can be seen that while some reached their highest enrichment ratio in the lower voltage range (e.g., Cu had μ = 7.49 at 20 kV in contrast with an μ = 7.26 at 41.5 kV), others exhibited the converse relation (e.g., Sb had μ = 9.15 at 39 kV compared to μ =4.54 at 22.5 kV).

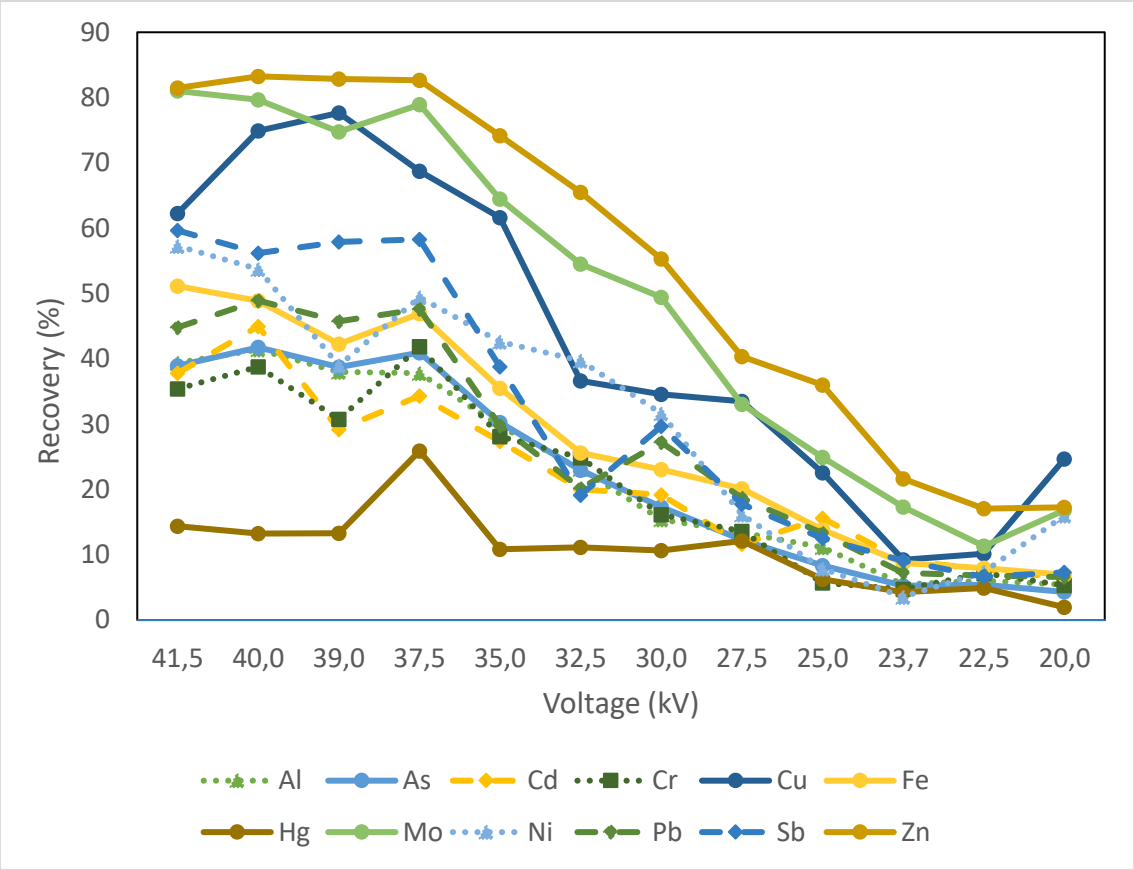

Figure 16.- Recovery in the conductive fraction for each PTE (plus Al and Fe). Average of three experimental runs at each voltage with a standard error <5%.

As with the yield, recovery (ε) in the conductive fraction also demonstrated a clear, positive correlation with voltage. Considering the recovery of individual elements, here Zn removal was the most successful, with recovery values of about 80% for voltages from 37 kV to 41.5 kV. The maximum recovery value for this element was 83.25 % with a yield, γ = 9 %, at an operating voltage of 40 kV. Recovery for this element decreased abruptly at 37 kV, a pattern seen for all 10 elements studied (Fig. 4). Referring back to Fig. 3 we see that the enrichment ratio for this element was high and varied very little with voltage (9 to 16%). Taking 39 kV, in the middle of this high-recovery range, the enrichment ratio μ=13.09% for which γ = 6.33% and ε = 82.86%.

Mo concentrations in the soil tested were bellow reference levels, however, we mention it here as its recovery levels were almost as high as those seen for Zn (see Fig. 6). That this method appears to be highly effective at separating this particular PTE is significant due to Mo's geochemical importance and economic interest.

The third best recovery values were recorded for Cu, the most important PTE in the soil tested. The maximum recovery value was 77.65% and this was achieved at 39 kV where

the enrichment ratio recorded was 12.27 %. As for the other PTE's examined here, the best results came at the highest voltages, with recovery values decreasing rapidly at lower voltages.

Regarding Sb, Ni and Pb, the maximum recovery values for these PTEs were 59.65% (41.5 kV), 53.73% (41.5 kV), and 48.92% (40 kV), respectively (Fig. 5). At these high voltages, the enrichment ratios for these elements were between 5 and 9%. As with the other elements tested, recovery fell dramatically at lower voltages.

Satisfactory yields were also obtained for Cd, Cr, and As, for which the maximum recovery values were 44.97% (40 kV), 41.85% (37.5 kV), and 41.75% (40 kV) respectively, with enrichment ratios ranging from 4 to 6 %. Mercury was the lowest yielding element in these experiments with a maximum recovery value of 25.88% (37.5 kV) and a corresponding enrichment ratio of 3.31%.Total concentrations results after the separation are presented in SM4.

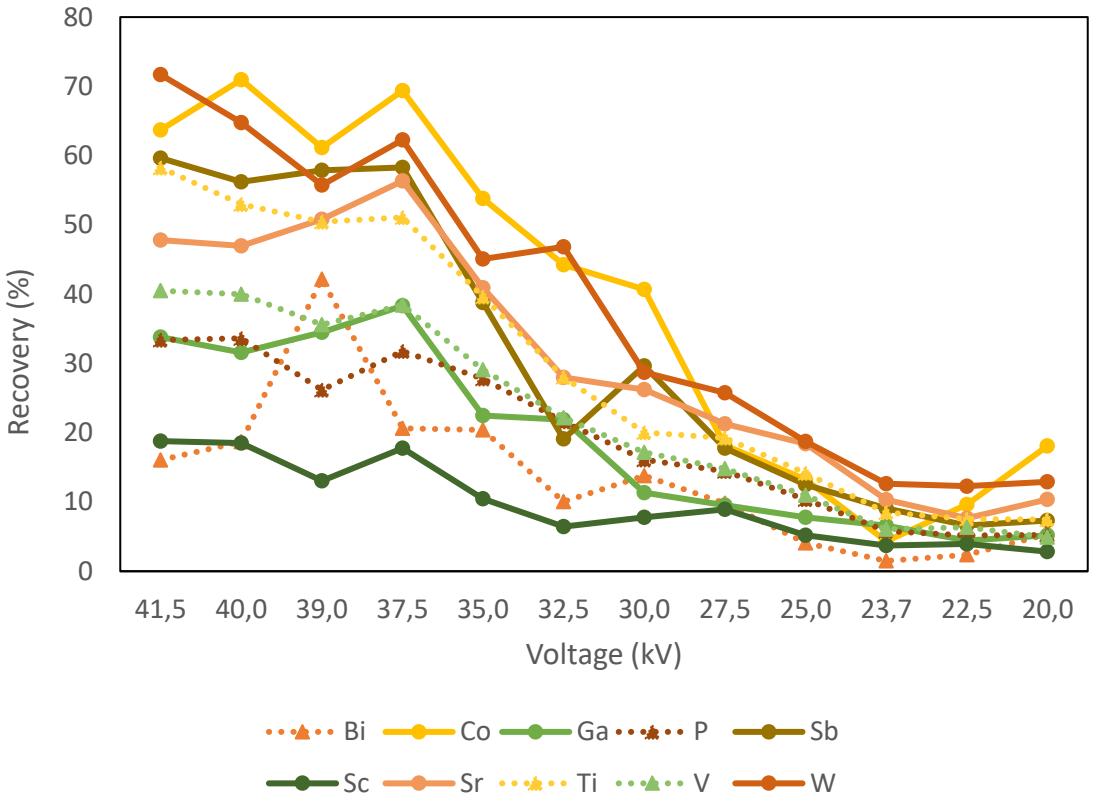

Figure 17.- Recovery of PTEs with significant economic value. Average of three experimental runs at each voltage with a standard error <5%.

3.3. Mineralogical analysis of the separated fractions

In order to evaluate the electrostatic separation method from a mineralogical point of view, the three fractions generated were examined under a binocular microscope. In this way, three main types of particles were identified (species 1, 2, and 3) and these were manually separated and studied using SEM-EDX to determine their mineralogical composition. Species 1 (spc.1) particles were found in the insulating fraction (nonconductive material) and were identified as feldspar (Fig. 6a). Further analysis revealed that these particles (Fig. 6, spc. a) were not pollutant bearing, suggesting a geogenic origin for the feldspar in these soil samples. Species 2 (spc. 2) type particles were found to be mica (Fig. 6b), and these were present in highest abundance among the middlings fraction. Analysis of the chemical composition of these particles revealed the presence of Pb and Zn, although in low concentrations (Fig. 6b, spc b). Finally, the most abundant particle in the conductive fraction (Fig. 6c), species 3 (spc. 3), corresponds to the slags identified in previous work on other soils in the region surrounding the site sampled here (Sierra et al., 2013). The presence of Cu, Pb, and Zn in conjunction with high levels of Fe, O, and S (indicating iron oxides and sulphides) points to the existing mineralization and/or mining and metallurgy activities as possible origin of these elements.

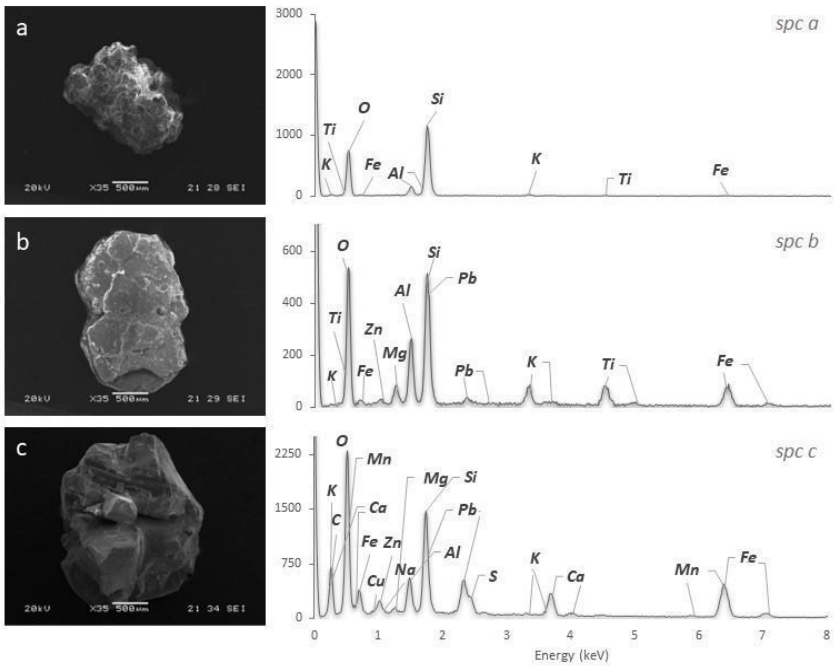

Figure 18.- Selected SEM images of each of the three predominant particle species present in soil fractions obtained after electrostatic separation with representative EDS spectra. a) Feldspar particle found in the insulating fraction, b) mica particle found in the middlings fraction, and c) slag particle found in the conductive fraction.

3.4. Selecting the conditions for optimal soil washing

We applied the technique of attributive analysis to our experimental results to determine the optimal experimental conditions (specifically the voltage used) for soil washing by electrostatic separation. This technique was designed by Sierra et al. (2010) and details of its derivation can be found in that article. Attributive analysis calculates a merit index (Q) for each experimental test based on the main parameters involved in the mineralogical concentration process thereby enabling tests to be ranked according to their effectiveness.

Optimal separation minimises yields while at the same time maximizing recovery values. Thus, the merit index of experiment i (where *i*=1, 2, …*m* representing each of the experimental voltages) with respect to PTE j (where *j*=1, 2, …*n* representing each of the PTEs tested) is as follows:

$$Q_j^i = \frac{Min\{\gamma\}}{\gamma^i} + \frac{\varepsilon_j^i}{Max\{\varepsilon\}_j} \quad (Eq.1)$$

Where:

- γ^i: Yield of experiment *i*.
- ε_{Ct}^i: Recovery value for the PTE *j* in experiment *i*.
- Q_j^i: Merit index for experiment *i* with respect to element *j*.

Of course, we wish to find a merit index that takes into account a particular experiment's performance across all elements of interest. However, we cannot simply add the individual merit indices for each experiment and element, since firstly, not all pollutants are equally abundant, and secondly, they each have very different maximum limits. Thus, a weighting factor, A, had to be introduced for each PTE (Eq.2, Eq.3):

$$A_j^i = \frac{\alpha_j^i}{TV} \quad (Eq.2)$$

$$A'^i_j = \frac{A_j^i}{\sum_i^m TV_j} \quad (Eq.3)$$

Where:

- α_j^i: Grade of the feed for the test *i* and element *j*.

- TV_j: Target value (international standard, see Table 1) for element j.
- A_j^i: Correction factor.
- A'^i_j: Adjusted correction factor.

Finally, the global merit index for each experiment was calculated as follows (Eq. 4):

$$Q^i_T = \sum_{j=1}^{n} Q^i_j A^{i\prime}_j \ (Eq. 4)$$

In this way, we have an indicator of how effectively each experimental voltage achieved separation: minimising yield and maximising recovery for each PTE taking into account its individual target levels. The results obtained using this formula for each voltage and PTE are shown in Table 2. It can be observed that higher voltages produce higher merit indices, indicating that broadly, higher voltages lead to more effective separation suggesting that these are the best operating conditions. Attributive analysis of this sort is expected to give an absolute maximum on the side of higher recoveries (41.5 kV) and thus, we conclude that, for optimal one-step separation, 41.5 kV is the best operating voltage.

Table 2.- Partial merit index (Q_j^i), adjusted correction factor ($A_j^{i\prime}$) and global merit index ($\boldsymbol{Q^i_T}$) for each experiment (i) and element (j).

		j																				
	Tens. (kV)	**As**		**Cd**		**Cr**		**Cu**		**Hg**		**Mo**		**Ni**		**Pb**		**Sb**		**Zn**		$\boldsymbol{Q^i_T}$
		Q_j^i	$Q_j^iA_j^{i\prime}$	Q_j^i	$Q_j^iA_j^{i\prime}$	Q_j^i	$Q_j^iA_j^{i\prime}$	Q_j^i	$Q_j^iA_j^{i\prime}$	Q_j^i	$Q_j^iA_j^{i\prime}$	Q_j^i	$Q_j^iA_j^{i\prime}$	Q_j^i	$Q_j^iA_j^{i\prime}$	Q_j^i	$Q_j^iA_j^{i\prime}$	Q_j^i	$Q_j^iA_j^{i\prime}$	Q_j^i	$Q_j^iA_j^{i\prime}$	
i	**41.5**	1.013	0.092	0.921	0.106	0.926	0.080	0.881	0.094	0.636	0.104	1.081	0.185	1.081	0.111	0.997	0.111	1.081	0.108	1.059	0.176	1.142
	40	1.077	0.096	1.077	0.095	1.003	0.076	1.041	0.129	0.588	0.085	1.060	0.165	1.015	0.089	1.077	0.089	1.019	0.094	1.077	0.173	1.089
	39	1.037	0.075	0.758	0.067	0.843	0.053	1.109	0.125	0.622	0.083	1.032	0.102	0.790	0.039	1.044	0.039	1.080	0.078	1.104	0.118	0.818
	37.5	1.069	0.093	0.852	0.074	1.088	0.092	0.973	0.159	1.088	0.113	1.063	0.112	0.951	0.098	1.061	0.098	1.066	0.103	1.081	0.134	1.067
	35	0.842	0.052	0.725	0.046	0.788	0.054	0.911	0.055	0.536	0.042	0.913	0.066	0.861	0.046	0.725	0.046	0.767	0.054	1.008	0.078	0.559
	32.5	0.722	0.049	0.617	0.039	0.766	0.043	0.643	0.039	0.602	0.032	0.845	0.050	0.865	0.053	0.584	0.053	0.493	0.053	0.959	0.053	0.469
	30	0.616	0.041	0.628	0.044	0.587	0.041	0.647	0.052	0.613	0.035	0.812	0.051	0.754	0.050	0.758	0.050	0.699	0.047	0.866	0.051	0.467
	27.5	0.506	0.040	0.471	0.038	0.536	0.046	0.643	0.041	0.681	0.030	0.620	0.041	0.494	0.040	0.594	0.040	0.510	0.036	0.697	0.043	0.402
	25	0.443	0.034	0.589	0.049	0.379	0.049	0.533	0.027	0.484	0.020	0.550	0.032	0.379	0.033	0.514	0.033	0.452	0.031	0.675	0.035	0.339
	23.7	0.535	0.037	0.610	0.036	0.521	0.040	0.527	0.020	0.574	0.023	0.622	0.017	0.471	0.055	0.556	0.055	0.561	0.027	0.668	0.018	0.302
	22.5	0.603	0.038	0.648	0.048	0.646	0.039	0.605	0.029	0.663	0.020	0.614	0.030	0.603	0.042	0.614	0.042	0.585	0.031	0.679	0.025	0.334
	20	0.592	0.043	0.631	0.036	0.615	0.038	0.807	0.029	0.565	0.039	0.697	0.023	0.768	0.036	0.623	0.036	0.612	0.036	0.696	0.023	0.341

4. Conclusions

Soils in regions with a history of mining and metallurgy often contain high levels of PTEs that require treatment. In this study, we treated soil samples taken from the La Cruz site in the Linares-La Carolina mining district. This sandy loam soil, typical of the Mediterranean region, contained significant levels of several PTEs, particularly Cu, Zn, and Pb.

Physical and chemical soil washing are well-established remediation strategies for PTE-contaminated soils. Electrostatic separation offers the possibility of separating virtually any mix of materials provided there is enough conductivity difference between components in that mix. Thus, we feel electrostatic separation should be considered among the available tools for soil separation in soil washing operations. The main limitation of electrostatic separation is the need for low moisture levels in the feed and thus the high cost that would be entailed in drying soils before processing. Fortunately, due to the local climate conditions of the site studied here, the soil to be treated was entirely dry.

The results presented here prove that electrostatic separation is a potentially useful tool for decontaminating the coarser fractions of sandy, dry, slag containing soils. In addition, the semi-industrial rig used in this investigation offers the immediate possibility of scaling up operations. The yields obtained in this work ranged from 0.69% to 9% with high recovery values for three PTEs: Zn (83.25%), Cu (77.65%), and Mo (81.01%); and significant recovery levels for six others: Sb, Pb, As, Ni, Cr, and Cd (45-60%). This suggests that substantial quantities of contaminated soil might be economically treated in a single, real-scale stage, which is unusual for a soil washing procedure. This initial success makes it feasible to envisage subsequent rewashing cycles aiming for a complete soil treatment.

Finally, we have demonstrated that attributive analysis can provide a quality index to establish an optimal separation voltage. According to this analysis, optimal concentrations for the PTEs tested are obtained at 41.5 kV. We suggest that programmes for soil remediation should make use of this mathematical procedure to improve outcomes. Further quotients could be included in this methodology to take account of not only separation performance but also environmental and economic aspects so incorporating the concept of the circular economy into soil remediation operations.

References

Adamo, P., Dudka, S., Wilson, M. J., & McHardy, W. J. (1996). Chemical and mineralogical forms of Cu and Ni in contaminated soils from the Sudbury mining and smelting region, Canada. *Environmental Pollution*, *91*(1), 11–19. https://doi.org/10.1016/0269-7491(95)00035-P

Aitani, A. M. (2004). Oil Refining and Products. *Encyclopedia of Energy*, 715–729. https://www.academia.edu/21206560/Oil_Refining_and_Products

Anderson, R., Rasor, E., & van Ryn, F. (1999). Particle size separation via soil washing to obtain volume reduction. *Journal of Hazardous Materials*, *66*(1–2), 89–98. https://doi.org/10.1016/S0304-3894(98)00210-6

Bedeković, G., & Trbović, R. (2020). Electrostatic separation of aluminium from residue of electric cables recycling process. *Waste Management*, *108*, 21–27. https://doi.org/10.1016/j.wasman.2020.04.033

Beiyuan, J., Tsang, D. C. W., Valix, M., Baek, K., Ok, Y. S., Zhang, W., Bolan, N. S., Rinklebe, J., & Li, X. D. (2018). Combined application of EDDS and EDTA for removal of potentially toxic elements under multiple soil washing schemes. *Chemosphere*, *205*, 178–187. https://doi.org/10.1016/J.CHEMOSPHERE.2018.04.081

Buchman, M., & Office of Response, N. (n.d.). *SQuiRT Cards, 2008*.

Chen, X., Xia, X., Zhao, Y., & Zhang, P. (2010). Heavy metal concentrations in roadside soils and correlation with urban traffic in Beijing, China. *Journal of Hazardous Materials*, *181*(1–3), 640–646. https://doi.org/10.1016/J.JHAZMAT.2010.05.060

Dermont, G., Bergeron, M., Mercier, G., & Richer-Laflèche, M. (2008). Soil washing for metal removal: A review of physical/chemical technologies and field applications. *Journal of Hazardous Materials*, *152*(1), 1–31. https://doi.org/10.1016/J.JHAZMAT.2007.10.043

EEA. (2009). *Overview of economic activities causing soil contamination in some WCE and SEE countries*. European Environment Agency (EEA). https://www.eea.europa.eu/data-and-maps/figures/overview-of-economic-activities-causing-soil-contamination-in-some-wce-and-see-countries-pct-of-investigated-sites

Feng, W., Zhang, S., Zhong, Q., Wang, G., Pan, X., Xu, X., Zhou, W., Li, T., Luo, L., & Zhang, Y. (2020). Soil washing remediation of heavy metal from contaminated soil with EDTMP and PAA: Properties, optimization, and risk assessment. *Journal of Hazardous Materials*, *381*, 120997. https://doi.org/10.1016/J.JHAZMAT.2019.120997

França, F. C. S. S., Albuuerque, A. M. A., Almeida, A. C., Silveira, P. B., Filho, C. A., Hazin, C. A., & Honorato, E. v. (2017). Heavy metals deposited in the culture of lettuce (Lactuca sativa L.) by the influence of vehicular traffic in Pernambuco, Brazil. *Food Chemistry*, *215*, 171–176. https://doi.org/10.1016/J.FOODCHEM.2016.07.168

Gu, Y., Yeung, A. T., & Li, H. (2018). Enhanced electrokinetic remediation of cadmium-contaminated natural clay using organophosphonates in comparison with EDTA. *Chinese Journal of Chemical Engineering*, *26*(5), 1152–1159. https://doi.org/10.1016/J.CJCHE.2017.10.012

Inculet, I. I. (1984). *Electrostatic mineral separation*. 153. https://books.google.com/books/about/Electrostatic_Mineral_Separation.html?hl=es&id=m_XmAAAAMAAJ

Kawatra, S. K., & Young, C. (2019). *SME mineral processing & extractive metallurgy handbook*. 2203.

Kdidi, S., Vaca-Medina, G., Peydecastaing, J., Oukarroum, A., Fayoud, N., & Barakat, A. (2019). Electrostatic separation for sustainable production of rapeseed oil cake protein concentrate: Effect of mechanical disruption on protein and lignocellulosic fiber separation. *Powder Technology*, *344*, 10–16. https://doi.org/10.1016/j.powtec.2018.11.107

Khalid, S., Shahid, M., Niazi, N. K., Murtaza, B., Bibi, I., & Dumat, C. (2017). A comparison of technologies for remediation of heavy metal contaminated soils. *Journal of Geochemical Exploration*, *182*, 247–268. https://doi.org/10.1016/J.GEXPLO.2016.11.021

Li, Q., Guo, L., Cao, H., Li, A., Xu, W., & Wang, Z. (2021). Effects of an effective adsorption region on removing catalyst particles from an FCC slurry under a DC electrostatic field. *Powder Technology*, *377*, 676–683. https://doi.org/10.1016/j.powtec.2020.09.038

Li, Q., Zhang, Z., Wu, Z., Wang, Z., & Guo, L. (2019). Effects of electrostatic field and operating parameters on removing catalytic particles from FCCS. *Powder Technology*, *342*, 817–828. https://doi.org/10.1016/j.powtec.2018.10.060

Li, X., & Thornton, I. (1993). Multi-element contamination of soils and plants in old mining areas, U.K. *Applied Geochemistry*, *8*, 51–56. https://doi.org/10.1016/S0883-2927(09)80010-3

Li, X., & Thornton, I. (2001). Chemical partitioning of trace and major elements in soils contaminated by mining and smelting activities. *Applied Geochemistry*, *16*(15), 1693–1706. https://doi.org/10.1016/S0883-2927(01)00065-8

Li, Y., Liao, X., & Li, W. (2019). Combined sieving and washing of multi-metal-contaminated soils using remediation equipment: A pilot-scale demonstration. *Journal of Cleaner Production*, *212*, 81–89. https://doi.org/10.1016/J.JCLEPRO.2018.11.294

Lillo Ramos, F. J. (1992). *Geology and geochemistry of Linares-La Carolina Pb-ore field (southeastern border of the Hesperian Massif)*.

Loredo, J., Ordóñez, A., Gallego, J. R., Baldo, C., & García-Iglesias, J. (1999). Geochemical characterisation of mercury mining spoil heaps in the area of Mieres (Asturias, northern Spain). *Journal of Geochemical Exploration*, *67*(1–3), 377–390. https://doi.org/10.1016/S0375-6742(99)00066-7

Lorite, I. J., Castilla, A., Cabezas, J. M., Alza, J., Santos, C., Porras, R., ... & Sillero, J. C. (2023). Analyzing the impact of extreme heat events and drought on wheat yield and protein concentration, and adaptation strategies using long-term cultivar trials under semi-arid conditions. Agricultural and Forest Meteorology, 329, 109279. https://doi.org/10.1016/j.agrformet.2022.109279.

Makino, T., Sugahara, K., Sakurai, Y., Takano, H., Kamiya, T., Sasaki, K., Itou, T., & Sekiya, N. (2006). Remediation of cadmium contamination in paddy soils by washing with chemicals: Selection of washing chemicals. *Environmental Pollution*, *144*(1), 2–10. https://doi.org/10.1016/J.ENVPOL.2006.01.017

Martínez, J., Llamas, J., de Miguel, E., Rey, J., & Hidalgo, M. C. (2007a). Determination of the geochemical background in a metal mining site: example of the mining district of Linares (South Spain). *Journal of Geochemical Exploration*, *94*(1–3), 19–29. https://doi.org/10.1016/j.gexplo.2007.05.001

Martínez, J., Llamas, J. F., de Miguel, E., Rey, J., & Hidalgo, M. C. (2007b). Application of the Visman method to the design of a soil sampling campaign in the mining district of Linares (Spain). *Journal of Geochemical Exploration*, *92*(1), 73–82. https://doi.org/10.1016/j.gexplo.2006.07.004

Martínez, J., Rey, J., Hidalgo, M. C., & Benavente, J. (2012). Characterizing abandoned mining dams by geophysical (ERI) and geochemical methods: The Linares-La Carolina district (Southern Spain). *Water, Air, and Soil Pollution*, *223*(6), 2955–2968. https://doi.org/10.1007/s11270-012-1079-7

Park, C. H., Subasinghe, N., & Jeon, H. S. (2015). Separation of covering plastics from particulate copper in cable wastes by induction electrostatic separation. *Materials Transactions*, *56*(7), 1140–1143. https://doi.org/10.2320/matertrans.M2015138

Piccolo, A., Spaccini, R., de Martino, A., Scognamiglio, F., & di Meo, V. (2019). Soil washing with solutions of humic substances from manure compost removes heavy metal contaminants as a function of humic molecular composition. *Chemosphere*, *225*, 150–156. https://doi.org/10.1016/J.CHEMOSPHERE.2019.03.019

Pfeifroth, Uwe; Kothe, Steffen; Müller, Richard; Trentmann, Jörg; Hollmann, Rainer; Fuchs, Petra; Werscheck, Martin (2017): Surface Radiation Data Set - Heliosat (SARAH) - Edition 2, Satellite Application Facility on Climate Monitoring, https://doi.org/10.5676/EUM_SAF_CM/SARAH/V002

Rui, D., Wu, Z., Ji, M., Liu, J., Wang, S., & Ito, Y. (2019). Remediation of Cd- and Pb-contaminated clay soils through combined freeze-thaw and soil washing. *Journal of Hazardous Materials*, *369*, 87–95. https://doi.org/10.1016/J.JHAZMAT.2019.02.038

Sierra, C., Gallego, J. R., Afif, E., Menéndez-Aguado, J. M., & González-Coto, F. (2010). Analysis of soil washing effectiveness to remediate a brownfield polluted with pyrite ashes. *Journal of Hazardous Materials*, *180*(1–3), 602–608. https://doi.org/10.1016/j.jhazmat.2010.04.075

Sierra, C., Martínez, J., Menéndez-Aguado, J. M., Afif, E., & Gallego, J. R. (2013). High intensity magnetic separation for the clean-up of a site polluted by lead metallurgy. *Journal of Hazardous Materials*, *248–249*(1), 194–201. https://doi.org/10.1016/j.jhazmat.2013.01.011

Tabtabaei, S., Konakbayeva, D., Rajabzadeh, A. R., & Legge, R. L. (2019). Functional properties of navy bean (Phaseolus vulgaris) protein concentrates obtained by pneumatic tribo-electrostatic separation. *Food Chemistry*, *283*, 101–110. https://doi.org/10.1016/j.foodchem.2019.01.031

Tabtabaei, S., Vitelli, M., Rajabzadeh, A. R., & Legge, R. L. (2017). Analysis of protein enrichment during single- and multi-stage tribo-electrostatic bioseparation processes for dry fractionation of legume flour. *Separation and Purification Technology*, *176*, 48–58. https://doi.org/10.1016/j.seppur.2016.11.050

Uchimiya, M., Wartelle, L. H., Klasson, K. T., Fortier, C. A., & Lima, I. M. (2011). Influence of pyrolysis temperature on biochar property and function as a heavy metal sorbent in soil. *Journal of Agricultural and Food Chemistry*, *59*(6), 2501–2510. https://doi.org/10.1021/JF104206C/SUPPL_FILE/JF104206C_SI_001.PDF

Villot, A., Gonthier, Y., Gonze, E., Bernis, A., Ravel, S., Grateau, M., & Guillaudeau, J. (2012). Separation of particles from syngas at high-temperatures with an electrostatic precipitator. *Separation and Purification Technology*, *92*, 181–190. https://doi.org/10.1016/j.seppur.2011.04.028

Wang, G., Zhang, S., Zhong, Q., Xu, X., Li, T., Jia, Y., Zhang, Y., Peijnenburg, W. J. G. M., & Vijver, M. G. (2018). Effect of soil washing with biodegradable chelators on the toxicity of residual metals and soil biological properties. *Science of The Total Environment*, *625*, 1021–1029. https://doi.org/10.1016/J.SCITOTENV.2018.01.019

Wills, B. A., & Napier-Munn, T. J. (2006). Mineral Processing Technology: An Introduction to the Practical Aspects of Ore Treatment and Mineral Recovery. In Butterworth-Heinemann (Ed.), *Wills' Mineral Processing Technology* (7th ed). Butterworth-Heinemann. https://doi.org/10.1016/C2010-0-65478-2

Wu, Q., Leung, J. Y. S., Geng, X., Chen, S., Huang, X., Li, H., Huang, Z., Zhu, L., Chen, J., & Lu, Y. (2015). Heavy metal contamination of soil and water in the vicinity of an abandoned e-waste recycling site: Implications for dissemination of heavy metals. *Science of The Total Environment*, *506–507*, 217–225. https://doi.org/10.1016/J.SCITOTENV.2014.10.121

Xu, J., Kleja, D. B., Biester, H., Lagerkvist, A., & Kumpiene, J. (2014). Influence of particle size distribution, organic carbon, pH and chlorides on washing of mercury

contaminated soil. *Chemosphere*, *109*, 99–105. https://doi.org/10.1016/J.CHEMOSPHERE.2014.02.058

Yang, X., Wang, H., Peng, Z., Hao, J., Zhang, G., Xie, W., & He, Y. (2018). Triboelectric properties of ilmenite and quartz minerals and investigation of triboelectric separation of ilmenite ore. *International Journal of Mining Science and Technology*, *28*(2), 223–230. https://doi.org/10.1016/j.ijmst.2018.01.003

Zhao, F. J., Ma, Y., Zhu, Y. G., Tang, Z., & McGrath, S. P. (2015). Soil contamination in China: Current status and mitigation strategies. *Environmental Science and Technology*, *49*(2), 750–759. https://doi.org/10.1021/ES5047099/SUPPL_FILE/ES5047099_SI_001.PDF

Zhao, L., Ding, Z., Sima, J., Xu, X., & Cao, X. (2017). Development of phosphate rock integrated with iron amendment for simultaneous immobilization of Zn and Cr (VI) in an electroplating contaminated soil. *Chemosphere*, *182*, 15–21. https://doi.org/10.1016/J.CHEMOSPHERE.2017.05.004

Universidad de Oviedo

CHAPTER III: A novel heuristic tool for selecting the best upgrading conditions for the removal of potentially toxic elements by soil washing

X. Corres, C. Sierra, A.J. Diez-Mestas, J.R. Gallego, D. Baragaño

Journal of Hazardous Materials 466 (2024) 133529

Abstract

Here we propose two-parameter penalized attributive analysis, PPAA-U, a novel heuristic tool for selecting the best upgrading conditions (BUCs) for soil washing. Given a multicomponent feed and a specific set of operating conditions, PPAA-U generates a quality index based on how well recoveries for key components are maximized while minimizing the yield. We demonstrate, through the calculation of families of curves, that this quality index is related linearly to recovery and to the inverse of the yield meaning that reducing yield values is more important than maximizing recovery. To test our method, electrostatic separation at 12 different voltages was carried out on soil samples from an ex-industrial site in Spain. Values of recovery, yield and grade were analyzed using basic attributive analysis and PPAA-U with and without target-to-distance correction. Both methods identified the same optimal separation voltage and the power of PPAA-U to correct for high variation in yields and recoveries was observed as a divergence between results produced by each method at low voltages where variation in these values was greatest. PPAA_U thus offers a convenient tool for soil washing optimization and we suggest that it could be applied successfully to other industrial processes.

Keywords

Soil pollution, soil remediation, optimization, circular economy.

Environmental implications

Two-parameter penalized attribute analysis for upgrading (PPAA-U) provides a way to optimize soil remediation operations and is, thus, a valuable tool to improve environmental outcomes. The method assesses how well a given set of operating conditions maximizes recovery while simultaneously minimizing the concentrate yield and its primary advantage lies in the way it provides a single value, the quality index, to identify optimal separation conditions. Furthermore, PPAA-U could be adapted easily to various processes and thus has numerous potential applications in a range of industries; in particular, its capacity to address multiple variables opens new avenues for sustainable materials processing and manufacturing.

1. Introduction

Many industrial processes lead to the accumulation of potentially toxic elements (PTEs) in soils, and the need to remove them is driving research into soil remediation techniques in several countries (Sun et al., 2019; Wu et al., 2015). Existing soil remediation technologies include various physical, chemical, and biological methods (Ashraf et al., 2019; Khalid et al., 2017). Originally developed in the mining industry to obtain metal concentrates from mineral ores, physical separation technologies have been used for soil remediation in the case of both organic and inorganic pollutants (Aparicio et al., 2022; Baragaño et al., 2023; Wan et al., 2020). Physical separation can be used to remove potentially toxic elements (PTEs) from soil either directly, where PTEs are present as discrete particles, or, since many PTEs are strongly absorbed by clay, by separating the fraction onto which they are preferentially sorbed (Baragaño et al., 2021; Gu et al., 2022; Liu et al., 2022). Although physical soil washing can be a terminal process, it is usually followed by chemical soil washing (Sierra et al., 2014; Tran et al., 2022).

Physical soil remediation shares many common processes with mineral beneficiating and recycling. In all cases, the objective is to separate a concentrate of perhaps two, or more, target components from a multicomponent feed. However, whereas in mineral beneficiation (and recycling), optimization may occur for either elements or mineral compounds, in the case of soil washing, we tend to be concerned only with elements.

The principal distinction between soil remediation and mineral processing (beneficiation or recycling) lies in the different economics of these processes. These considerations mean that the concentrate-to-tailings ratio achieved in mineral processing operations is generally closer to one than it is in soil remediation (Bunge et al., 1995). In mineral beneficiation, for example, the cost of further processing the concentrate (through the pyro- and hydrometallurgical routes) is offset due to the value of the final product (Nishiyama et al., 2000; Richardson et al., 1999); however, for soil washing, a high initial concentrate-to-tailing ratio is crucial to avoid compromising the economic viability of the operation (Schulz, 1970).

This means that, for soil remediation, in contrast to mineral beneficiation and recycling, concentrate yield minimization is the most important criterion. Moreover, in soil remediation, the washed fraction (tailings) must adhere to environmental standards in

terms of grade for it to be declared decontaminated, whereas in mineral recycling and beneficiation, the grade of tailings is dictated more by economic considerations and may remain quite high provided that the process is profitable (Gupta & Yan, 2016; Weiss, 1985).

In any mineral separation process, whether this be a beneficiation or soil remediation process, improving performance implies increasing the concentration of a target element or compound in one of the process flows. Thus, the total mass of the initial material flow, known as the feed (F), is normally separated into two products, the concentrate (C) and the tailings (T), corresponding to the fractions in which the grade of the target element or compound is, respectively, higher or lower than that in the feed. A third fraction is sometimes collected, the middlings (M), which has a grade intermediate between that of the concentrate and the tailings.

The total mass balance is then (Wills & Finch, 2015):

$$\mathrm{F} = \mathrm{C} + \mathrm{M} + \mathrm{T} \ (\mathrm{Eq.}\ 1)$$

Dividing Equation 1 by the mass of the feed gives the yield or weight recovery for each mass flow (Eq. 2) (Drzymala, 2006):

$$\frac{\mathrm{F}}{\mathrm{F}} = 1 = \frac{\mathrm{C}}{\mathrm{F}} + \frac{\mathrm{M}}{\mathrm{F}} + \frac{\mathrm{T}}{\mathrm{F}} \ (\mathrm{Eq.}\ 2)$$

Of the three yields, that of most interest is the concentrate yield, $\frac{\mathrm{C}}{\mathrm{F}} = \gamma$, which contains the highest concentration of the target element or compound.

A parameter known as the grade or assay is used to indicate the proportion of the target element or compound in each of the mass flows. Its value for the concentrate is usually denoted as λ, and this value can be used as an assessment of the quality of the separation process. The grades for the feed, middlings and tailings are denoted by α, β, and ϑ, respectively. In a successful separation process, the following inequalities should be true: $\lambda > \alpha$; $\vartheta < \alpha$; and $\lambda > \beta > \alpha$ (Drzymala, 2006). The recovery, ε, refers to the mass of the target element or compound found in a given mass flow relative to the feed. Thus, for the concentrate fraction, recovery is defined as (Drzymala, 2006):

$$\varepsilon = \frac{\lambda}{\alpha}\gamma \ (\mathrm{Eq.}\ 3)$$

The same value for the tailings fraction is usually denoted as η, such that (Drzymala, 2006):

$$\varepsilon + \eta = 1 \text{ (Eq. 4)}$$

Intuitively, it would seem that ε alone could be used as a measure of separation performance due to its relationship to the parameters α, λ and γ. However, this is not the case and, in fact, assessing separation performance requires consideration of not only ε but at least two of either α, λ or γ. For example, ε=100% may seem to imply perfect separation, but accompanied by high γ and low λ, this is clearly not so. Thus, if we wish to optimize a separation process, we must maximize ε and λ while simultaneously minimizing γ (Drzymala, 2006; Taggart. A.F., 1947; Wills & Finch, 2015).

Bearing in mind the above discussion, the aim of this research is to develop a robust method for determining the best upgrading conditions for a given soil washing operation. Specifically, we will:

- Offer an exhaustive analysis of basic attributive analysis in terms of families of curves.
- Discuss the distortion of quality statistics due to the data dispersion of particular experimental set-ups.
- Show how attributive analysis can be modified to address this type of distortion.
- Provide a practical example of the use of attributive analysis.

2. Materials and methods

In this section, we discuss the sources of the soil samples and the separation technique used to demonstrate the practical application of attributive analysis. We then explain the principles of basic and penalized attributive analysis.

2.1. Sample preparation and analysis

The site of interest is the Linares mining district (Andalusia, Spain), a center for intense Pb mining, mineral processing, and metallurgical activities for several centuries (Cortada et al., 2018; Rosendo et al., 2022). Ten 2.5 kg samples were collected from the top 35 cm layer of soil at random points across the study site to form a bulk sample of 25 kg. The bulk sample was homogenized and wet sieved (water flow = 0.3 l/min) using sodium carbonate and sodium hexametaphosphate as dispersing agents to produce six granulometric fractions: 63 μm, 63-125 μm, 125-250 μm, 250-500 μm, 500-1000 μm, and 1000-2000 μm (ASTM D-422-63). Wet sieving continued until 3 kg of the 1000-2000 μm fraction was obtained. This fraction was then divided into 36 subsamples for electrostatic separation. Each of these subsamples was subjected to chemical analysis.

Subsequently, representative subsamples weighing 1 g each were extracted. These specimens were digested using "Aqua regia" (a mixture of HCl and HNO_3) before analysis via inductively coupled plasma optical emission spectroscopy (ICP–OES) (HP 7700, Agilent Technologies).

Separation of the feed samples was achieved using an EHTP Outotec (Fig. S1) high-tension electrostatic separator. This advanced specification model is equipped with an AC wiper electrode operating at 18 kV and two DC electrodes—one corona and the other static—adjustable to a maximum of 41.5 kV, known as the separation voltage. Additionally, it features a grounded roller brush with interchangeable bristles and infrared roller heating for particle removal. Three fractions are collected, the nonconductive, intermediate, and conductive fractions.

The most important parameters in the separation process include the conductivity of the sample particles, the rotation speed of the roller, the placement of the electrodes, and the corona electrode tension. This enables the separation of materials based on their

conductivity properties, making electrostatic separation an invaluable tool for many industrial and research applications.

Samples are loaded onto the roller via the feed hopper and travel towards the corona electrode. The air surrounding the corona electrode is ionized; thus, as the particles on the roller approach the corona electrode, they pick up charge. Conductive particles will lose their charge most rapidly; therefore, the roller's centrifugal force ejects these particles first, and they are collected in the conductors bin. More insulating particles keep their charge and remain on the roller until they are brushed off and fall into either the insulators or the middlings bin.

The apparatus was operated at 12 different separating voltages in a range from 20 kV to 41.5 kV. Separations were repeated three times at each separation voltage, and the results presented here correspond to the average values recorded for the three experiments completed at each voltage. A comprehensive description of the apparatus is provided in the supplementary material section (SM1).

2.2. Basic attributive analysis

The basic model for attributive analysis was developed and applied to soil washing by Sierra et al. (2010) and Boente et al. (2017). Given the results of a number of soil-washing experiments using a particular separation technique, this method seeks to determine the set of experimental parameters that provides optimal separation. As discussed this is done by seeking the conditions where the recovery of target elements is maximized while minimizing the yield.

Considering a set of *m* experiments to separate out *n* contaminating elements, the performance of a given experiment, *i*, with respect to target element, *j*, is expressed as a quality factor Q_j^i (Eq. 5):

$$Q_j^i = \frac{\mathrm{Min}\{\gamma\}}{\gamma^i} + \frac{\varepsilon_j^i}{\mathrm{Max}\{\varepsilon_j\}} \quad (\mathrm{Eq.}\,5)$$

Where:

- $i = 1, \ldots, m$ and refers to the results produced by a specific set of experimental parameters.

- j = 1, …, n and refers to results for a specific target element or contaminant; in this study, m = 10 (see Table 3 for all target elements considered).
- Q_j^i: Quality factor of experiment i for element j.
- γ^i: Yield of experiment i.
- ε_j^i: Recovery of element j in experiment i;

In the present study, the main experimental variable is the separation voltage; thus, m =12 and ten target elements (the values of j) were considered (see Table 3). Table 3 presents the yields and recoveries of each element at each separation voltage tested; the values shown are an average of the results from three experimental runs at the same separation voltage.

As in the present study, there are generally numerous contaminants to consider, each of which has a specific target grade, that is, a safe threshold concentration after soil washing. Because some contaminants are significantly more toxic than others are, each element to be removed during the soil washing operation is given a weighting coefficient related to its target grade known as the target-to-distance correction. The sum of these coefficients must add up to 1; thus, we first define A_j^i $(Eq. 6)$:

$$A_j^i = \frac{\alpha_j^i}{\propto_j^{target}} \text{ (Eq. 6)}$$

Where:

- i and j are defined as before.
- α_j^i: Feed grade of element j in experiment i.
- $\propto_j^{target}$: Target grade for element j.

Then, to obtain the correct weighting for each element's contribution to overall contamination levels, the following transformation is implemented (Eq. 7):

$$A_j^{i\prime} = \frac{A_j^i}{\sum_i^m A_j^i} (Eq. 7)$$

A global quality index for a given experiment, *i*, for all elements $\left(Q_T^i\right)$ can then be defined as follows (Eq. 8):

$$Q_T^i = \sum_{j=1}^{n} Q_j^i A_j^{i\prime} \ (Eq. 8)$$

Finally, the best experimental set up is, then, that for which this value is maximal (Eq. 9):

$$Q_{optimal} = \ \mathrm{Max}\left\{\sum_{j=1}^{n} Q_j^i A_j^{i\prime}\right\} \ (Eq. 9)$$

where the following restrictions apply:

$$\left\{\forall \alpha_j^i, \gamma^i, \varepsilon_j^i, m, n, Q_T^i: \alpha_j^i \in \left[\alpha_j^{target}, 10^6\right], \gamma^i, \varepsilon_j^i \in (0,100], m, n \in \mathbb{N}, Q_T^i \in (0,2n)\right\}$$

2.3. Two parameter penalized attribute analysis (PPAA-U)

As can be appreciated from Equation 5 and Equation 6, experiments for which the yield, recovery, or grade varies greatly compared to the mean values will be given disproportionally more weight than those resulting in less variance. This will clearly bias the final quality assessment; thus, we present a modified method to address and eliminate this problem. Specifically, the inverse of the standard deviation can be used as a weighting factor to penalize large variations in each of the parameters of interest, yield, recovery, and grade, all of which vary for each element and every experiment. In addition, because the range of variation will be of a different order of magnitude for each parameter (for instance, in our case study, ε [%] is in the range {2, 83.3}, while γ [%] is in the range {0.7, 9}, and α [mg/kg] is in the range {0.32, 3108.21}, see Table 3), the weighting factors must be normalized to between 0 and 1.

In this way, we obtain a new value for the quality factor of each experiment and target element, C_j^i (Eq. 10—Eq. 14):

$$\Gamma^i = \frac{\mathrm{Min}\{\gamma\}}{\gamma^i}\left(\frac{\sum_{i=1}^{m}\left|\gamma^i - \bar{\gamma}\right|}{m}\right)^{-1} \ (Eq. 10)$$

$$\Gamma^{i\prime} = \frac{\Gamma^i}{\sum_i^m \Gamma^i} \ (Eq. 11)$$

$$E_j^i = \frac{\varepsilon_j^i}{Max\{\varepsilon_j\}}\left(\frac{\sum_{i=1}^{m}\left|\varepsilon_j^i - \overline{\varepsilon}_j\right|}{m}\right)^{-1} (Eq. 12)$$

$$E_j^{i'} = \frac{E_j^i}{\sum_i^m E_j^i} (Eq. 13)$$

$$C_j^i = \Gamma^{i'} + E_j^{i'} (Eq. 14)$$

and a new target-to-distance correction coefficient, $B_j^{i'}$ (Eq. 15 - Eq. 16):

$$B_j^i = \frac{\alpha_j^i}{\propto_j^{target}}\left(\frac{\sum_{i=1}^{m}\left|\propto_j^i - \overline{\alpha}_j\right|}{m}\right)^{-1} (Eq. 15)$$

$$B_j^{i\prime} = \frac{B_j^i}{\sum_i^m B_j^i} (Eq. 16)$$

Thus, the corrected global quality index for an experiment *i* for all elements *j* to *n* is:

$$C_T^i = \sum_{j=1}^{n} C_j^i B_j^{i\prime} \text{ (Eq. 17)}$$

Finally, the optimal experimental set up can be found as follows:

$$C_{optimal} = Max\left\{\sum_{j=1}^{n} C_j^i B_j^{i\prime}\right\} (Eq. 18)$$

Where:

- *i*, *j*, and *n* are defined as before.
- γ: Yield of experiment *i*.
- $\overline{\gamma}$: Mean yield for element j.
- ε: Recovery of element *j* in experiment i.
- $\overline{\varepsilon}_j$: Mean recovery for element *j*.
- α_j^i: Grade of the feed of *j* element in experiment *i*.
- $\overline{\alpha}_j$: Mean grade for element *j*.
- $\propto_j^{target}$: Target grade for element *j*.

and the following restrictions apply:

$$\left\{\forall \alpha_j^i, \gamma^i, \varepsilon_j^i, m, n, C_T^i: \alpha_j^i \in \left[\alpha_j^{target}, 10^6\right], \gamma^i, \varepsilon_j^i \in (0,100], m, n \in \mathbb{N}, C_T^i \in (0,2n)\right\}$$

The supplementary material section (SM2) contains an example of this methodology used in a scenario involving two experimental set-ups with two elements to be separated.

3. Results and discussion

3.1. Separation results

We conducted 12 experimental runs with separation voltages ranging from 41.5 kV to 17.5 kV (Table 3). There was a positive correlation between yield (γ) and voltage with γ=1.4% at 20 kV and γ=8.6% at 41.5 kV with a maximum of γ=9.0% at 40.0 kV (peak-yield voltage). Similarly, the recovery (ε) in the conductive fraction was also positively correlated with the voltage. The peak-yield voltage (40 kV) also produced the highest maximum recoveries for six PTEs of interest: Zn (83.3%), followed by Mo (81.0%), Cu (62.2%), Cu (62.2%), Sb (59.6%) and Ni (57.3%). The same voltage, however, resulted in the lowest recoveries for the other four PTEs studied: Hg (13.2%), Cr (38.8%), Cd (45.0%) and As (41.7%). Considering the variation in the values recorded the three parameters of interest, yield, recovery and grade, while the first of these parameters varied in a range from 1.4% to 8.6%, the other two had far wider ranges: 2%-83.3% and 0.3 mg/kg to 3108 mg/kg, for recovery and grade respectively. All the data are summarized in Table 3.

Attributive analysis generates a family of curves describing the relationships between yield, recovery, and the quality index for a particular experimental set up. In the following sections we will consider these curves and compare the performances of basic and penalized attributive analysis in evaluating the quality indices of the 12 separation experiments undertaken here.

Table 3.- Yield (γ) for each experiment, grade (α), and recovery (ε) for each element in each experiment. Average of three experimental runs at each voltage with a standard error <5%.

		As		Cd		Cr		Cu		Hg		Mo		Ni		Pb		Sb		Zn	
Voltage	γ	α	ε	α	ε	α	ε	α	ε	α	ε	α	ε	α	ε	α	ε	α	ε	α	ε
(kV)	(%)	(mg/kg)	(%)	(mg/kg)	(%)	(mg/kg)	(%)	(mg/kg)	(%)	(mg/kg)	(%)	(mg/kg)	(%)	(mg/kg)	(%)	(mg/kg)	(%)	(mg/kg)	(%)	(mg/kg)	(%)
41.5	8.6	57.8	38.9	11.3	37.8	11.6	35.4	523.5	62.2	1.7	14.4	4.0	81.0	12.3	57.3	2731.75	44.8	15.7	59.6	2375.37	81.5
40	9.0	56.5	41.7	8.7	45.0	10.2	38.8	610.7	74.9	1.5	13.2	3.6	79.7	10.5	53.7	2521.85	48.9	14.5	56.2	2293.01	83.3
39	6.3	45.9	38.7	8.6	29.2	8.4	30.7	555.1	77.7	1.4	13.3	2.3	74.7	6.0	39.0	2311.17	45.7	11.4	57.9	1535.38	82.9
37.5	7.8	55.3	40.9	8.5	34.3	11.4	41.8	802.3	68.7	1.1	25.9	2.4	78.9	12.3	49.4	2691.02	47.6	15.1	58.3	1776.63	82.6
35	5.9	39.2	30.3	6.2	27.4	9.3	28.1	296.0	61.6	0.8	10.9	1.7	64.5	6.4	42.6	2837.74	29.8	11.1	38.8	1106.05	74.2
32.5	4.0	43.5	23.0	6.2	20.0	7.6	24.8	294.8	36.6	0.6	11.1	1.4	54.5	7.4	39.7	3108.21	20.1	16.8	19.1	790.23	65.5
30	3.4	42.7	17.3	6.9	19.1	9.5	16.1	394.5	34.6	0.6	10.6	1.4	49.4	8.0	31.6	2238.23	27.2	10.6	29.6	834.86	55.3
27.5	3.3	50.0	12.3	7.9	11.6	11.5	13.6	314.5	33.5	0.5	12.1	1.5	33.0	9.7	16.1	2522.95	18.7	10.9	17.8	886.28	40.3
25	2.8	49.0	8.4	8.1	15.6	17.4	5.7	245.0	22.5	0.4	6.2	1.3	24.9	10.5	7.8	1797.21	13.3	10.7	12.5	751.50	36.0
23.7	1.7	43.6	5.3	5.8	9.1	10.4	4.7	188.6	9.2	0.4	4.3	0.6	17.3	14.0	3.6	1620.25	7.2	7.5	9.1	376.06	21.6
22.5	1.5	39.6	5.4	7.2	7.8	8.1	7.2	235.1	10.2	0.3	4.9	1.1	11.3	8.3	7.4	1684.47	6.8	8.3	6.6	520.28	17.1
20	1.4	46.2	4.3	5.6	6.4	8.3	5.3	176.1	24.7	0.7	2.0	0.7	16.8	5.6	16.0	2016.94	6.6	9.1	7.3	473.96	17.3
17.5	0.7	66.6	2.0	6.9	2.7	11.4	1.9	286.4	5.1	0.4	2.0	0.9	7.0	8.7	3.0	3455.43	2.9	15.0	3.0	590.56	6.9
Target value (mg/kg)		0.9		0.8		0.35		3.4		0.3		3		0.26		55		3		16	

3.2. Families of curves

Taking Equation 5, the attributive analysis equation, and substituting in values for yield (γ) and recovery (Ɛ), it is possible to produce a family of surfaces that share a similar shape and functional relationship. These surfaces represent the ways in which the quality index of an experiment (Q) will vary with changes in either γ or Ɛ. Figure 19 shows a surface plot of Q for all possible combinations for γ^i and ε_j^i ranging from 0.01 to 0.99.

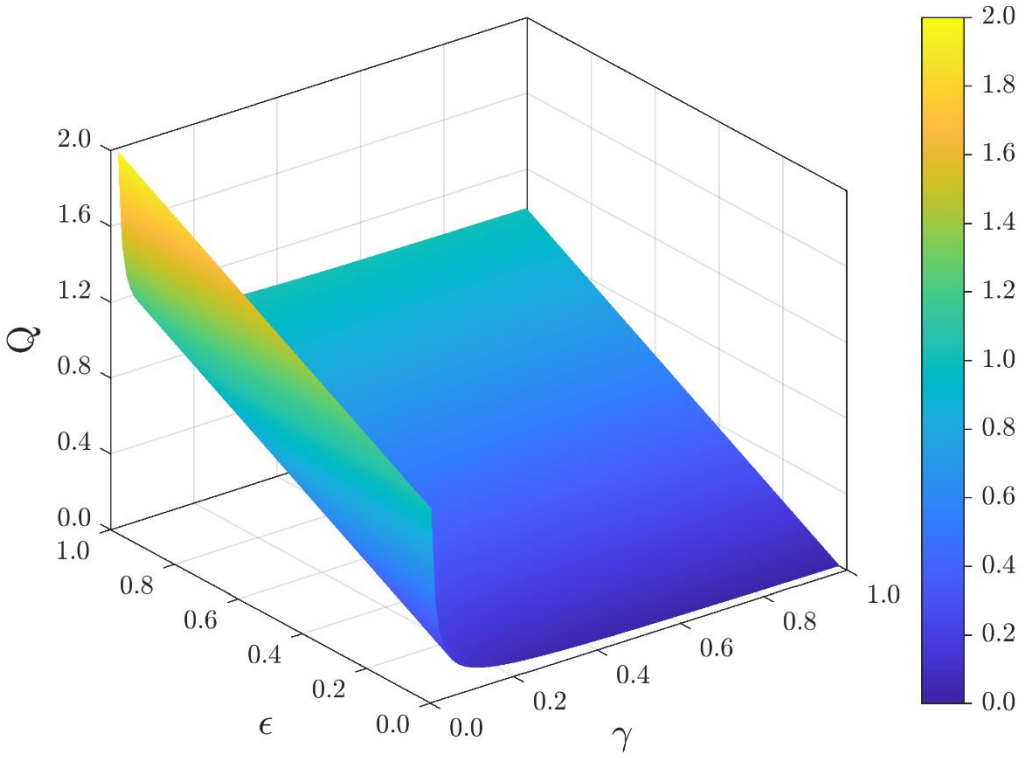

Figure 19.- General shape of a quality index function.

Sierra et al. (2010) applied the attributive analysis function to process engineering; however, they did not analyze the family of surfaces created. Such analysis enables an exploration of the theoretical consistency of the proposed methodology. In this way, as part of the present study we will perform a sensitivity analysis and a comparative analysis with known values from our electrostatic separation experiment (see section 3.1). In the present work, our comparative analysis involves an examination of results derived from the basic version of attributive analysis in comparison to those derived from PPAA-U without target-to-distance correction. Concerning the former, this considers the relative sensitivity of quality index with respect to changes in yield and recovery values.

As demonstrated in Figure 19, the relationship between Q and γ is very different from its relationship with Ɛ; thus, it is useful to examine these two relationships separately. This can be done by keeping either one of the two addends in Equation 5 ($\frac{\varepsilon_j^i}{\mathrm{Max}\{\varepsilon_j\}}$ or ε_j^i) constant to give two families of curves, one for Q varying with γ and another for Q varying with Ɛ.

Starting with the recovery addend, $\frac{\varepsilon_j^i}{\mathrm{Max}\{\varepsilon_j\}}$, setting $\mathrm{Max}\{\varepsilon_j\}$ to 0.99 and varying ε_j^i between 0.01 and 0.99, we obtain a set of curves corresponding to different values of γ (for values of γ from γ_{min}=0.01 to 0.99). These curves correspond to Q-Ɛ plane (see Figure 19) at different points along the γ-axis and as can be seen in Figure 20, the quality index, Q, and Ɛ are related by a straight line:

$$\mathrm{Q} = \frac{\varepsilon_j^i}{\mathrm{Max}\{\varepsilon_j\}} + K$$

The gradient of the line can be found by taking the derivative of Q with respect to Ɛ:

$$\mathrm{dQ} = \frac{d\varepsilon_j^i}{\mathrm{Max}\{\varepsilon_j\}}$$

such that (Eq. 19):

$$\frac{\mathrm{dQ}}{d\varepsilon_j^i} = \frac{1}{\mathrm{Max}\{\varepsilon_j\}} \ (\mathrm{Eq.}\ 19)$$

This tells us that as the maximum recovery increases, the slope of the curve generated decreases. Moreover, when $\mathrm{Max}\{\epsilon_j\}$ is large, the variation in Q with recovery will decrease.

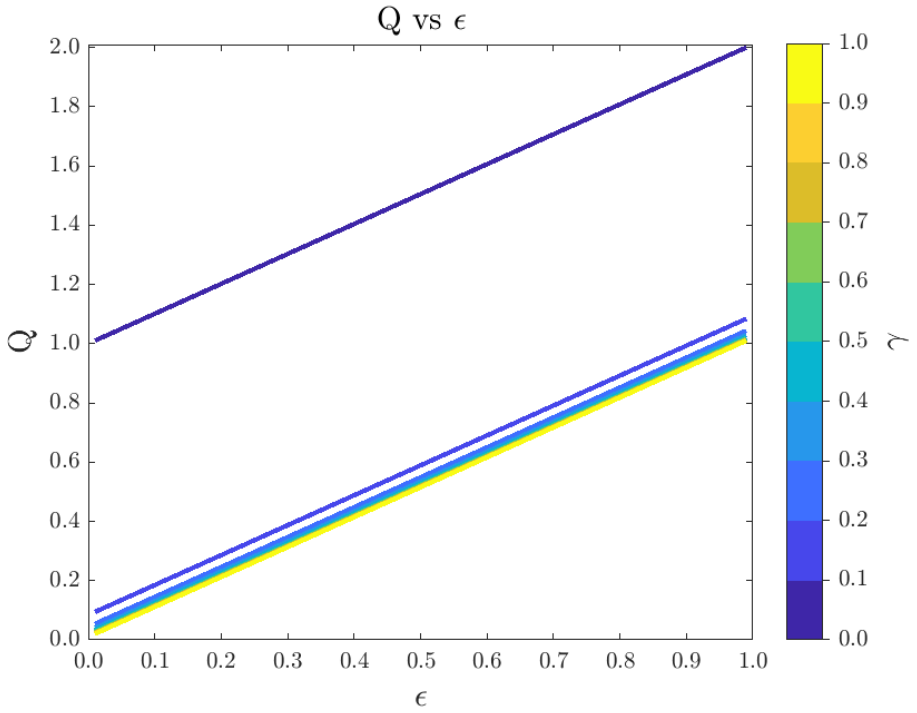

Figure 20.- Quality index function (parallel to the Q-ε plane).

Taking the yield addend, $\frac{\text{Min}\{\gamma\}}{\gamma^i}$, setting Min{γ}=0.01 and varying Ɛ from 0.01 to Ɛ= Max$\{\varepsilon_j\}$ = 0.99 gives a second set of curves. These curves are Q-γ planes at different points along the Ɛ axis; see Figure 21. In contrast to Ɛ, γ has a nonlinear relationship with Q, and calculating the gradient of the curve gives an inverse square function (Eq. 20):

$$\frac{dQ}{d\gamma} = \frac{-\text{Min}\{\gamma\}}{(\gamma^i)^2} \quad \text{(Eq. 20)}$$

This result shows that the quality index is highly sensitive to yield for values of $\gamma^i < 0.1$; however, for $\gamma^i > 0.1$, the quality index remains almost stable. In this way, reducing yield values is more important than maximizing recovery since, at very low yields, small changes in this parameter have a very large impact on the quality index.

Equation 20 also demonstrates that the sensitivity of the quality index to changes in yield decreases for higher values of Min{γ}. This fact could be useful under particularly noisy experimental conditions.

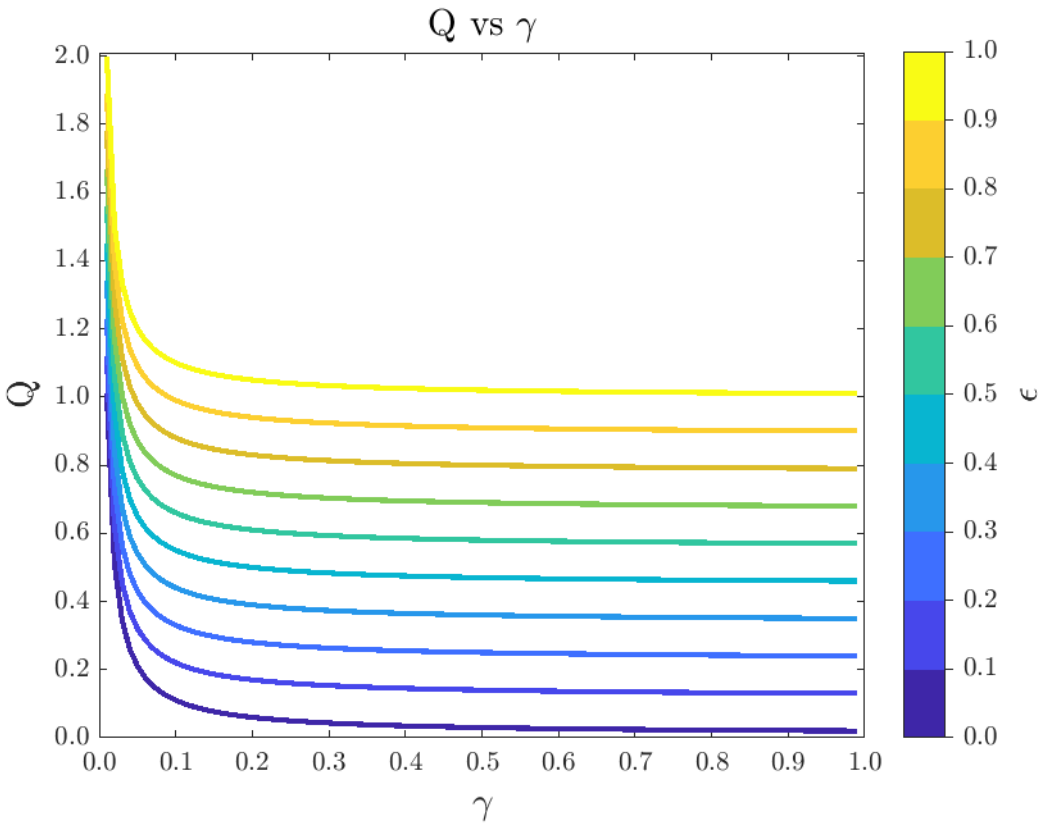

Figure 21.- Quality index parallel to the Q-γ plane.

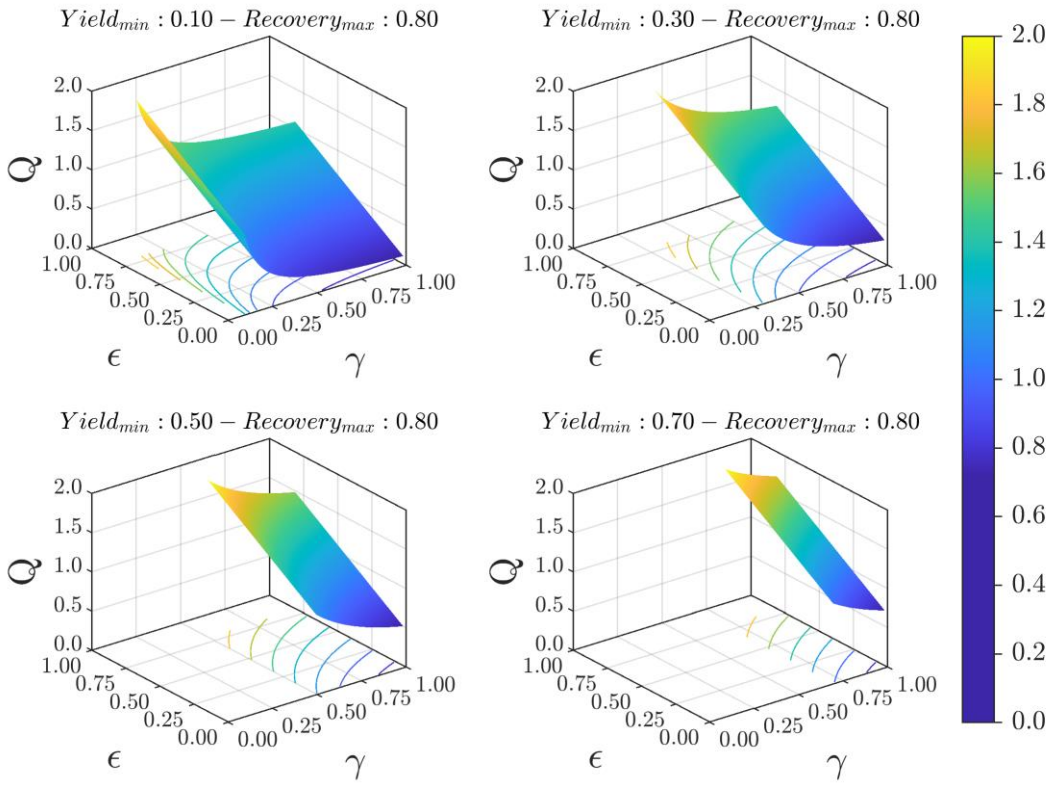

Figure 22.- Quality index function for different minimum yields.

From the above analysis it becomes apparent that Q should be considered a function of four variables: γ^i and ε_j^i, $\text{Min}\{\gamma\}$ and $\text{Max}\{\varepsilon_j\}$. We will now explore in more detail the effect of variations in $\text{Min}\{\gamma\}$ and $\text{Max}\{\varepsilon_j\}$.

Starting this time with the yield addend, $\frac{\text{Min}\{\gamma\}}{\gamma^i}$, increasing $\text{Min}\{\gamma\}$ reduces the function domain from [0,1] to [$\text{Min}\{\gamma\}$,1]. As was mentioned, while this function is highly sensitive to $\gamma^i < 0.1$, at larger values of γ^i the curve is relatively flat Figure 21); thus, increasing $\text{Min}\{\gamma\}$ places the quality function in a largely stable zone. Furthermore, as Figure 22 demonstrates, higher values of $\text{Min}\{\gamma\}$ lead to flatter curves, meaning that Q becomes increasingly insensitive to variation in γ^i.

Similarly, considering the recovery addend, $\frac{\varepsilon_j^i}{\text{Max}\{\varepsilon_j\}}$, if $\text{Max}\{\varepsilon_j\}$ decreases this also narrows the function domain from [0,1] to [0, $\text{Max}\{\varepsilon_j\}$]. In addition, since the gradient of the curve (see Equation 19) is constant and equal to $\frac{1}{\text{Max}\{\varepsilon_j\}}$, increasing $\text{Max}\{\varepsilon_j\}$, will decrease the gradient angle, given by $\tan^{-1}\left(\frac{1}{Max\{\varepsilon_j\}}\right)$. This is demonstrated in Figure 23.

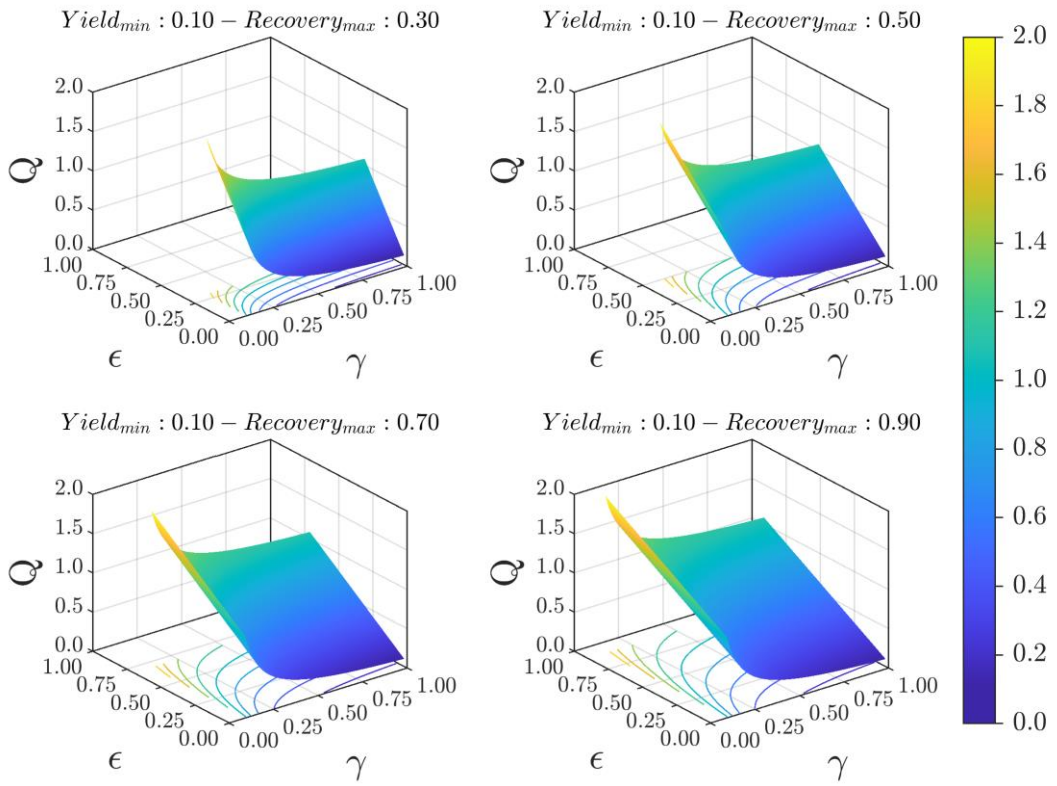

Figure 23.- Quality index function for different maximum recoveries.

3.3. Results of Penalized Attributive Analysis (PAA-U)

Bearing in mind the insights of the previous section, we now consider a comparison of basic attributive analysis, AA, and its inverse standard deviation weighted or penalized version, PPAA-U. Figure 24 presents a comparison between results obtained using AA and PPAA-U (without target-to-distance correction) for the electrostatic soil washing operation described in section 3.1. We observe significant agreement between AA and PPAA-U, particularly for lower voltages (<25 kV). This is because the variation in recoveries for the elements tested is less at lower voltages (see Table 3) than at higher voltages. In this way, the weighting used in PPAA-U makes little difference at lower voltages; however, at high voltages, the high variances are strongly penalized, lowering the Q values of these experiments and thus causing a divergence in the results obtained via the basic and penalized versions of the method. In addition, both AA and PPAA-U predict the presence of two maxima in the quality index: one at low voltages where despite low recoveries, the lower yield leads to a peak in the quality index, and a second at high voltages where there is high recovery.

When the target-to-distance correction is introduced, while both methods once again give similar results and, as expected PPA diverges from AA at higher voltages, the overall pattern is very different: specifically, the peak in the quality index at lower voltages disappears Figure 25). The target-to-distance correction allows us to compare how different experimental set-ups perform with respect to particularly harmful elements. This in turn enables attributive analysis to identify not simply the best overall separation conditions, but those that are most environmentally optimal. In the present case, voltages greater than 37.5 kV stand out as providing the best separation conditions giving priority to the removal of the most harmful PTEs.

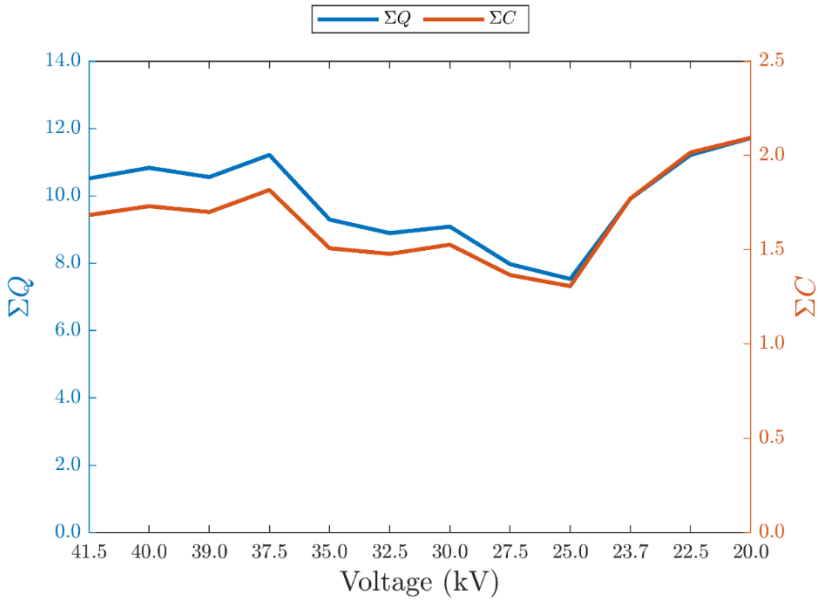

Figure 24.- AA (ΣQ) and PPAA-U (ΣC) quality index results before target-to-distance correction.

The work presented here demonstrates that PPAA-U is a promising tool for identifying the optimal conditions for electrostatic soil washing operations. To further improve the methodology, additional quotients should be incorporated to account for components reporting to the middlings fraction instead of considering it as part of the concentrate, as is done here. In addition, the method could be modified to encompass some of the economic factors involved in the soil washing process, especially those relating to the circular economy, to further optimize conditions.

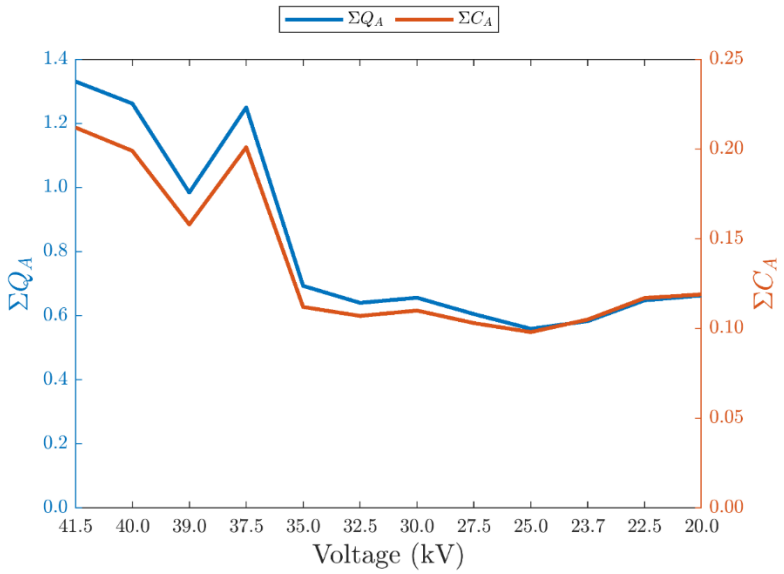

Figure 25.- Quality index as calculated via basic AA (ΣQA) and PPAA-U (ΣCA) with target-to-distance correction.

4. Conclusions

Currently, the available literature offers few means to evaluate the quality of a separation process. Methods that do exist tend to use only two parameters, typically recovery and yield, however, on their own, these two variables do not provide a sufficiently robust way to identify separation conditions that are genuinely optimal.

In its original form, attributive analysis addresses the short-comings of other methods providing a tool to assess optimal separation conditions through a comparison of three variables: yield, recovery, and grade. However, this basic method suffers where there are large variations in the yields and recoveries of the components or elements separated.

Indeed, examination of the attributive analysis function reveals that it exhibits significant sensitivity to dispersion within both the yield dataset and the recovery dataset. However, the sensitivity to variations in yield is greatest, something that can be attributed to the fact that while the quality index is linearly related to recovery (with the slope being dependent on the maximum recovery value), it has an inverse relationship with yield and thus an inverse squared relationship to changes in yield. Penalized attributive analysis, PAA-U, directly addresses the issue of variations in yields and recoveries, most strongly penalizing contributions to the quality index from experimental set-ups for which the largest variations are recorded.

Target-to-distance correction improved the performance of both AA and PPAA-U. For the separation technique used in this work, without this correction, two maxima (one at higher and one at lower voltages) in the quality index were observed, making it difficult to distinguish the true optimum conditions. When the target-to-distance correction was introduced, however, the lower voltage maximum was removed. This shows that while lower voltages might provide effective separation on average, they are poor at removing particularly harmful PTEs; this more targeted separation is achieved only at higher voltages.

Future work should focus not only on the application of PPAA-U to evaluate the soil washing methods used in the remediation of metal(loid)-polluted soil but also as part of feasibility studies for bioremediation or chemical oxidation technologies (where numerous organic contaminants each with different target concentrations are addressed simultaneously). Furthermore, this methodology can not only be applied to environmental

remediation operations, but could also be used to determine optimal operating conditions in a variety of materials processing or manufacturing contexts. In such contexts, the quality factor used in this method might involve variables such as temperature, pressure, or particle size and also the environmental and economic factors such as the costs associated with particular operating conditions which might depend on energy use or manpower requirements.

Acknowledgements

Carlos Sierra would like to thank the EURECA-PRO phase I 2020-2023 co-funded by the European Union's Erasmus+ Programme (Ref.: 101004049).

References

American Society for Testing and Materials. (1963). ASTM D422-63: Standard Test Method for Particle-Size Analysis of Soils (reapproved 2007). ASTM International.

Aparicio, J. D., Raimondo, E. E., Saez, J. M., Costa-Gutierrez, S. B., Álvarez, A., Benimeli, C. S., & Polti, M. A. (2022). The current approach to soil remediation: A review of physicochemical and biological technologies, and the potential of their strategic combination. *Journal of Environmental Chemical Engineering*, *10*(2). https://doi.org/10.1016/J.JECE.2022.107141

Baragaño, D., Gallego, J.R., Menéndez-Aguado, J., Marina, M.A., Sierra, C., 2021. As sorption onto Fe-based nanoparticles and recovery from soils by means of wet high intensity magnetic separation. *Chem. Eng. J.* 408, 127325 https://doi.org/10.1016/J.CEJ.2020.127325.

Baragaño, D., Berrezueta, E., Komárek, M., Menéndez-Aguado, J.M., 2023. Magnetic separation for arsenic and metal recovery from polluted sediments within a circular economy. *J. Env. Manag*. 339, 117884. https://doi.org/10.1016/j.jenvman.2023.117884

Boente, C., Sierra, C., Rodríguez-Valdés, Menéndez-Aguado, J.M., & Gallego, J.R. (2017). Soil washing optimization by means of attributive analysis: Case study for the removal of potentially toxic elements from soil contaminated with pyrite ash. Journal of Cleaner Production 142, 2693-2699 http://dx.doi.org/10.1016/j.jclepro.2016.11.007

Bunge, R., Bachmann, A., & Ngo, C. D. (1995). *Soil-washing: Mineral processing technology in environmental engineering*.

Cortada, U., Hidalgo, C., Martínez, J.M., & Rey, J. (2018). Impact in soils caused by metal(loid)s in lead metallurgy. The case of La Cruz Smelter (Southern Spain). Journal of Geochemical Exploration 190(5a). http://dx.doi.org/10.1016/j.gexplo.2018.04.001

Drzymala, J. (2006). Atlas of upgrading curves used in separation and mineral science and technology. In *Physicochemical Problems of Mineral Processing* (Vol. 40).

Gu, F., Zhang, J., Shen, Z., Li, Y., Ji, R., Li, W., Zhang, L., Han, J., Xue, J., & Cheng, H. (2022). A review for recent advances on soil washing remediation technologies. *Bulletin of Environmental Contamination and Toxicology*, *109*(4), 651–658. https://doi.org/10.1007/S00128-022-03584-6/METRICS

Gupta, A., & Yan, D. (2016). Mineral Processing Design and Operations: An Introduction: Second Edition. *Mineral Processing Design and Operations: An Introduction: Second Edition*, 1–850.

Liu, J., Zhao, L., Liu, Q., Li, J., Qiao, Z., Sun, P., & Yang, Y. (2022). A critical review on soil washing during soil remediation for heavy metals and organic pollutants. *International Journal of Environmental Science and Technology*, *19*(1), 601–624. https://doi.org/10.1007/S13762-021-03144-1/METRICS

Nishiyama, T., Tomoguchi, M., & Sasamoto, N. (2000). Soil washing using mineral processing plant in Hanaoka Mine, Dowa Mining Co., Ltd. *Second International Conference on Processing Materials for Properties*, 601–624. https://www.researchgate.net/publication/290268173_Soil_washing_using_mineral_processing_plant_in_Hanaoka_Mine_Dowa_Mining_Co_Ltd

Richardson, W. S., Phillips, C. R., Luttrell, J., Hicks, R., & Cox, C. (1999). Application of remedy studies to the development of a soil washing pilot plant that uses mineral processing technology: a practical experience. *Journal of Hazardous Materials*, *66*(1–2), 47–65. https://doi.org/10.1016/S0304-3894(98)00211-8

Rosendo, R., Rey, J., Martínez, J.M., & Hidalgo, C. (2022). Geological and mining heritage as a driver of development: The NE sector of the Linares-La Carolina district (Southeastern Spain). Geosciences 12(2), 76. http://dx.doi.org/10.3390/geosciences12020076

Schulz, N. F. (1970). "Separation Efficiency." *Trans. SME/AIME*, *247*, 81–87. https://cir.nii.ac.jp/crid/1570572701370836096

Sierra, C., Martínez-Blanco, D., Blanco, J. A., & Gallego, J. R. (2014). Optimisation of magnetic separation: A case study for soil washing at a heavy metals polluted site. *Chemosphere*, *107*, 290–296. https://doi.org/10.1016/J.CHEMOSPHERE.2013.12.063

Taggart. A.F. (1947). *Handbook of Mineral Dressing*. John Wiley & Sons. https://www.abebooks.com/first-edition/Handbook-Mineral-Dressing-Ores-Industrial-Minerals/4800302279/bd

Tran, H. T., Lin, C., Hoang, H. G., Bui, X. T., Le, V. G., & Vu, C. T. (2022). Soil washing for the remediation of dioxin-contaminated soil: A review. *Journal of Hazardous Materials*, *421*. https://doi.org/10.1016/J.JHAZMAT.2021.126767

Wan, X., Lei, M., & Chen, T. (2020). Review on remediation technologies for arsenic-contaminated soil. *Frontiers of Environmental Science and Engineering*, *14*(2), 1–14. https://doi.org/10.1007/S11783-019-1203-7/METRICS

Weiss, N. L. (1985). Metallurgical Accounting and Mill Reports. In *SME mineral processing handbook*. Society of Mining Engineers of the American Institute of Mining, Metallurgical, and Petroleum Engineers.

Wills, B. A., & Finch, J. A. (2015). Wills' mineral processing technology: An introduction to the practical aspects of ore treatment and mineral recovery. *Wills' Mineral Processing Technology: An Introduction to the Practical Aspects of Ore Treatment and Mineral Recovery*, 1–498.

Suplementary Materials - 1

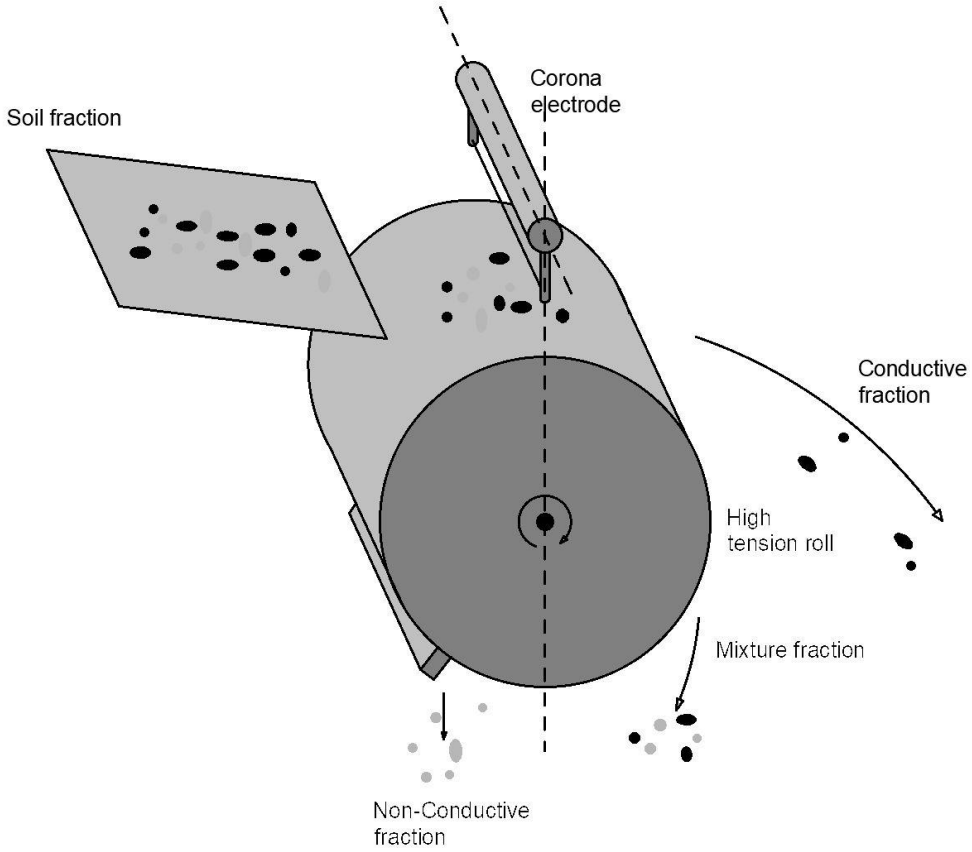

Figure 26.- eForce high-tension electrostatic separator.

Suplementary Materials – 2: Calculations example

In this example an electrostatic separation process is considered. The main variable of control is voltage (40 kV and 41.5 kV) and the elements of interest to be separated are Cu and Zn. The experimental results are summarized in Table 4.

Table 4.- Grade, recovery and yields for two separation experiments.

Voltage	α		α^{target}		γ	ε	
(kV)	Cu	Zn	Cu	Zn		Cu	Zn
40	610.692	2293.012	3.4	16	9.005	74.905	83.253
41.5	523.518	2375.374			8.564	62.165	81.483

To identify the best operating conditions, we use PAA, and the calculations are as follows:

1) Considering the 40 kV separation:

Uncorrected quality index for Cu:

$$\gamma^{41.5} = 8.564\ ;\ \varepsilon_{Cu}^{41.5} = 62.165\ ;\ \alpha_{Cu}^{41.5} = 523.518$$

$$\gamma^{40} = 9.005\ ;\ \varepsilon_{Cu}^{40} = 74.905\ ;\ \propto_{Cu}^{40} = 610.692$$

$$Min\{\gamma\} = 8.564\ ;\ Max\{\varepsilon_{Cu}\} = 74.905\ ;\ \propto_{Cu}^{target} = 3.4$$

$$\bar{\gamma} = 8.785\ ;\ \overline{\varepsilon}_{Cu} = 68.535\ ;\ \overline{\alpha}_{Cu} = 567.105$$

$$\Gamma^{40} = \frac{Min\{\gamma\}}{\gamma^{40}}\left(\frac{|\gamma^{41.5} - \bar{\gamma}| + |\gamma^{40} - \bar{\gamma}|}{2}\right)^{-1};\ \Gamma^{40\prime} = \frac{\Gamma^{40}}{\Gamma^{41.5} + \Gamma^{40}}$$

$$\Gamma^{40} = \frac{8.564}{9.005}\left(\frac{|8.564 - 8.785| + |9.005 - 8.785|}{2}\right)^{-1} = 4.319;$$

$$\Gamma^{40\prime} = \frac{4.319}{4.541 + 4.319} = 0.487$$

$$E_{Cu}^{40} = \frac{\varepsilon_{Cu}^{40}}{Max\{\varepsilon_{Cu}\}}\left(\frac{\left|\varepsilon_{Cu}^{41.5} - \overline{\varepsilon}_{Cu}\right| + |\varepsilon_{Cu}^{40} - \overline{\varepsilon}_{Cu}|}{2}\right)^{-1};\ E_{Cu}^{40\prime} = \frac{E_{Cu}^{40}}{E_{Cu}^{41.5} + E_{Cu}^{40}}$$

$$E_{Cu}^{40} = \frac{74.905}{74.905}\left(\frac{|62.165 - 68.535| + |74.905 - 68.535|}{2}\right)^{-1} = 0.157;$$

$$E_{Cu}^{40\prime} = \frac{0.157}{0.130 + 0.157} = 0.546$$

$$C_{Cu}^{40} = \Gamma^{40\prime} + E_{Cu}^{40\prime} = 0.487 + 0.546 = 1.034$$

Target-to-distance correction for Cu:

$$B_{Cu}^{40} = \frac{\alpha_{Cu}^{40}}{\propto_{Cu}^{target}} \left(\frac{\left| \propto_{Cu}^{41.5} - \overline{\alpha}_{Cu} \right| + \left| \propto_{Cu}^{40} - \overline{\alpha}_{Cu} \right|}{2} \right)^{-1};\ B_{Cu}^{40\prime} = \frac{B_{Cu}^{40}}{B_{Cu}^{41.5} + B_{Cu}^{40}}$$

$$B_{Cu}^{40} = \frac{610.692}{3.4} \left(\frac{|523.518 - 567.105| + |610.692\ - 567.105|}{2} \right)^{-1} = 4.121;$$

$$B_{Cu}^{40\prime} = \frac{4.121}{3.533 + 4.121} = 0.538$$

Uncorrected quality index for Zn:

$$\gamma^{41.5} = 8.564;\ \varepsilon_{Zn}^{41.5} = \ 81.483;\ \alpha_{Zn}^{41.5} = 2375.374$$

$$\gamma^{40} = 9.005;\ \varepsilon_{Zn}^{40} = 83.253;\ \propto_{Zn}^{40} = 2293.012$$

$$Min\{\gamma\} = 8.564;\ Max\{\varepsilon_{Zn}\} = 83.253;\ \propto_{Zn}^{target} = 16$$

$$\bar{\gamma} = 8.785;\ \overline{\varepsilon}_{Zn} = 82.368;\ \overline{\alpha}_{Zn} = 2334.193$$

$$\Gamma^{40} = 4.319;$$
$$\Gamma^{40\prime} = 0.487$$

$$E_{Zn}^{40} = \frac{\varepsilon_{Zn}^{40}}{Max\{\varepsilon_{Zn}\}} \left(\frac{\left| \varepsilon_{Zn}^{41.5} - \overline{\varepsilon}_{Zn} \right| + \left| \varepsilon_{Zn}^{40} - \overline{\varepsilon}_{Zn} \right|}{2} \right)^{-1};\ E_{Zn}^{40\prime} = \frac{E_{Zn}^{40}}{E_{Zn}^{41.5} + E_{Zn}^{40}}$$

$$E_{Zn}^{40} = \frac{83.253}{83.253} \left(\frac{|81.483 - 82.368| + |83.253 - 82.368|}{2} \right)^{-1} = 1.130;$$

$$E_{Zn}^{40\prime} = \frac{1.130}{1.106 + 1.130} = 0.505$$

$$\mathrm{C}_{Zn}^{40} = \ \Gamma^{40\prime} + E_{Zn}^{40\prime} = \ 0.487 + 0.505 = 0.993$$

Target-to-distance correction for Zn:

$$B_{Zn}^{40} = \frac{\alpha_{Zn}^{40}}{\propto_{Zn}^{target}} \left(\frac{\left| \propto_{Zn}^{41.5} - \overline{\alpha}_{Zn} \right| + \left| \propto_{Zn}^{40} - \overline{\alpha}_{Zn} \right|}{2} \right)^{-1};\ B_{Zn}^{40\prime} = \frac{B_{Zn}^{40}}{B_{Zn}^{41.5} + B_{Zn}^{40}}$$

$$B_{Zn}^{40} = \frac{2293.012}{16} \left(\frac{|2375.374 - 2334.193| + |2293.012 - 2334.193|}{2} \right)^{-1} = 3.480;$$

$$B_{Zn}^{40\prime} = \frac{3.480}{3.605 + 3.480} = 0.491$$

This gives a total corrected quality index for the 40 kV experiment of:

$$C_T^{40} = C_{Cu}^{40} B_{Cu}^{40\prime} + C_{Zn}^{40} B_{Zn}^{40\prime}$$

Substituting in the values obtained:

$$= (1.034 \cdot 0.538) + (0.993 \cdot 0.491) = 0.557 + 0.488 = 1.045$$

2) Considering the 41.5 kV separation:

Uncorrected quality index for Cu:

$$\gamma^{41.5} = 8.564\ ;\ \varepsilon_{\mathrm{Cu}}^{41.5} = 62.165\ ;\ \alpha_{\mathrm{Cu}}^{41.5} = 523.518$$

$$\gamma^{40} = 9.005\ ;\ \varepsilon_{\mathrm{Cu}}^{40} = 74.905\ ;\ \propto_{\mathrm{Cu}}^{40} = 610.692$$

$$\mathrm{Min}\{\gamma\} = 8.564\ ;\ \mathrm{Max}\{\varepsilon_{\mathrm{Cu}}\} = 74.905\ ;\ \propto_{\mathrm{Cu}}^{\mathrm{target}} = 3.4$$

$$\bar{\gamma} = 8.785\ ;\ \bar{\varepsilon}_{\mathrm{Cu}} = 68.535\ ;\ \bar{\alpha}_{\mathrm{Cu}} = 567.105$$

$$\Gamma^{41.5} = \frac{\mathrm{Min}\{\gamma\}}{\gamma^{41.5}} \left(\frac{|\gamma^{41.5} - \bar{\gamma}| + |\gamma^{40} - \bar{\gamma}|}{2} \right)^{-1} ; \Gamma^{41.5\prime} = \frac{\Gamma^{41.5}}{\Gamma^{41.5} + \Gamma^{40}}$$

$$\Gamma^{41.5} = \frac{8.564}{8.564} \left(\frac{|8.564 - 8.785| + |9.005 - 8.785|}{2} \right)^{-1} = 4.541;$$

$$\Gamma^{41.5\prime} = \frac{4.541}{4.541 + 4.319} = 0.513$$

$$\mathrm{E}_{\mathrm{Cu}}^{41.5} = \frac{\varepsilon_{\mathrm{Cu}}^{41.5}}{\mathrm{Max}\{\varepsilon_{\mathrm{Cu}}\}} \left(\frac{\left|\varepsilon_{\mathrm{Cu}}^{41.5} - \bar{\varepsilon}_{\mathrm{Cu}}\right| + \left|\varepsilon_{\mathrm{Cu}}^{40} - \bar{\varepsilon}_{\mathrm{Cu}}\right|}{2} \right)^{-1} ; \mathrm{E}_{\mathrm{Cu}}^{41.5\prime} = \frac{\mathrm{E}_{\mathrm{Cu}}^{41.5}}{\mathrm{E}_{\mathrm{Cu}}^{41.5} + \mathrm{E}_{\mathrm{Cu}}^{40}}$$

$$\mathrm{E}_{\mathrm{Cu}}^{41.5} = \frac{62.165}{74.905} \left(\frac{|62.165 - 68.535| + |74.905 - 68.535|}{2} \right)^{-1} = 0.130;$$

$$\mathrm{E}_{\mathrm{Cu}}^{41.5\prime} = \frac{0.130}{0.130 + 0.157} = 0{,}454$$

$$C_{\mathrm{Cu}}^{41.5} = \Gamma^{41.5\prime} + \mathrm{E}_{\mathrm{Cu}}^{41.5\prime} = 0.513 + 0.454 = 0.966$$

Target-to-distance correction for Cu:

$$\mathrm{B}_{\mathrm{Cu}}^{41.5} = \frac{\alpha_{\mathrm{Cu}}^{41.5}}{\propto_{\mathrm{Cu}}^{\mathrm{target}}} \left(\frac{\left|\propto_{\mathrm{Cu}}^{41.5} - \bar{\alpha}_{\mathrm{Cu}}\right| + \left|\propto_{\mathrm{Cu}}^{40} - \bar{\alpha}_{\mathrm{Cu}}\right|}{2} \right)^{-1} ; \mathrm{B}_{\mathrm{Cu}}^{41.5\prime} = \frac{\mathrm{B}_{\mathrm{Cu}}^{41.5}}{\mathrm{B}_{\mathrm{Cu}}^{41.5} + \mathrm{B}_{\mathrm{Cu}}^{40}}$$

$$\mathrm{B}_{\mathrm{Cu}}^{41.5} = \frac{523.518}{3.4} \left(\frac{|523.518 - 567.105| + |610.692 - 567.105|}{2} \right)^{-1} = 3.533;$$

$$\mathrm{B}_{\mathrm{Cu}}^{41.5\prime} = \frac{3.533}{3.533 + 4.121} = 0.462$$

Uncorrected quality index for Zn:

$$\gamma^{41.5} = 8.564;\ \varepsilon_{\mathrm{Zn}}^{41.5} = \ 81.483;\ \alpha_{\mathrm{Zn}}^{41.5} = 2375.374$$

$$\gamma^{40} = 9.005;\ \varepsilon_{\mathrm{Zn}}^{40} = 83.253;\ \propto_{\mathrm{Zn}}^{40} = 2293.012$$

$$\mathrm{Min}\{\gamma\} = 8.564;\ \mathrm{Max}\{\varepsilon_{\mathrm{Zn}}\} = 83.253;\ \propto_{\mathrm{Zn}}^{\mathrm{target}} = 16$$

$$\bar{\gamma} = 8.785;\ \overline{\varepsilon}_{Zn} = 82.368;\ \overline{\alpha}_{Zn} = 2334.193$$

$$\Gamma^{41.5} = 4.541;$$
$$\Gamma^{41.5\prime} = 0.513$$

$$E_{Zn}^{41.5} = \frac{\varepsilon_{Zn}^{41.5}}{Max\{\varepsilon_{Zn}\}}\left(\frac{\left|\varepsilon_{Zn}^{41.5} - \overline{\varepsilon}_{Zn}\right| + |\varepsilon_{Zn}^{40} - \overline{\varepsilon}_{Zn}|}{2}\right)^{-1};\ E_{Zn}^{41.5\prime} = \frac{E_{Zn}^{41.5}}{E_{Zn}^{41.5} + E_{Zn}^{40}}$$

$$E_{Zn}^{41.5} = \frac{81.483}{83.253}\left(\frac{|81.483 - 82.368| + |83.253 - 82.368|}{2}\right)^{-1} = 1.106;$$

$$E_{Zn}^{41.5\prime} = \frac{1.106}{1.106 + 1.130} = 0.495$$

$$\mathrm{C}_{Zn}^{41.5} = \ \Gamma^{41.5\prime} + E_{Zn}^{41.5\prime} = 0.513 + 0.495 = 1.008$$

Target-to-distance correction for Zn:

$$B_{Zn}^{41.5} = \frac{\alpha_{Zn}^{41.5}}{\propto_{Zn}^{target}}\left(\frac{\left|\propto_{Zn}^{41.5} - \overline{\alpha}_{Zn}\right| + |\propto_{Zn}^{40} - \overline{\alpha}_{Zn}|}{2}\right)^{-1};\ B_{Zn}^{41.5\prime} = \frac{B_{Zn}^{41.5}}{B_{Zn}^{41.5} + B_{Zn}^{40}}$$

$$B_{Zn}^{41.5} = \frac{2375.374}{16}\left(\frac{|2375.374 - 2334.193| + |2293.012 - 2334.193|}{2}\right)^{-1} = 3.605;$$

$$B_{Zn}^{41.5\prime} = \frac{3.605}{3.605 + 3.480} = 0.509$$

This gives a total corrected quality index for the 41.5 kV experiment of:

$$\mathrm{C}_{T}^{41.5} = \ \mathrm{C}_{Cu}^{41.5} B_{Cu}^{41.5\prime} + \mathrm{C}_{Zn}^{41.5} B_{Zn}^{41.5\prime}$$

Substituting in the values obtained:

$$= (0.966 \cdot 0.462) + (1.008 \cdot 0.509) = 0.446 + 0.513 = 0.959$$

The optimal experimental conditions are defined as those for which the total corrected quality index is greatest; in this case, the experiment at 40 kV:

$$\mathrm{C}_{optimal} = \ Max\left\{\sum_{j=1}^{n} \mathrm{C}_{j}^{i} B_{j}^{i\prime}\right\} = \mathrm{C}_{T}^{40} = 1.045$$

Universidad de Oviedo

CHAPTER IV: A novel algorithm for optimizing hydrocyclone operations in the decontamination of potentially toxic elements in soils

X. Corres, N. Gómez, C. Boente, J.R. Gallego, C. Sierra

Chemosphere 358 (2024) 142135

Abstract

We present the Three-Parameter Penalized Attributive Analysis for Upgrading (3PPAA-U) method as a tool for selecting the Best Upgrading Condition (BUC) in process engineering. Conventional approaches tend to consider only maximizing recovery (ε) and minimizing yield (γc); in contrast, the proposed 3PPAA-U introduces and seeks to maximize a third parameter, the grade (λ). This multi-parameter approach has not yet been explored in existing literature. In addition to controlling multiple parameters, the method is also superior to others as it includes inverse standard deviation weighting to avoid the distortion of results due to data dispersion. This reduces the possibility of drawing conclusions based on extreme values. Furthermore, the method can be used with a target-to-distance correction to optimize separation for multi-component feeds. To illustrate our method, we present a practical application of 3PPAA-U. Soil contaminated with potentially toxic elements (PTEs) was subject to hydrocycloning under 12 different experimental conditions. Results of these 12 experiments were compared using 3PPAA-U and conventional methods to identify the best upgrading conditions (BUC). Analysis reveals that the 3PPAA-U approach offers a simple and effective criterion for selecting BUC. Furthermore, 3PPAA-U has uses beyond soil remediation. It offers a versatile tool for optimizing operations across various processing and manufacturing environments offering a way to manage factors such as concentration, temperature, pressure, pH, Eh, grain size, and even broader environmental and economic considerations.

Keywords

Metallurgical accounting, process efficiency, process design, control of experiments

1. Introduction

1.1. Soil washing: key concepts

Soil pollution includes numerous potentially toxic elements (PTEs) such as lead, cadmium, arsenic, and mercury, as well as polycyclic aromatic hydrocarbons (PAHs) (c.f., Sun et al., 2019; Wu et al., 2015). PTEs not only affect soil fertility but also pose a risk to human health . For example, ingesting or inhaling contaminated soil particles can lead to serious health issues including cancer, respiratory problems, and neurological disorders (Liu et al., 2017; Rieuwerts et al., 2013). Furthermore, PTEs are known to leach into watercourses and this can cause even more widespread environmental degradation and risks to public health (Khalid et al., 2017).

Therefore, it is crucial to address the issue of contaminated soil through effective remediation strategies, for instance, phytoremediation (Ashraf, 2019; Chen et al., 2016), microbial remediation (Chen et al., 2023), electrokinetic remediation (Wang et al., 2021), and soil washing (Guo et al., 2022; Khum-in et al., 2023; Lee & Kim, 2010; Pinto et al., 2014)These strategies can help to reduce the levels of PTEs and other pollutants, restoring the soil and preventing further damage to the environment and human health.

Soil washing is a highly efficient and rapid technique (Khum-in et al., 2023) for the removal of PTEs and organic compounds from soil (Guo et al., 2022). Additionally, this technique represents one of the few methods able to provide a permanent solution for soil contamination, particularly in cases where levels of pollutants are significant (Lee & Kim, 2010; Pinto et al., 2014).

There are two types of soil washing, namely physical and chemical. The latter involves mixing the soil with an extraction solution to chemically dissolve or mobilize the contaminants. Physical soil washing, on the other hand, separates and extracts pollutants by exploiting the differences in physical properties, for example, size, density, magnetic properties, and hydrophobicity, that exist between soil particles and pollutant-bearing particles (Dermont et al., 2008). The strategies involved in physical soil washing are based on well-established methods employed in the mining industry for the extraction of elements from mineral ores (Ye et al., 2022; Sierra et al., 2013). However, these techniques can be expensive and time-consuming, thus there is a need for reducing costs and improving the efficiency of these remediation methods.

1.2. Determining Best Upgrading Conditions (BUC)

Assessing the performance of an upgrading process requires the definition of several parameters. Firstly, if the material subject to the upgrading process has a feed mass flow rate, F, then the products of the upgrading process are the concentrate and the tailings with, respectively, mass flow rates, C, and F. In some cases, there may be intermediate outputs, known as middlings, which will have a mass flow rate, M. These flow rates are related thus:

$$F = C+M+T \quad \text{(Eq. 1a)}$$

Dividing Eq. 1a by F, we get the yield (γ) for each fraction, that is, the mass percentage of the feed (F) reporting to each fraction: γ_c, the concentrate yield; γ_m, the midlings yield; and γ_t, the tailings yield; $\gamma_F = 1$, the feed yield (Eq. 1b):

$$\gamma_F = \gamma_c + \gamma_m + \gamma_t \quad \text{(Eq. 1b)}$$

The grade of a fraction is defined as the concentration of a given element or compound in that fraction, and it is denoted as α for the feed and λ for the concentrate.

Finally, the percentage of useful (or desired) content that reports to a specific fraction relative to the feed is known as the recovery, ε, and this is used to assess the quality of the upgrading process. Of most relevance here is the concentrate fraction and, for the concentrate mass stream, the recovery for this fraction is expressed as (Eq. 2):

$$\varepsilon = \frac{\lambda}{\alpha}\gamma_c \quad \text{(Eq. 2)}$$

In physical soil washing scenarios, the pollutants to be removed are held in the concentrate fraction while the tailings comprise the partially decontaminated soil. Thus, to optimise soil decontamination, the goal is to minimise γ_c and maximise λ.

Traditionally, to find optimal operating conditions, pairs of the parameters γ_c, λ and ε can be plotted on separation curves (e.g., Drzymała, 2006). However, such methods are naturally limited to a consideration of only two components at a time and this can be misleading. For example, an apparently optimal experiment with a high value of ε and low γ_c might simply contain very little material that would report to the concentrate, thus it is necessary to consider λ too. Similarly, an experiment might provide a high value of ε

might also give a high λ, however we cannot tell if this is truly an optimal set up without looking at γ_c since a high λ might simply be a consequence of a low γ_c.

Furthermore, most traditional methods are only able to consider single component separations and many soil washing operations involve soils with multiple contaminants. By including λ, in its calculations, 3PPAA-U enables optimization for multicomponent separations and allows the identification of operating conditions that will preferentially address the most dangerous pollutants.

1.3. Aim and specific objectives

Following from the previous discussion, the aim of this research, is to develop an effective method to select the optimal conditions for soil upgrading operations. In this way we will:

a) introduce the 3PPAA-U method

b) apply the method to a real-life soil washing operation using a hydrocyclone to decontaminate soil from an ex-industrial site in Asturias, Spain.

We will then compare the results of traditional separation-curve optimisation to 3PPAA-U with and without target-to-distance correctionand discuss the implications of this new method.

2. Materials and methods: A real-life soil washing operation

2.1. Soil sampling and chemical analysis

The soil sample used in this study was collected from a 35,000 m^2 brownfield location in Asturias (Northern Spain). Figure 27 depicts the location of the brownfield and the sampling area. More information about the site and its environment can be found in Boente et al., 2020. Superficial soil samples were collected from various points across the study site to obtain a bulk sample of 50 kg. Rocks, gravel, and other large debris were removed in situ by passing the soil through a 2 cm mesh. The sample was then dried at ambient temperature before being passed through a 4 mm mesh. Finally, the soil sample was sieved using standardized Restch separating screens, and two major fractions were recovered (0 µm −125 µm and 125 µm −4000 µm).

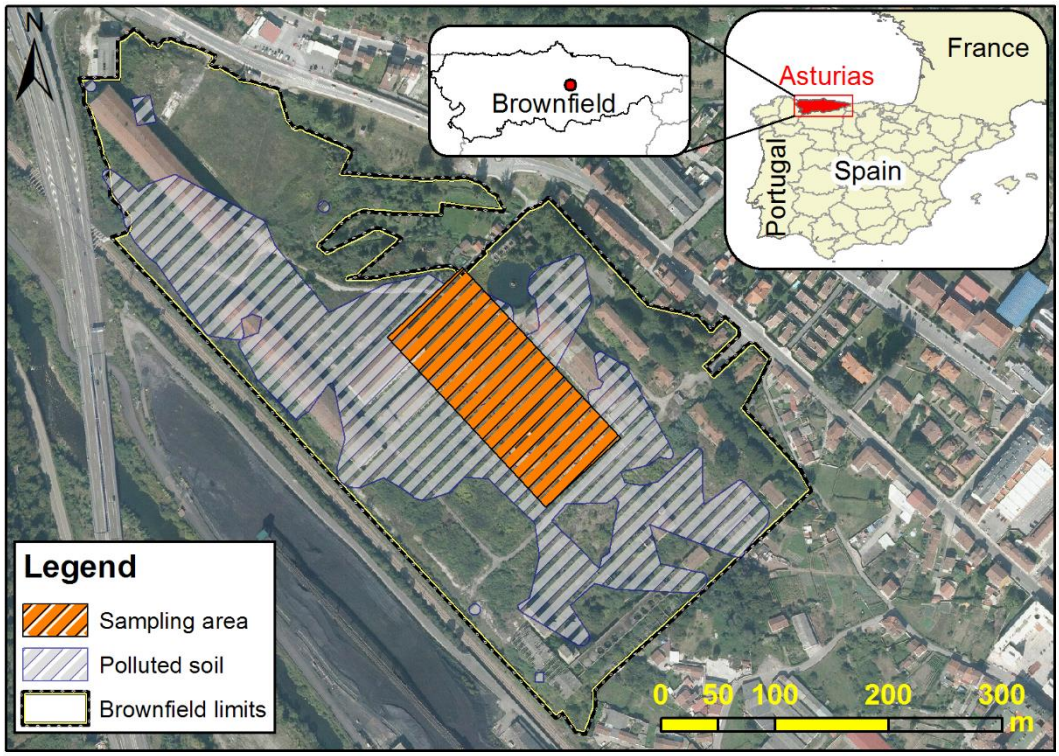

Figure 27.- Brownfield location and sampling location in Asturias, Spain (Latitude: 43.2964; Longitude: -5.68254).

Of the two major fractions recovered, the finer (grain size < 125 µm) had the highest PTE content. Thus, this fraction was divided into 12 subsamples for separation. Representative 1g subsamples from each subsample were subjected to chemical analysis: first they were leached using an "Aqua regia" solution (HCl + HNO_3) and the digested samples were

analysed by ICP-MS instrument (model HP 7700 from Agilent Technologies)for major and trace element content.

2.2. Separation experiments

Separation tests were completed in a lab-scale plant (C700 Mozley) capable of running hydrocyclones from 10 mm to 50 mm in diameter. The hydrocyclone uses gravity to separate aqueous suspensions of particles (slurries) into fractions based on particle density (Karim et al., 2021). It comprises a conical chamber with two outlets, one at the top and one at the bottom, and is fed tangentially with high pressure slurry. When the slurry enters the hydrocyclone chamber, it experiences a centrifugal force which pushes denser fractions outwards and downwards towards the lower outlet (underflow) while lower-density fractions exit via the upper outlet (overflow). The hydrocyclone used in this experiment offers four operating configurations: conic with apex diameters of 9.5mm, 6.4 mm, and 3 mm; or flat bottom (FB). Samples were tested in each of the available configurations at pressures of 100 kPa, 200 kPa, and 300 kPa, thus there were twelve experimental runs in total. The solid concentration of the feed slurry was maintained at a constant 20% by weight.

For each experimental run, once a steady state was attained, samples from both the hydrocyclone underflow and overflow were collected in borosilicate flasks. Samples (from the overflow and underflow) were subjected to low temperature drying (45° C) in an oven to minimize the potential loss of Hg and As due to volatilization. The dry weights of these samples were then measured before representative sub-samples were taken for ICP-MS analysis (model HP 7700 from Agilent Technologies).

Table 5.- Operating conditions for the twelve experimental runs.

Run	Apex	Pressure
	mm	kPa
1	9.5	100
2		200
3		300
4	6.4	100
5		200
6		300
7	3	100
8		200
9		300
10	FB	100
11		200
12		300

2.3. 2.3 Attributive analysis

2.3.1. Selection of the concentrate, tailings, and middlings fractions in multicomponent separations

A major consideration in designing an algorithm to find the BUC is the fact that soil washing operations generally deal with multicomponent contamination. Thus, the first issue to address is which fraction should be considered the concentrate (to be removed for further processing) and which the tailings (to be isolated and returned to original site) as this may vary for each PTE. For our purposes, the concentrate fraction (CF) is taken as that for which $\varepsilon > \gamma_c$ (c.f., Fuerstenau & Han, 2003) for more than half of the PTEs under consideration. Those experiments in which $\gamma_c >$ 50% were not included in our analysis, as soil washing is not interested in scenarios where the concentrated fraction is larger than the tailings fraction.

2.3.2. Basic Attributive analysis

Basic Attributive Analysis (BAA) was developed as a means of optimising soil washing by Sierra et al. (2010) and applied first in the context of remediating soils contaminated with Pyrite ash (Sierra et al, 2010; Boente et al., 2017).

In the case where a set of *m* soil-washing experiments have been carried out under a range of experimental conditions, BAA aims to identify which conditions maximize the recovery of a number, *n*, of target elements while minimizing the yield. The performance

of a given experiment, *i*, for target element, *j*, is then expressed as a quality factor Q_j^i calculated as (Eq. 3):

$$Q_j^i = \frac{Min\{\gamma\}}{\gamma^i} + \frac{\varepsilon_j^i}{Max\{\varepsilon_j\}} \ (Eq. 3)$$

Where:

- i =1,…, m and identifies a specific experiment with a particular set of separation parameters.
- j = 1,…, n and refers to results for a specific target element or contaminant and in this study, m = 10 (see Table 5 for all target elements considered)
- Q_j^i= Efficiency factor of experiment *i* for element *j*.
- γ^i = Yield of experiment *i*.
- ε_j^i = Recovery of element *j* for experiment *i*.

As discussed in 2.3.1, there are generally numerous PTEs to consider and, due to their differing toxicity levels, each will have a safe threshold concentration (the *target grade*) after soil washing. This consideration can be included in the quality factor for each experiment as a weighting coefficient. For each PTE, this coefficient is the ratio of the PTE's grade after soil washing and its target grade; it is known as the target-to-distance correction and for an element *j* separated in experiment *i* it is defined as ($Eq. 4$):

$$A_j^i = \frac{\alpha_j^i}{\propto_j^{target}} \ (\text{Eq. } 4)$$

Where:

- *i* and *j* are defined as before.
- α_j^i = Feed grade of element *j* in experiment *i*.
- $\propto_j^{target}$= Target grade for element *j*

The sum of these coefficients for all *j*=1,…, *n* elements must add up to 1.

To obtain the correct weighting for each element's contribution to overall contamination levels, the following transformation is implemented (Eq. 5):

$$A_j^{i\prime} = \frac{A_j^i}{\sum_i^m A_j^i} (Eq. 5)$$

This allows us to define a global quality index for a given experiment, *i*, for all elements under consideration (Eq. 6):

$$Q_T^i = \sum_{j=1}^{n} Q_j^i A_j^{i\prime} \text{ (Eq. 6)}$$

The experiment with optimal separation conditions is that for which this value is maximal (Eq. 7):

$$Q_{optimal} = Max\left\{\sum_{j=1}^{n} Q_j^i A_j^{i\prime}\right\} \text{ (Eq. 7)}$$

2.3.3. Three-Parameter Penalized Attributive Analysis (3PPAA)

Here we present the Three-Parameter Penalized Attributive Analysis (3PPAA) as a tool to find the BUC. This method builds on the BAA model and is an extension of a previous, two parameter (yield and recovery) version, Penalized Attributive Analysis (PAA) which was described in Corres et al. (2024).

The three parameters in question are: $\Gamma^{i\prime}$, $\mathrm{E}_j^{i\prime}$, and $\Lambda_j^{i\prime}$, respectively, the normalised weighted values of the yield in experiment *i*, and the normalised weighted values of recovery, and grade concentration in experiment *i* for element *j*. The weighting of parameters in this way reduces the influence of noisier experiments in the final analysis of experimental quality.

Our aim is to minimize yield while maximizing the recovery of a range of PTEs and their grade concentrations. Recalling the relationship between γ_c, $\mathcal{E}$ and λ (Eq.2), then, as in PPA, the appropriate parameters for yield and recovery are defined as (Eqs.8-11):

$$\Gamma^i = \frac{Min\{\gamma_c\}}{\gamma^i}\left(\frac{\sum_{i=1}^m \left|\gamma_c^i - \overline{\gamma_c}\right|}{m}\right)^{-1} (Eq. 8)$$

$$\Gamma^{i\prime} = \frac{\Gamma^i}{\sum_i^m \Gamma^i} \quad (Eq. 9)$$

$$\mathrm{E}_j^i = \frac{\varepsilon_j^i}{Max\{\varepsilon_j\}}\left(\frac{\sum_{i=1}^m \left|\varepsilon_j^i - \overline{\varepsilon}_j\right|}{n}\right)^{-1} (Eq. 10)$$

$$\mathrm{E}_j^{i\prime} = \frac{\mathrm{E}_j^i}{\sum_i^m \mathrm{E}_j^i} \quad (Eq.11)$$

The newly introduced grade parameter is similarly defined thus (Eqs. 12-13):

$$\Lambda_j^i = \frac{\lambda_j^i}{Max\{\lambda_j\}} \left(\frac{\sum_{i=1}^m \left| \lambda_j^i - \overline{\lambda}_j \right|}{n} \right)^{-1} \quad (Eq.12)$$

$$\Lambda_j^{i\prime} = \frac{\Lambda_j^i}{\sum_i^m \Lambda_j^i} \quad (Eq.13)$$

The sum of these three parameters gives us C_j^i the quality index of experiment *i* for element *j* (Eq. 14):

$$\mathrm{C}_j^i = \Gamma^{i\prime} + E_j^{i\prime} + \Lambda_j^{i\prime} \quad (Eq.14)$$

Where:

- i = experiment
- m = number of experiments
- j = specific PTE or another contaminant
- n = number of elements
- γ_c^i= yield of experiment "i"
- $\overline{\gamma_c}$ = mean yield
- ε_j^i= recovery of element "j" at experiment "i"
- $\overline{\varepsilon}_j$ = mean recovery for element "j"
- λ_j^i= concentrate grade of element "j" at experiment "i"
- $\overline{\lambda}_j$ = Mean concentrate grade of element "j"
- C_j^i= quality index of element "j" at experiment "i".

As in BAA, to account for the fact that different PTE's have different safe soil concentrations a target-to-distance correction can be used B_j^i (Eq. 15):

$$B_j^i = \frac{\alpha_j^i}{\propto_j^{tg}} \left(\frac{\sum_{i=1}^{m} \left| \propto_j^i - \overline{\alpha}_j \right|}{n} \right)^{-1} \quad (Eq. 15)$$

Where:

- B_j^i= Weighting factor for element *j* in experiment *i*
- $\propto_j^{tg}$= Target decontamination grade, i.e., the acceptable threshold grade after decontamination
- $\propto_j^i =$ Grade of element *j* in experiment *i*
- $\overline{\alpha}_j$= Grade of element *j* in experiment *i*

Here, the ratio of the post separation grade, α_j^i, to the target grade, $\propto_j^{tg}$ for the PTE of interest is weighted to minimize the final standard deviation of the result.

Normalizing this relative to its weight in the sum of *m* similar parameters B_j^i we obtain (Eq. 16):

$$B_j^{i'} = \frac{B_j^i}{\sum_i^m B_j^i} \quad (Eq. 16)$$

Although optional, this correction factor is immensely useful given the diverse nature of soils and their varying levels and types of contamination. As will be demonstrated in the case study, its use can make a significant difference to the choice of an optimal separation method. It enables the prioritisation of certain PTEs based on their initial concentration in the soil and their corresponding safe concentration as specified by regulatory standards (Boente et al., 2017).

Finally, we define the decontamination quality index $\left(Q_T^i\right)$ for all PTEs for a given experiment as (Eq. 17):

$$Q_T^i = \sum_{j=1}^{n} \mathrm{C}_j^i B_j^{i'} \quad (Eq. 17)$$

The maximum value of Q_T^i corresponds to the BUC (Eq. 18):

$$Q_{optimal} = Max \left\{ \sum_{=1}^{n} \mathrm{C}_j^i B_j^{i\prime} \right\} \quad (Eq. 18)$$

A worked example with this methodology is provided in SM1.

3. Results and discussion

3.1. Separation results

Soil from the study site was tested to find the feed concentration grades (α) of a nine PTEs (Cr, Ni, As, Cu, Zn, Pb, Sb, Cd, Mo) and the values obtained were compared against Dutch standards (e.g., Buchman & Office of Response, n.d.) (Table 6). These standards provide an intervention value (IV) and target value (TV) for a range of PTEs and were chosen as being among the most well-known and respected of available standards.

As can be seen on Table 6, out of the 9 PTEs studied, 7 (As, Cr, Cu, Ni, Pb, Sb, Zn) exceeded their respective IVs, while As, Cu and Zn also exceeded their TVs. To compare the severity of contamination associated with the PTEs under investigation, the ratio of the soil concentration of a given PTE to its TV was calculated to give a contamination level (CL). The PTEs were ranked in order of CL with the highest value, 159.3 recorded for Cr and the lowest, 1.37, recorded for Mo. Beyond the quality factor calculated for different experimental set ups (see 3.2) this provides a further criterion for selecting the optimum conditions. Specifically, optimal separation conditions should not only produce a high overall quality factor but also target the most serious pollutants.

Table 6.- Bulk sample mean α for the nine PTEs compared to their Dutch standard (e.g., Buchman & Office of Response, n.d.) intervention values (IV) and target values (TV). Elements are ordered by contamination level (CL) from the highest to the lowest.

PTE	***Grade (α)***	***Intervention value (IV)***	***Target value (TV)***	***Contamination level (CL)***
	ppm	*ppm*	*ppm*	*TV/α*
Cr	**55.7**	0.35	220	159.03
Ni	**37.3**	0.26	100	143.38
As	**60.7**	0.9	55	67.45
Cu	**111.1**	3.4	96	32.67
Zn	**377.1**	16	350	23.57
Pb	**319.9**	55	530	5.82
Sb	**9.5**	3	15	3.16
Cd	1.3	0.8	12	1.67
Mo	4.1	3	190	1.37

Separation of soil samples was conducted under the 12 different experimental conditions identified on Table 5, and, in each case, the experimental concentrate yield, (γ_c^i) was

calculated as were the recoveries (ε_j^i) of all PTEs off interest. The results are shown in Figure 28.

In the following analysis, we shall discuss only the separation results for those experiments complied with the constraint $\overline{\varepsilon^i} < \gamma_c^i$ (thus experiments 5, 6, 7, and 10 have been omitted). The full set of raw separation results is presented in SM2 (Table 5 and Table 6).

Figure 28 ranks experiments, from left to right, in descending order of mean recovery value for the nine PTEs studied ($\overline{\varepsilon^i}$). Experiments 8 and 9 have by far the lowest mean recovery values ($\overline{\varepsilon^8}$ = 36.2% and $\overline{\varepsilon^9}$ = 30.4%) while mean recovery values for the remaining experiments are similar, varying within a range from 54.6% (Experiment 4) to 59.8% (Experiment 3).

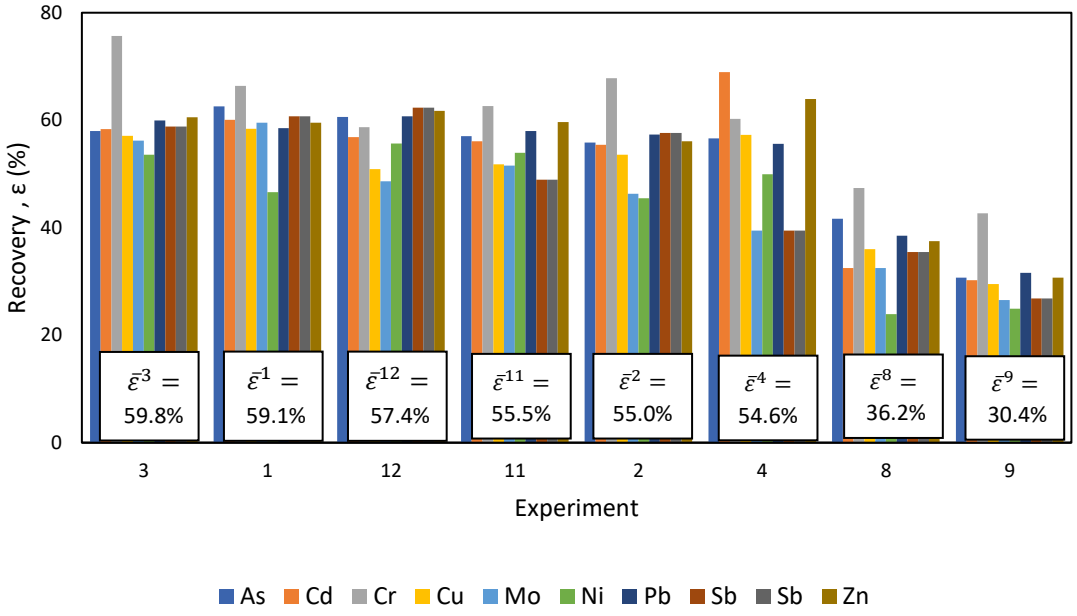

Figure 28.- Recovery values for each experiment and PTE in the concentrated fraction (ε_j^i). Results are in descending order of mean recovery, $\overline{\varepsilon^i}$, (left to right). Only experiments in which $\overline{\varepsilon^i} < \gamma_c^i$ are shown.

Referring to Figure 29, the values for γ_c^i found in each experiment show a similar trend to that seen for $\overline{\varepsilon^i}$ (Figure 28). Specifically, experiments 8 and 9 have the lowest values of γ_c^i (γ_c^8 = 16.1 and γ_c^9 = 14.8), while for the remaining experiments these values are not only significantly higher but also very similar: γ_c^i ranges from 34.1% (Experiment 2) to 43.5% (Experiment 3).

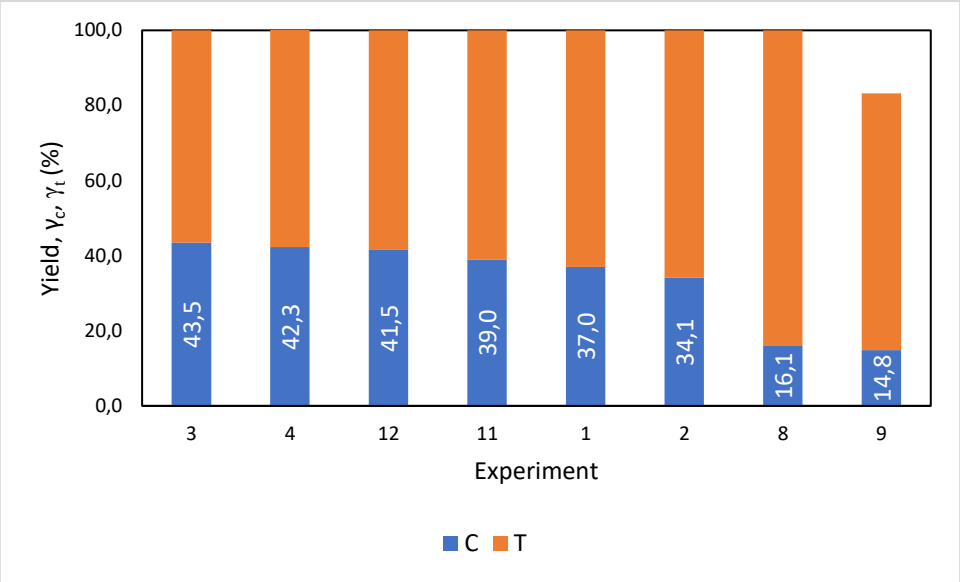

Figure 29.- Yield for the concentrated ($\gamma^i c$) and tailings ($\gamma^i t$) fractions. Results are ordered by descending value of γ_c^i. Only experiments in which $\bar{\varepsilon}^i < \gamma_c^i$ are shown.

Based on these results it is unclear which experimental conditions would be optimal. Experiment 3 maximizes overall recovery but has the highest yield, while the experiments with the lowest yield (8 and 9) also have the lowest overall recoveries. Based on Cr recovery, six experiments record their highest recovery for this PTE, however, for all except Experiment 3, the recovery of Ni (the next most important contaminant in the sample, see Table 6) is their lowest recovery value.

To further assess the efficiency of our separation experiments, we can plot the mean PTE recovery value for each experiment ($\bar{\varepsilon}^i$) against the experimental concentrate fraction yield (γ_c^i) and compare our results to the theoretical perfect, typical and non-separation curves (PSC, TSC and NSC: see for e.g., Richardson and Morrison, 2003). Experiments for which separation has been most successful should approach the PSC while less successful separation experiments will be closer to the NSC.

Referring to Figure 31, the points representing Experiments 8 and 9 lie closest to the TSC. This suggests that these two experiments might provide the best upgrading conditions.

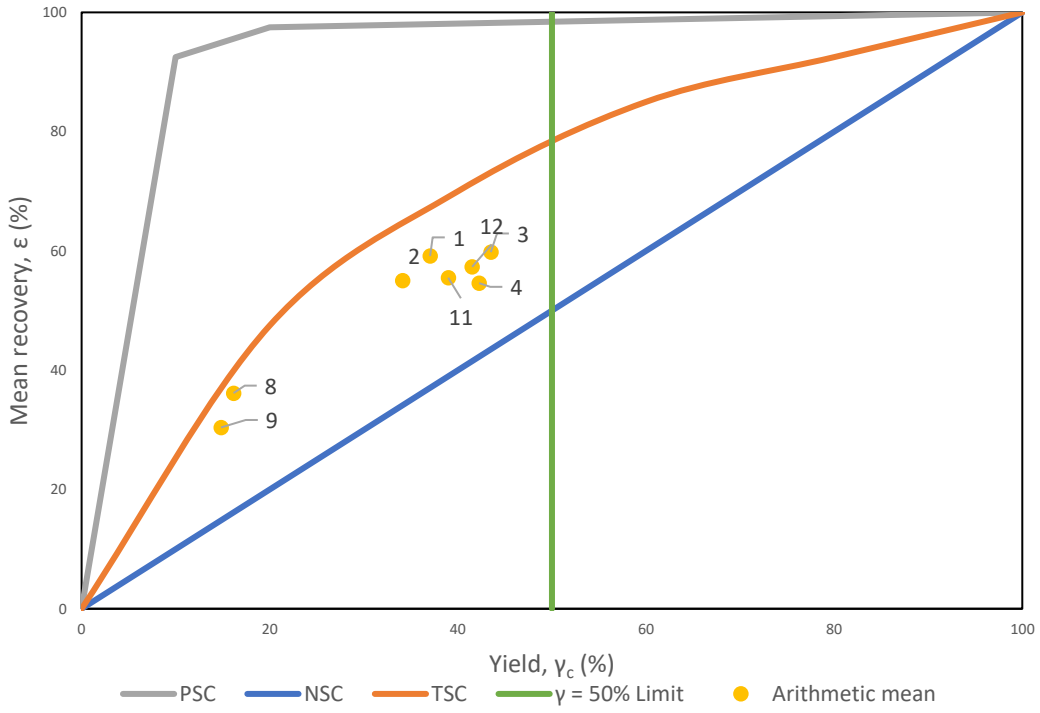

Figure 30.- Mean recovery and concentrate yield for each experiment ($\bar{\varepsilon}^{i} < \gamma_c^i$) plotted for comparison to curves for perfect separation (PSC), non-separation (NSC), and typical separation (TSC).

3.2. Three-parameter Attributive Analysis for optimising soil upgrading

While comparing experimental results to theoretical separation curves is adequate in many scenarios, that this method uses mean recovery values across all contaminants is a severe limitation since some PTEs are significantly more harmful than others. By its incorporation of a target-to-distance correction, B_j^i, 3PPAA-U offers a superior approach in this respect because it is able to consider recovery values for individual elements and therefore enables optimization of soil upgrading for specific PTEs.

In the following we compare 3PPAA-U with and without target-to-distance correction in order to highlight its importance. Without this correction, the 3PPAA-U quality index ($Q_{optimal}$) offers information on which experimental parameters lead to the overall most efficient soil upgrading process, that is, it ranks experiments according to their average performance with respect to all PTEs considered without addressing the relative toxicity of different elements. With target-to-distance correction, 3PPAA-U can help adapt and optimize a soil washing process to the precise contamination properties of a given soil.

Table 7 shows the quality indices for all of the experiments calculated using 3PPAA-U without target-to-distance correction. The best performing experiments still appear to be Experiments 8 and 9 with quality indices 0.6 and 0.7 units greater than the third best performer (Experiment 2) (Table 7).

Table 7.- 3PPAA-U before the target-to-distance-to target correction for experiments where $\overline{\varepsilon^i} < \gamma_c^i$.

Experiment	C_j^i									$\sum_{j=1}^{n} C_j^i$
	As	*Cd*	*Cr*	*Cu*	*Mo*	*Ni*	*Pb*	*Sb*	*Zn*	
1	0.3974	0.3692	0.3772	0.3796	0.3958	0.3462	0.3939	0.4292	0.3648	3.4533
2	0.3961	0.3719	0.4022	0.3869	0.3674	0.3616	0.4032	0.4295	0.3813	3.5003
3	0.3384	0.3339	0.4002	0.3506	0.3724	0.3646	0.3454	0.3425	0.3458	3.1937
4	0.3262	0.4407	0.3084	0.3444	0.2744	0.3593	0.3172	0.2528	0.3770	3.0004
8	0.4768	0.4384	0.4989	0.4526	0.4447	0.4137	0.4737	0.4799	0.4460	4.1247
9	0.4795	0.4584	0.4798	0.4650	0.4479	0.4362	0.4861	0.4944	0.4571	4.2044
11	0.2914	0.2928	0.2791	0.3102	0.3690	0.3570	0.2864	0.2672	0.3110	2.7640
12	0.2942	0.2947	0.2542	0.3107	0.3283	0.3615	0.2941	0.3045	0.3170	2.7592

However, as previous results show (see Figure 28 and Figure 29), these two experiments have not only the lowest values of γ_c^i (both are nearly half the value found for Experiment 2 which has the next lowest γ_c^i) but also the lowest values of $\overline{\varepsilon^i}$ ($\overline{\varepsilon^8}$ = 36.2% and $\overline{\varepsilon^9}$ = 30.4% corresponding to, respectively, nearly half and two thirds that the next lowest mean recovery, $\overline{\varepsilon^4}$ = 54.6%). That 3PPAA-U points to these experiments as potentially giving the BUC suggests that optimal conditions are favoured more by minimising γ_c^i than maximising $\overline{\varepsilon^i}$. This becomes clear if we consider that both these values are higher for Experiment 8 than for Experiment 9 but the difference is greatest for $\overline{\varepsilon^i}$ (for γ_c^i is 1.33% higher and $\overline{\varepsilon^i}$ is 5.76% higher); thus, since Experiment 9 has the higher quality index, it would seem that more is gained by a marginal minimisation of γ_c^i compared to a far larger gain in $\overline{\varepsilon^i}$.

Referring back to Figure 31, it can be seen that compared to the points representing all other experiments, those representing Experiments 8 and 9 were closest to the TSC. Thus,

3PPAA-U without target-to-distance correction suggests similar BUCs to those derived from conventional separation curve methods.

Table 8 shows the quality indices of each experiment calculated with target-to-distance correction. In this way, the quality index now includes a consideration of the grade concentrations for individual PTEs of interest for each experimental set up studied. Referring to Table 8, while Experiment 9 still comes out as one of the best methods, Experiment 2, ranked third before target-to-distance correction, now appears to be optimal with Experiments 1 and 3 also performing well.

Table 8.- 3PPAA-U after the distance to target correction for experiments where $\overline{\varepsilon^{i}} < \gamma_c^i$.

Experiment	$C_j^i B_j^{i\prime}$									$\sum_{j=1}^{n} C_j^i B_j^{i\prime}$
	As	*Cd*	*Cr*	*Cu*	*Mo*	*Ni*	*Pb*	*Sb*	*Zn*	
1	0.0612	0.0486	0.0598	0.0508	0.0467	0.0440	0.0668	0.0742	0.0496	0.5017
2	0.0654	0.0510	0.0630	0.0563	0.0514	0.0471	0.0658	0.0721	0.0570	0.5290
3	0.0514	0.0462	0.0735	0.0516	0.0547	0.0525	0.0511	0.0444	0.0513	0.4768
4	0.0446	0.0853	0.0425	0.0455	0.0334	0.0549	0.0411	0.0292	0.0602	0.4368
8	0.0496	0.0506	0.0608	0.0447	0.0419	0.0475	0.0545	0.0589	0.0448	0.4533
9	0.0656	0.0542	0.0500	0.0547	0.0475	0.0442	0.0659	0.0811	0.0541	0.5173
11	0.0220	0.0227	0.0199	0.0319	0.0529	0.0394	0.0186	0.0172	0.0276	0.2524
12	0.0223	0.0260	0.0167	0.0379	0.0426	0.0431	0.0217	0.0191	0.0314	0.2608

Figure 31 shows a plot of quality indices for each of our experimental set ups to highlight the differences between which separation conditions would seem optimal without (curve A) and with (curve B) target-to-distance correction.

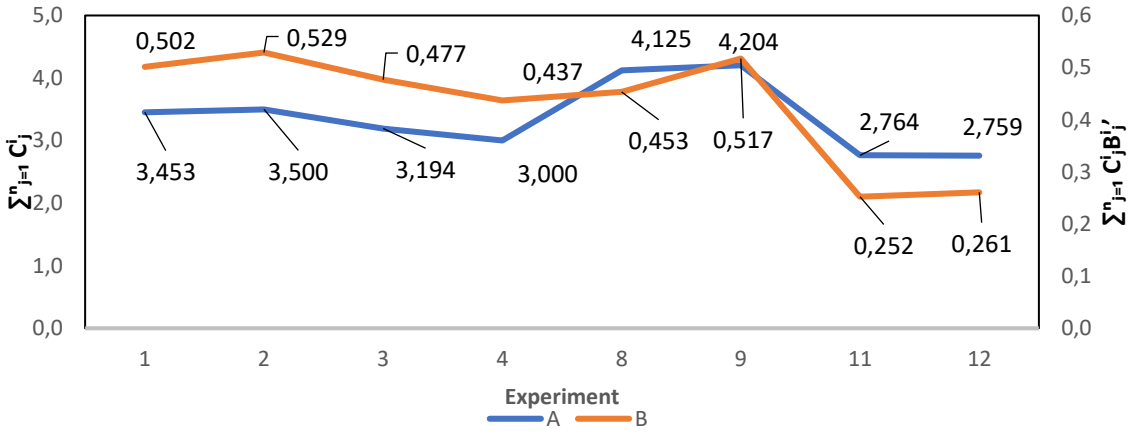

Figure 31.- Results of 3PPAA-U without (A) and with (B) target-to-distance correction for experiments with $\bar{\varepsilon}^{i} < \gamma_c^i$

As can be seen in the tables included in SM2, while recovery and yield vary relatively little between experiments (the standard deviation is between 10.02 and 12.73 for both these values), the grades found for different PTEs varies greatly in each experiment (the standard deviation in λ for some elements [for instance Cd] is as low as 0.67 while for others [such as Pb] it is as high as 181). In this way, it is no surprise that the calculation with target-to-distance correction produces very different results compared to previous methods.

Our results show 3PPAA-U provides a good general method for the identification of promising experimental configurations for soil upgrading operations. However, it is only a guide, and to select the BUCs for a particular soil, it is recommended that the top 2 or 3 configurations identified by 3PPAA-U be examined more closely to fine tune values of γ_c and ε. This is particularly important where, as in the current set of experiments, the analysis shows two configurations (Experiments 2 and 9) to have very similar efficiencies.

The 3PPAA methodology extends beyond identifying BUCs for soil washing, offering potential to identify optimal operating conditions across a broad spectrum of materials processing and manufacturing scenarios. The methodology could be extended to include a range of variables— from temperature and pressure to particle size, alongside environmental and economic considerations, such as energy consumption or CO_2 generation—to address a number of complex operational challenges simultaneously.

4. Conclusions

Three Parameter Attribute Analysis for soil upgrading is a method that allows the identification of and prioritizing of operational outcomes; thus, it can enable the fine tuning of operations to the specific problems of a given site.

A particular strength of 3PPAA-U for soil upgrading lies in how it deals with multicomponent feeds to derive the BUC. Firstly, the method has a clear criterion for establishing which fraction constitutes the concentrate and which the tailings so avoiding the issue that in some experiments, pollutants might report to different fractions. In addition, its target-to-distance correction selects the optimal upgrading conditions based on preferential contribution of the most harmful pollutants. The method is also robust to extremes of variation in parameters due to the way in which these are weighted.

3PPAA-U assess separation experiments based on three parameters, the grade (λ) and recovery (ε) of pollutants to be targeted and the concentrate yield (γ_c). The method ranks different experimental configurations dependent upon how well they maximize the grade and recovery while minimizing yield and appears to prioritize the minimisation of yield over maximising recovery. Without target-to-distance correction, 3PPAA-U is at least as good at selecting optimal experimental conditions as methods based on other criteria, such as the proximity to the perfect separation curve. The additional correction enables 3PPAA-U to exceed these traditional methods and so potentially improve the outcome of soil washing processes.

It is important to recognize that the 3PPAA-U is not an absolute guide for identifying the BUC, but rather a heuristic methodology. Thus, although it provides a structured and objective approach for evaluating and comparing different options, it is based on a set of assumptions and simplifications, so it may not capture the full complexity of a given soil washing operation. In this way, researchers and practitioners are advised to take this methodology only as an indicator of which experimental configurations are most promising and worth looking into further. The full decision-making process for choosing the best approach for a particular site must also consider a full range of subjective and qualitative factors such as cost, feasibility and risk. Consequently, although 3PPAA-U can be a useful tool for decision-making, it should be used in conjunction with other methods and criteria and should be applied with caution and critical thinking. One of the most

obvious improvements of this method would be to include a third parameter, the grade, as part of the calculation for the experimental quality index (C_j^i). This additional constraint could potentially mitigate the impact of anomalous values and improve the overall accuracy of the method. Further research might include expanding the 3PPAA-U methodology to assess a fuller range of criteria important to the success of soil washing operations.

Acknowledgements

Carlos Sierra thanks the EURECA-PRO phase I 2020–2023 co-funded by the Erasmus+ Program of the European Union (Ref.: 101004049).

References

Ashraf, S., Ali, Q., Zahir, Z. A., Ashraf, S., & Asghar, H. N. (2019). Phytoremediation: Environmentally sustainable way for reclamation of heavy metal polluted soils. *Ecotoxicology and Environmental Safety*, *174*, 714–727. https://doi.org/10.1016/J.ECOENV.2019.02.068

Boente, C., Gerassis, S., Albuquerque, M.T.D., Taboada, J., Gallego, J.R., 2020. Local versus Regional Soil Screening Levels to Identify Potentially Polluted Areas. *Mathematical Geosciences*, 52, 381–396. https://doi.org/10.1007/s11004-019-09792-x

Boente, C., Sierra, C., Rodríguez-Valdés, E., Menéndez-Aguado, J.M., Gallego, J.R., 2017. Soil washing optimization by means of attributive analysis: Case study for the removal of potentially toxic elements from soil contaminated with pyrite ash. *Journal of Cleaner Production*, 142, 2693–2699. https://doi.org/10.1016/j.jclepro.2016.11.007

Buchman, M., & Office of Response, N. (n.d.). SQuiRT Cards, 2008.

Chen, L., Wang, F., Zhang, Z., Chao, H., He, H., Hu, W., Zeng, Y., Duan, C., Liu, J., Fang, L., 2023. Influences of arbuscular mycorrhizal fungi on crop growth and potentially toxic element accumulation in contaminated soils: A meta-analysis. *Critical Reviews in Environmental Science and Technology*, 53, 1795–1816. https://doi.org/10.1080/10643389.2023.2183700

Chen, Z., Ma, Y., & Liao, X. (2016). Phytoremediation of heavy metal pollution from mining and smelting activities: a review. Journal of Cleaner Production, 127, 19-30.

Corres, X., Sierra, C., Diez-Mestas, A.J., Gallego, J.R., Baragaño, D., 2024. A novel heuristic tool for selecting the best upgrading conditions for the removal of potentially toxic elements by soil washing. Journal of Hazardous Materials, 466, 133529. https://10.1016/j.jhazmat.2024.133529

Deacon, C. M., Blackwell, M. S., Bol, R., Reimann, C., & Zhao, F. J. (2012). PAHs in soil: long-term changes following land-use change and influence on PAH bioaccessibility. Environmental Pollution, 162, 330-335.

Dermont, G., Bergeron, M., Mercier, G., & Richer-Laflèche, M. (2008). Soil washing for metal removal: A review of physical/chemical technologies and field applications.

Journal of Hazardous Materials, *152*(1), 1–31. https://doi.org/10.1016/J.JHAZMAT.2007.10.043

Drzymała, J. (2006). Atlas of upgrading curves used in separation and mineral science and technology. *Physicochemical Problems of Mineral Processing*, *40*(1), 19-29.

Richardson, JM &. Morrison, R.D (2003) Metallurgical Balances and Efficiency. In: Fuerstenau, M. C., & Han, K. N. (2003). *Principles of mineral processing*. Society for Mining, Metallurgy, and Exploration.

Gallego, J. L. R., Ordóñez, A., & Loredo, J. (2002). Investigation of trace element sources from an industrialized area (Avilés, northern Spain) using multivariate statistical methods. *Environment International*, *27*(7), 589–596. https://doi.org/10.1016/S0160-4120(01)00115-5

Gee, G. W., & Or, D. (2018). 2.4 Particle-Size Analysis. *Methods of Soil Analysis, Part 4: Physical Methods*, 255–293. https://doi.org/10.2136/SSSABOOKSER5.4.C12

Guo, J., Yuan, C., Zhao, Z., He, Q., Zhou, H., & Wen, M. (2022). Soil washing by biodegradable GLDA and PASP: Effects on metals removal efficiency, distribution, leachability, bioaccessibility, environmental risk and soil properties. *Process Safety and Environmental Protection*, *158*, 172–180. https://doi.org/10.1016/J.PSEP.2021.12.004

Karim, A. V., Jiao, Y., Zhou, M., Nidheesh, P.V., 2021. Iron-based persulfate activation process for environmental decontamination in water and soil. *Chemosphere 265, 129057*. https://doi.org/10.1016/j.chemosphere.2020.129057

Khalid, S., Shahid, M., Niazi, N. K., Murtaza, B., Bibi, I., & Dumat, C. (2017). A comparison of technologies for remediation of heavy metal contaminated soils. *Journal of Geochemical Exploration*, *182*, 247–268. https://doi.org/10.1016/J.GEXPLO.2016.11.021

Khum-in, V., Suk-in, J., In-ai, P., Piaowan, K., Praimeesub, Y., Rintachai, K., Supanpaiboon, W., Phenrat, T., 2023. Combining magnet-assisted soil washing and soil amendment with zero-valent iron to restore safe rice cultivation in real cadmium-contaminated paddy fields. *Chemosphere 340, 139816*. https://doi.org/10.1016/j.chemosphere.2023.139816

Lee, K. Y., & Kim, K. W. (2010). Heavy metal removal from shooting range soil by hybrid electrokinetics with bacteria and enhancing agents. *Environmental Science and Technology*, *44*(24), 9482–9487. https://doi.org/10.1021/ES102615A/SUPPL_FILE/ES102615A_SI_001.PDF

Martínez López, J., Llamas Borrajo, J., de Miguel García, E., Rey Arrans, J., Hidalgo Estévez, M. C., & Sáez Castillo, A. J. (2008). Multivariate analysis of contamination in the mining district of Linares (Jaén, Spain). *Applied Geochemistry*, *23*(8), 2324–2336. https://doi.org/10.1016/J.APGEOCHEM.2008.03.014

Pearl, M., Pruijn, M., & Bovendeur, J. (2006). The application of soil washing to the remediation of contaminated soils. *Land Contamination and Reclamation*, *14*(3), 713–726. https://doi.org/10.2462/09670513.680

Pinto, I. S. S., Neto, I. F. F., & Soares, H. M. V. M. (2014). Biodegradable chelating agents for industrial, domestic, and agricultural applications—a review. *Environmental Science and Pollution Research*, *21*(20), 11893–11906. https://doi.org/10.1007/S11356-014-2592-6/METRICS

Sierra, C., Martínez, J., Menéndez-Aguado, J. M., Afif, E., & Gallego, J. R. (2013). High intensity magnetic separation for the clean-up of a site polluted by lead metallurgy. *Journal of Hazardous Materials*, *248–249*(1), 194–201. https://doi.org/10.1016/j.jhazmat.2013.01.011

Sierra, C., Gallego, J.R., Afif, E., Menéndez-Aguado, J.M., González-Coto, F., 2010. Analysis of soil washing effectiveness to remediate a brownfield polluted with pyrite ashes. *Journal of Hazardous Materials*, 180, 602–608. https://10.1016/j.jhazmat.2010.04.075

Sun, Y., Li, H., Guo, G., Semple, K. T., & Jones, K. C. (2019). Soil contamination in China: Current priorities, defining background levels and standards for heavy metals. *Journal of Environmental Management*, *251*, 109512. https://doi.org/10.1016/J.JENVMAN.2019.109512

Turečková, K., Nevima, J., Duda, D., & Tuleja, P. (2021). Latent structures of brownfield regeneration: A case study of regions of the Czech Republic. *Journal of Cleaner Production*, *311*, 127478. https://doi.org/10.1016/J.JCLEPRO.2021.127478

Wang, Y., Li, A., Cui, C., 2021. Remediation of heavy metal-contaminated soils by electrokinetic technology: Mechanisms and applicability. *Chemosphere*, 265, 129071. https://10.1016/j.chemosphere.2020.129071

Wills, B. A., & Napier-Munn, T. J. (2006). Mineral Processing Technology: An Introduction to the Practical Aspects of Ore Treatment and Mineral Recovery. In Butterworth-Heinemann (Ed.), *Wills' Mineral Processing Technology* (7th ed). Butterworth-Heinemann. https://doi.org/10.1016/C2010-0-65478-2

Wu, Q., Leung, J. Y. S., Geng, X., Chen, S., Huang, X., Li, H., Huang, Z., Zhu, L., Chen, J., & Lu, Y. (2015). Heavy metal contamination of soil and water in the vicinity of an abandoned e-waste recycling site: Implications for dissemination of heavy metals. *Science of The Total Environment*, *506–507*, 217–225. https://doi.org/10.1016/J.SCITOTENV.2014.10.121

Ye, B., Lan, J., Nong, Z., Qin, C., Ye, M., Liang, J., Li, J., Bi, J., Huang, W., 2022. Efficiently combined technology of precipitation, bipolar membrane electrodialysis, and adsorption for salt-containing soil washing wastewater treatment. *Process Safety and Environmental Protection, 165*, 205–216. https://doi.org/10.1016/j.psep.2022.07.015

Suplementary Materials – 1: Attributive analysis: A case study using two experimental set-ups and 2 contaminants

To demonstrate TPAA, for simplicity we have selected two experimental configurations from the 12 investigated and we shall focus on only two PTEs, As and Cd. Table 9 below shows initial and target concentrations of the two chosen PTEs (left) and the yield, and recovery after separation of these two PTEs for two different experimental configurations:

Table 9.- Initial and target concentrations of the two chosen PTEs (left) and the yield, and recovery after separation of these two PTEs for two different experimental configurations.

	λ		α		α^{target}		γ	ε	
Exp.	**As**	**Cd**	**As**	**Cd**	**As**	**Cd**		**As**	**Cd**
1	122	2.3	72.27	1.42	0.9	0.9	37.048	62.543	60.064
2	127	2.4	77.58	1.48			34.101	55.827	55.396

The TPAA methodology is as follows:

- **Exp. 1 (As):**

$$\gamma^1 = 37.048\ ;\ \varepsilon_{As}^1 = 62.543\ ;\ \alpha_{As}^1 = 72.27\ ;\ \lambda_{As}^1 = 122$$

$$\gamma^2 = 34.101\ ;\ \varepsilon_{As}^2 = 55.827\ ;\ \propto_{As}^2 = 77.58\ ;\ \lambda_{As}^2 = 127$$

$$Min\{\gamma\} = 34.101\ \ ;\ Max\{\varepsilon_{As}\} = 62.543\ ;\ \propto_{As}^{target} = 0.9$$

$$\bar{\gamma} = 35.5745\ ;\ \overline{\varepsilon}_{As} = 59.185\ ;\ \overline{\alpha}_{As} = 74.925\ ;\ \overline{\lambda}_{As} = 124.5$$

$$\Gamma^1 = \frac{Min\{\gamma\}}{\gamma^1}\left(\frac{|\gamma^1 - \bar{\gamma}| + |\gamma^2 - \bar{\gamma}|}{2}\right)^{-1} = 0.625$$

$$\Gamma^{1\prime} = \frac{\Gamma^1}{\Gamma^1 + \Gamma^2} = 0.479$$

$$\mathrm{E}_{As}^1 = \frac{\varepsilon_{As}^1}{Max\{\varepsilon_{As}\}}\left(\frac{|\varepsilon_{As}^1 - \overline{\varepsilon}_{As}| + |\varepsilon_{As}^2 - \overline{\varepsilon}_{As}|}{2}\right)^{-1} = 0.298$$

$$\mathrm{E}_{As}^{1}{}' = \frac{\mathrm{E}_{As}^{1}}{\mathrm{E}_{As}^{1} + \mathrm{E}_{As}^{2}} = 0.528$$

$$\Lambda_{As}^{1} = \frac{\lambda_{As}^{1}}{Max\{\lambda_{As}\}}\left(\frac{\left|\lambda_{As}^{1} - \overline{\lambda}_{As}\right| + \left|\lambda_{As}^{2} - \overline{\lambda}_{As}\right|}{2}\right)^{-1} = 0.384$$

$$\Lambda_{As}^{1}{}' = \frac{\Lambda_{As}^{1}}{\Lambda_{As}^{1} + \Lambda_{As}^{2}} = 0.490$$

$$\mathrm{C}_{As}^{1} = \Gamma^{1\prime} + \mathrm{E}_{As}^{1}{}' + \Lambda_{As}^{1}{}' = 1.498$$

$$B_{As}^{1} = \frac{\alpha_{As}^{1}}{\propto_{As}^{target}}\left(\frac{|\propto_{As}^{1} - \overline{\alpha}_{As}| + |\propto_{As}^{2} - \overline{\alpha}_{As}|}{2}\right)^{-1} = 30.256$$

$$B_{As}^{1}{}' = \frac{B_{As}^{1}}{B_{As}^{1} + B_{As}^{2}} = 0.482$$

- **Exp. 1 (Cd):**

$$\gamma^{1} = 37.048\ ;\ \varepsilon_{Cd}^{1} = 60.064\ ;\ \alpha_{Cd}^{1} = 1.42\ ;\ \lambda_{Cd}^{1} = 2.3$$

$$\gamma^{2} = 34.101\ ;\ \varepsilon_{Cd}^{2} = 55.396;\ \propto_{Cd}^{2} = 1.48\ ;\ \lambda_{Cd}^{2} = 2.4$$

$$Min\{\gamma\} = 34.101\ ;\ Max\{\varepsilon_{Cd}\} = 60.06;\ \propto_{Cd}^{target} = 0.8$$

$$\bar{\gamma} = 35.5745\ ;\ \overline{\varepsilon}_{Cd} = 57.73\ ;\ \overline{\alpha}_{Cd} = 1.45\ ;\ \overline{\lambda}_{Cd} = 2.35$$

$$\mathrm{E}_{Cd}^{1} = \frac{\varepsilon_{Cd}^{1}}{Max\{\varepsilon_{Cd}\}}\left(\frac{\left|\varepsilon_{Cd}^{1} - \overline{\varepsilon}_{Cd}\right| + \left|\varepsilon_{Cd}^{2} - \overline{\varepsilon}_{Cd}\right|}{2}\right)^{-1} = 0.428$$

$$\mathrm{E}_{Cd}^{1}{}' = \frac{\mathrm{E}_{Cd}^{1}}{\mathrm{E}_{Cd}^{1} + \mathrm{E}_{Cd}^{2}} = 0.520$$

$$\Lambda_{Cd}^{1} = \frac{\lambda_{Cd}^{1}}{Max\{\lambda_{Cd}\}}\left(\frac{\left|\lambda_{Cd}^{1} - \overline{\lambda}_{Cd}\right| + \left|\lambda_{Cd}^{2} - \overline{\lambda}_{Cd}\right|}{2}\right)^{-1} = 19.167$$

$$\Lambda_{Cd}^{1}{}' = \frac{\Lambda_{Cd}^{1}}{\Lambda_{Cd}^{1} + \Lambda_{Cd}^{2}} = 0.489$$

$$\mathrm{C}_{As}^{1} = \Gamma^{1'} + \mathrm{E}_{Cd}^{1}{}' + \Lambda_{Cd}^{1}{}' = 1.489$$

$$B_{As}^{1} = \frac{\alpha_{Cd}^{1}}{\propto_{Cd}^{target}}\left(\frac{|\propto_{Cd}^{1} - \overline{\alpha}_{Cd}| + |\propto_{Cd}^{2} - \overline{\alpha}_{Cd}|}{2}\right)^{-1} = 60.375$$

$$B_{Cd}^{1}{}' = \frac{B_{Cd}^{1}}{B_{Cd}^{1} + B_{Cd}^{2}} = 0.510$$

- **Quality performance index without distance-target correction ($\boldsymbol{Q_{T\,nc}^{i}}$) for Experiment 1:**

$$Q_{T\,nc}^{i} = \mathrm{C}_{As}^{1} + \mathrm{C}_{Cd}^{1} = 1.489 + 1.498 = 2.986$$

- **Quality performance index with distance-target correction for Experiment 1:**

$$Q_{T}^{i} = \mathrm{C}_{As}^{1} B_{As}^{1}{}' + \mathrm{C}_{Cd}^{1} B_{Cd}^{1}{}' = 0.722 + 0.729 = 1.452$$

Experiment 2

- **Exp. 2 (As):**

$$\Gamma^2 = \frac{Min\{\gamma\}}{\gamma^2}\left(\frac{|\gamma^1 - \bar{\gamma}| + |\gamma^2 - \bar{\gamma}|}{2}\right)^{-1} = 0.679$$

$$\Gamma^{2\prime} = \frac{\Gamma^2}{\Gamma^1 + \Gamma^2} = 0.521$$

$$\mathrm{E}_{As}^2 = \frac{\varepsilon_{As}^2}{Max\{\varepsilon_{As}\}}\left(\frac{|\varepsilon_{As}^1 - \overline{\varepsilon}_{As}| + |\varepsilon_{As}^2 - \overline{\varepsilon}_{As}|}{2}\right)^{-1} = 0.266$$

$$\mathrm{E}_{As}^{2\prime} = \frac{\mathrm{E}_{As}^2}{\mathrm{E}_{As}^1 + \mathrm{E}_{As}^2} = 0.472$$

$$\Lambda_{As}^2 = \frac{\lambda_{As}^2}{Max\{\lambda_{As}\}}\left(\frac{\left|\lambda_{As}^1 - \overline{\lambda}_{As}\right| + \left|\lambda_{As}^2 - \overline{\lambda}_{As}\right|}{2}\right)^{-1} = 0.4$$

$$\Lambda_{As}^{1\prime} = \frac{\Lambda_{As}^1}{\Lambda_{As}^1 + \Lambda_{As}^2} = 0.51$$

$$\mathrm{C}_{As}^2 = \Gamma^{2\prime} + \mathrm{E}_{As}^{2\prime} + \Lambda_{As}^{2\prime} = 1.502$$

$$B_{As}^1 = \frac{\alpha_{As}^1}{\propto_{As}^{target}}\left(\frac{|\propto_{As}^1 - \overline{\alpha}_{As}| + |\propto_{As}^2 - \overline{\alpha}_{As}|}{2}\right)^{-1} = 32.478$$

$$B_{As}^{2\prime} = \frac{B_{As}^2}{B_{As}^1 + B_{As}^2} = 0.518$$

- **Exp. 2 (Cd):**

$$\mathrm{E}_{Cd}^2 = \frac{\varepsilon_{Cd}^2}{Max\{\varepsilon_{Cd}\}}\left(\frac{|\varepsilon_{Cd}^1 - \overline{\varepsilon}_{d}| + |\varepsilon_{Cd}^2 - \overline{\varepsilon}_{Cd}|}{2}\right)^{-1} = 0.395$$

$$\mathrm{E}_{Cd}^{2\prime} = \frac{\mathrm{E}_{Cd}^2}{\mathrm{E}_{Cd}^1 + \mathrm{E}_{Cd}^2} = 0.48$$

$$\Lambda_{Cd}^{2} = \frac{\lambda_{Cd}^{2}}{Max\{\lambda_{Cd}\}}\left(\frac{\left|\lambda_{Cd}^{1} - \overline{\lambda}_{Cd}\right| + \left|\lambda_{Cd}^{2} - \overline{\lambda}_{Cd}\right|}{2}\right)^{-1} = 20$$

$$\Lambda_{Cd}^{2}{}' = \frac{\Lambda_{Cd}^{2}}{\Lambda_{Cd}^{1} + \Lambda_{Cd}^{2}} = 0.511$$

$$\mathrm{C}_{As}^{2} = \Gamma^{2'} + \mathrm{E}_{Cd}^{2}{}' + \Lambda_{Cd}^{2}{}' = 1.511$$

$$B_{As}^{2} = \frac{\alpha_{Cd}^{2}}{\propto_{Cd}^{target}}\left(\frac{|\propto_{Cd}^{1} - \overline{\alpha}_{Cd}| + |\propto_{Cd}^{2} - \overline{\alpha}_{Cd}|}{2}\right)^{-1} = 62.875$$

$$B_{Cd}^{2}{}' = \frac{B_{Cd}^{2}}{B_{Cd}^{1} + B_{Cd}^{2}} = 0.510$$

- **Quality performance index without distance-target correction ($\boldsymbol{Q_{T\,nc}^{i}}$) for Experiment 2:**

$$Q_{T\,nc}^{i} = \mathrm{C}_{As}^{1} + \mathrm{C}_{Cd}^{1} = 1.502 + 1.511 = 3.014$$

- **Quality decontamination index with distance-target correction for Experiment 2:**

$$Q_{T}^{i} = \mathrm{C}_{As}^{2} B_{As}^{2}{}' + \mathrm{C}_{Cd}^{2} B_{Cd}^{2}{}' = 0.778 + 0.771 = 1.549$$

Suplementary Materials – 2: Complete separation results

Table 10.- Separation results for As, Cd, Cr, Cu and Mo.

Apex Φ	Pressure	Experiment	Fraction	γ_c	As			Cd			Cr			Cu			Mo		
(mm)	(kPa)			(%)	α (ppm)	λ (ppm)	ε (%)	α (ppm)	λ (ppm)	ε (%)	α (ppm)	λ (ppm)	ε (%)	α (ppm)	λ (ppm)	ε (%)	α (ppm)	λ (ppm)	ε (%)
9.5	100	1	UF	63.0	72.3	43.0	37.5	1.4	0.9	39.9	58.0	31.0	33.6	113.5	75.0	41.6	3.1	2.0	40.5
			OF	37.0	72.3	122.0	62.5	1.4	2.3	60.1	58.0	104.0	66.4	113.5	179.0	58.4	3.1	5.0	59.5
	200	2	UF	65.9	77.6	52.0	44.2	1.5	1.0	44.6	57.3	28.0	32.2	123.5	87.0	46.4	3.7	3.0	53.7
			OF	34.1	77.6	127.0	55.8	1.5	2.4	55.4	57.3	114.0	67.8	123.5	194.0	53.6	3.7	5.0	46.3
	300	3	UF	56.5	71.3	53.0	42.0	1.5	1.1	41.7	67.3	29.0	24.4	125.0	95.0	42.9	3.9	3.0	43.8
			OF	43.5	71.3	95.0	58.0	1.5	2.0	58.3	67.3	117.0	75.6	125.0	164.0	57.1	3.9	5.0	56.2
6.4	100	4	UF	64.8	64.2	43.0	43.4	2.1	1.0	31.1	50.5	31.0	39.8	112.2	74.0	42.7	3.2	3.0	60.5
			OF	42.3	64.2	86.0	56.6	2.1	3.4	68.9	50.5	72.0	60.2	112.2	152.0	57.3	3.2	3.0	39.5
	200	5	UF	64.7	111.8	138.0	79.8	2.0	2.4	75.8	73.1	66.0	58.4	163.8	197.0	77.8	4.4	3.0	43.9
			OF	35.3	111.8	64.0	20.2	2.0	1.4	24.2	73.1	86.0	41.6	163.8	103.0	22.2	4.4	7.0	56.1
	300	6	UF	69.5	63.4	71.0	77.8	1.3	1.5	77.3	73.1	49.0	46.5	122.6	140.0	79.3	5.8	4.0	47.6
			OF	30.5	63.4	46.0	22.2	1.3	1.0	22.7	73.1	128.0	53.5	122.6	83.0	20.7	5.8	10.0	52.4
3	100	7	UF	44.2	50.2	39.0	34.4	1.1	0.9	37.3	111.7	28.0	11.1	83.2	67.0	35.6	9.1	3.0	14.5
			OF	55.8	50.2	59.0	65.6	1.1	1.2	62.7	111.7	178.0	88.9	83.2	96.0	64.4	9.1	14.0	85.5
	200	8	UF	83.9	48.9	34.0	58.4	1.2	1.0	67.5	44.6	28.0	52.6	83.9	64.0	64.0	2.5	2.0	67.5
			OF	16.1	48.9	126.0	41.6	1.2	2.5	32.5	44.6	131.0	47.4	83.9	187.0	36.0	2.5	5.0	32.5
	300	9	UF	68.4	64.2	65.0	69.3	1.3	1.3	69.8	38.2	32.0	57.3	100.0	103.0	70.5	2.8	3.0	73.5
			OF	14.8	64.2	133.0	30.7	1.3	2.6	30.2	38.2	110.0	42.7	100.0	199.0	29.5	2.8	5.0	26.5
Flat Bottom	100	10	UF	49.3	33.6	24.0	35.2	0.8	0.6	36.8	43.8	20.0	22.5	114.5	79.0	34.0	3.5	2.0	28.0
			OF	50.7	33.6	43.0	64.8	0.8	1.0	63.2	43.8	67.0	77.5	114.5	149.0	66.0	3.5	5.0	72.0
	200	11	UF	61.0	35.5	25.0	43.0	0.8	0.6	43.9	26.1	16.0	37.4	87.3	69.0	48.2	3.8	3.0	48.4
			OF	39.0	35.5	52.0	57.0	0.8	1.2	56.1	26.1	42.0	62.6	87.3	116.0	51.8	3.8	5.0	51.6
	300	12	UF	58.5	35.6	24.0	39.4	0.9	0.7	43.1	24.1	17.0	41.3	103.6	87.0	49.1	3.4	3.0	51.4
			OF	41.5	35.6	52.0	60.6	0.9	1.3	56.9	24.1	34.0	58.7	103.6	127.0	50.9	3.4	4.0	48.6

Table 11.- Separation results for Ni, Pb, Sb and Zn

Apex Φ (mm)	Pressure (kPa)	Experiment	Fraction	γ_c (%)	Ni			Pb			Sb			Zn		
					α (ppm)	λ (ppm)	ε (%)	α (ppm)	λ (ppm)	ε (%)	α (ppm)	λ (ppm)	ε (%)	α (ppm)	λ (ppm)	ε (%)
9.5	100	1	UF	63.0	36.6	31.0	53.4	420.4	277.0	41.5	12.8	8.0	39.3	396.5	255.0	40.5
			OF	37.0	36.6	46.0	46.6	420.4	664.0	58.5	12.8	21.0	60.7	396.5	637.0	59.5
	200	2	UF	65.9	37.5	31.0	54.5	404.5	262.0	42.7	12.4	8.0	42.4	435.3	290.0	43.9
			OF	34.1	37.5	50.0	45.5	404.5	680.0	57.3	12.4	21.0	57.6	435.3	716.0	56.1
	300	3	UF	56.5	41.4	34.0	46.4	367.0	260.0	40.0	9.6	7.0	41.2	432.5	302.0	39.5
			OF	43.5	41.4	51.0	53.6	367.0	506.0	60.0	9.6	13.0	58.8	432.5	602.0	60.5
6.4	100	4	UF	64.8	44.0	34.0	50.1	320.9	220.0	44.4	8.6	8.0	60.5	465.3	259.0	36.1
			OF	42.3	44.0	52.0	49.9	320.9	422.0	55.6	8.6	8.0	39.5	465.3	704.0	63.9
	200	5	UF	64.7	42.1	47.0	72.3	607.4	752.0	80.0	18.5	22.0	77.0	595.0	729.0	79.2
			OF	35.3	42.1	33.0	27.7	607.4	343.0	20.0	18.5	12.0	23.0	595.0	350.0	20.8
	300	6	UF	69.5	45.6	49.0	74.6	325.7	381.0	81.3	7.4	8.0	75.2	452.5	531.0	81.5
			OF	30.5	45.6	38.0	25.4	325.7	200.0	18.7	7.4	6.0	24.8	452.5	274.0	18.5
3	100	7	UF	44.2	37.3	30.0	35.6	260.8	205.0	34.7	8.1	7.0	38.1	294.1	231.0	34.7
			OF	55.8	37.3	43.0	64.4	260.8	305.0	65.3	8.1	9.0	61.9	294.1	344.0	65.3
	200	8	UF	83.9	33.1	30.0	76.1	284.9	209.0	61.5	9.1	7.0	64.5	292.4	218.0	62.5
			OF	16.1	33.1	49.0	23.9	284.9	679.0	38.5	9.1	20.0	35.5	292.4	679.0	37.5
	300	9	UF	68.4	29.2	32.0	75.1	336.1	336.0	68.4	12.2	13.0	73.2	344.6	349.0	69.3
			OF	14.8	29.2	49.0	24.9	336.1	717.0	31.6	12.2	22.0	26.8	344.6	714.0	30.7
Flat Bottom	100	10	UF	49.3	34.6	25.0	35.6	166.8	113.0	33.4	5.5	4.0	35.7	269.9	173.0	31.6
			OF	50.7	34.6	44.0	64.4	166.8	219.0	66.6	5.5	7.0	64.3	269.9	364.0	68.4
	200	11	UF	61.0	31.8	24.0	46.1	161.3	111.0	42.0	4.8	4.0	51.1	258.7	171.0	40.3
			OF	39.0	31.8	44.0	53.9	161.3	240.0	58.0	4.8	6.0	48.9	258.7	396.0	59.7
	300	12	UF	58.5	34.3	26.0	44.3	183.2	123.0	39.3	4.7	3.0	37.6	288.6	189.0	38.3
			OF	41.5	34.3	46.0	55.7	183.2	268.0	60.7	4.7	7.0	62.4	288.6	429.0	61.7

Table 12.- Separation results after classification of separated fractions into concentrate (C) and tailings (T).

Experiment	Fraction	γ_c	As		Cd		Cr		Cu		Mo		Ni		Pb		Sb		Zn	
		(%)	λ (ppm)	ε (%)	λ (ppm)	ε (%)	λ (ppm)	ε (%)	λ (ppm)	ε (%)	λ (ppm)	ε (%)	λ (ppm)	ε (%)	λ (ppm)	ε (%)	λ (ppm)	ε (%)	λ (ppm)	ε (%)
1	T	63.0	43.0	37.5	0.9	39.9	31.0	33.6	75.0	41.6	2.0	40.5	31.0	53.4	277.0	41.5	8.0	39.3	255.0	40.5
	C	37.0	122.0	62.5	2.3	60.1	104.0	66.4	179.0	58.4	5.0	59.5	46.0	46.6	664.0	58.5	21.0	60.7	637.0	59.5
2	T	65.9	52.0	44.2	1.0	44.6	28.0	32.2	87.0	46.4	3.0	53.7	31.0	54.5	262.0	42.7	8.0	42.4	290.0	43.9
	C	34.1	127.0	55.8	2.4	55.4	114.0	67.8	194.0	53.6	5.0	46.3	50.0	45.5	680.0	57.3	21.0	57.6	716.0	56.1
3	T	56.5	53.0	42.0	1.1	41.7	29.0	24.4	95.0	42.9	3.0	43.8	34.0	46.4	260.0	40.0	7.0	41.2	302.0	39.5
	C	43.5	95.0	58.0	2.0	58.3	117.0	75.6	164.0	57.1	5.0	56.2	51.0	53.6	506.0	60.0	13.0	58.8	602.0	60.5
4	T	64.8	43.0	43.4	1.0	31.1	31.0	39.8	74.0	42.7	3.0	60.5	34.0	50.1	220.0	44.4	8.0	60.5	259.0	36.1
	C	42.3	86.0	56.6	3.4	68.9	72.0	60.2	152.0	57.3	3.0	39.5	52.0	49.9	422.0	55.6	8.0	39.5	704.0	63.9
5	T	35.3	64.0	20.2	1.4	24.2	86.0	41.6	103.0	22.2	7.0	56.1	33.0	27.7	343.0	20.0	12.0	23.0	350.0	20.8
	C	64.7	138.0	79.8	2.4	75.8	66.0	58.4	197.0	77.8	3.0	43.9	47.0	72.3	752.0	80.0	22.0	77.0	729.0	79.2
6	T	30.5	46.0	22.2	1.0	22.7	128.0	53.5	83.0	20.7	10.0	52.4	38.0	25.4	200.0	18.7	6.0	24.8	274.0	18.5
	C	69.5	71.0	77.8	1.5	77.3	49.0	46.5	140.0	79.3	4.0	47.6	49.0	74.6	381.0	81.3	8.0	75.2	531.0	81.5
7	T	44.2	39.0	34.4	0.9	37.3	28.0	11.1	67.0	35.6	3.0	14.5	30.0	35.6	205.0	34.7	7.0	38.1	231.0	34.7
	C	55.8	59.0	65.6	1.2	62.7	178.0	88.9	96.0	64.4	14.0	85.5	43.0	64.4	305.0	65.3	9.0	61.9	344.0	65.3
8	T	83.9	34.0	58.4	1.0	67.5	28.0	52.6	64.0	64.0	2.0	67.5	30.0	76.1	209.0	61.5	7.0	64.5	218.0	62.5
	C	16.1	126.0	41.6	2.5	32.5	131.0	47.4	187.0	36.0	5.0	32.5	49.0	23.9	679.0	38.5	20.0	35.5	679.0	37.5
9	T	68.4	65.0	69.3	1.3	69.8	32.0	57.3	103.0	70.5	3.0	73.5	32.0	75.1	336.0	68.4	13.0	73.2	349.0	69.3
	C	14.8	133.0	30.7	2.6	30.2	110.0	42.7	199.0	29.5	5.0	26.5	49.0	24.9	717.0	31.6	22.0	26.8	714.0	30.7
10	T	49.3	24.0	35.2	0.6	36.8	20.0	22.5	79.0	34.0	2.0	28.0	25.0	35.6	113.0	33.4	4.0	35.7	173.0	31.6
	C	50.7	43.0	64.8	1.0	63.2	67.0	77.5	149.0	66.0	5.0	72.0	44.0	64.4	219.0	66.6	7.0	64.3	364.0	68.4
11	T	61.0	25.0	43.0	0.6	43.9	16.0	37.4	69.0	48.2	3.0	48.4	24.0	46.1	111.0	42.0	4.0	51.1	171.0	40.3
	C	39.0	52.0	57.0	1.2	56.1	42.0	62.6	116.0	51.8	5.0	51.6	44.0	53.9	240.0	58.0	6.0	48.9	396.0	59.7
12	T	58.5	24.0	39.4	0.7	43.1	17.0	41.3	87.0	49.1	3.0	51.4	26.0	44.3	123.0	39.3	3.0	37.6	189.0	38.3
	C	41.5	52.0	60.6	1.3	56.9	34.0	58.7	127.0	50.9	4.0	48.6	46.0	55.7	268.0	60.7	7.0	62.4	429.0	61.7

Universidad de Oviedo

CHAPTER V: General Discussion

Separation Methods

-Electrostatic Separation

The feasibility of electrostatic separation for soil remediation was assessed at an ancient Pb mining site in Southern Spain. Using a high-tension electrostatic separator (EHTP Outotec), high recovery rates were achieved for various potentially toxic elements (PTEs), including Zn (83%), Cu (78%), and Mo (81%). These results demonstrate that electrostatic separation is particularly effective for coarser fractions of sandy, dry, slag-containing soils, suggesting that it may be a viable method for soil remediation in specific scenarios.

The unique electrical characteristics of the contaminating particles (primarily slags) and the base soil, which allow for their separation, are key to the technique's efficacy. However, its efficiency is limited in situations involving finer soil fractions or high soil moisture, where these conditions reduce the process's overall effectiveness.

-Hydrocyclone Separation

The feasibility of hydrocyclone separation for soil remediation was assessed at an ancient fertilizer plant site. Experiments were conducted using twelve different designs with varying apex diameters and pressures. This technique proved to be effective in cleaning soils contaminated with various PTEs, particularly when the contaminants were associated with smaller particle sizes. However, its effectiveness decreased as the contaminating particles became more dispersed in coarser fractions. Additionally, the findings indicated that PTE separation generally improved with designs featuring smaller apex diameters and higher pressures. The results demonstrated the effectiveness of this type of separation for the remediation of multi-metal(loid)-polluted soil, particularly from pyrite ashes.

Attributive Analysis variants

Through the present research, the attributive analysis (AA) approach has undergone significant evolution, leading to more optimized evaluations of soil washing operations for soil remediation. Initially, basic AA focused on maximizing recovery (ε) while minimizing yield (γ) to assess separation conditions. However, these two factors alone do not provide a sufficiently robust method for determining optimal separation conditions,

as a large increase in concentrate purity is not necessarily associated with good recovery and low yield alone.

Moreover, the basic attributive analysis function exhibits significant sensitivity to variability in both the yield and recovery datasets. The quality index is inversely related to yield and, consequently, shows an inverse squared relationship with changes in yield. In contrast, it maintains a linear relationship with recovery, where the slope depends on the maximum recovery value. This relationship explains the increased sensitivity to variations in yield.

The issue of discrepancies between yield and recovery is directly addressed by the penalized attributive analysis (PAA-U). This method penalizes contributions to the quality index from experimental setups where the largest variances are observed. It incorporates parameter normalization and inverse standard deviation weighting to mitigate the impact of significant fluctuations in yield and recovery data. As a result, this approach improves the accuracy of determining optimal conditions for PTE separation by penalizing variability and weighting the most detrimental factors. Moreover, the three-parameter penalized attributive analysis (3PPAA-U) enhances the accuracy of PAA-U by introducing a third parameter (concentrate grade). This technique has proven more effective in mitigating fluctuations in the studied variables, thus reducing the impact of outlier values and further improving the overall accuracy of AA.

It is important to emphasize that all AA methodologies, including 3PPAA-U, are heuristic tools designed to guide decision-making, rather than providing absolute solutions for identifying the best upgrading conditions (BUC). The selection of the most appropriate approach for a specific case should consider a wide array of subjective and qualitative factors, including cost, feasibility, and risk. Therefore, the results generated by these methodologies should be viewed as indicators of the most promising conditions and thus worth further investigation.

Finally, although with these procedures, we aimed to provide a reliable tool for the assessment and improvement of physical separation processes, their application of presents significant potential for deployment in a wide range of materials processing and manufacturing contexts. In these cases, the quality factors considered might include variables like time, temperature, pressure, or particle size, as well as environmental and economic factors such as energy consumption, labour requirements and risk assessment.

Universidad de Oviedo

CHAPTER VI: Conclusions

Conclusions.

Physical separation of potentially toxic elements (PTEs) from soil is feasible through electrostatic separation, under specific conditions, and hydrocycloning in a more versatile manner. The attributive analysis technique has progressed significantly throughout the research, enabling continuous improvements in the accuracy and efficiency of separation procedures.

Initially, the basic attributive analysis (BAA) provided a solid foundation for assessing separation conditions by focusing on maximizing recovery (ε) and minimizing yield (γ). This approach successfully identified the most promising experimental configurations for electrostatic separation, demonstrating the effectiveness of the technique in specific soil conditions.

The subsequent development of penalized attributive analysis (PPAA-U) introduced standard deviation correction and parameter normalization, which enhanced the accuracy of the analysis in highly variable experimental settings. This iteration allowed for more precise identification of optimal PTE separation conditions, thereby improving the efficiency and recovery outcomes of the electrostatic separation process.

Ultimately, the three-parameter penalized attributive analysis (3PPAA-U) further advanced the methodology by incorporating yield (γ), recovery (ε), and grade concentration (λ) into the analysis. This comprehensive approach not only optimized hydrocyclone operations but also provided a reliable tool for determining ideal separation conditions in soils polluted by various pollutants.

The 3PPAA-U approach is heuristic rather than definitive in determining optimal upgrading conditions (BUC). While it offers a systematic and objective means to evaluate and compare different options, it is based on assumptions and simplifications that may overlook some complexities inherent in soil washing processes. Therefore, this methodology should not be considered a final decision-making tool but rather as an indicator of promising experimental configurations for researchers and professionals. Subjective and qualitative factors such as risk, cost, and feasibility must be integrated into the overall decision-making process. Consequently, 3PPAA-U should be applied with caution and critical judgment, alongside other methodologies. Future studies may expand the 3PPAA-U approach to encompass a broader range of factors critical to the success of soil washing operations.

In conclusion, the 3PPAA-U approach prioritizes minimizing yield over maximizing recovery, ranking various experimental configurations based on their effectiveness in maximizing grade and recovery while minimizing yield. Without target-to-distance correction, 3PPAA-U is at least as effective as methods that rely on other criteria, such as proximity to the ideal separation curve. With the additional correction, 3PPAA-U outperforms conventional techniques, potentially improving the results of soil washing procedures. The advancement of the attributive analysis method represents a valuable tool for enhancing the effectiveness of separation techniques used in soil remediation. By implementing these advancements, soil remediation practices are likely to continue evolving and improving, effectively addressing contemporary environmental issues.

Conclusiones.

La separación física de elementos potencialmente tóxicos (EPTs) del suelo es factible mediante la separación electrostática, bajo condiciones específicas, y la separación por hidrociclón de una manera más versátil. La técnica de análisis atributivo ha progresado significativamente a lo largo de la investigación, permitiendo mejoras continuas en la precisión y eficiencia de los procedimientos de separación.

Inicialmente, el análisis atributivo básico (BAA) proporcionó una base sólida para evaluar las condiciones de separación al centrarse en maximizar la recuperación (ε) y minimizar el rendimiento (γ). Este enfoque identificó con éxito las configuraciones experimentales más prometedoras para la separación electrostática, demostrando la efectividad de la técnica en condiciones específicas del suelo.

El desarrollo posterior del análisis atributivo penalizado (PPAA-U) introdujo la corrección de desviación estándar y la normalización de parámetros, lo que mejoró la precisión del análisis en entornos experimentales altamente variables. Esta iteración permitió una identificación más precisa de las condiciones óptimas de separación de elementos traza (PTE), mejorando así la eficiencia y los resultados de recuperación del proceso de separación electrostática.

En última instancia, el análisis atributivo penalizado de tres parámetros (3PPAA-U) avanzó aún más en la metodología al incorporar el rendimiento (γ), la recuperación (ε) y la concentración de grado (λ) en el análisis. Este enfoque integral no solo optimizó las operaciones de los hidrociclones, sino que también proporcionó una herramienta confiable para determinar las condiciones ideales de separación en suelos contaminados por múltiples contaminantes.

El enfoque 3PPAA-U es heurístico más que definitivo en la determinación de las condiciones óptimas de mejora (BUC). Aunque ofrece un medio sistemático y objetivo para evaluar y comparar diferentes opciones, se basa en suposiciones y simplificaciones que pueden pasar por alto algunas complejidades inherentes a los procesos de lavado de suelos. Por lo tanto, esta metodología no debe considerarse una herramienta de toma de decisiones final, sino más bien un indicador de configuraciones experimentales prometedoras para investigadores y profesionales. Factores subjetivos y cualitativos, como el riesgo, el costo y la viabilidad, deben integrarse en el proceso general de toma de decisiones. En consecuencia, el 3PPAA-U debe aplicarse con cautela y juicio crítico,

junto con otras metodologías. Los estudios futuros pueden ampliar el enfoque 3PPAA-U para abarcar una gama más amplia de factores críticos para el éxito de las operaciones de lavado de suelos.

En conclusión, el enfoque 3PPAA-U prioriza la minimización del rendimiento sobre la maximización de la recuperación, clasificando diversas configuraciones experimentales según su efectividad en maximizar el grado y la recuperación mientras se minimiza el rendimiento. Sin la corrección de distancia objetivo, el 3PPAA-U es al menos tan efectivo como los métodos que se basan en otros criterios, como la proximidad a la curva de separación ideal. Con la corrección adicional, el 3PPAA-U supera a las técnicas convencionales, mejorando potencialmente los resultados de los procedimientos de lavado de suelos. El avance del método de análisis atributivo representa una herramienta valiosa para mejorar la efectividad de las técnicas de separación utilizadas en la remediación de suelos. Al implementar estos avances, es probable que las prácticas de remediación de suelos continúen evolucionando y mejorando, abordando eficazmente los problemas ambientales contemporáneos.

Universidad de Oviedo

APPENDIX I

Environmental Technology & Innovation 32 (2023) 103237

Contents lists available at ScienceDirect

Environmental Technology & Innovation

journal homepage: www.elsevier.com/locate/eti

An evaluation of the feasibility of electrostatic separation for physical soil washing

X. Corres [a], D. Baragaño [b], J.M. Menéndez-Aguado [c], J.R. Gallego [a], C. Sierra [d,e,*]

[a] INDUROT and Environmental Biogeochemistry & Raw Materials Group, Campus de Mieres, Universidad de Oviedo, Mieres, Asturias, Spain
[b] Escuela Politécnica de Ingeniería de Minas y Energía. Boulevard Ronda Rufino Peón nº, 254. Universidad de Cantabria, Torrelavega, Cantabria, Spain
[c] Escuela Politécnica de Mieres. c/Gonzalo Gutiérrez Quirós s/n, 33600, Mieres, Asturias, Spain
[d] Department of Mining, Topography and Structure Technology, University of León, Campus de Vegazana, 24006, León, Spain
[e] European University on Responsible Consumption and Production, University of León, Campus de Vegazana, 24006, León, Spain

ARTICLE INFO

Article history:
Received 17 April 2023
Received in revised form 23 May 2023
Accepted 3 June 2023
Available online 7 June 2023

Keywords:
Potentially toxic elements (PTEs)
Sandy soil
Mineral processing
Lead
Circular economy

ABSTRACT

We present the first application of electrostatic separation for soil washing. Soil samples were collected from the PTE-containing area of La Cruz in Linares, southern Spain. Using a single-phase high-tension roll separator with voltages ranging from 20 kV to 41.5 kV, we achieved yield values between 0.69% and 9%, with high recovery rates for certain elements such as Zn, Cu, and Mo. SEM-EDX analysis revealed three particle types, including a non-conductive fraction composed of feldspar, a middling fraction composed of mica, and a conductive fraction consisting of PTE-bearing slag grains. Attributive analysis showed that 41.5 kV was the optimal voltage for maximizing PTE concentration. Overall, electrostatic separation is a promising approach for treating soils contaminated with PTEs, particularly in dry climate areas impacted by mining activities.

1. Introduction

Potentially Toxic Elements (PTEs) are known to be widespread and present complex challenges due to their failure to decompose, difficulties with remediation, toxicity to plants and in the food chain, and damage to soil ecosystems (Beiyuan et al., 2018; Gu et al., 2018; Li et al., 2019a,b). These pollutants are well-known by-products of human activity, including mining, waste disposal, agriculture, electroplating, and coal combustion (Piccolo et al., 2019; Rui et al., 2019; Wu et al., 2015), thus, soil contamination with PTEs is currently one of the most pressing environmental issues we are faced with. Several million hectares of PTE-contaminated soils are found in Europe alone, accounting for nearly 40% of all contaminated soil worldwide (EEA, 2009). Beyond Europe, this issue affects many other nations, principally the USA (Uchimiya et al., 2011), Japan (Makino et al., 2006), and Brazil (França et al., 2017).

PTE-polluted soils can be remediated using physical (soil replacement, physical soil washing, thermal desorption), chemical (chemical soil washing, solidification/stabilization electrokinetic, vitrification), and biological (phytoremediation, microorganism remediation, animal remediation) (Anderson et al., 1999; Beiyuan et al., 2018; Dermont et al., 2008) treatment methods. Soil washing techniques have their origin in the mining industry and involve either the separation of soils by particle size and density generally using water as the carrier agent (physical washing) or the use of a chemical to

* Corresponding author at: Department of Mining, Topography and Structure Technology, University of León, Campus de Vegazana, 24006, León, Spain.
E-mail address: csief@unileon.es (C. Sierra).

https://doi.org/10.1016/j.eti.2023.103237

extract the contaminant (chemical washing) (Anderson et al., 1999). Such techniques result in a clean fraction that can be backfilled on site and a contaminated fraction that can be disposed of appropriately. In comparison to other methods, physical soil washing is one of the most remarkable decontamination techniques due to its capacity to permanently remove PTEs, fast processing, waste volume reduction, and significant cost/effectiveness ratio (Baragaño et al., 2021, 2023; Feng et al., 2020; Khalid et al., 2017; Wang et al., 2018; Xu et al., 2014; Zhao et al., 2017).

Electrostatic separation makes use of differences in electrical conductivity between minerals (Inculet, 1984) and on the face of it, this method would seem to be a universal method of separation because all materials exhibit some variation in conductivity. In reality, however, it has several limitations, specifically, its low capacity for fine grain sizes, the processing requirement of a dry monolayer feed, limitations with soil sample variability, sensitivity to moisture and moderate to high energy consumption (mainly due to drying) (Kawatra and Young, 2019). Typically, this method is used with granular feeds with particle sizes ranging from 40 μm to 1 mm (Kawatra and Young, 2019).

As discussed in Yang et al. (2018), electrostatic separation is widely used for the recovery of ilmenite ore, rutile, and zircon from sands. It also plays a part in many recycling processes, for example in the separation of metal from plastic in lots of scrap electrical cabling (Bedeković and Trbović, 2020; Park et al., 2015), and in the food industry to isolate or concentrate proteins found in various foodstuffs (Kdidi et al., 2019; Tabtabaei et al., 2017, 2019). In addition, the technique is used in the petrochemical industry for desalting crude oil (Aitani, 2004) and for the purification of certain products (Li et al., 2019a,b, 2021; Villot et al., 2012).

Despite its proven effectiveness in many areas, however, electrostatic separation does not appear to have been investigated as a method for soil decontamination. As stated above, one reason for this may be the fact that this method requires a dry feed. The costs involved in drying soils before processing represent a major obstacle to the use of electrostatic separation in a soil washing operation. The site we are considering in this research, La Cruz in the Linares-La Carolina mining district (Southern Andalusia, Spain), side-steps this problem as its Mediterranean climate means there is little rainfall, and its soils are thus completely dry for most of the year (Lorite et al., 2023). Thus, with its arid climate it is an ideal site to test electrostatic separation of soils.

Following from the discussion above, the primary goals of the current study are:

- To evaluate the feasibility of electrostatic separation as part of physical soil washing treatments for soils containing PTEs.
- To explain the underlying aspects of the separation by means of a detailed mineralogical study.
- To test a novel formulation (attributive analysis) for the assessment of separation efficiency and thus determine optimal separation conditions.

2. Materials and methods

2.1. Site description

Galena (PbS) has been mined at La Cruz for over two centuries making it one of the most important led ore mining regions in the world (Lillo Ramos, 1992; Martínez et al., 2007b,a, 2012). The led ore is found in veins with sphalerite (ZnS), chalcopyrite ($CuFeS_2$), and barite ($BaSO_4$) thus processing and extracting the useful ore creates a significant quantity of waste which is often dumped on the land next to mining operations. Moreover, much of the mineral processing at the site considered here involved gravity separation and froth flotation resulting in both medium and fine grain rejects that were then sent to nearby landfills or dumps. In addition, the solid, liquid, and gaseous contaminants produced by the district's foundries remain on these sites in the form of slag and dust, an environmental problem discussed by Adamo et al. (1996) and Li and Thornton (2001) at similar sites in Canada and the UK, respectively. When these industrial residues, containing fractions with a high concentration of heavy metals, are dispersed and dumped on the ground without any prior remediation treatment the action of weathering increases their chemical availability (Loredo et al., 1999; Martínez et al., 2007a) making them even more environmentally hazardous. In this way, mining waste in all its forms constitutes a significant problem for the extensive agricultural areas of the zone (Sierra et al., 2013). Location map is presented in SM1. According to Heliosat (SARAH), the study site receives an average of 3.3 h of sunlight per day, with 5.82 peak sun hours (PSHs) and an average annual solar radiation of over 5 kwh/m^2 on a horizontal surface (H) (e.g., Pfeifroth et al. (2017)). Based on this information, it is evident that solar energy can serve as a viable alternative energy source to power the electrostatic separation process.

2.2. Sample preparation

Samples were taken from 10 randomly selected sites across the location of interest. All samples were taken from the top 35 cm layer of soil; the depth was measured using a stainless-steel calliper and a shovel was used to collect the sample. In total a bulk sample of 25 kg was collected. The sample was then homogenized and kept at room temperature in inert plastic containers until further preparation and analysis. All soil analysis was completed within 15 days of the initial sampling.

The bulk sample was wet sieved in batches for five minutes with a water flow of 0.3 l/min to obtain granulometric fractions of 63, 63–125, 125–250, 250–500, 500–1000, and 1000–2000 μm (ASTM D-422-63, Standard Test Method

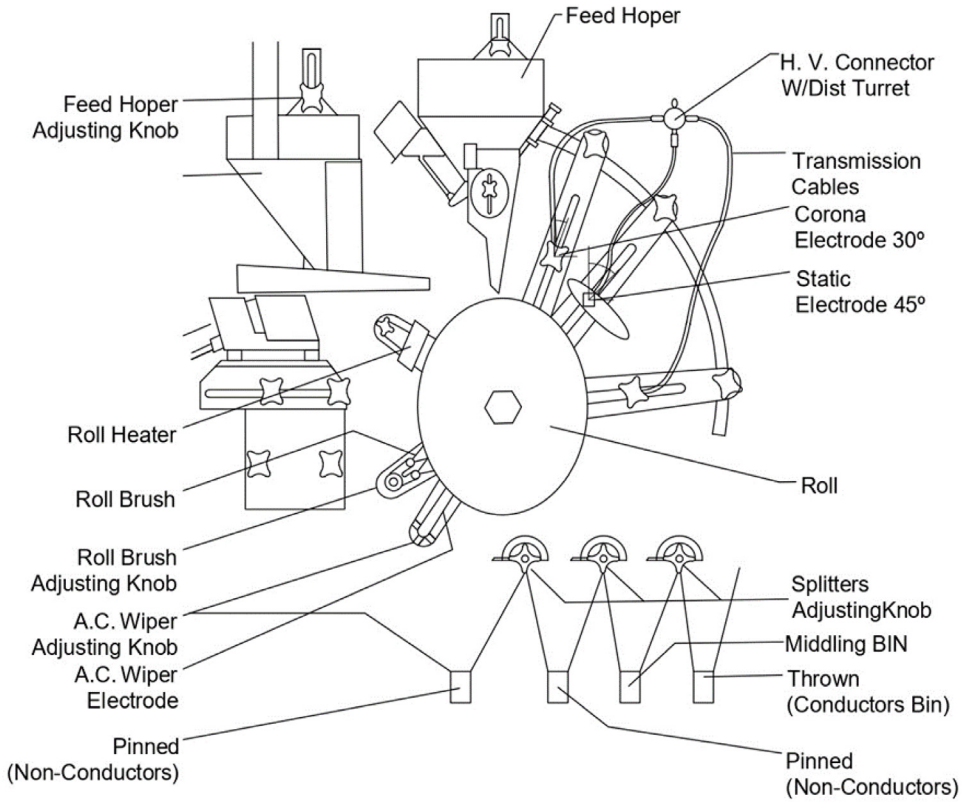

Fig. 1. Scheme of the high voltage electrostatic separation process.

for Particle-Size Analysis of Soils). Note that, sodium hexametaphosphate and sodium carbonate were used to aid the separation of the silt-clay fraction (<63 μm) from the larger particles. The process was repeated until 3 kg of the 1000–2000 μm fraction was obtained. This fraction was divided into twelve subsamples, which were reserved for further processing in the electrostatic separator. Additional subsamples were taken from each fraction, and these were air dried at 40 °C before being sent for chemical analysis.

2.3. Electrostatic separation

As described above, twelve samples were made from the 1–2 mm fraction of soil collected from the site of interest. Each sample was tested at a different separation voltage with experimental runs at each voltage repeated three times. An average of these results was taken and is presented in this article. The apparatus used was an eForce high voltage electrostatic separator (model EHTP by Outotec) (Fig. 1 and SM2) which is one the few semi-industrial electrostatic separators operating in Europe.

The apparatus employed has the following design characteristics:

- Feed particle size range: 0.074–10 mm.
- Treatment capacity: up to 150 kg/h.
- Vibratory tray and hopper with variable speed control for coarser particles and a positive speed feed chute and vibrator hopper for finer particles.
- Hopper with 2 adjustable dividers for the collection of non-conductive, intermediate (middling), and conductive products.
- 2 interchangeable stainless-steel rollers:
    - Of sizes 25.4 and 35.56 cm (10 and 14″) in diameter by 15.24 cm (6″) wide (industry standards) and
    - Of variable roll speed with a 1/4 HP direct drive motor.
- 2 DC electrodes, one corona and the other static, which can be set at a range of voltages to a maximum of 41.5 kV; and 1 AC wiper electrode at 18 kV.
- High voltage transformer, adjustable up to 12,000 VAC.

- Grounded roller brush for particle removal: adjustable and with infrared roller heating capability.

The module was operated under the following conditions:

- Corona electrode angle: 30° with respect to the vertical.
- Electrostatic electrode angle: 45° with respect to vertical.
- Roll speed: 50 rpm.

Samples were fed into the feed hopper and onto the roller. The corona electrode ionizes the surrounding air and charges the particles on the roller as they approach the electrode. Conductive particles lose their charge quickly to the earthed roller and are thrown into the conductors bin due to the centrifugal force of the roller. The more insulating particles retain their charge and will stay on the roller until they are brushed off and fall into either the middlings or insulators bin (depending on particle size and roller speed).

The degree of separation that can be achieved for a given sample will depend on the composition of the sample, roller speed, electrode positions, and separation voltage (the voltage of the corona electrode). In this work, the only variable was the separation voltage which was set at a range of values from 20 kV to 41.5 kV in order to determine the optimum voltage for the soils sampled here.

2.4. Chemical and mineralogical analysis

Before chemical analysis, subsamples (6 from the grain size fractioning and 108 from the separation experiments) needed to be standardized thus, all fractions >125 μm were milled using a vibrating disk mill (RS 100 Retsch) at 400 rpm for 40 s Then, representative samples of 1 g were taken from each subsample, and these were subjected to "Aqua regia" ($HCl + HNO_3$) digestion before being sent for ICP-OES analysis at the ISO 9002 accredited laboratories, Actlabs International (Ancaster, Ontario, Canada). Tests returned the total concentrations of the following 36 major and trace elements: Ag, Al, As, Au, B, Ba, Bi, Ca, Cd, Co, Cr, Cu, Fe, Ga, Hg, K, La, Mg, Mn, Mo, Na, Ni, P, Pb, S, Sb, Sc, Se, Sr, Te, Th, Ti, Tl, V, W, Zn. Samples that exceeded the limit of quantification for the previous method (13 in total) were treated in triplicate with Fusion-Inductively Coupled Plasma-Sodium Peroxide Oxidation (FUS-Na_2O_2) in the same laboratories. This process involves sintering the sample at 650 °C after oxidizing it with sodium peroxide. The resulting oxidized material was then dissolved in aqueous HNO_3, and various elements in the resulting solution are quantified using ICP-OES (report number: A19-03313).

The subsamples were also examined using a stereoscopic binocular microscope (Nikon SMZ1000) and micrographs were obtained with a high-resolution Nikon DS-Ri1 camera. The morphology and composition of minerals was examined using an SEM-EDX system, comprising a Jeol JSM-6100 scanning electron microscope and an energy dispersive X-ray analyser (INCA Energy 200).

3. Results and discussion

3.1. PTEs concentration in soils

Nine PTEs tested for in this study (As, Cd, Cu, Cr, Hg, Ni, Pb, Sb, and Zn), were found in quantities above the target limits set by current international standards (Buchman and Office of Response, 2008) and three (Cu, Zn, Pb) were significantly above both the intervention limit (Table 1), and the contamination ratio (CR: the quotient of sample concentration and the target value for the element of interest). The concentration of Mo in the soil samples was determined to be below the reference levels. Nevertheless, it was included in the study due to its geochemical importance and economic significance, as well as its notable performance in the separation process. Furthermore, the analysis also incorporated Al and Fe due to their high conductivity. Cu was the most significant soil PTE at the site of interest (176.13 mg/kg to 802.32 mg/kg, mean: 362.7 mg/kg; CR: 106.68) followed by Zn (376.06 mg/kg to 2375.37 mg/kg, mean: 1051.03 mg/kg; CR: 65.69), and, as expected, Pb (1620.25 mg/kg to 3455.43 mg/kg, mean: 2412.81 mg/kg; CR:43.87). Another PTE, As was found to have a CR of similar order to the main 3 PTEs (53.84). In this way, there is a major case for a soil decontamination programme at the site of interest focusing principally on Cu, Zn, and Pb but which might be extended first to As, and later to Ni, Cr, Cd, Sb, and Hg. The soil exhibited a sandy loam texture, like many soils found in Mediterranean regions.

3.2. Electrostatic separation

The results of electrostatic separation were initially assessed according to three standard ore processing parameters: yield (γ), recovery (ε), and enrichment ratio (μ) (Wills and Napier-Munn, 2006). The yield or weight recovery is the quotient of the feed mass and that of the conductive fraction collected for a given experimental run. The recovery is the quotient of the mass of an element of interest found in the conductive fraction and that of the feed for a given experimental run. Finally, the enrichment ratio is the quotient of the concentration of an element of interest found in the conductive fraction and that of the feed for a given experimental run.

Table 1
PTEs concentrations in the bulk sample, the international standard (target and intervention limits), and contamination ratio for each PTE tested for in addition to Al, Mo and Fe. Elements marked with an asterisk are those with concentrations surpassing both the intervention and target values.

Element	Concentration (mg/kg)	Dutch standards (mg/kg) (Buchman and Office of Response, 2008)		Contamination ratio
		Intervention	Target	
Al	4681.2	–	–	–
As	48.46	55	0.9	53.84
Cd	7.48	12	0.8	9.35
Cr	10.41	220	0.35	29.75
Cu*	362.70	96	3.4	106.68
Fe	19 590.53	–	–	-
Hg	0.76	10	0.3	2.54
Mo	1.71	115	190	3
Ni	9.17	100	0.26	35.28
Pb*	2412.81	530	55	43.87
Sb	11.96	15	3	3.99
Zn*	1051.03	350	16	65.69

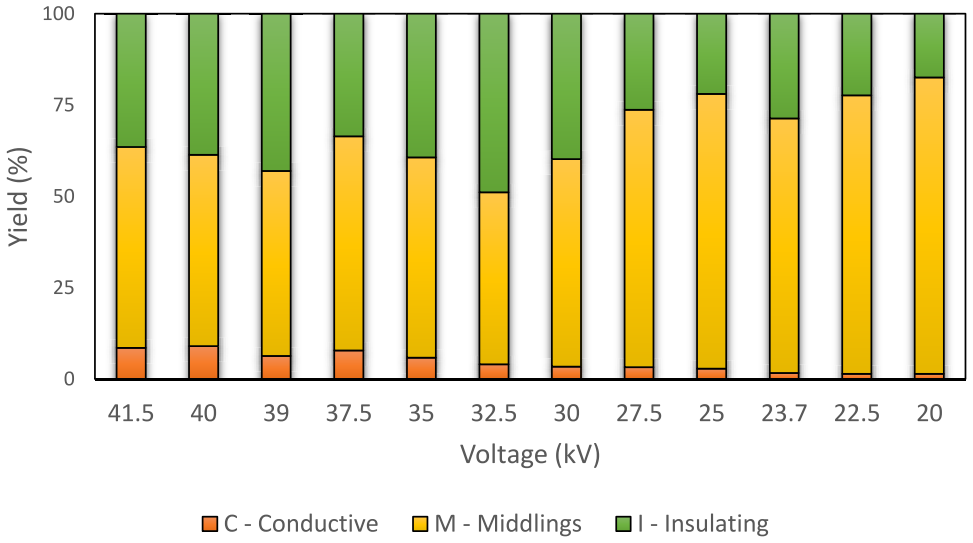

Fig. 2. Yield (γ) distribution between fractions for experimental runs.

Experimental runs were completed for 12 values of corona electrode voltage starting with the highest voltage available (41.5 kV). The voltage was gradually reduced on each subsequent run to determine the optimal operating conditions. At all voltages, we observed lowest yields ($\gamma = 0.69\% - 9\%$) for the conductive fraction compared to the middlings ($\gamma = 50.68\% - 90.59\%$) and insulating fraction ($\gamma = 8.72\% - 48.89\%$) (Fig. 2).

Looking in detail at the relationship between the yield for the conductive faction and applied voltage, here we found a positive correlation: the higher the voltage, the higher the yield with an almost directly proportional relationship (SM3). This suggests that higher voltages increased the number of conductive particles collected from the feed. However, higher voltages may also increase the capture of insulating particles, which could reduce recovery, and this highlights the need for more exhaustive study into the selection of an optimal operating voltage.

For most PTEs, the enrichment ratio, μ, is lower for the middlings and insulating fractions (<1% in all cases) compared to the conductive fraction (Table 2). This is a reflection of the fact that most pollutants tested here were metallic or semi-metallic and thus would be expected to report to the conductive fraction.

No clear tendencies were seen with respect to the enrichment ratios for any of the separated fractions (insulating, middlings, or conductive) and voltage. Considering the specific elements of interest (Fig. 3), here it can be seen that while some reached their highest enrichment ratio in the lower voltage range (e.g., Cu had $\mu = 7.49$ at 20 kV in contrast with an $\mu = 7.26$ at 41.5 kV), others exhibited the converse relation (e.g., Sb had $\mu = 9.15$ at 39 kV compared to $\mu = 4.54$ at 22.5 kV).

As with the yield, recovery (ε) in the conductive fraction also demonstrated a clear, positive correlation with voltage. Considering the recovery of individual elements, here Zn removal was the most successful, with recovery values of about 80% for voltages from 37 kV to 41.5 kV. The maximum recovery value for this element was 83.25% with a yield, $\gamma = 9$ %, at an operating voltage of 40 kV. Recovery for this element decreased abruptly at 37 kV, a pattern seen for all 10 elements studied (Fig. 4). Referring back to Fig. 3 we see that the enrichment ratio for this element was high and varied very little

Table 2
Partial merit index (Q_j^i), adjusted correction factor ($A_j^{i'}$) and global merit index ($\boldsymbol{Q_T^i}$) for each experiment (i) and element (j).

	Tens. (kV)	j																			Q_T^i
		As		Cd		Cr		Cu		Hg		Mo		Ni		Pb		Sb		Zn	
		Q_j^i	$Q_j^i A_j^{i'}$	Q_j^i	$Q_j^i A_j^{i'}$	Q_j^i	$Q_j^i A_j^{i'}$	Q_j^i	$Q_j^i A_j^{i'}$	Q_j^i	$Q_j^i A_j^{i'}$	Q_j^i	$Q_j^i A_j^{i'}$	Q_j^i	$Q_j^i A_j^{i'}$	Q_j^i	$Q_j^i A_j^{i'}$	Q_j^i	$Q_j^i A_j^{i'}$	Q_j^i	$Q_j^i A_j^{i'}$	
i	41.5	1.013	0.092	0.921	0.106	0.926	0.080	0.881	0.094	0.636	0.104	1.081	0.185	1.081	0.111	0.997	0.111	1.081	0.108	1.059	0.176	1.142
	40	1.077	0.096	1.077	0.095	1.003	0.076	1.041	0.129	0.588	0.085	1.060	0.165	1.015	0.089	1.077	0.089	1.019	0.094	1.077	0.173	1.089
	39	1.037	0.075	0.758	0.067	0.843	0.053	1.109	0.125	0.622	0.083	1.032	0.102	0.790	0.039	1.044	0.039	1.080	0.078	1.104	0.118	0.818
	37.5	1.069	0.093	0.852	0.074	1.088	0.092	0.973	0.159	1.088	0.113	1.063	0.112	0.951	0.098	1.061	0.098	1.066	0.103	1.081	0.134	1.067
	35	0.842	0.052	0.725	0.046	0.788	0.054	0.911	0.055	0.536	0.042	0.913	0.066	0.861	0.046	0.725	0.046	0.767	0.054	1.008	0.078	0.559
	32.5	0.722	0.049	0.617	0.039	0.766	0.043	0.643	0.039	0.602	0.032	0.845	0.050	0.865	0.053	0.584	0.053	0.493	0.053	0.959	0.053	0.469
	30	0.616	0.041	0.628	0.044	0.587	0.041	0.647	0.052	0.613	0.035	0.812	0.051	0.754	0.050	0.758	0.050	0.699	0.047	0.866	0.051	0.467
	27.5	0.506	0.040	0.471	0.038	0.536	0.046	0.643	0.041	0.681	0.030	0.620	0.041	0.494	0.040	0.594	0.040	0.510	0.036	0.697	0.043	0.402
	25	0.443	0.034	0.589	0.049	0.379	0.049	0.533	0.027	0.484	0.020	0.550	0.032	0.379	0.033	0.514	0.033	0.452	0.031	0.675	0.035	0.339
	23.7	0.535	0.037	0.610	0.036	0.521	0.040	0.527	0.020	0.574	0.023	0.622	0.017	0.471	0.055	0.556	0.055	0.561	0.027	0.668	0.018	0.302
	22.5	0.603	0.038	0.648	0.048	0.646	0.039	0.605	0.029	0.663	0.020	0.614	0.030	0.603	0.042	0.614	0.042	0.585	0.031	0.679	0.025	0.334
	20	0.592	0.043	0.631	0.036	0.615	0.038	0.807	0.029	0.565	0.039	0.697	0.023	0.768	0.036	0.623	0.036	0.612	0.036	0.696	0.023	0.341

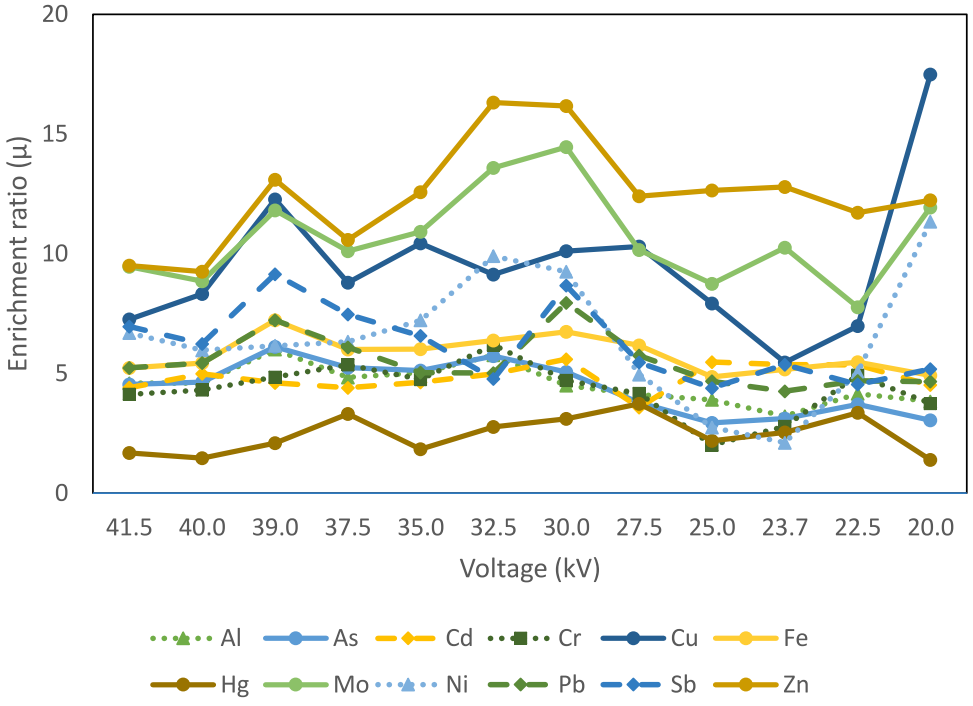

Fig. 3. Enrichment ratio in the conductive fraction for each PTE (plus Al and Fe). Average of three experimental runs at each voltage with a standard error <5%.

with voltage (9 to 16%). Taking 39 kV, in the middle of this high-recovery range, the enrichment ratio $\mu = 13.09\%$ for which $\gamma = 6.33\%$ and $\varepsilon = 82.86\%$.

Mo concentrations in the soil tested were below reference levels, however, we mention it here as its recovery levels were almost as high as those seen for Zn (see Fig. 6). That this method appears to be highly effective at separating this particular PTE is significant due to Mo's geochemical importance and economic interest.

The third best recovery values were recorded for Cu, the most important PTE in the soil tested. The maximum recovery value was 77.65% and this was achieved at 39 kV where the enrichment ratio recorded was 12.27%. As for the other PTE's examined here, the best results came at the highest voltages, with recovery values decreasing rapidly at lower voltages.

Regarding Sb, Ni and Pb, the maximum recovery values for these PTEs were 59.65% (41.5 kV), 53.73% (41.5 kV), and 48.92% (40 kV), respectively (Fig. 5). At these high voltages, the enrichment ratios for these elements were between 5 and 9%. As with the other elements tested, recovery fell dramatically at lower voltages.

Satisfactory yields were also obtained for Cd, Cr, and As, for which the maximum recovery values were 44.97% (40 kV), 41.85% (37.5 kV), and 41.75% (40 kV) respectively, with enrichment ratios ranging from 4 to 6%. Mercury was the lowest yielding element in these experiments with a maximum recovery value of 25.88% (37.5 kV) and a corresponding enrichment ratio of 3.31%. Total concentrations results after the separation are presented in SM4.

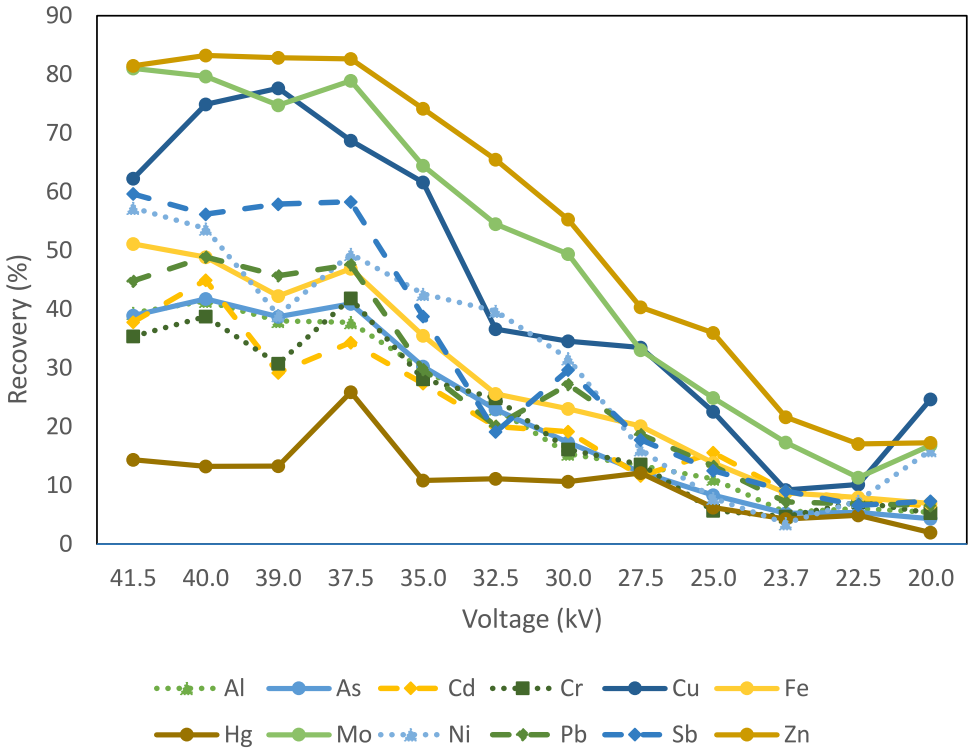

Fig. 4. Recovery in the conductive fraction for each PTE (plus Al and Fe). Average of three experimental runs at each voltage with a standard error <5%.

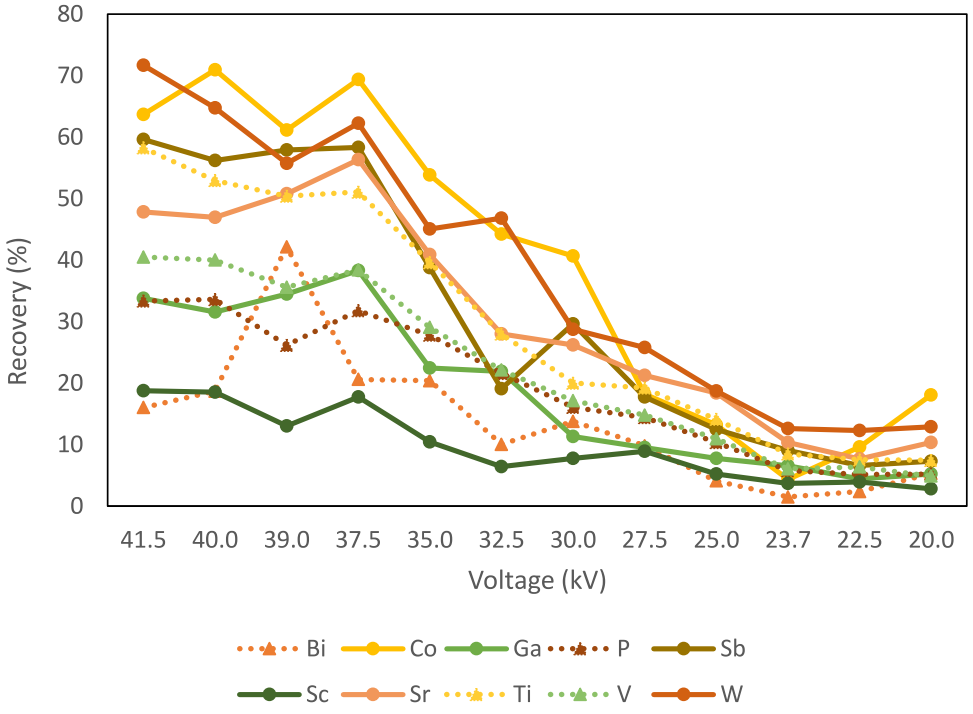

Fig. 5. Recovery of PTEs with significant economic value. Average of three experimental runs at each voltage with a standard error <5%.

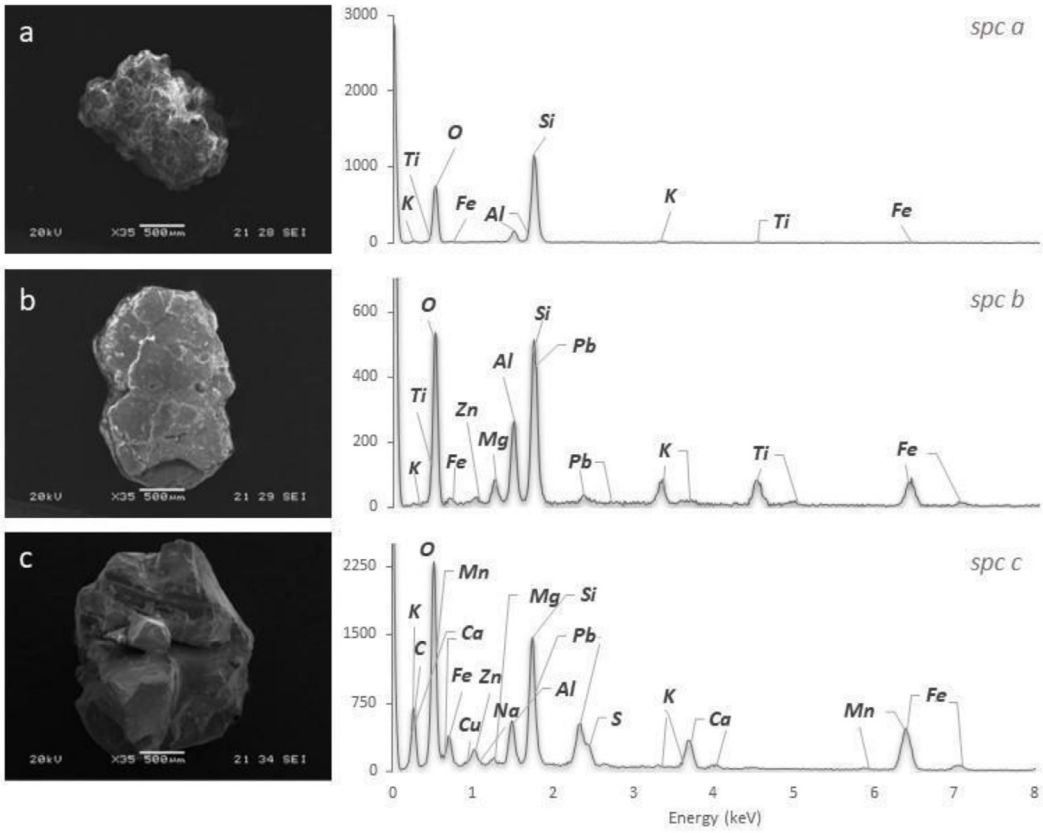

Fig. 6. Selected SEM images of each of the three predominant particle species present in soil fractions obtained after electrostatic separation with representative EDS spectra. (a) Feldspar particle found in the insulating fraction, (b) mica particle found in the middlings fraction, and (c) slag particle found in the conductive fraction.

3.3. Mineralogical analysis of the separated fractions

In order to evaluate the electrostatic separation method from a mineralogical point of view, the three fractions generated were examined under a binocular microscope. In this way, three main types of particles were identified (species 1, 2, and 3) and these were manually separated and studied using SEM-EDX to determine their mineralogical composition. Species 1 (spc.1) particles were found in the insulating fraction (nonconductive material) and were identified as feldspar (Fig. 6a). Further analysis revealed that these particles (Fig. 6, spc. a) were not pollutant bearing, suggesting a geogenic origin for the feldspar in these soil samples. Species 2 (spc. 2) type particles were found to be mica (Fig. 6b), and these were present in highest abundance among the middlings fraction. Analysis of the chemical composition of these particles revealed the presence of Pb and Zn, although in low concentrations (Fig. 6b, spc b). Finally, the most abundant particle in the conductive fraction (Fig. 6c), species 3 (spc. 3), corresponds to the slags identified in previous work on other soils in the region surrounding the site sampled here (Sierra et al., 2013). The presence of Cu, Pb, and Zn in conjunction with high levels of Fe, O, and S (indicating iron oxides and sulphides) points to the existing mineralization and/or mining and metallurgy activities as possible origin of these elements.

3.4. Selecting the conditions for optimal soil washing

We applied the technique of attributive analysis to our experimental results to determine the optimal experimental conditions (specifically the voltage used) for soil washing by electrostatic separation. This technique was designed by Sierra et al. (2010) and details of its derivation can be found in that article. Attributive analysis calculates a merit index (Q) for each experimental test based on the main parameters involved in the mineralogical concentration process thereby enabling tests to be ranked according to their effectiveness.

Optimal separation minimizes yields while at the same time maximizing recovery values. Thus, the merit index of experiment i (where $i = 1, 2, \ldots m$ representing each of the experimental voltages) with respect to PTE j (where $j = 1, 2,$

…n representing each of the PTEs tested) is as follows:

$$Q_j^i = \frac{Min\{\gamma\}}{\gamma^i} + \frac{\varepsilon_j^i}{Max\{\varepsilon\}_j} \tag{1}$$

where:

- γ^i: Yield of experiment i.
- ε_{Ct}^i: Recovery value for the PTE j in experiment i.
- Q_j^i: Merit index for experiment i with respect to element j.

Of course, we wish to find a merit index that takes into account a particular experiment's performance across all elements of interest. However, we cannot simply add the individual merit indices for each experiment and element, since firstly, not all pollutants are equally abundant, and secondly, they each have very different maximum limits. Thus, a weighting factor, A, had to be introduced for each PTE (Eqs. (2), (3)):

$$A_j^i = \frac{\alpha_j^i}{TV} \tag{2}$$

$$A_j'^i = \frac{A_j^i}{\sum_i^m TV_j} \tag{3}$$

where:

- α_j^i: Grade of the feed for the test i and element j.
- TV_j: Target value (international standard, see Table 1) for element j.
- A_j^i: Correction factor.
- $A_j'^i$: Adjusted correction factor.

Finally, the global merit index for each experiment was calculated as follows (Eq. (4)):

$$Q_T^i = \sum_{j=1}^{n} Q_j^i A_j^{i\prime} \tag{4}$$

In this way, we have an indicator of how effectively each experimental voltage achieved separation: minimizing yield and maximizing recovery for each PTE taking into account its individual target levels. The results obtained using this formula for each voltage and PTE are shown in Table 2. It can be observed that higher voltages produce higher merit indices, indicating that broadly, higher voltages lead to more effective separation suggesting that these are the best operating conditions. Attributive analysis of this sort is expected to give an absolute maximum on the side of higher recoveries (41.5 kV) and thus, we conclude that, for optimal one-step separation, 41.5 kV is the best operating voltage.

4. Conclusions

Soils in regions with a history of mining and metallurgy often contain high levels of PTEs that require treatment. In this study, we treated soil samples taken from the La Cruz site in the Linares-La Carolina mining district. This sandy loam soil, typical of the Mediterranean region, contained significant levels of several PTEs, particularly Cu, Zn, and Pb.

Physical and chemical soil washing are well-established remediation strategies for PTE-contaminated soils. Electrostatic separation offers the possibility of separating virtually any mix of materials provided there is enough conductivity difference between components in that mix. Thus, we feel electrostatic separation should be considered among the available tools for soil separation in soil washing operations. The main limitation of electrostatic separation is the need for low moisture levels in the feed and thus the high cost that would be entailed in drying soils before processing. Fortunately, due to the local climate conditions of the site studied here, the soil to be treated was entirely dry.

The results presented here prove that electrostatic separation is a potentially useful tool for decontaminating the coarser fractions of sandy, dry, slag containing soils. In addition, the semi-industrial rig used in this investigation offers the immediate possibility of scaling up operations. The yields obtained in this work ranged from 0.69% to 9% with high recovery values for three PTEs: Zn (83.25%), Cu (77.65%), and Mo (81.01%); and significant recovery levels for six others: Sb, Pb, As, Ni, Cr, and Cd (45%–60%). This suggests that substantial quantities of contaminated soil might be economically treated in a single, real-scale stage, which is unusual for a soil washing procedure. This initial success makes it feasible to envisage subsequent rewashing cycles aiming for a complete soil treatment.

Finally, we have demonstrated that attributive analysis can provide a quality index to establish an optimal separation voltage. According to this analysis, optimal concentrations for the PTEs tested are obtained at 41.5 kV. We suggest that programmes for soil remediation should make use of this mathematical procedure to improve outcomes. Further quotients could be included in this methodology to take account of not only separation performance but also environmental and economic aspects so incorporating the concept of the circular economy into soil remediation operations.

CRediT authorship contribution statement

X. Corres: Conceptualization and design, Investigation, Data curation, Writing – original draft. **D. Baragaño:** Methodology, Data curation. **J.M. Menéndez-Aguado:** Methodology, Investigation. **J.R. Gallego:** Conceptualization and design, Methodology, Funding acquisition. **C. Sierra:** Conceptualization, Data curation, Formal analysis, Writing - Original Draft, Writing – review & editing.

Declaration of competing interest

The authors declare that they have no known competing financial interests or personal relationships that could have appeared to influence the work reported in this paper.

Data availability

Data will be made available on request.

Funding

Diego Baragaño would like to express his gratitude to the European Union-Next Generation EU, the Spanish Ministry of Universities, and The Recovery, Transformation and Resilience Plan for providing the funding for his postdoctoral grant which was administered by the University of Oviedo (Ref. MU-21-UP2021-03032892642). Carlos Sierra thanks the EURECA-PRO phase I 2020–2023 co-funded by the Erasmus+ Programme of the European Union (Ref.: 101004049).

Appendix A. Supplementary data

Supplementary material related to this article can be found online at https://doi.org/10.1016/j.eti.2023.103237.

References

Adamo, P., Dudka, S., Wilson, M.J., McHardy, W.J., 1996. Chemical and mineralogical forms of cu and Ni in contaminated soils from the sudbury mining and smelting region, Canada. Environ. Pollut. 91 (1), 11–19. http://dx.doi.org/10.1016/0269-7491(95)00035-P.

Aitani, A.M., 2004. Oil refining and products. Encycl. Energy 71, 5–729, https://www.academia.edu/21206560/Oil_Refining_and_Products.

Anderson, R., Rasor, E., van Ryn, F., 1999. Particle size separation via soil washing to obtain volume reduction. J. Hard Mater. 66 (1–2), 89–98. http://dx.doi.org/10.1016/S0304-3894(98)00210-6.

Baragaño, D., Berrezueta, E., Komárek, M., Menéndez-Aguado, J.M., 2023. Magnetic separation for arsenic and metal recovery from polluted sediments within a circular economy. J. Env. Manag. 339, 117884. http://dx.doi.org/10.1016/j.jenvman.2023.117884.

Baragaño, D., Gallego, J.L.R., María Menéndez-Aguado, J., Marina, M.A., Sierra, C., 2021. As sorption onto fe-based nanoparticles and recovery from soils by means of wet high intensity magnetic separation. Chem. Eng. J. 408, 127325. http://dx.doi.org/10.1016/J.CEJ.2020.127325.

Bedeković, G., Trbović, R., 2020. Electrostatic separation of aluminium from residue of electric cables recycling process. Waste Manage. 108, 21–27. http://dx.doi.org/10.1016/j.wasman.2020.04.033.

Beiyuan, J., Tsang, D.C.W., Valix, M., Baek, K., Ok, Y.S., Zhang, W., Bolan, N.S., Rinklebe, J., Li, X.D., 2018. Combined application of EDDS and EDTA for removal of potentially toxic elements under multiple soil washing schemes. Chemosphere 205, 178–187. http://dx.doi.org/10.1016/J.CHEMOSPHERE.2018.04.081.

Buchman, M., Office of Response, N., 2008. SQuiRT cards. (n.d.).

Dermont, G., Bergeron, M., Mercier, G., Richer-Laflèche, M., 2008. Soil washing for metal removal: A review of physical/chemical technologies and field applications. J. Hard Mater. 152 (1), 1–31. http://dx.doi.org/10.1016/J.JHAZMAT.2007.10.043.

EEA, 2009. Overview of Economic Activities Causing Soil Contamination in Some WCE and SEE Countries. European Environment Agency (EEA), https://www.eea.europa.eu/data-and-maps/figures/overview-of-economic-activities-causing-soil-contamination-in-some-wce-and-see-countries-pct-of-investigated-sites.

Feng, W., Zhang, S., Zhong, Q., Wang, G., Pan, X., Xu, X., Zhou, W., Li, T., Luo, L., Zhang, Y., 2020. Soil washing remediation of heavy metal from contaminated soil with EDTMP and PAA: Properties, optimization, and risk assessment. J. Hard Mater. 381, 120997. http://dx.doi.org/10.1016/J.JHAZMAT.2019.120997.

França, F.C.S.S., Albuuerque, A.M.A., Almeida, A.C., Silveira, P.B., Filho, C.A., Hazin, C.A., Honorato, E. v., 2017. Heavy metals deposited in the culture of lettuce (Lactuca sativa L.) by the influence of vehicular traffic in pernambuco, Brazil. Food Chem. 215, 171–176. http://dx.doi.org/10.1016/J.FOODCHEM.2016.07.168.

Gu, Y., Yeung, A.T., Li, H., 2018. Enhanced electrokinetic remediation of cadmium-contaminated natural clay using organophosphonates in comparison with EDTA. Chin. J. Chem. Eng. 26 (5), 1152–1159. http://dx.doi.org/10.1016/J.CJCHE.2017.10.012.

Inculet, I.I., 1984. Electrostatic mineral separation. p. 153, https://books.google.com/books/about/Electrostatic_Mineral_Separation.html?hl=es&id=m_XmAAAAMAAJ.

Kawatra, S.K., Young, C., 2019. SME Mineral Processing & Extractive Metallurgy HandBook. p. 2203.

Kdidi, S., Vaca-Medina, G., Peydecastaing, J., Oukarroum, A., Fayoud, N., Barakat, A., 2019. Electrostatic separation for sustainable production of rapeseed oil cake protein concentrate: Effect of mechanical disruption on protein and lignocellulosic fiber separation. Powder Technol. 344, 10–16. http://dx.doi.org/10.1016/j.powtec.2018.11.107.

Khalid, S., Shahid, M., Niazi, N.K., Murtaza, B., Bibi, I., Dumat, C., 2017. A comparison of technologies for remediation of heavy metal contaminated soils. J. Geochem. Explor. 182, 247–268. http://dx.doi.org/10.1016/J.GEXPLO.2016.11.021.

Li, Q., Guo, L., Cao, H., Li, A., Xu, W., Wang, Z., 2021. Effects of an effective adsorption region on removing catalyst particles from an FCC slurry under a DC electrostatic field. Powder Technol. 377, 676–683. http://dx.doi.org/10.1016/j.powtec.2020.09.038.

Li, Y., Liao, X., Li, W., 2019a. Combined sieving and washing of multi-metal-contaminated soils using remediation equipment: A pilot-scale demonstration. J. Clean. Prod. 212, 81–89. http://dx.doi.org/10.1016/J.JCLEPRO.2018.11.294.
Li, X., Thornton, I., 2001. Chemical partitioning of trace and major elements in soils contaminated by mining and smelting activities. Appl. Geochem. 16 (15), 1693–1706. http://dx.doi.org/10.1016/S0883-2927(01)00065-8.
Li, Q., Zhang, Z., Wu, Z., Wang, Z., Guo, L., 2019b. Effects of electrostatic field and operating parameters on removing catalytic particles from FCCS. Powder Technol. 342, 817–828. http://dx.doi.org/10.1016/j.powtec.2018.10.060.
Lillo Ramos, F.J., 1992. Geology and geochemistry of linares-la carolina pb-ore field (southeastern border of the hesperian massif).
Loredo, J., Ordóñez, A., Gallego, J.R., Baldo, C., García-Iglesias, J., 1999. Geochemical characterisation of mercury mining spoil heaps in the area of mieres (asturias, northern Spain). J. Geochem. Explor. 67 (1–3), 377–390. http://dx.doi.org/10.1016/S0375-6742(99)00066-7.
Lorite, I.J., Castilla, A., Cabezas, J.M., Alza, J., Santos, C., Porras …, R., Sillero, J.C., 2023. Analyzing the impact of extreme heat events and drought on wheat yield and protein concentration, and adaptation strategies using long-term cultivar trials under semi-arid conditions. Agricult. Forest Meteorol. 329, 109279. http://dx.doi.org/10.1016/j.agrformet.2022.109279.
Makino, T., Sugahara, K., Sakurai, Y., Takano, H., Kamiya, T., Sasaki, K., Itou, T., Sekiya, N., 2006. Remediation of cadmium contamination in paddy soils by washing with chemicals: Selection of washing chemicals. Environ. Pollut. 144 (1), 2–10. http://dx.doi.org/10.1016/J.ENVPOL.2006.01.017.
Martínez, J., Llamas, J., de Miguel, E., Rey, J., Hidalgo, M.C., 2007a. Determination of the geochemical background in a metal mining site: example of the mining district of linares (south Spain). J. Geochem. Explor. 94 (1–3), 19–29. http://dx.doi.org/10.1016/j.gexplo.2007.05.001.
Martínez, J., Llamas, J.F., de Miguel, E., Rey, J., Hidalgo, M.C., 2007b. Application of the visman method to the design of a soil sampling campaign in the mining district of linares (Spain). J. Geochem. Explor. 92 (1), 73–82. http://dx.doi.org/10.1016/j.gexplo.2006.07.004.
Martínez, J., Rey, J., Hidalgo, M.C., Benavente, J., 2012. Characterizing abandoned mining dams by geophysical (ERI) and geochemical methods: The linares-la carolina district (southern Spain). Water Air Soil Pollut. 223 (6), 2955–2968. http://dx.doi.org/10.1007/s11270-012-1079-7.
Park, C.H., Subasinghe, N., Jeon, H.S., 2015. Separation of covering plastics from particulate copper in cable wastes by induction electrostatic separation. Mater. Trans. 56 (7), 1140–1143. http://dx.doi.org/10.2320/matertrans.M2015138.
Pfeifroth, Uwe, Kothe, Steffen, Müller, Richard, Trentmann, Jörg, Hollmann, Rainer, Fuchs, Petra, Werscheck, Martin, 2017. Surface Radiation Data Set - Heliosat (SARAH) - Edition 2. Satellite Application Facility on Climate Monitoring, http://dx.doi.org/10.5676/EUM_SAF_CM/SARAH/V002.
Piccolo, A., Spaccini, R., de Martino, A., Scognamiglio, F., di Meo, V., 2019. Soil washing with solutions of humic substances from manure compost removes heavy metal contaminants as a function of humic molecular composition. Chemosphere 225, 150–156. http://dx.doi.org/10.1016/J.CHEMOSPHERE.2019.03.019.
Rui, D., Wu, Z., Ji, M., Liu, J., Wang, S., Ito, Y., 2019. Remediation of Cd- and Pb- contaminated clay soils through combined freeze-thaw and soil washing. J. Hard Mater. 369, 87–95. http://dx.doi.org/10.1016/J.JHAZMAT.2019.02.038.
Sierra, C., Gallego, J.R., Afif, E., Menéndez-Aguado, J.M., González-Coto, F., 2010. Analysis of soil washing effectiveness to remediate a brownfield polluted with pyrite ashes. J. Hard Mater. 180 (1–3), 602–608. http://dx.doi.org/10.1016/j.jhazmat.2010.04.075.
Sierra, C., Martínez, J., Menéndez-Aguado, J.M., Afif, E., Gallego, J.R., 2013. High intensity magnetic separation for the clean-up of a site polluted by lead metallurgy. J. Hazard. Mater. 248–249 (1), 194–201. http://dx.doi.org/10.1016/j.jhazmat.2013.01.011.
Tabtabaei, S., Konakbayeva, D., Rajabzadeh, A.R., Legge, R.L., 2019. Functional properties of navy bean (phaseolus vulgaris) protein concentrates obtained by pneumatic tribo-electrostatic separation. Food Chem. 283, 101–110. http://dx.doi.org/10.1016/j.foodchem.2019.01.031.
Tabtabaei, S., Vitelli, M., Rajabzadeh, A.R., Legge, R.L., 2017. Analysis of protein enrichment during single- and multi-stage tribo-electrostatic bioseparation processes for dry fractionation of legume flour. Sep. Purif. Technol. 176, 48–58. http://dx.doi.org/10.1016/j.seppur.2016.11.050.
Uchimiya, M., Wartelle, L.H., Klasson, K.T., Fortier, C.A., Lima, I.M., 2011. Influence of pyrolysis temperature on biochar property and function as a heavy metal sorbent in soil. J. Agricult. Food Chem. 59 (6), 2501–2510. http://dx.doi.org/10.1021/JF104206C/SUPPL_FILE/JF104206C_SI_001.PDF.
Villot, A., Gonthier, Y., Gonze, E., Bernis, A., Ravel, S., Grateau, M., Guillaudeau, J., 2012. Separation of particles from syngas at high-temperatures with an electrostatic precipitator. Sep. Purif. Technol. 92, 181–190. http://dx.doi.org/10.1016/j.seppur.2011.04.028.
Wang, G., Zhang, S., Zhong, Q., Xu, X., Li, T., Jia, Y., Zhang, Y., Peijnenburg, W.J.G.M., Vijver, M.G., 2018. Effect of soil washing with biodegradable chelators on the toxicity of residual metals and soil biological properties. Sci. Total Environ. 625, 1021–1029. http://dx.doi.org/10.1016/J.SCITOTENV.2018.01.019.
Wills, B.A., Napier-Munn, T.J., 2006. Mineral processing technology: An introduction to the practical aspects of ore treatment and mineral recovery. In: Butterworth-Heinemann (Ed.), Wills' Mineral Processing Technology, seventh ed. Butterworth-Heinemann, http://dx.doi.org/10.1016/C2010-0-65478-2.
Wu, Q., Leung, J.Y.S., Geng, X., Chen, S., Huang, X., Li, H., Huang, Z., Zhu, L., Chen, J., Lu, Y., 2015. Heavy metal contamination of soil and water in the vicinity of an abandoned e-waste recycling site: Implications for dissemination of heavy metals. Sci. Total Environ. 506–507, 217–225. http://dx.doi.org/10.1016/J.SCITOTENV.2014.10.121.
Xu, J., Kleja, D.B., Biester, H., Lagerkvist, A., Kumpiene, J., 2014. Influence of particle size distribution, organic carbon, pH and chlorides on washing of mercury contaminated soil. Chemosphere 109, 99–105. http://dx.doi.org/10.1016/J.CHEMOSPHERE.2014.02.058.
Yang, X., Wang, H., Peng, Z., Hao, J., Zhang, G., Xie, W., He, Y., 2018. Triboelectric properties of ilmenite and quartz minerals and investigation of triboelectric separation of ilmenite ore. Int. J. Mining Sci. Technol. 28 (2), 223–230. http://dx.doi.org/10.1016/j.ijmst.2018.01.003.
Zhao, L., Ding, Z., Sima, J., Xu, X., Cao, X., 2017. Development of phosphate rock integrated with iron amendment for simultaneous immobilization of Zn and Cr (VI) in an electroplating contaminated soil. Chemosphere 182, 15–21. http://dx.doi.org/10.1016/J.CHEMOSPHERE.2017.05.004.

Journal of Hazardous Materials 466 (2024) 133529

Contents lists available at ScienceDirect

Journal of Hazardous Materials

journal homepage: www.elsevier.com/locate/jhazmat

A novel heuristic tool for selecting the best upgrading conditions for the removal of potentially toxic elements by soil washing

X. Corres [a], C. Sierra [b], A.J. Diez-Mestas [c], J.R. Gallego [a], D. Baragaño [d,e,*]

[a] INDUROT and Environmental Biogeochemistry & Raw Materials Group, Campus de Mieres, Universidad de Oviedo, Mieres, Asturias, Spain
[b] Department of Mining, Topography and Structure Technology, University of León, Campus de Vegazana, 24006, León, Spain
[c] Freelance data analysis consultant. Mieres, Asturias, Spain
[d] School of Mines and Energy Engineering, University of Cantabria, Blvr. Ronda Rufino Peón 254, 39300 Torrelavega, Cantabria, Spain
[e] Instituto de Ciencia y Tecnología del Carbono, INCAR-CSIC, Francisco Pintado Fe, 26, 33011 Oviedo, Spain

HIGHLIGHTS

- We introduce PPAA-U for soil-washing optimization.
- PPAA-U maximizes recovery and minimizes concentrate yield.
- PAAA-U penalizes experimental contributions with high variability.
- This methodology yields consistently good results.
- PPAA-U has many potential applications in other separation technologies.

GRAPHICAL ABSTRACT

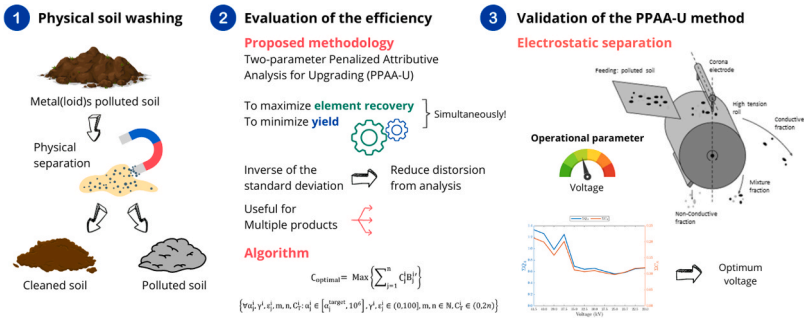

ARTICLE INFO

Keywords:
Soil pollution
Soil remediation
Optimization
Circular economy

ABSTRACT

Here, we propose two-parameter penalized attributive analysis, PPAA-U, a novel heuristic tool for selecting the best upgrading conditions (BUCs) for soil washing. Given a multi-component feed and a specific set of operating conditions, PPAA-U generates a quality index based on how well recoveries for key components are maximized while minimizing the yield. We demonstrate, through the calculation of families of curves, that this quality index is related linearly to recovery and to the inverse of the yield, meaning that reducing yield values is more important than maximizing recovery. To evaluate our method, electrostatic separation at 12 different voltages was carried out on soil samples from an ex-industrial site in Spain. Values of recovery, yield, and grade were analyzed using basic attributive analysis and PPAA-U with and without target-to-distance correction. Both methods identified the same optimal separation voltage, and the power of PPAA-U to correct for high variation in yields and recoveries was observed as a divergence between results produced by each method at low voltages where variation in these values was greatest. PPAA-U thus offers a convenient tool for soil washing optimization, and we suggest that it could be applied successfully to other industrial processes.

* Corresponding author at: School of Mines and Energy Engineering, University of Cantabria, Blvr. Ronda Rufino Peón 254, 39300 Torrelavega, Cantabria, Spain.
E-mail address: diego.baragano@unican.es (D. Baragaño).

https://doi.org/10.1016/j.jhazmat.2024.133529
Received 11 October 2023; Received in revised form 11 January 2024; Accepted 12 January 2024
Available online 17 January 2024

1. Introduction

Many industrial processes lead to the accumulation of potentially toxic elements (PTEs) in soils, and the need to remove them is driving research into soil remediation techniques in several countries [1,2]. Existing soil remediation technologies include various physical, chemical, and biological methods [3,4]. Originally developed in the mining industry to obtain metal concentrates from mineral ores, physical separation technologies have been used for soil remediation in the case of both organic and inorganic pollutants [5-7]. Physical separation can be used to remove potentially toxic elements (PTEs) from soil either directly, where PTEs are present as discrete particles, or, since many PTEs are strongly absorbed by clay, by separating the fraction onto which they are preferentially sorbed [8-10]. Although physical soil washing can be a terminal process, it is usually followed by chemical soil washing [11,12].

Physical soil remediation shares many common processes with mineral beneficiating and recycling. In all cases, the objective is to separate a concentrate of perhaps two or more target components from a multi-component feed. However, whereas in mineral beneficiation (and recycling), optimization may occur for either elements or mineral compounds, in the case of soil washing, we tend to be concerned only with elements.

The principal distinction between soil remediation and mineral processing (beneficiation or recycling) lies in the different economics of these processes. These considerations mean that the concentrate-to-tailings ratio achieved in mineral processing operations is generally closer to one than it is in soil remediation [13]. In mineral beneficiation, for example, the cost of further processing the concentrate (through the pyro- and hydrometallurgical routes) is offset due to the value of the final product [14,15]; however, for soil washing, a high initial concentrate-to-tailing ratio is crucial to avoid compromising the economic viability of the operation [16].

This means that, for soil remediation, in contrast to mineral beneficiation and recycling, concentrate yield minimization is the most important criterion. Moreover, in soil remediation, the washed fraction (tailings) must adhere to environmental standards in terms of grade for it to be declared decontaminated, whereas in mineral recycling and beneficiation, the grade of tailings is dictated more by economic considerations and may remain quite high provided that the process is profitable [17,18].

In any mineral separation process, whether this be a beneficiation or soil remediation process, improving performance implies increasing the concentration of a target element or compound in one of the process flows. Thus, the total mass of the initial material flow, known as the feed (F), is normally separated into two products, the concentrate (C) and the tailings (T), corresponding to the fractions in which the grade of the target element or compound is, respectively, higher or lower than that in the feed. A third fraction is sometimes collected, the middlings (M), which has a grade intermediate between that of the concentrate and the tailings.

The total mass balance is then [19]:

$$F = C + M + T \tag{1}$$

Dividing Eq. (1) by the mass of the feed gives the yield or weight recovery for each mass flow (Eq. (2)) [20]:

$$\frac{F}{F} = 1 = \frac{C}{F} + \frac{M}{F} + \frac{T}{F} \tag{2}$$

Of the three yields, that of most interest is the concentrate yield, $\frac{C}{F} = \gamma$, which contains the highest concentration of the target element or compound.

A parameter known as the grade or assay is used to indicate the proportion of the target element or compound in each of the mass flows. Its value for the concentrate is usually denoted as λ, and this value can be used as an assessment of the quality of the separation process. The grades for the feed, middlings, and tailings are denoted by α, β, and ϑ, respectively. In a successful separation process, the following inequalities should be true: $\lambda > \alpha$; $\vartheta < \alpha$; and $\lambda > \beta > \alpha$ [20]. The recovery, ε, refers to the mass of the target element or compound found in a given mass flow relative to the feed. Thus, for the concentrate fraction, recovery is defined as [20]:

$$\varepsilon = \frac{\lambda}{\alpha}\gamma \tag{3}$$

The same value for the tailings fraction is usually denoted as η, such that [20]:

$$\varepsilon + \eta = 1 \tag{4}$$

Intuitively, it would seem that ε alone could be used as a measure of separation performance due to its relationship to the parameters α, λ, and γ. However, this is not the case and, in fact, assessing separation performance requires consideration of not only ε but at least two of either α, λ, or γ. For example, $\varepsilon = 100\%$ may seem to imply perfect separation, but accompanied by high γ and low λ, this is clearly not so. Thus, if we wish to optimize a separation process, we must maximize ε and λ while simultaneously minimizing γ [20,21,19].

Bearing in mind the above discussion, the aim of this research is to develop a robust method for determining the best upgrading conditions for a given soil washing operation. Specifically, we will:

- Offer an exhaustive analysis of basic attributive analysis in terms of families of curves.
- Discuss the effect of experimental noise on the overall quality of a given experimental set-up.
- Show how attributive analysis can be modified to address this type of distortion.
- Provide a practical example of the use of attributive analysis.

2. Materials and methods

In this section, we discuss the sources of the soil samples and the separation technique used to demonstrate the practical application of attributive analysis. We then explain the principles of basic and penalized attributive analysis.

2.1. Sample preparation and analysis

The site of interest is the Linares mining district (Andalusia, Spain), a center for intense Pb mining, mineral processing, and metallurgical activities for several centuries [22,23]. Ten 2.5 kg samples were collected from the top 35 cm layer of soil at random points across the study site to form a bulk sample of 25 kg. The bulk sample was homogenized and wet sieved (water flow = 0.3 l/min) using sodium carbonate and sodium hexametaphosphate as dispersing agents to produce six granulometric fractions: 63 μm, 63–125 μm, 125–250 μm, 250–500 μm, 500–1000 μm, and 1000–2000 μm (ASTM D-422–63) [24]. Wet sieving continued until 3 kg of the 1000–2000 μm fraction was obtained. This fraction was then divided into thirty-six subsamples for electrostatic separation. Each of these subsamples was subjected to chemical analysis.

Subsequently, representative subsamples weighing 1 g each were extracted. These specimens were digested using "aqua regia" (a mixture of HCl and HNO_3) before analysis via inductively coupled plasma optical emission spectroscopy (ICP—OES) (HP 7700, Agilent Technologies).

Separation of the feed samples was achieved using an EHTP Outotec (Fig. S1) high-tension electrostatic separator. This advanced specification model is equipped with an AC wiper electrode operating at 18 kV and two DC electrodes—one corona and the other static—adjustable to a maximum of 41.5 kV, known as the separation voltage. Additionally, it features a grounded roller brush with interchangeable bristles and infrared roller heating for particle removal. Three fractions are collected: the nonconductive, intermediate, and conductive fractions.

The most important parameters in the separation process include the conductivity of the sample particles, the rotation speed of the roller, the placement of the electrodes, and the corona electrode tension. This enables the separation of materials based on their conductivity properties, making electrostatic separation an invaluable tool for many industrial and research applications.

Samples are loaded onto the roller via the feed hopper and travel towards the corona electrode. The air surrounding the corona electrode is ionized; thus, as the particles on the roller approach the corona electrode, they pick up charge. Conductive particles will lose their charge most rapidly; therefore, the roller's centrifugal force ejects these particles first, and they are collected in the conductors bin. More insulating particles keep their charge and remain on the roller until they are brushed off and fall into either the insulators or the middlings bin.

The apparatus was operated at 12 different separating voltages in a range from 20 kV to 41.5 kV. Separations were repeated three times at each separation voltage, and the results presented here correspond to the average values recorded for the three experiments completed at each voltage. A comprehensive description of the apparatus is provided in the Supplementary material section (SM1).

2.2. Basic attributive analysis

The basic model for attributive analysis was developed and applied to soil washing by Sierra et al. (2010) and Boente et al. [25]. Given the results of a number of soil-washing experiments using a particular separation technique, this method seeks to determine the set of experimental parameters that provides optimal separation. As discussed, this is done by seeking the conditions where the recovery of target elements is maximized while minimizing the yield.

Considering a set of m experiments to separate out n contaminating elements, the performance of a given experiment, i, with respect to target element, j, is expressed as a quality factor Q_j^i (Eq. (5)):

$$Q_j^i = \frac{\mathrm{Min}\{\gamma\}}{\gamma^i} + \frac{\varepsilon_j^i}{\mathrm{Max}\{\varepsilon_j\}} \tag{5}$$

where

- $i = 1, \ldots, m$ and refers to the results produced by a specific set of experimental parameters.
- $j = 1, \ldots, n$ and refers to results for a specific target element or contaminant; in this study, m = 10 (see Table 1 for all target elements considered).
- Q_j^i: Quality factor of experiment i for element j.
- γ^i: Yield of experiment i.
- ε_j^i: Recovery of element j in experiment i.

In the present study, the main experimental variable is the separation voltage; thus, $m = 12$, and ten target elements (the values of j) were considered (see Table 1). Table 1 presents the yields and recoveries of each element at each separation voltage tested; the values shown are an average of the results from three experimental runs at the same separation voltage.

As in the present study, there are generally numerous contaminants to consider, each of which has a specific target grade, that is, a safe threshold concentration after soil washing. Because some contaminants are significantly more toxic than others, each element to be removed during the soil washing operation is given a weighting coefficient related to its target grade, known as the target-to-distance correction. The sum of these coefficients must add up to 1; thus, we first define $A_j^i (Eq.6)$:

$$A_j^i = \frac{\alpha_j^i}{\alpha_j^{\mathrm{target}}} \tag{6}$$

Table 1
Yield (γ) for each experiment, grade (α), and recovery (ε) for each element in each experiment. Average of three experimental runs at each voltage with a standard error < 5%.

		As		Cd		Cr		Cu		Hg		Mo		Ni		Pb		Sb		Zn	
Voltage (kV)	γ (%)	α (mg/kg)	ε (%)	α (mg/kg)	ε (%)	α (mg/kg)	ε (%)	α (mg/kg)	ε (%)	α (mg/kg)	ε (%)	α (mg/kg)	ε (%)	α (mg/kg)	ε (%)	α (mg/kg)	ε (%)	α (mg/kg)	ε (%)	α (mg/kg)	ε (%)
41.5	8.6	57.8	38.9	11.3	37.8	11.6	35.4	523.5	62.2	1.7	14.4	4.0	81.0	12.3	57.3	2731.75	44.8	15.7	59.6	2375.37	81.5
40	9.0	56.5	41.7	8.7	45.0	10.2	38.8	610.7	74.9	1.5	13.2	3.6	79.7	10.5	53.7	2521.85	48.9	14.5	56.2	2293.01	83.3
39	6.3	45.9	38.7	8.6	29.2	8.4	30.7	555.1	77.7	1.4	13.3	2.3	74.7	6.0	39.0	2311.17	45.7	11.4	57.9	1535.38	82.9
37.5	7.8	55.3	40.9	8.5	34.3	11.4	41.8	802.3	68.7	1.1	25.9	2.4	78.9	12.3	49.4	2691.02	47.6	15.1	58.3	1776.63	82.6
35	5.9	39.2	30.3	6.2	27.4	9.3	28.1	296.0	61.6	0.8	10.9	1.7	64.5	6.4	42.6	2837.74	29.8	11.1	38.8	1106.05	74.2
32.5	4.0	43.5	23.0	6.2	20.0	7.6	24.8	294.8	36.6	0.6	11.1	1.4	54.5	7.4	39.7	3108.21	20.1	16.8	19.1	790.23	65.5
30	3.4	42.7	17.3	6.9	19.1	9.5	16.1	394.5	34.6	0.6	10.6	1.4	49.4	8.0	31.6	2238.23	27.2	10.6	29.6	834.86	55.3
27.5	3.3	50.0	12.3	7.9	11.6	11.5	13.6	314.5	33.5	0.5	12.1	1.5	33.0	9.7	16.1	2522.95	18.7	10.9	17.8	886.28	40.3
25	2.8	49.0	8.4	8.1	15.6	17.4	5.7	245.0	22.5	0.4	6.2	1.3	24.9	10.5	7.8	1797.21	13.3	10.7	12.5	751.50	36.0
23.7	1.7	43.6	5.3	5.8	9.1	10.4	4.7	188.6	9.2	0.4	4.3	0.6	17.3	14.0	3.6	1620.25	7.2	7.5	9.1	376.06	21.6
22.5	1.5	39.6	5.4	7.2	7.8	8.1	7.2	235.1	10.2	0.3	4.9	1.1	11.3	8.3	7.4	1684.47	6.8	8.3	6.6	520.28	17.1
20	1.4	46.2	4.3	5.6	6.4	8.3	5.3	176.1	24.7	0.7	2.0	0.7	16.8	5.6	16.0	2016.94	6.6	9.1	7.3	473.96	17.3
17.5	0.7	66.6	2.0	6.9	2.7	11.4	1.9	286.4	5.1	0.4	2.0	0.9	7.0	8.7	3.0	3455.43	2.9	15.0	3.0	590.56	6.9
Target value (mg/kg)		0.9		0.8		0.35		3.4		0.3		3		0.26		55		3		16	

where

- i and j are defined as before.
- α_j^i: Feed grade of element j in experiment i.
- α_j^{target}: Target grade for element j.

Then, to obtain the correct weighting for each element's contribution to overall contamination levels, the following transformation is implemented (Eq. (7)):

$$A_j^{i'} = \frac{A_j^i}{\sum_i^m A_j^i} \tag{7}$$

A global quality index for a given experiment, i, for all elements $\left(Q_T^i\right)$ can then be defined as follows (Eq. (8)):

$$Q_T^i = \sum\nolimits_{j=1}^{n} Q_j^i A_j^{i\prime} \tag{8}$$

Finally, the best experimental set-up is, then, that for which this value is maximal (Eq. (9)):

$$Q_{optimal} = Max\left\{\sum\nolimits_{j=1}^{n} Q_j^i A_j^{i\prime}\right\} \tag{9}$$

where the following restrictions apply:

$$\left\{\forall \alpha_j^i, \gamma^i, \varepsilon_j^i, m, n, Q_T^i : \alpha_j^i \in \left[\alpha_j^{target}, 10^6\right], \gamma^i, \varepsilon_j^i \in (0, 100), m, n \in \mathbb{N}, Q_T^i \in (0, 2n)\right\}$$

2.3. Two-parameter penalized attribute analysis (PPAA-U)

As can be appreciated from Eqs. (5) and (6), experiments for which the yield, recovery, or grade varies greatly compared to the mean values will be given disproportionally more weight than those resulting in less variance. This will clearly bias the final quality assessment; thus, we present a modified method to address and eliminate this problem. Specifically, the inverse of the standard deviation can be used as a weighting factor to penalize large variations in each of the parameters of interest, yield, recovery, and grade, all of which vary for each element and every experiment. In addition, because the range of variation will be of a different order of magnitude for each parameter (for instance, in our case study, ε [%] is in the range {2, 83.3}, while γ [%] is in the range {0.7, 9}, and α [mg/kg] is in the range {0.32, 3108.21}, see Table 1), the weighting factors must be normalized to between 0 and 1.

In this way, we obtain a new value for the quality factor of each experiment and target element, C_j^i (Eqs. (10)–(14)):

$$\Gamma^i = \frac{Min\{\gamma\}}{\gamma^i}\left(\frac{\sum_{i=1}^{m}|\gamma^i - \overline{\gamma}|}{m}\right)^{-1} \tag{10}$$

$$\Gamma^{i'} = \frac{\Gamma^i}{\sum_i^m \Gamma^i} \tag{11}$$

$$E_j^i = \frac{\varepsilon_j^i}{Max\{\varepsilon_j\}}\left(\frac{\sum_{i=1}^{m}\left|\varepsilon_j^i - \overline{\varepsilon}_j\right|}{m}\right)^{-1} \tag{12}$$

$$E_j^{i'} = \frac{E_j^i}{\sum_i^m E_j^i} \tag{13}$$

$$C_j^i = \Gamma^{i'} + E_j^{i'} \tag{14}$$

and a new target-to-distance correction coefficient, $B_j^{i'}$ (Eq. (15)–(16)):

$$B_j^i = \frac{\alpha_j^i}{\alpha_j^{target}}\left(\frac{\sum_{i=1}^{m}\left|\alpha_j^i - \overline{\alpha}_j\right|}{m}\right)^{-1} \tag{15}$$

$$B_j^{i\prime} = \frac{B_j^i}{\sum_i^m B_j^i} \tag{16}$$

Thus, the corrected global quality index for an experiment i for all elements j to n is:

$$C_T^i = \sum\nolimits_{j=1}^{n} C_j^i B_j^{i\prime} \tag{17}$$

Finally, the optimal experimental set up can be found as follows:

$C_{optimal} = Max\left\{\sum_{j=1}^{n} C_j^i B_j^{i'}\right\}$ (18).

where

- i, j, and n are defined as before.
- γ: Yield of experiment i.
- $\overline{\gamma}$: Mean yield for element j.
- ε: Recovery of element j in experiment i.
- $\overline{\varepsilon}_j$: Mean recovery for element j.
- α_j^i: Grade of the feed of j element in experiment i.
- $\overline{\alpha}_j$: Mean grade for element j.
- α_j^{target}: Target grade for element j.

and the following restrictions apply:

$$\left\{\forall \alpha_j^i, \gamma^i, \varepsilon_j^i, m, n, C_T^i : \alpha_j^i \in \left[\alpha_j^{target}, 10^6\right], \gamma^i, \varepsilon_j^i \in (0, 100], m, n \in \mathbb{N}, C_T^i \in (0, 2n)\right\}$$

The Supplementary material section (SM2) contains an example of this methodology used in a scenario involving two experimental set-ups with two elements to be separated.

3. Results and discussion

3.1. Separation results

We conducted twelve experimental runs with separation voltages ranging from 41.5 kV to 17.5 kV (Table 1). There was a positive correlation between yield (γ) and voltage with $\gamma = 1.4\%$ at 20 kV and $\gamma = 8.6\%$ at 41.5 kV with a maximum of $\gamma = 9.0\%$ at 40.0 kV (peak-yield voltage). Similarly, the recovery (ε) in the conductive fraction was also positively correlated with the voltage. The peak-yield voltage (40 kV) also produced the highest maximum recoveries for six PTEs of interest: Zn (83.3%), followed by Mo (81.0%), Cu (62.2%), Cu (62.2%), Sb (59.6%) and Ni (57.3%). The same voltage, however, resulted in the lowest recoveries for the other four PTEs studied: Hg (13.2%), Cr (38.8%), Cd (45.0%), and As (41.7%). Considering the variation in the values recorded for the three parameters of interest, yield, recovery, and grade, while the first of these parameters varied in a range from 1.4% to 8.6%, the other two had far wider ranges: 2%–83.3% and 0.3 mg/kg to 3108 mg/kg, for recovery and grade, respectively. All the data are summarized in Table 1.

Attributive analysis generates a family of curves describing the relationships between yield, recovery, and the quality index for a particular experimental set-up. In the following sections, we will consider these curves and compare the performances of basic and penalized

attributive analysis in evaluating the quality indices of the twelve separation experiments undertaken here.

3.2. Families of curves

Taking Eq. 5, the attributive analysis equation, and substituting in values for yield (γ) and recovery (Ɛ), it is possible to produce a family of surfaces that share a similar shape and functional relationship. These surfaces represent the ways in which the quality index of an experiment (Q) will vary with changes in either γ or Ɛ. Fig. 1 shows a surface plot of Q for all possible combinations for γ^i and ε^i_j ranging from 0.01 to 0.99.

Sierra et al. (2010) applied the attributive analysis function to process engineering; however, they did not analyze the family of surfaces created. Such analysis enables an exploration of the theoretical consistency of the proposed methodology. In this way, as part of the present study, we will perform a sensitivity analysis and a comparative analysis with known values from our electrostatic separation experiment (see Section 2.1). Concerning the former type of analysis, this considers the relative sensitivity of the quality index to changes in yield and recovery values. Meanwhile, our comparative analysis involves an examination of results derived from the basic version of attributive analysis in comparison to those derived from PPAA-U without target-to-distance correction.

As demonstrated in Fig. 1, the relationship between Q and γ is very different from its relationship with Ɛ; thus, it is useful to examine these two relationships separately. This can be done by keeping either one of the two addends in Eq. 5 ($\frac{\varepsilon^i_j}{\mathrm{Max}\{\varepsilon_j\}}$ or ε^i_j) constant to give two families of curves, one for Q varying with γ and another for Q varying with Ɛ.

Starting with the recovery addend, $\frac{\varepsilon^i_j}{\mathrm{Max}\{\varepsilon_j\}}$, setting $\mathrm{Max}\{\varepsilon_j\}$ to 0.99 and varying ε^i_j between 0.01 and 0.99, we obtain a set of curves corresponding to different values of γ (for values of γ from γ_{min}=0.01 to 0.99). These curves correspond to the Q-Ɛ plane (see Fig. 1) at different points along the γ-axis, and as can be seen in Fig. 2, the quality index, Q, and Ɛ are related by a straight line:

$$Q = \frac{\varepsilon^i_j}{\mathrm{Max}\{\varepsilon_j\}} + K$$

The gradient of the line can be found by taking the derivative of Q with respect to Ɛ:

$$dQ = \frac{d\varepsilon^i_j}{\mathrm{Max}\{\varepsilon_j\}}$$

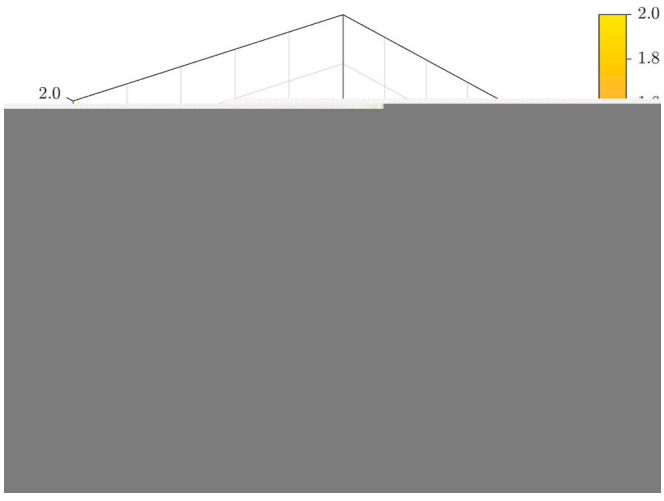

Fig. 1. General shape of a quality index function.

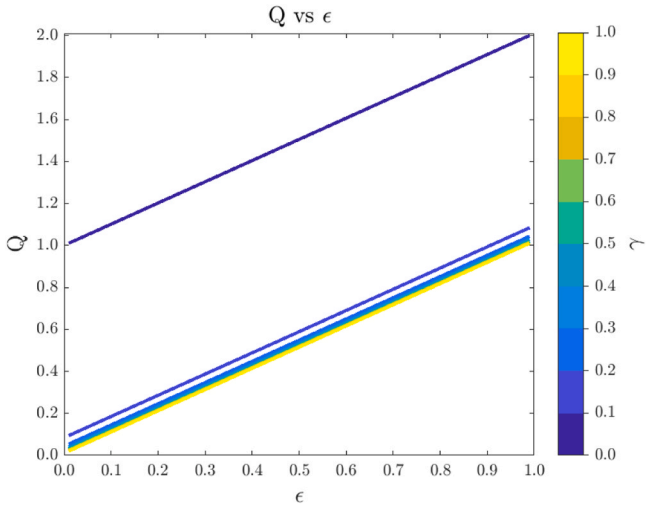

Fig. 2. Quality index function (parallel to the Q-ε plane).

such that (Eq. (19)):

$$\frac{dQ}{d\varepsilon^i_j} = \frac{1}{\mathrm{Max}\{\varepsilon_j\}} \tag{19}$$

This tells us that as the maximum recovery increases, the slope of the curve generated decreases. Moreover, when $\mathrm{Max}\{\epsilon_j\}$ is large, the variation in Q with recovery will decrease.

Taking the yield addend, $\frac{\mathrm{Min}\{\gamma\}}{\gamma^i}$, setting $\mathrm{Min}\{\gamma\}$= 0.01 and varying Ɛ from 0.01 to Ɛ= $\mathrm{Max}\{\varepsilon_j\}$ = 0.99 gives a second set of curves. These curves are Q-γ planes at different points along the Ɛ axis; see Fig. 3. In contrast to Ɛ, γ has a nonlinear relationship with Q, and calculating the gradient of the curve gives an inverse square function (Eq. (20)):

$$\frac{dQ}{d\gamma} = \frac{-\mathrm{Min}\{\gamma\}}{(\gamma^i)^2} \tag{20}$$

This result shows that the quality index is highly sensitive to yield for values of $\gamma^i < 0.1$; however, for $\gamma^i > 0.1$, the quality index remains almost stable. In this way, reducing yield values is more important than maximizing recovery since, at very low yields, small changes in this parameter have a very large impact on the quality index.

Eq. 20 also demonstrates that the sensitivity of the quality index to changes in yield decreases for higher values of $\mathrm{Min}\{\gamma\}$. This fact could be

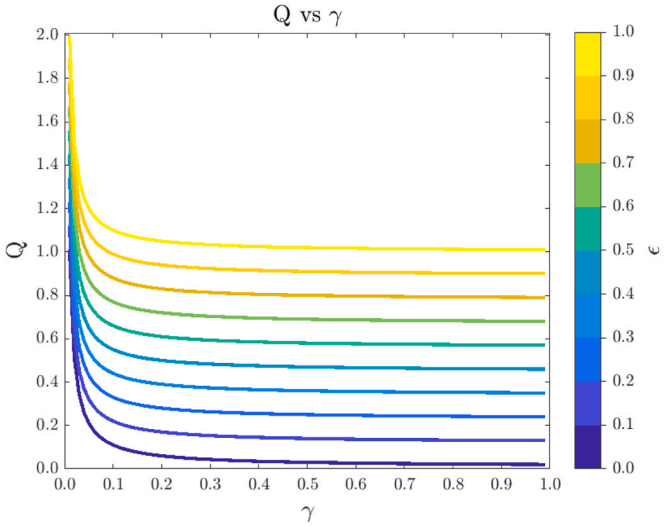

Fig. 3. Quality index parallel to the Q-γ plane.

useful under particularly noisy experimental conditions.

From the above analysis, it becomes apparent that Q should be considered a function of four variables: γ^i and ε_j^i, $\mathrm{Min}\{\gamma\}$ and $\mathrm{Max}\{\varepsilon_j\}$. We will now explore in more detail the effect of variations in $\mathrm{Min}\{\gamma\}$ and $\mathrm{Max}\{\varepsilon_j\}$.

Starting this time with the yield addend, $\frac{\mathrm{Min}\{\gamma\}}{\gamma^i}$, increasing $\mathrm{Min}\{\gamma\}$ reduces the function domain from [0,1] to [$\mathrm{Min}\{\gamma\}$,1]. As was mentioned, while this function is highly sensitive to $\gamma^i < 0.1$, at larger values of γ^i the curve is relatively flat (Fig. 3); thus, increasing $\mathrm{Min}\{\gamma\}$ places the quality function in a largely stable zone. Furthermore, as Fig. 4 demonstrates, higher values of $\mathrm{Min}\{\gamma\}$ lead to flatter curves, meaning that Q becomes increasingly insensitive to variation in γ^i.

Similarly, considering the recovery addend, $\frac{\varepsilon_j^i}{\mathrm{Max}\{\varepsilon_j\}}$, if $\mathrm{Max}\{\varepsilon_j\}$ decreases, this also narrows the function domain from [0,1] to [0, $\mathrm{Max}\{\varepsilon_j\}$]. In addition, since the gradient of the curve (see Eq. 19) is constant and equal to $\frac{1}{\mathrm{Max}\{\varepsilon_j\}}$, increasing $\mathrm{Max}\{\varepsilon_j\}$ will decrease the gradient angle, given by $\tan^{-1}\left(\frac{1}{Max\{\varepsilon_j\}}\right)$. This is demonstrated in Fig. 5.

3.3. Results of Penalized Attributive Analysis (PAA-U)

Bearing in mind the insights of the previous section, we now consider a comparison of basic attributive analysis, AA, and its inverse standard deviation weighted or penalized version, PPAA-U. Fig. 6 presents a comparison between results obtained using AA and PPAA-U (without target-to-distance correction) for the electrostatic soil washing operation described in Section 2.1. We observe significant agreement between AA and PPAA-U, particularly for lower voltages (<25 kV). This is because the variation in recoveries for the elements tested is less at lower voltages (see Table 1) than at higher voltages. In this way, the weighting used in PPAA-U makes little difference at lower voltages; however, at high voltages, the high variances are strongly penalized, lowering the Q values of these experiments and thus causing a divergence in the results obtained via the basic and penalized versions of the method. In addition, both AA and PPAA-U predict the presence of two maxima in the quality index: one at low voltages where, despite low recoveries, the lower yield leads to a peak in the quality index and a second at high voltages where there is high recovery.

When the target-to-distance correction is introduced, while both methods once again give similar results and, as expected PPA diverges from AA at higher voltages, the overall pattern is very different: specifically, the peak in the quality index at lower voltages disappears (Fig. 7). The target-to-distance correction allows us to compare how different experimental set-ups perform with respect to particularly harmful elements. This, in turn, enables attributive analysis to identify not simply the best overall separation conditions but those that are most environmentally optimal. In the present case, voltages greater than 37.5 kV stand out as providing the best separation conditions, giving priority to the removal of the most harmful PTEs.

The work presented here demonstrates that PPAA-U is a promising tool for identifying the optimal conditions for electrostatic soil washing operations. To further improve the methodology, additional quotients should be incorporated to account for components reporting to the middlings fraction instead of considering it as part of the concentrate, as is done here. In addition, the method could be modified to encompass some of the economic factors involved in the soil washing process, especially those relating to the circular economy, to further optimize conditions.

4. Conclusions

Currently, the available literature offers few means to evaluate the quality of a separation process. Methods that do exist tend to use only two parameters, typically recovery and yield; however, on their own, these two variables do not provide a sufficiently robust way to identify separation conditions that are genuinely optimal.

In its original form, attributive analysis addresses the shortcomings of other methods, providing a tool to assess optimal separation

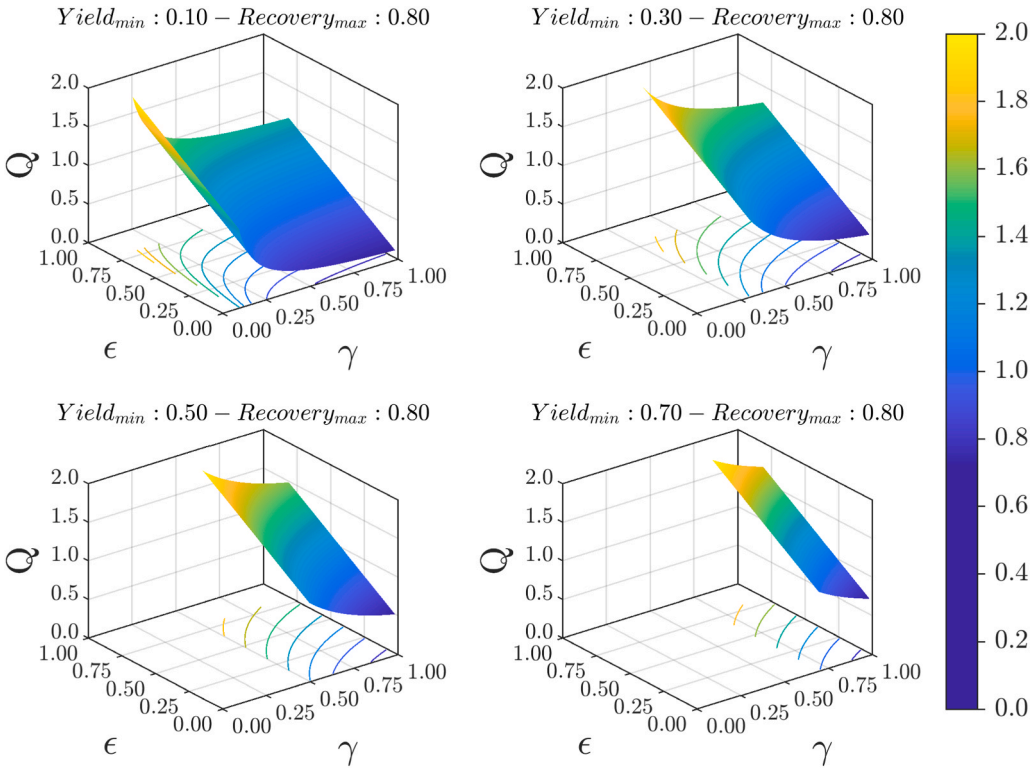

Fig. 4. Quality index function for different minimum yields.

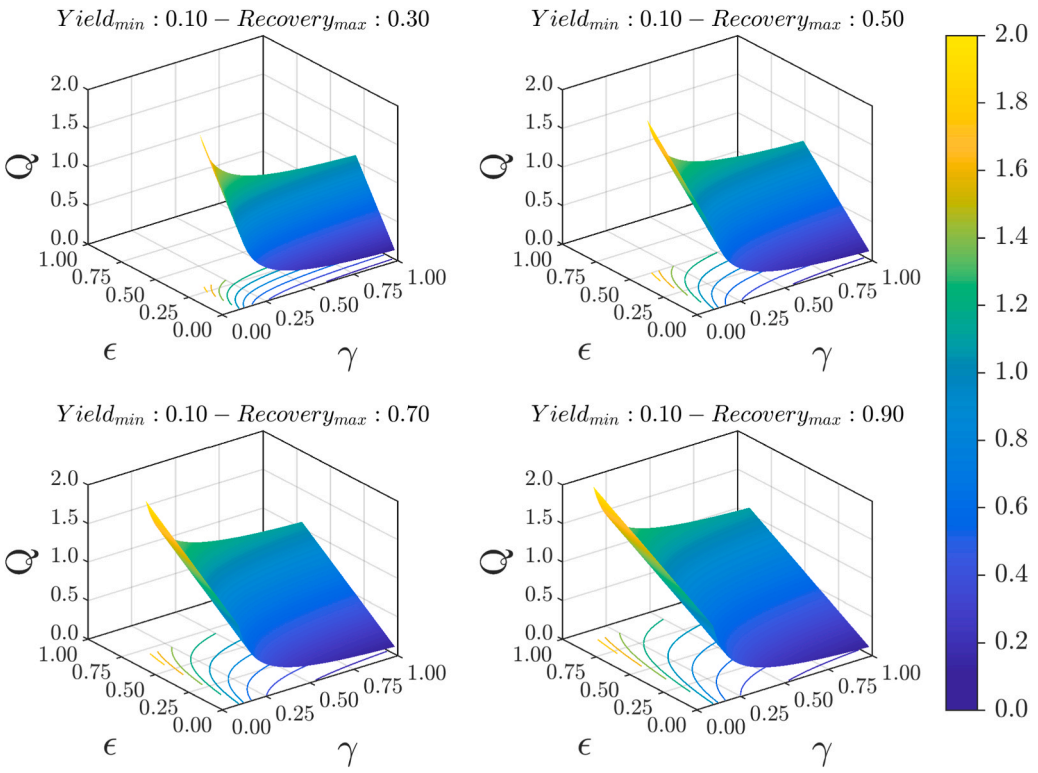

Fig. 5. Quality index function for different maximum recoveries.

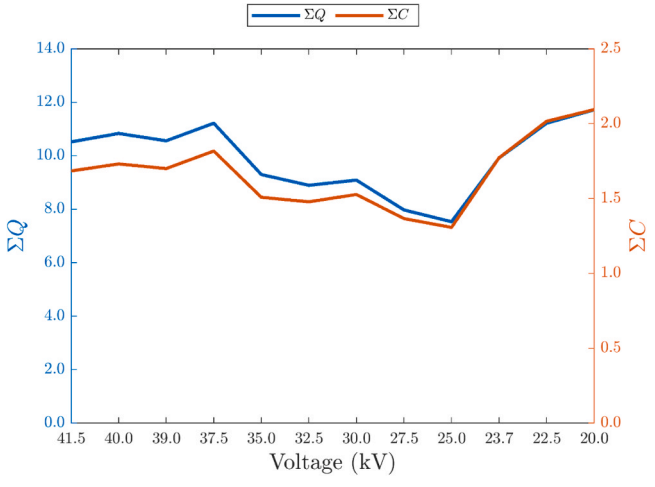

Fig. 6. AA (ΣQ) and PPAA-U (ΣC) quality index results before target-to-distance correction.

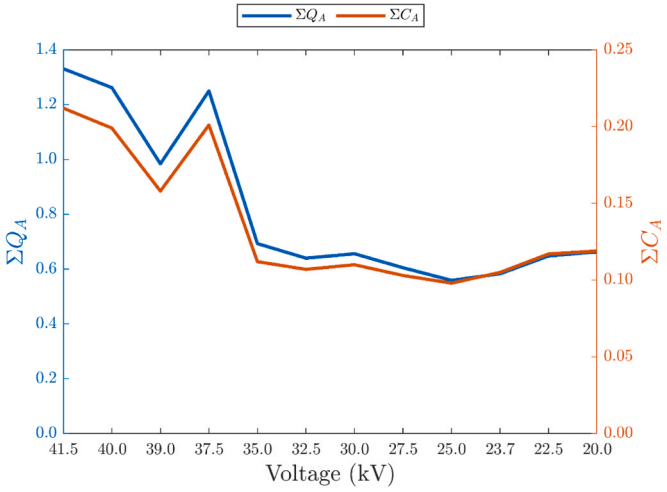

Fig. 7. Quality index as calculated via basic AA (ΣQ_A) and PPAA-U (ΣC_A) with target-to-distance correction.

conditions through a comparison of three variables: yield, recovery, and grade. However, this basic method suffers where there are large variations in the yields and recoveries of the components or elements separated.

Indeed, examination of the attributive analysis function reveals that it exhibits significant sensitivity to dispersion within both the yield dataset and the recovery dataset. However, the sensitivity to variations in yield is greatest, something that can be attributed to the fact that while the quality index is linearly related to recovery (with the slope being dependent on the maximum recovery value), it has an inverse relationship with yield and thus an inverse squared relationship to changes in yield. Penalized attributive analysis, PAA-U, directly addresses the issue of variations in yields and recoveries, most strongly penalizing contributions to the quality index from experimental set-ups for which the largest variations are recorded.

Target-to-distance correction improved the performance of both AA and PPAA-U. For the separation technique used in this work, without this correction, two maxima (one at higher and one at lower voltages) in the quality index were observed, making it difficult to distinguish the true optimum conditions. When the target-to-distance correction was introduced, however, the lower voltage maximum was removed. This shows that while lower voltages might provide effective separation on average, they are poor at removing particularly harmful PTEs; this more targeted separation is achieved only at higher voltages.

Future work should focus not only on the application of PPAA-U to evaluate the soil washing methods used in the remediation of metal (loid)-polluted soil but also as part of feasibility studies for

bioremediation or chemical oxidation technologies (where numerous organic contaminants, each with different target concentrations, are addressed simultaneously). Furthermore, this methodology can not only be applied to environmental remediation operations but could also be used to determine optimal operating conditions in a variety of materials processing or manufacturing contexts. In such contexts, the quality factor used in this method might involve variables such as temperature, pressure, or particle size and also the environmental and economic factors such as the costs associated with particular operating conditions, which might depend on energy use or manpower requirements.

Environmental implications

Two-parameter penalized attribute analysis for upgrading (PPAA-U) provides a way to optimize soil remediation operations and is, thus, a valuable tool to improve environmental outcomes. The method assesses how well a given set of operating conditions maximizes recovery while simultaneously minimizing the concentrate yield, and its primary advantage lies in the way it provides a single value, the quality index, to identify optimal separation conditions. Furthermore, PPAA-U could be adapted easily to various processes and thus has numerous potential applications in a range of industries; in particular, its capacity to address multiple variables opens new avenues for sustainable materials processing and manufacturing.

Declaration of Competing Interest

The authors declare that they have no known competing financial interests or personal relationships that could have appeared to influence the work reported in this paper.

Data availability

Data will be made available on request.

Acknowledgements

Carlos Sierra would like to thank the EURECA-PRO phase I 2020–2023 co-funded by the European Union's Erasmus + Programme (Ref.: 101004049). Diego Baragaño wants to acknowledge MCIU/AEI/CSIC for his JdC contract under the grant JDC2022-050209-I funded by MCIU/AEI/10.13039/501100011033 and by European Union NextGenerationEU/PRTR.

Appendix A. Supporting information

Supplementary data associated with this article can be found in the online version at doi:10.1016/j.jhazmat.2024.133529.

References

[1] Wu, Q., Leung, J.Y.S., Geng, X., Chen, S., Huang, X., Li, H., et al., 2015. Heavy metal contamination of soil and water in the vicinity of an abandoned e-waste recycling site: Implications ofr dissemination of heavy metals. Science of the Total Environment 506-507, 217–225. https://doi.org/10.1016/j.scitotenv.2014.10.121.

[2] Sun, L, Guo, D., Liu, K., Meng, H., Zheng, Y., Yuan, F., et al., 2019. Levels, sources, and spatial distribution of heavy metals in soils from a typical coal industrial city of Tangshan, China. Catena 175, 101–109. https://doi.org/10.1016/j.catena.2018.12.014.

[3] Ashraf, S., Ali, Q., Zahir, Z.A., Ashraf, S., Asghar, H.N., 2019. Phytoremediation: Environmentally sustainable way for reclamation of heavy metal polluted soils. Ecotoxicology and Environmental Safety 174, 714–727. https://doi.org/10.1016/j.ecoenv.2019.02.068.

[4] Khalid, S., Shahid, M., Niazi, N.K., Murtaza, B., Bibi, I., Dumat, C., 2017. A comparison of technologies for remediation of heavy metal contaminated soils. Journal of Geochemical Exploration 182, 247–268. https://doi.org/10.1016/j.gexplo.2016.11.021.

[5] Aparicio, J.D., Raimondo, E.E., Saez, J.M., Costa-Gutierrez, S.B., Álvarez, A., Benimeli, C.S., et al., 2022. The current approach to soil remediation: a review of physicochemical and biological technologies, and the potential of their strategic combination. J Environ Chem Eng 10 (2). https://doi.org/10.1016/J.JECE.2022.107141.

[6] Baragaño, D., Berrezueta, E., Komárek, M., Menéndez-Aguado, J.M., 2023. Magnetic separation for arsenic and metal recovery from polluted sediments within a circular economy. J Env Manag 339, 117884. https://doi.org/10.1016/j.jenvman.2023.117884.

[7] Wan, X., Lei, M., Chen, T., 2020. Review on remediation technologies for arsenic-contaminated soil. Front Environ Sci Eng 14 (2), 1–14. https://doi.org/10.1007/S11783-019-1203-7/METRICS.

[8] Baragaño, D., Gallego, J.R., Menéndez-Aguado, J., Marina, M.A., Sierra, C., 2021. As sorption onto Fe-based nanoparticles and recovery from soils by means of wet high intensity magnetic separation. Chem Eng J 408, 127325. https://doi.org/10.1016/J.CEJ.2020.127325.

[9] Gu, F., Zhang, J., Shen, Z., Li, Y., Ji, R., Li, W., et al., 2022. A review for recent advances on soil washing remediation technologies. Bull Environ Contam Toxicol 109 (4), 651–658. https://doi.org/10.1007/S00128-022-03584-6/METRICS.

[10] Liu, J., Zhao, L., Liu, Q., Li, J., Qiao, Z., Sun, P., et al., 2022. A critical review on soil washing during soil remediation for heavy metals and organic pollutants. Int J Environ Sci Technol 19 (1), 601–624. https://doi.org/10.1007/S13762-021-03144-1/METRICS.

[11] Sierra, C., Martínez-Blanco, D., Blanco, J.A., Gallego, J.R., 2014. Optimisation of magnetic separation: a case study for soil washing at a heavy metals polluted site. Chemosphere 107, 290–296. https://doi.org/10.1016/J.CHEMOSPHERE.2013.12.063.

[12] Tran, H.T., Lin, C., Hoang, H.G., Bui, X.T., Le, V.G., Vu, C.T., 2022. Soil washing for the remediation of dioxin-contaminated soil: a review. J Hazard Mater 421. https://doi.org/10.1016/J.JHAZMAT.2021.126767.

[13] Bunge, R., Bachmann, A., Ngo, C.D.1995. Soil-washing: Mineral processing technology in environmental engineering.

[14] Nishiyama, T., Tomoguchi, M., Sasamoto, N.,2000. Soil washing using mineral processing plant in Hanaoka Mine, Dowa Mining Co., Ltd. Second International Conference on Processing Materials for Properties, pp. 601–624. ⟨https://www.researchgate.net/publication/290268173_Soil_washing_using_mineral_processing_plant_in_Hanaoka_Mine_Dowa_Mining_Co_Ltd⟩.

[15] Richardson, W.S., Phillips, C.R., Luttrell, J., Hicks, R., Cox, C., 1999. Application of remedy studies to the development of a soil washing pilot plant that uses mineral processing technology: a practical experience. J Hazard Mater 66 (1–2), 47–65. https://doi.org/10.1016/S0304-3894(98)00211-8.

[16] Schulz, N.F.,1970. "Separation Efficiency." Trans. SME/AIME, 247, pp. 81–87. ⟨https://cir.nii.ac.jp/crid/1570572701370836096⟩.

[17] Gupta, A., Yan, D.2016. Mineral Processing Design and Operations: An Introduction: Second Edition. Mineral Processing Design and Operations: An Introduction: Second Edition, pp. 1–850.

[18] Weiss, N.L.,1985. Metallurgical Accounting and Mill Reports. In SME mineral processing handbook. Society of Mining Engineers of the American Institute of Mining, Metallurgical, and Petroleum Engineers.

[19] Wills, B.A., Finch, J.A., 2015. Wills' mineral processing technology: an introduction to the practical aspects of ore treatment and mineral recovery. Wills' Miner Process Technol. Introd Pract Asp Ore Treat Miner Recovery 1–498.

[20] Drzymala, J., 2006. Atlas of upgrading curves used in separation and mineral science and technology. Physicochem Probl Miner Process 40.

[21] Taggart. A.F.,1947. Handbook of Mineral Dressing. John Wiley & Sons. ⟨https://www.abebooks.com/first-edition/Handbook-Mineral-Dressing-Ores-Industrial-Minerals/4800302279/bd⟩.

[22] Cortada, U., Hidalgo, C., Martínez, J.M., Rey, J., 2018. Impact in soils caused by metal(loid)s in lead metallurgy. the case of La Cruz Smelter (Southern Spain). J Geochem Explor 190 (5a). https://doi.org/10.1016/j.gexplo.2018.04.001.

[23] Rosendo, R., Rey, J., Martínez, J.M., Hidalgo, C., 2022. Geological and mining heritage as a driver of development: the NE sector of the Linares-La Carolina district (Southeastern Spain). Geosciences 12 (2), 76. https://doi.org/10.3390/geosciences12020076.

[24] American Society for Testing and Materials, 1963. ASTM D422–63: Standard Test Method for Particle-Size Analysis of Soils (Reapproved 2007). ASTM International.

[25] Boente, C., Sierra, C., Rodríguez-Valdés, Menéndez-Aguado, J.M., Gallego, J.R., 2017. Soil washing optimization by means of attributive analysis: case study for the removal of potentially toxic elements from soil contaminated with pyrite ash. J Clean Prod 142, 2693–2699. https://doi.org/10.1016/j.jclepro.2016.11.007.

Chemosphere 358 (2024) 142135

Contents lists available at ScienceDirect

Chemosphere

journal homepage: www.elsevier.com/locate/chemosphere

A novel algorithm for optimizing hydrocyclone operations in the decontamination of potentially toxic elements in soils

X. Corres [a], N. Gómez [b], C. Boente [c,*], J.R. Gallego [a], C. Sierra [b,d]

[a] INDUROT and Environmental Biogeochemistry & Raw Materials Group, Campus de Mieres, Universidad de Oviedo, Mieres, Asturias, Spain
[b] Department of Mining, Topography and Structure Technology, Universidad de León, Campus de Vegazana, 24006, León, Spain
[c] Laboratorio de Estratigrafía Biomolecular, ETSI Minas y Energía, Universidad Politécnica de Madrid, 28003 Madrid, Spain
[d] European University on Responsible Consumption and Production, Campus de Vegazana, 24006, León, Spain

HIGHLIGHTS

- A novel method for optimizing yield parameters in soil washing is presented.
- The algorithm holds potential for determining optimal operating conditions.
- Grade, recovery and concentrate yield were the parameters to optimize.
- The key to the method is maximizing grade and recovery while minimizing yield.

GRAPHICAL ABSTRACT

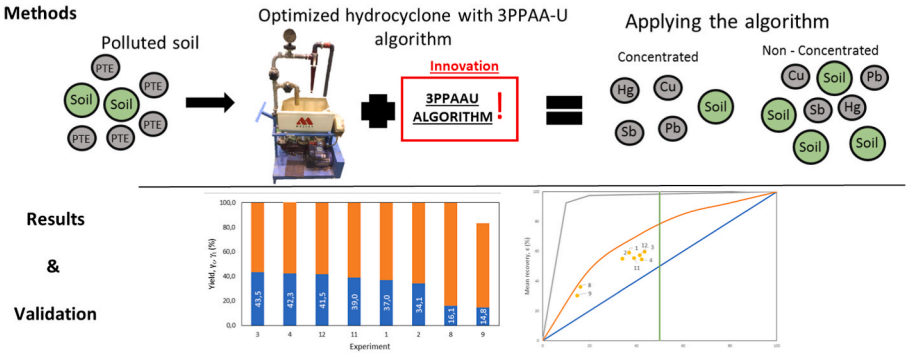

ARTICLE INFO

Handling Editor: Lena Q. Ma

Keywords:
Metallurgical accounting
Process efficiency
Process design
Control of experiments

ABSTRACT

We present the Three-Parameter Penalized Attributive Analysis for Upgrading (3PPAA-U) method as a tool for selecting the Best Upgrading Condition (BUC) in process engineering. Conventional approaches tend to consider only maximizing recovery (ε) and minimizing yield (γc); in contrast, the proposed 3PPAA-U introduces and seeks to maximize a third parameter, the grade (λ). This multi-parameter approach has not yet been explored in existing literature. In addition to controlling multiple parameters, the method is also superior to others as it includes inverse standard deviation weighting to avoid the distortion of results due to data dispersion. This reduces the possibility of drawing conclusions based on extreme values. Furthermore, the method can be used with a target-to-distance correction to optimize separation for multi-component feeds. To illustrate our method, we present a practical application of 3PPAA-U. Soil contaminated with potentially toxic elements (PTEs) was subject to hydrocycloning under 12 different experimental conditions. Results of these 12 experiments were compared using 3PPAA-U and conventional methods to identify the best upgrading conditions (BUC). Analysis reveals that the 3PPAA-U approach offers a simple and effective criterion for selecting BUC. Furthermore, 3PPAA-U has uses beyond soil remediation. It offers a versatile tool for optimizing operations across various

* Corresponding author.
E-mail address: c.boente@upm.es (C. Boente).

https://doi.org/10.1016/j.chemosphere.2024.142135
Received 3 January 2024; Received in revised form 13 April 2024; Accepted 22 April 2024
Available online 24 April 2024

processing and manufacturing environments offering a way to manage factors such as concentration, temperature, pressure, pH, Eh, grain size, and even broader environmental and economic considerations.

1. Introduction

1.1. Soil washing: key concepts

Soil pollution includes numerous potentially toxic elements (PTEs) such as lead, cadmium, arsenic, and mercury, as well as polycyclic aromatic hydrocarbons (PAHs) (c.f., Sun et al., 2019; Wu et al., 2015). PTEs not only affect soil fertility but also pose a risk to human health. For example, ingesting or inhaling contaminated soil particles can lead to serious health issues including cancer, respiratory problems, and neurological disorders (Rieuwerts et al., 2014). Furthermore, PTEs are known to leach into watercourses and this can cause even more widespread environmental degradation and risks to public health (Khalid et al., 2017).

Therefore, it is crucial to address the issue of contaminated soil through effective remediation strategies, for instance, phytoremediation (Ashraf et al., 2019; Chen et al., 2016), microbial remediation (Chen et al., 2023), electrokinetic remediation (Wang et al., 2021), and soil washing (Guo et al., 2022; Khum-in et al., 2023; Lee and Kim, 2010; Pinto et al., 2014)These strategies can help to reduce the levels of PTEs and other pollutants, restoring the soil and preventing further damage to the environment and human health.

Soil washing is a highly efficient and rapid technique (Khum-in et al., 2023) for the removal of PTEs and organic compounds from soil (Guo et al., 2022). Additionally, this technique represents one of the few methods able to provide a permanent solution for soil contamination, particularly in cases where levels of pollutants are significant (Lee and Kim, 2010; Pinto et al., 2014).

There are two types of soil washing, namely physical and chemical. The latter involves mixing the soil with an extraction solution to chemically dissolve or mobilize the contaminants. Physical soil washing, on the other hand, separates and extracts pollutants by exploiting the differences in physical properties, for example, size, density, magnetic properties, and hydrophobicity, that exist between soil particles and pollutant-bearing particles (Dermont et al., 2008). The strategies involved in physical soil washing are based on well-established methods employed in the mining industry for the extraction of elements from mineral ores (Ye et al., 2022; Sierra et al., 2013). However, these techniques can be expensive and time-consuming, thus there is a need for reducing costs and improving the efficiency of these remediation methods.

1.2. Determining best upgrading conditions (BUC)

Assessing the performance of an upgrading process requires the definition of several parameters. Firstly, if the material subject to the upgrading process has a feed mass flow rate, F, then the products of the upgrading process are the concentrate and the tailings with, respectively, mass flow rates, C, and F. In some cases, there may be intermediate outputs, known as middlings, which will have a mass flow rate, M. These flow rates are related thus:

$$F = C + M + T \tag{1a}$$

Dividing Eq. (1a) by F, we get the yield (γ) for each fraction, that is, the mass percentage of the feed (F) reporting to each fraction: γ_c, the concentrate yield; γ_m, the midlings yield; and γ_t, the tailings yield; $\gamma_F = 1$, the feed yield (Eq. (1b)):

$$\gamma_F = \gamma_c + \gamma_m + \gamma_t \tag{1b}$$

The grade of a fraction is defined as the concentration of a given element or compound in that fraction, and it is denoted as α for the feed and λ for the concentrate.

Finally, the percentage of useful (or desired) content that reports to a specific fraction relative to the feed is known as the recovery, ε, and this is used to assess the quality of the upgrading process. Of most relevance here is the concentrate fraction and, for the concentrate mass stream, the recovery for this fraction is expressed as (Eq. (2)):

$$\varepsilon = \frac{\lambda}{\alpha}\gamma_c \tag{2}$$

In physical soil washing scenarios, the pollutants to be removed are held in the concentrate fraction while the tailings comprise the partially decontaminated soil. Thus, to optimize soil decontamination, the goal is to minimize γ_c and maximize λ.

Traditionally, to find optimal operating conditions, pairs of the parameters γ_c, λ and ε can be plotted on separation curves (e.g., Drzymała, 2006). However, such methods are naturally limited to a consideration of only two components at a time and this can be misleading. For example, an apparently optimal experiment with a high value of ε and low γ_c might simply contain very little material that would report to the concentrate, thus it is necessary to consider λ too. Similarly, an experiment might provide a high value of ε might also give a high λ, however we cannot tell if this is truly an optimal set up without looking at γ_c since a high λ might simply be a consequence of a low γ_c.

Furthermore, most traditional methods are only able to consider single component separations and many soil washing operations involve soils with multiple contaminants. By including λ, in its calculations, 3PPAA-U enables optimization for multicomponent separations and allows the identification of operating conditions that will preferentially address the most dangerous pollutants.

1.3. Aim and specific objectives

Following from the previous discussion, the aim of this research, is to develop an effective method to select the optimal conditions for soil upgrading operations. In this way we will:

a) introduce the 3PPAA-U method
b) apply the method to a real-life soil washing operation using a hydrocyclone to decontaminate soil from an ex-industrial site in Asturias, Spain.

We will then compare the results of traditional separation-curve optimization to 3PPAA-U with and without target-to-distance correctionand discuss the implications of this new method.

2. Materials and methods: a real-life soil washing operation

2.1. Soil sampling and chemical analysis

The soil sample used in this study was collected from a 35,000 m^2 brownfield location in Asturias (Northern Spain). Fig. 1 depicts the location of the brownfield and the sampling area. More information about the site and its environment can be found in Boente et al. (2020). Superficial soil samples were collected from various points across the study site to obtain a bulk sample of 50 kg. Rocks, gravel, and other large debris were removed in situ by passing the soil through a 2 cm mesh. The sample was then dried at ambient temperature before being passed through a 4 mm mesh. Finally, the soil sample was sieved using standardized Restch separating screens, and two major fractions were recovered (0 μm − 125 μm and 125 μm − 4000 μm).

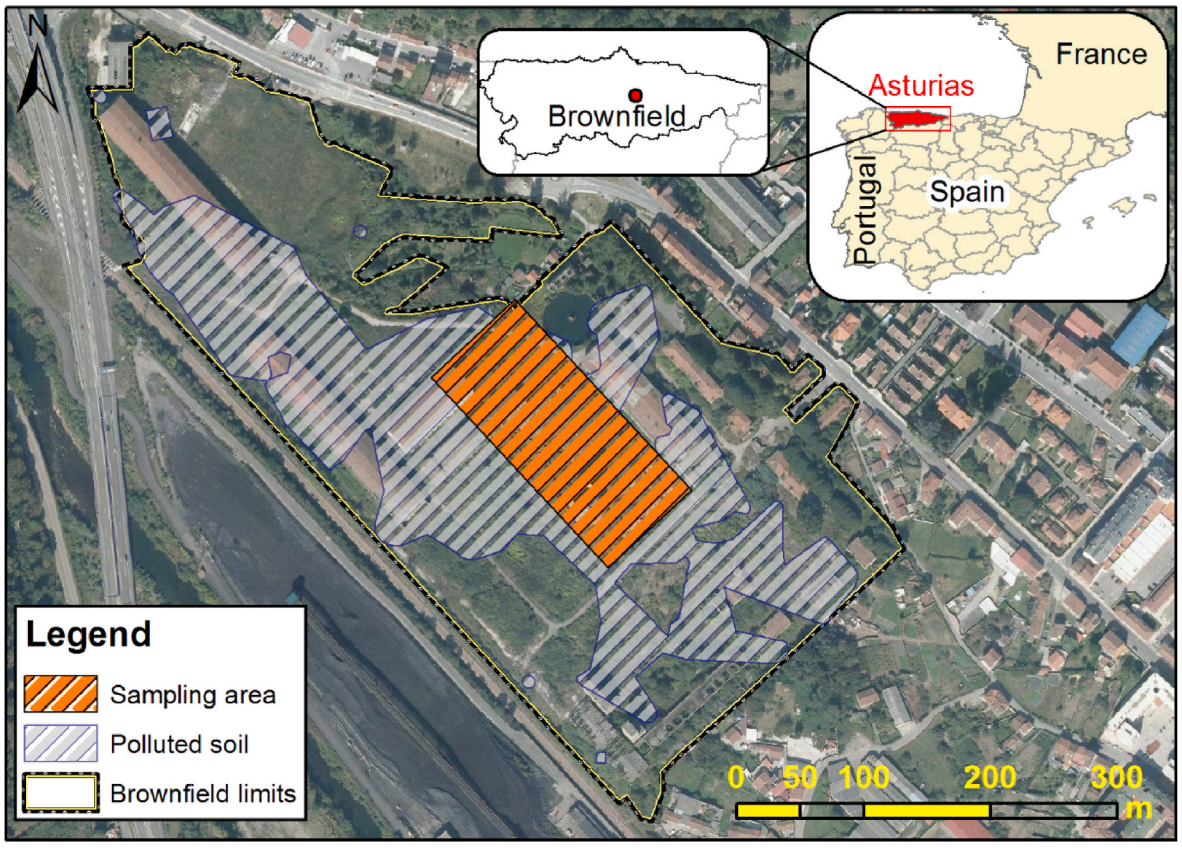

Fig. 1. Brownfield location and sampling location in Asturias, Spain (Latitude: 43.2964; Longitude: 5.68254).

Of the two major fractions recovered, the finer (grain size <125 μm) had the highest PTE content. Thus, this fraction was divided into 12 subsamples for separation. Representative 1g subsamples from each subsample were subjected to chemical analysis: first they were leached using an "Aqua regia" solution (HCl + HNO_3) and the digested samples were analysed by ICP-MS instrument (model HP 7700 from Agilent Technologies)for major and trace element content.

2.2. Separation experiments

Separation tests were completed in a lab-scale plant (C700 Mozley) capable of running hydrocyclones from 10 mm to 50 mm in diameter. The hydrocyclone uses gravity to separate aqueous suspensions of particles (slurries) into fractions based on particle density (Karim et al., 2021). It comprises a conical chamber with two outlets, one at the top and one at the bottom, and is fed tangentially with high pressure slurry. When the slurry enters the hydrocyclone chamber, it experiences a centrifugal force which pushes denser fractions outwards and downwards towards the lower outlet (underflow) while lower-density fractions exit via the upper outlet (overflow). The hydrocyclone used in this experiment offers four operating configurations: conic with apex diameters of 9.5 mm, 6.4 mm, and 3 mm; or flat bottom (FB). Samples were tested in each of the available configurations at pressures of 100 kPa, 200 kPa, and 300 kPa, thus there were twelve experimental runs in total. The solid concentration of the feed slurry was maintained at a constant 20% by weight.

For each experimental run, once a steady state was attained, samples from both the hydrocyclone underflow and overflow were collected in borosilicate flasks. Samples (from the overflow and underflow) were subjected to low temperature drying (45 °C) in an oven to minimize the potential loss of Hg and As due to volatilization. The dry weights of these samples were then measured before representative sub-samples were taken for ICP-MS analysis (model HP 7700 from Agilent Technologies).

2.3. Attributive analysis

2.3.1. Selection of the concentrate, tailings, and middlings fractions in multicomponent separations

A major consideration in designing an algorithm to find the BUC is the fact that soil washing operations generally deal with multicomponent contamination. Thus, the first issue to address is which fraction should be considered the concentrate (to be removed for further processing) and which the tailings (to be isolated and returned to original site) as this may vary for each PTE. For our purposes, the concentrate fraction (CF) is taken as that for which $\varepsilon > \gamma_c$ (c.f., Fuerstenau and Han, 2003) for more than half of the PTEs under consideration. Those experiments in which $\gamma_c >$ 50% were not included in our analysis, as soil washing is not interested in scenarios where the concentrated fraction is larger than the tailings fraction.

2.3.2. Basic attributive analysis

Basic Attributive Analysis (BAA) was developed as a means of optimizing soil washing by Sierra et al. (2010) and applied first in the context of remediating soils contaminated with Pyrite ash (Sierra et al., 2010; Boente et al., 2017).

In the case where a set of *m* soil-washing experiments have been carried out under a range of experimental conditions, BAA aims to identify which conditions maximize the recovery of a number, *n*, of target elements while minimizing the yield. The performance of a given experiment, *i*, for target element, *j*, is then expressed as a quality factor Q_j^i calculated as (Eq. (3)):

$$Q_j^i = \frac{Min\{\gamma\}}{\gamma^i} + \frac{\varepsilon_j^i}{Max\{\varepsilon_j\}} \tag{3}$$

Table 1
Operating conditions for the twelve experimental runs.

Run	Apex	Pressure
	mm	kPa
1	9.5	100
2		200
3		300
4	6.4	100
5		200
6		300
7	3	100
8		200
9		300
10	FB	100
11		200
12		300

Where:

- $i = 1, \ldots, m$ and identifies a specific experiment with a particular set of separation parameters.
- $j = 1, \ldots, n$ and refers to results for a specific target element or contaminant and in this study, m = 10 (see Table 1 for all target elements considered).
- Q_j^i = Efficiency factor of experiment i for element j.
- γ^i = Yield of experiment i.
- ε_j^i = Recovery of element j for experiment i.

As discussed in 2.3.1, there are generally numerous PTEs to consider and, due to their differing toxicity levels, each will have a safe threshold concentration (the *target grade*) after soil washing. This consideration can be included in the quality factor for each experiment as a weighting coefficient. For each PTE, this coefficient is the ratio of the PTE's grade after soil washing and its target grade; it is known as the target-to-distance correction and for an element j separated in experiment i it is defined as (*Eq.* 4):

$$A_j^i = \frac{\alpha_j^i}{\propto_j^{target}} \tag{4}$$

Where:

- i and j are defined as before.
- α_j^i = Feed grade of element j in experiment i.
- $\propto_j^{target}$ = Target grade for element j

The sum of these coefficients for all $j = 1, \ldots, n$ elements must add up to 1.

To obtain the correct weighting for each element's contribution to overall contamination levels, the following transformation is implemented (Eq. (5)):

$$A_j^{i'} = \frac{A_j^i}{\sum_i^m A_j^i} \tag{5}$$

This allows us to define a global quality index for a given experiment, i, for all elements under consideration (Eq. (6)):

$$Q_T^i = \sum\nolimits_{j=1}^{n} Q_j^i A_j^{i'} \tag{6}$$

The experiment with optimal separation conditions is that for which this value is maximal (Eq. (7)):

$$Q_{optimal} = Max\left\{\sum\nolimits_{j=1}^{n} Q_j^i A_j^{i'}\right\} \tag{7}$$

2.3.3. Three-Parameter Penalized Attributive Analysis (3PPAA)

Here we present the Three-Parameter Penalized Attributive Analysis (3PPAA) as a tool to find the BUC. This method builds on the BAA model and is an extension of a previous, two parameter (yield and recovery) version, Penalized Attributive Analysis (PAA) which was described in Corres et al. (2024).

The three parameters in question are: $\Gamma^{i'}$, $\mathrm{E}_j^{i'}$, and $\Lambda_j^{i'}$, respectively, the normalised weighted values of the yield in experiment i, and the normalised weighted values of recovery, and grade concentration in experiment i for element j. The weighting of parameters in this way reduces the influence of noisier experiments in the final analysis of experimental quality.

Our aim is to minimize yield while maximizing the recovery of a range of PTEs and their grade concentrations. Recalling the relationship between γ_c, $\mathcal{E}$ and λ (Eq. (2)), then, as in PPA, the appropriate parameters for yield and recovery are defined as (Eqs. (8)–(11)):

$$\Gamma^i = \frac{Min\{\gamma_c\}}{\gamma^i}\left(\frac{\sum_{i=1}^{m}\left|\gamma_c^i - \overline{\gamma_c}\right|}{m}\right)^{-1} \tag{8}$$

$$\Gamma^{i'} = \frac{\Gamma^i}{\sum_i^m \Gamma^i} \tag{9}$$

$$\mathrm{E}_j^i = \frac{\varepsilon_j^i}{Max\{\varepsilon_j\}}\left(\frac{\sum_{i=1}^{m}\left|\varepsilon_j^i - \overline{\varepsilon}_j\right|}{n}\right)^{-1} \tag{10}$$

$$\mathrm{E}_j^{i'} = \frac{\mathrm{E}_j^i}{\sum_i^m \mathrm{E}_j^i} \tag{11}$$

The newly introduced grade parameter is similarly defined thus (Eqs. (12) and (13)):

$$\Lambda_j^i = \frac{\lambda_j^i}{Max\{\lambda_j\}}\left(\frac{\sum_{i=1}^{m}\left|\lambda_j^i - \overline{\lambda}_j\right|}{n}\right)^{-1} \tag{12}$$

$$\Lambda_j^{i'} = \frac{\Lambda_j^i}{\sum_i^m \Lambda_j^i} \tag{13}$$

The sum of these three parameters gives us C_j^i the quality index of experiment i for element j (Eq. (14)):

$$\mathrm{C}_j^i = \Gamma^{i'} + E_j^{i'} + \Lambda_j^{i'} \tag{14}$$

Where:

- i = experiment.
- m = number of experiments.
- j = specific PTE or another contaminant.
- n = number of elements.
- γ_c^i = yield of experiment "i"
- $\overline{\gamma_c}$ = mean yield
- ε_j^i = recovery of element "j" at experiment "i"
- $\overline{\varepsilon}_j$ = mean recovery for element "j"
- λ_j^i = concentrate grade of element "j" at experiment "i"
- $\overline{\lambda}_j$ = Mean concentrate grade of element "j"
- C_j^i = quality index of element "j" at experiment "i".

As in BAA, to account for the fact that different PTE's have different safe soil concentrations a target-to-distance correction can be used B_j^i (Eq. (15)):

$$B_j^i = \frac{\alpha_j^i}{\alpha_j^{tg}} \left(\frac{\sum_{i=1}^{m} \left| \alpha_j^i - \overline{\alpha}_j \right|}{n} \right)^{-1} \quad (15)$$

Where:

- B_j^i = Weighting factor for element j in experiment i
- α_j^{tg} = Target decontamination grade, i.e., the acceptable threshold grade after decontamination
- α_j^i = Grade of element j in experiment i
- $\overline{\alpha}_j$ = Grade of element j in experiment iHere, the ratio of the post separation grade, α_j^i, to the target grade, α_j^{tg} for the PTE of interest is weighted to minimize the final standard deviation of the result.

Normalizing this relative to its weight in the sum of m similar parameters B_j^i we obtain (Eq. (16)):

$$B_j^{i'} = \frac{B_j^i}{\sum_i^m B_j^i} \quad (16)$$

Although optional, this correction factor is immensely useful given the diverse nature of soils and their varying levels and types of contamination. As will be demonstrated in the case study, its use can make a significant difference to the choice of an optimal separation method. It enables the prioritisation of certain PTEs based on their initial concentration in the soil and their corresponding safe concentration as specified by regulatory standards (Boente et al., 2017).

Finally, we define the decontamination quality index (Q_T^i) for all PTEs for a given experiment as (Eq. (17)):

$$Q_T^i = \sum_{j=1}^{n} \mathbb{C}_j^i B_j^{i'} \quad (17)$$

The maximum value of Q_T^i corresponds to the BUC (Eq. (18)):

$$Q_{optimal} = Max\left\{ \sum_{j=1}^{n} \mathbb{C}_j^i B_j^{i'} \right\} \quad (18)$$

A worked example with this methodology is provided in SM1.

3. Results and discussion

3.1. Separation results

Soil from the study site was tested to find the feed concentration grades (α) of a nine PTEs (Cr, Ni, As, Cu, Zn, Pb, Sb, Cd, Mo) and the values obtained were compared against Dutch standards (e.g., Buchman and Office of Response, n.d.) (Table 2). These standards provide an intervention value (IV) and target value (TV) for a range of PTEs and were chosen as being among the most well-known and respected of available standards.

Table 2
Bulk sample mean α for the nine PTEs compared to their Dutch standard (e.g., Buchman and Office of Response, n.d.) intervention values (IV) and target values (TV). Elements are ordered by contamination level (CL) from the highest to the lowest.

PTE	Grade (α)	Intervention value (IV)	Target value (TV)	Contamination Level (CL)
	ppm	ppm	ppm	TV/α
Cr	**55.7**	0.35	220	159.03
Ni	**37.3**	0.26	100	143.38
As	**60.7**	0.9	55	67.45
Cu	**111.1**	3.4	96	32.67
Zn	**377.1**	16	350	23.57
Pb	**319.9**	55	530	5.82
Sb	**9.5**	3	15	3.16
Cd	1.3	0.8	12	1.67
Mo	4.1	3	190	1.37

As can be seen on Table 2, out of the 9 PTEs studied, 7 (As, Cr, Cu, Ni, Pb, Sb, Zn) exceeded their respective IVs, while As, Cu and Zn also exceeded their TVs. To compare the severity of contamination associated with the PTEs under investigation, the ratio of the soil concentration of a given PTE to its TV was calculated to give a contamination level (CL). The PTEs were ranked in order of CL with the highest value, 159.3 recorded for Cr and the lowest, 1.37, recorded for Mo. Beyond the quality factor calculated for different experimental set ups (see 3.2) this provides a further criterion for selecting the optimum conditions. Specifically, optimal separation conditions should not only produce a high overall quality factor but also target the most serious pollutants.

Separation of soil samples was conducted under the 12 different experimental conditions identified on Table 1, and, in each case, the experimental concentrate yield, (γ_c^i) was calculated as were the recoveries (ε_j^i) of all PTEs off interest. The results are shown in Fig. 2.

In the following analysis, we shall discuss only the separation results for those experiments complied with the constraint $\overline{\varepsilon^i} < \gamma_c^i$ (thus experiments 5, 6, 7, and 10 have been omitted). The full set of raw separation results is presented in SM2 (Tables 1 and 2).

Fig. 2 ranks experiments, from left to right, in descending order of mean recovery value for the nine PTEs studied ($\overline{\varepsilon^i}$). Experiments 8 and 9 have by far the lowest mean recovery values ($\overline{\varepsilon^8}$ = 36.2% and $\overline{\varepsilon^9}$ = 30.4%) while mean recovery values for the remaining experiments are similar, varying within a range from 54.6% (Experiment 4) to 59.8% (Experiment 3).

Referring to Fig. 3, the values for γ_c^i found in each experiment show a similar trend to that seen for $\overline{\varepsilon^i}$ (Fig. 2). Specifically, experiments 8 and 9 have the lowest values of γ_c^i (γ_c^8 = 16.1 and γ_c^9 = 14.8), while for the remaining experiments these values are not only significantly higher but also very similar: γ_c^i ranges from 34.1% (Experiment 2) to 43.5% (Experiment 3).

Based on these results it is unclear which experimental conditions would be optimal. Experiment 3 maximizes overall recovery but has the highest yield, while the experiments with the lowest yield (8 and 9) also have the lowest overall recoveries. Based on Cr recovery, six experiments record their highest recovery for this PTE, however, for all except Experiment 3, the recovery of Ni (the next most important contaminant in the sample, see Table 2) is their lowest recovery value.

To further assess the efficiency of our separation experiments, we can plot the mean PTE recovery value for each experiment ($\overline{\varepsilon^i}$) against the experimental concentrate fraction yield (γ_c^i) and compare our results to the theoretical perfect, typical and non-separation curves (PSC, TSC and NSC: see for e.g., Richardson and Morrison, 2003). Experiments for which separation has been most successful should approach the PSC while less successful separation experiments will be closer to the NSC.

Referring to Fig. 4, the points representing Experiments 8 and 9 lie closest to the TSC. This suggests that these two experiments might provide the best upgrading conditions.

3.2. Three-parameter attributive analysis for optimizing soil upgrading

While comparing experimental results to theoretical separation curves is adequate in many scenarios, that this method uses mean recovery values across all contaminants is a severe limitation since some PTEs are significantly more harmful than others. By its incorporation of a target-to-distance correction, B_j^i, 3PPAA-U offers a superior approach in this respect because it is able to consider recovery values for individual elements and therefore enables optimization of soil upgrading for specific PTEs.

In the following we compare 3PPAA-U with and without target-to-distance correction in order to highlight its importance. Without this correction, the 3PPAA-U quality index ($Q_{optimal}$) offers information on

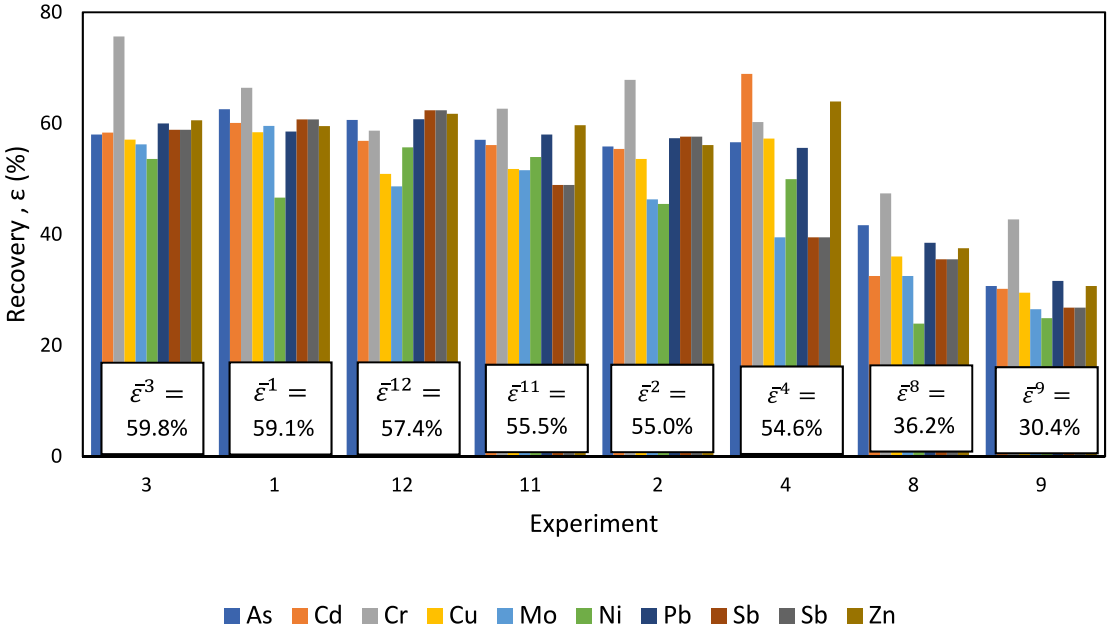

Fig. 2. Recovery values for each experiment and PTE in the concentrated fraction (ε_j^i). Results are in descending order of mean recovery, $\overline{\varepsilon^i}$, (left to right). Only experiments in which $\overline{\varepsilon^i} < \gamma_c^i$ are shown.

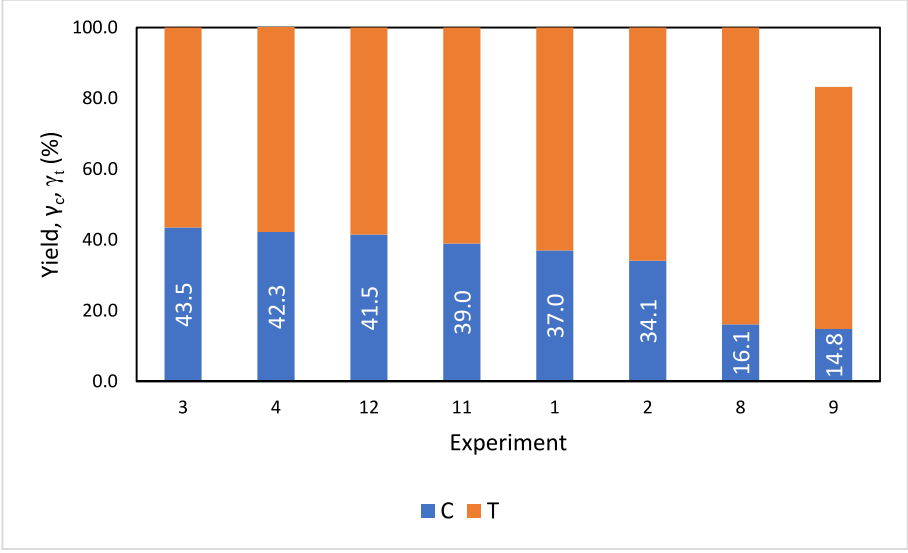

Fig. 3. Yield for the concentrated (γ^i_c) and tailings (γ^i_t) fractions. Results are ordered by descending value of γ_c^i. Only experiments in which $\overline{\varepsilon^i} < \gamma_c^i$ are shown.

which experimental parameters lead to the overall most efficient soil upgrading process, that is, it ranks experiments according to their average performance with respect to all PTEs considered without addressing the relative toxicity of different elements. With target-to-distance correction, 3PPAA-U can help adapt and optimize a soil washing process to the precise contamination properties of a given soil.

Table 3 shows the quality indices for all of the experiments calculated using 3PPAA-U without target-to-distance correction. The best performing experiments still appear to be Experiments 8 and 9 with quality indices 0.6 and 0.7 units greater than the third best performer (Experiment 2) (Table 3).

However, as previous results show (see Figs. 1 and 2), these two experiments have not only the lowest values of γ_c^i (both are nearly half the value found for Experiment 2 which has the next lowest γ_c^i) but also the lowest values of $\overline{\varepsilon^i}$ ($\overline{\varepsilon^8}$ = 36.2% and $\overline{\varepsilon^9}$ = 30.4% corresponding to, respectively, nearly half and two thirds that the next lowest mean recovery, $\overline{\varepsilon^4}$ = 54.6%). That 3PPAA-U points to these experiments as potentially giving the BUC suggests that optimal conditions are favoured more by minimizing γ_c^i than maximizing $\overline{\varepsilon^i}$. This becomes clear if we consider that both these values are higher for Experiment 8 than for Experiment 9 but the difference is greatest for $\overline{\varepsilon^i}$ (for γ_c^i is 1.33% higher and $\overline{\varepsilon^i}$ is 5.76% higher); thus, since Experiment 9 has the higher quality index, it would seem that more is gained by a marginal minimisation of γ_c^i compared to a far larger gain in $\overline{\varepsilon^i}$.

Referring back to Fig. 4, it can be seen that compared to the points representing all other experiments, those representing Experiments 8 and 9 were closest to the TSC. Thus, 3PPAA-U without target-to-distance

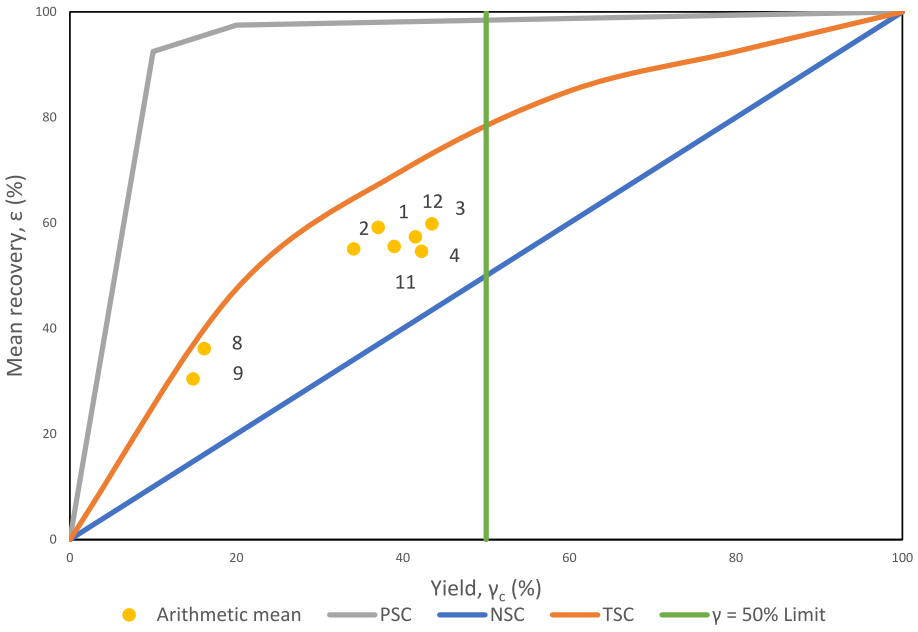

Fig. 4. Mean recovery and concentrate yield for each experiment ($\overline{\varepsilon^i} < \gamma_c^i$) plotted for comparison to curves for perfect separation (PSC), non-separation (NSC), and typical separation (TSC).

Table 3
3PPAA-U before the target-to-distance-to target correction for experiments where $\overline{\varepsilon^i} < \gamma_c^i$.

Experiment	$\mathcal{C}_j^i$									$\sum_{j=1}^{n}\mathcal{C}_j^i$
	As	Cd	Cr	Cu	Mo	Ni	Pb	Sb	Zn	
1	0.3974	0.3692	0.3772	0.3796	0.3958	0.3462	0.3939	0.4292	0.3648	3.4533
2	0.3961	0.3719	0.4022	0.3869	0.3674	0.3616	0.4032	0.4295	0.3813	3.5003
3	0.3384	0.3339	0.4002	0.3506	0.3724	0.3646	0.3454	0.3425	0.3458	3.1937
4	0.3262	0.4407	0.3084	0.3444	0.2744	0.3593	0.3172	0.2528	0.3770	3.0004
8	0.4768	0.4384	0.4989	0.4526	0.4447	0.4137	0.4737	0.4799	0.4460	4.1247
9	0.4795	0.4584	0.4798	0.4650	0.4479	0.4362	0.4861	0.4944	0.4571	4.2044
11	0.2914	0.2928	0.2791	0.3102	0.3690	0.3570	0.2864	0.2672	0.3110	2.7640
12	0.2942	0.2947	0.2542	0.3107	0.3283	0.3615	0.2941	0.3045	0.3170	2.7592

Table 4
3PPAA-U after the distance to target correction for experiments where $\overline{\varepsilon^i} < \gamma_c^i$.

Experiment	$\mathcal{C}_j^i \boldsymbol{B}_j^{i'}$									$\sum_{j=1}^{n}\mathcal{C}_j^i \boldsymbol{B}_j^{i'}$
	As	Cd	Cr	Cu	Mo	Ni	Pb	Sb	Zn	
1	0.0612	0.0486	0.0598	0.0508	0.0467	0.0440	0.0668	0.0742	0.0496	0.5017
2	0.0654	0.0510	0.0630	0.0563	0.0514	0.0471	0.0658	0.0721	0.0570	0.5290
3	0.0514	0.0462	0.0735	0.0516	0.0547	0.0525	0.0511	0.0444	0.0513	0.4768
4	0.0446	0.0853	0.0425	0.0455	0.0334	0.0549	0.0411	0.0292	0.0602	0.4368
8	0.0496	0.0506	0.0608	0.0447	0.0419	0.0475	0.0545	0.0589	0.0448	0.4533
9	0.0656	0.0542	0.0500	0.0547	0.0475	0.0442	0.0659	0.0811	0.0541	0.5173
11	0.0220	0.0227	0.0199	0.0319	0.0529	0.0394	0.0186	0.0172	0.0276	0.2524
12	0.0223	0.0260	0.0167	0.0379	0.0426	0.0431	0.0217	0.0191	0.0314	0.2608

correction suggests similar BUCs to those derived from conventional separation curve methods.

Table 4 shows the quality indices of each experiment calculated with target-to-distance correction. In this way, the quality index now includes a consideration of the grade concentrations for individual PTEs of interest for each experimental set up studied. Referring to Table 4, while Experiment 9 still comes out as one of the best methods, Experiment 2, ranked third before target-to-distance correction, now appears to be optimal with Experiments 1 and 3 also performing well.

Fig. 5 shows a plot of quality indices for each of our experimental set ups to highlight the differences between which separation conditions would seem optimal without (curve A) and with (curve B) target-to-distance correction.

As can be seen in the tables included in SM2, while recovery and yield vary relatively little between experiments (the standard deviation is between 10.02 and 12.73 for both these values), the grades found for different PTEs varies greatly in each experiment (the standard deviation in λ for some elements [for instance Cd] is as low as 0.67 while for others [such as Pb] it is as high as 181). In this way, it is no surprise that the calculation with target-to-distance correction produces very different results compared to previous methods.

Our results show 3PPAA-U provides a good general method for the

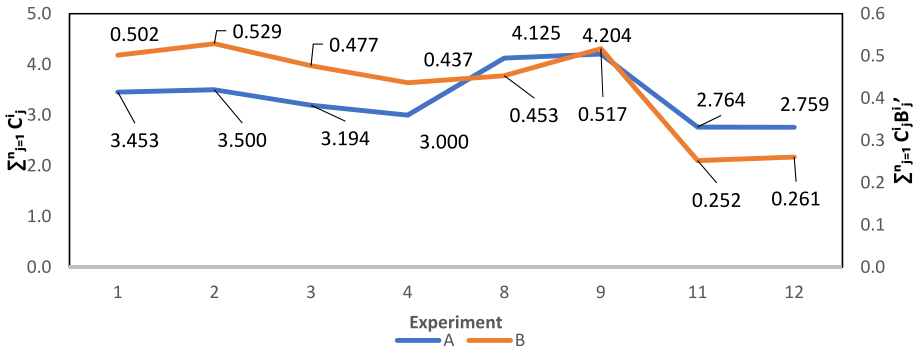

Fig. 5. Results of 3PPAA-U without (A) and with (B) target-to-distance correction for experiments with $\overline{\varepsilon^i} < \gamma_c^i$

identification of promising experimental configurations for soil upgrading operations. However, it is only a guide, and to select the BUCs for a particular soil, it is recommended that the top 2 or 3 configurations identified by 3PPAA-U be examined more closely to fine tune values of γ_c and ε. This is particularly important where, as in the current set of experiments, the analysis shows two configurations (Experiments 2 and 9) to have very similar efficiencies.

The 3PPAA methodology extends beyond identifying BUCs for soil washing, offering potential to identify optimal operating conditions across a broad spectrum of materials processing and manufacturing scenarios. The methodology could be extended to include a range of variables— from temperature and pressure to particle size, alongside environmental and economic considerations, such as energy consumption or CO_2 generation—to address a number of complex operational challenges simultaneously.

4. Conclusions

Three Parameter Attribute Analysis for soil upgrading is a method that allows the identification of and prioritizing of operational outcomes; thus, it can enable the fine tuning of operations to the specific problems of a given site.

A particular strength of 3PPAA-U for soil upgrading lies in how it deals with multicomponent feeds to derive the BUC. Firstly, the method has a clear criterion for establishing which fraction constitutes the concentrate and which the tailings so avoiding the issue that in some experiments, pollutants might report to different fractions. In addition, its target-to-distance correction selects the optimal upgrading conditions based on preferential contribution of the most harmful pollutants. The method is also robust to extremes of variation in parameters due to the way in which these are weighted.

3PPAA-U assess separation experiments based on three parameters, the grade (λ) and recovery (ε) of pollutants to be targeted and the concentrate yield (γ_c). The method ranks different experimental configurations dependent upon how well they maximize the grade and recovery while minimizing yield and appears to prioritize the minimisation of yield over maximizing recovery. Without target-to-distance correction, 3PPAA-U is at least as good at selecting optimal experimental conditions as methods based on other criteria, such as the proximity to the perfect separation curve. The additional correction enables 3PPAA-U to exceed these traditional methods and so potentially improve the outcome of soil washing processes.

It is important to recognize that the 3PPAA-U is not an absolute guide for identifying the BUC, but rather a heuristic methodology. Thus, although it provides a structured and objective approach for evaluating and comparing different options, it is based on a set of assumptions and simplifications, so it may not capture the full complexity of a given soil washing operation. In this way, researchers and practitioners are advised to take this methodology only as an indicator of which experimental configurations are most promising and worth looking into further. The full decision-making process for choosing the best approach for a particular site must also consider a full range of subjective and qualitative factors such as cost, feasibility and risk. Consequently, although 3PPAA-U can be a useful tool for decision-making, it should be used in conjunction with other methods and criteria and should be applied with caution and critical thinking. One of the most obvious improvements of this method would be to include a third parameter, the grade, as part of the calculation for the experimental quality index (C_j^i). This additional constraint could potentially mitigate the impact of anomalous values and improve the overall accuracy of the method. Further research might include expanding the 3PPAA-U methodology to assess a fuller range of criteria important to the success of soil washing operations.

CRediT authorship contribution statement

X. Corres: Writing – original draft, Visualization, Investigation, Formal analysis, Data curation. **N. Gómez:** Writing – review & editing, Validation, Methodology. **C. Boente:** Writing – review & editing, Methodology, Formal analysis. **J.R. Gallego:** Writing – review & editing, Supervision, Resources, Funding acquisition. **C. Sierra:** Writing – original draft, Visualization, Supervision, Project administration, Methodology, Investigation, Formal analysis, Conceptualization.

Declaration of competing interest

The authors declare that they have no known competing financial interests or personal relationships that could have appeared to influence the work reported in this paper.

Data availability

Data will be made available on request.

Acknowledgements

Carlos Sierra thanks the EURECA-PRO phase I 2020–2023 co-funded by the Erasmus+ Program of the European Union (Ref.: 101004049). Open Access funding provided thanks to the Read and Publish. Nacional. Periodo 2021-2024 agreement between Universidad Politécnica de Madrid and Elsevier.

Appendix A. Supplementary data

Supplementary data to this article can be found online at https://doi.org/10.1016/j.chemosphere.2024.142135.

References

Ashraf, S., Ali, Q., Zahir, Z.A., Ashraf, S., Asghar, H.N., 2019. Phytoremediation: environmentally sustainable way for reclamation of heavy metal polluted soils. Ecotoxicol. Environ. Saf. 174, 714–727. https://doi.org/10.1016/J.ECOENV.2019.02.068.

Boente, C., Sierra, C., Rodríguez-Valdés, E., Menéndez-Aguado, J.M., Gallego, J.R., 2017. Soil washing optimization by means of attributive analysis: case study for the removal of potentially toxic elements from soil contaminated with pyrite ash. J. Clean. Prod. 142, 2693–2699. https://doi.org/10.1016/j.jclepro.2016.11.007.

Boente, C., Gerassis, S., Albuquerque, M.T.D., Taboada, J., Gallego, J.R., 2020. Local versus regional soil screening levels to identify potentially polluted areas. Math. Geosci. 52, 381–396. https://doi.org/10.1007/s11004-019-09792-x.

Buchman, M., Office of Response, N., 2008. SQuiRT Cards.

Chen, Z., Ma, Y., Liao, X., 2016. Phytoremediation of heavy metal pollution from mining and smelting activities: a review. J. Clean. Prod. 127, 19–30.

Chen, L., Wang, F., Zhang, Z., Chao, H., He, H., Hu, W., Zeng, Y., Duan, C., Liu, J., Fang, L., 2023. Influences of arbuscular mycorrhizal fungi on crop growth and potentially toxic element accumulation in contaminated soils: a meta-analysis. Crit. Rev. Environ. Sci. Technol. 53, 1795–1816. https://doi.org/10.1080/10643389.2023.2183700.

Corres, X., Sierra, C., Diez-Mestas, A.J., Gallego, J.R., Baragaño, D., 2024. A novel heuristic tool for selecting the best upgrading conditions for the removal of potentially toxic elements by soil washing. J. Hazard Mater. 466, 133529. https://10.1016/j.jhazmat.2024.133529.

Dermont, G., Bergeron, M., Mercier, G., Richer-Laflèche, M., 2008. Soil washing for metal removal: a review of physical/chemical technologies and field applications. J. Hazard Mater. 152 (1), 1–31. https://doi.org/10.1016/J.JHAZMAT.2007.10.043.

Drzymała, J., 2006. Atlas of upgrading curves used in separation and mineral science and technology. Physicochem. Probl. Miner. Process. 40 (1), 19–29.

Guo, J., Yuan, C., Zhao, Z., He, Q., Zhou, H., Wen, M., 2022. Soil washing by biodegradable GLDA and PASP: effects on metals removal efficiency, distribution, leachability, bioaccessibility, environmental risk and soil properties. Process Saf. Environ. Protect. 158, 172–180. https://doi.org/10.1016/J.PSEP.2021.12.004.

Karim, A.V., Jiao, Y., Zhou, M., Nidheesh, P.V., 2021. Iron-based persulfate activation process for environmental decontamination in water and soil. Chemosphere 265, 129057. https://doi.org/10.1016/j.chemosphere.2020.129057.

Khalid, S., Shahid, M., Niazi, N.K., Murtaza, B., Bibi, I., Dumat, C., 2017. A comparison of technologies for remediation of heavy metal contaminated soils. J. Geochem. Explor. 182, 247–268. https://doi.org/10.1016/J.GEXPLO.2016.11.021.

Khum-in, V., Suk-in, J., In-ai, P., Piaowan, K., Praimeesub, Y., Rintachai, K., Supanpaiboon, W., Phenrat, T., 2023. Combining magnet-assisted soil washing and soil amendment with zero-valent iron to restore safe rice cultivation in real cadmium-contaminated paddy fields. Chemosphere 340, 139816. https://doi.org/10.1016/j.chemosphere.2023.139816.

Lee, K.Y., Kim, K.W., 2010. Heavy metal removal from shooting range soil by hybrid electrokinetics with bacteria and enhancing agents. Environ. Sci. Technol. 44 (24), 9482–9487. https://doi.org/10.1021/ES102615A/SUPPL_FILE/ES102615A_SI_001.PDF.

Pinto, I.S.S., Neto, I.F.F., Soares, H.M.V.M., 2014. Biodegradable chelating agents for industrial, domestic, and agricultural applications—a review. Environ. Sci. Pollut. Control Ser. 21 (20), 11893–11906. https://doi.org/10.1007/S11356-014-2592-6/METRICS.

Richardson, J.M., Morrison, R.D., 2003. Metallurgical balances and efficiency. In: Fuerstenau, M.C., Han, K.N. (Eds.), Principles of Mineral Processing. Society for Mining, Metallurgy, and Exploration, 2003.

Rieuwerts, J.S., Mighanetara, K., Braungardt, C.B., Rollinson, G.K., Pirrie, D., Azizi, F., 2014. Geochemistry and mineralogy of arsenic in mine wastes and stream sediments in a historic metal mining area in the UK. Sci. Total Environ. 472, 226–234. https://doi.org/10.1016/j.scitotenv.2013.11.029.

Sierra, C., Gallego, J.R., Afif, E., Menéndez-Aguado, J.M., González-Coto, F., 2010. Analysis of soil washing effectiveness to remediate a brownfield polluted with pyrite ashes. J. Hazard Mater. 180, 602–608. https://10.1016/j.jhazmat.2010.04.075.

Sierra, C., Martínez, J., Menéndez-Aguado, J.M., Afif, E., Gallego, J.R., 2013. High intensity magnetic separation for the clean-up of a site polluted by lead metallurgy. J. Hazard Mater. 248–249 (1), 194–201. https://doi.org/10.1016/j.jhazmat.2013.01.011.

Sun, Y., Li, H., Guo, G., Semple, K.T., Jones, K.C., 2019. Soil contamination in China: current priorities, defining background levels and standards for heavy metals. J. Environ. Manag. 251, 109512 https://doi.org/10.1016/J.JENVMAN.2019.109512.

Wang, Y., Li, A., Cui, C., 2021. Remediation of heavy metal-contaminated soils by electrokinetic technology: mechanisms and applicability. Chemosphere 265, 129071. https://10.1016/j.chemosphere.2020.129071.

Wu, Q., Leung, J.Y.S., Geng, X., Chen, S., Huang, X., Li, H., Huang, Z., Zhu, L., Chen, J., Lu, Y., 2015. Heavy metal contamination of soil and water in the vicinity of an abandoned e-waste recycling site: implications for dissemination of heavy metals. Sci. Total Environ. 506–507, 217–225. https://doi.org/10.1016/J.SCITOTENV.2014.10.121.

Ye, B., Lan, J., Nong, Z., Qin, C., Ye, M., Liang, J., Li, J., Bi, J., Huang, W., 2022. Efficiently combined technology of precipitation, bipolar membrane electrodialysis, and adsorption for salt-containing soil washing wastewater treatment. Process Saf. Environ. Protect. 165, 205–216. https://doi.org/10.1016/j.psep.2022.07.015.